

A NOVEL APPROACH FOR ARCHAEOLOGICAL PREDICTIVE  
MODELLING: CASE STUDY FROM WESTERN TÜRKİYE HELLENISTIC  
SETTLEMENTS

A THESIS SUBMITTED TO  
THE GRADUATE SCHOOL OF NATURAL AND APPLIED SCIENCES  
OF  
MIDDLE EAST TECHNICAL UNIVERSITY

BY

MELEK ER

IN PARTIAL FULFILLMENT OF THE REQUIREMENTS  
FOR  
THE DEGREE OF DOCTOR OF PHILOSOPHY  
IN  
ARCHAEOOMETRY

MARCH 2023



Approval of the thesis:

**A NOVEL APPROACH FOR ARCHAEOLOGICAL PREDICTIVE  
MODELLING: CASE STUDY FROM WESTERN TÜRKİYE  
HELLENISTIC SETTLEMENTS**

submitted by **MELEK ER** in partial fulfillment of the requirements for the degree of  
**Doctor of Philosophy in Archaeometry Department, Middle East Technical  
University** by,

Prof. Dr. Halil Kalıpçılar  
Dean, Graduate School of **Natural and Applied Sciences**

\_\_\_\_\_

Prof. Dr. Gülay Ertuş  
Head of Department, **Archaeometry**

\_\_\_\_\_

Prof. Dr. Zeynep Kalaylıođlu  
Supervisor, **Archaeometry, METU**

\_\_\_\_\_

Assoc. Prof. Dr. Elif Koparal  
Co-Supervisor, **Archaeology, Mimar Sinan Fine Arts Univ.**

\_\_\_\_\_

**Examining Committee Members:**

Prof. Dr. Burcu Erciyas  
City and Regional Planning, METU

\_\_\_\_\_

Prof. Dr. Zeynep Kalaylıođlu  
Statistics, METU

\_\_\_\_\_

Prof. Dr. Lütfi Süzen  
Geological Engineering, METU

\_\_\_\_\_

Assist. Prof. Dr. Emine Sökmen Adalı  
Anthropology, Social Sciences Univ. of Ankara

\_\_\_\_\_

Assoc. Prof. Dr. Michele Massa  
Archaeology, Bilkent University

\_\_\_\_\_

Date: 15.03.2023

**I hereby declare that all information in this document has been obtained and presented in accordance with academic rules and ethical conduct. I also declare that, as required by these rules and conduct, I have fully cited and referenced all material and results that are not original to this work.**

Name, Surname: Melek Er

Signature :

## ABSTRACT

### **A NOVEL APPROACH IN ARCHAEOLOGICAL PREDICTIVE MODELLING: CASE STUDY FROM WESTERN TÜRKİYE HELLENISTIC SETTLEMENTS**

Er, Melek

Doctor of Philosophy, Archaeometry

Supervisor: Prof. Dr. Zeynep Kalaylıođlu

Co-Supervisor: Assoc. Prof. Dr. Elif Koparal

March 2023, 242 pages

The archaeological predictive models (APMs) have been developed since 1980s to locate unknown archaeological sites. However, the major elements for the development of APMs are still criticized: the archaeological input data, the variables used in prediction, the statistical analysis and the testing of resulting model.

This study aims to address each of these criticisms through a case study focused on the poleis of the Hellenistic period in western Türkiye. A high quality of archaeological data and relevant variables for prediction are accepted into the analysis. Elevation, ruggedness, slope, aspect, arable land, access to water and rock types used in the city walls were assessed as possible predictive variables. The study found that variables such as ruggedness, slope, aspect, and arable land were highly predictive. Additionally, the study introduced a new way of use for the road network as a socio-cultural variable, along with APMs.

Unlike previous studies, this study developed a statistical method that allows for polygonal representation of archaeological settlements while deriving landscape characteristics of the site. At each step, the suggested statistical approaches were tested for their repeatability and sensitivity to the sample size. The resulting variables

were selected based on their performance, repeatability, and sensitivity to proceed the unification of them as a final predictive map.

Keywords: Archaeological predictive modelling, statistics, Hellenistic Western Türkiye

## ÖZ

### **ARKEOLOJİK ÖNGÖRÜ MODELLEMESİNDE YENİ BİR YAKLAŞIM: BATI TÜRKİYE HELENİSTİK DÖNEM YERLEŞİMLERİ ÜZERİNE ÖRNEK BİR ÇALIŞMA**

Er, Melek  
Doktora, Arkeometri  
Tez Danışmanı: Prof. Dr. Zeynep Kalaylıođlu  
Ortak Tez Danışmanı: Doç. Dr. Elif Koparal

Mart 2023, 242 sayfa

Arkeolojik öngörü modelleri (AÖM), 1980'lerden beri bilinmeyen arkeolojik alanların yerini belirlemek için geliştirilmektedir. Ancak, AÖM'lerin geliştirilmesinde kilit unsurlar olan arkeolojik veriler, tahmin deđişkenleri, istatistiksel analiz ve ortaya çıkan modelin test edilmesi hala eleştirilmektedir.

Bu çalışma, batı Türkiye'deki Hellenistik Dönem polis yerleşimlerine odaklanan bir vaka çalışması aracılığıyla her bir eleştiriye ele almayı amaçlamaktadır. Analize yüksek kaliteli arkeolojik veriler ve tahmin için ilgili deđişkenler kabul edilmiştir. Rakım, engebелilik, eğim, bakı, tarım arazisi, suya erişim ve şehir surlarında kullanılan kaya türleri olası deđişkenler olarak değerlendirildi. Engebелilik, eğim, bakı ve tarım arazisi deđişkenlerinin yerleşim yeri tahminine önemli katkıları olduğu tespit edildi. Ek olarak, çalışmada, AÖM'lerde yol ađı için yeni bir kullanım yöntemi ortaya kondu.

Önceki çalışmalardan farklı olarak, bu çalışma, arkeolojik yerleşimlerin poligonal temsiline izin veren, bu alanın topoğrafik özelliklerini değerlendiren istatistiksel bir yöntem geliştirdi. Her adımda, önerilen istatistiksel yaklaşım, tekrarlanabilirliği ve örneklem büyüklüğüne duyarlılığı açısından test edildi. Sonunda, deđişkenler

performanslarına, tekrarlanabilirliklerine ve hassasiyetlerine göre seçildi ve bunlar birleştirilerek nihai bir tahmin haritası elde edildi.

Anahtar Kelimeler: Arkeolojik öngörü modellemesi, istatistik, Hellenistik Batı Türkiye

To Mavi

## ACKNOWLEDGMENTS

I am deeply grateful to many individuals who have provided me with invaluable support and guidance throughout the course of my thesis. First and foremost, I would like to express my heartfelt appreciation to my supervisor, Prof. Dr. Zeynep Kalaylıođlu, for her constant encouragement and guidance. Without her continuous support, this thesis would not have been possible.

I would also like to extend my gratitude to my co-supervisor, Assoc. Prof. Elif Koparal, for her valuable advice and guidance during the realization of this study.

Additionally, I owe a great debt of gratitude to Prof. Dr. Burcu Erciyas and Prof. Dr. Lutfi S ezen for their constant support and guidance during the thesis monitoring meetings, drawing on their vast knowledge to enrich my work.

Special thanks are also due to Assist. Prof. Dr. Emine S okmen Adalı from the Anthropology Department at the Social Sciences University of Ankara and Assoc. Prof. Dr. Michele Massa from the Archaeology Department at Bilkent University for their constructive comments and encouragement, particularly during the final stages of the thesis. I am fortunate to count them among my friends.

I would like to express my deepest gratitude to Prof. Dr. Vedat Toprak for inspiring my passion for this field of study, and for his invaluable experiences and enlightening conversations that have greatly enriched both my thesis and my life.

Finally, I would like to thank my friends Aylin Karakuşçu, Emre Duran, Cansu Ünüştü, Onur Ahıskalı, Emre Işıkay, and Serhat Uğural for their firm support.

I am also immensely grateful to my family for their love and support throughout my long PhD education. My warmest thanks go to my mother Makbule Tendürüs, my father İbrahim Tendürüs, my sister Dilek Tendürüs, my brothers Cengiz Tendürüs and Oğuz Tendürüs, my mother-in-law Şehriban Er, my father-in-law Kazım Er, and

my sisters-in-law Şencan Tendürüs and Menşure Tendürüs, as well as my beloved nephews.

Finally, I am at a loss for words to express my gratitude to my husband Mehmet Bilgi Er and my daughter Melis Doğa Er for their unwavering love and support in all that I do.

## TABLE OF CONTENTS

ABSTRACT .....	v
ÖZ.....	vii
ACKNOWLEDGMENTS .....	x
TABLE OF CONTENTS .....	xii
LIST OF TABLES .....	xvi
LIST OF FIGURES.....	xix
CHAPTERS	
1. INTRODUCTION.....	1
1.1. Predictive Modelling Concept .....	2
1.1.1. Model Objective(s).....	3
1.1.2. Model Components .....	4
1.1.3. Modelling Method.....	5
1.1.4. Modelling Techniques.....	8
1.1.5. Model Performance .....	13
1.1.6. Model Validation.....	14
1.2. Overview of APM Studies.....	15
1.3. Criticisms in APM.....	21
1.3.1. Archaeological input data.....	22
1.3.2. Variables.....	23
1.3.3. Statistical methods.....	24
1.3.4. Model Validation.....	26

1.4.	Archaeological Predictive Modelling in Türkiye .....	26
1.5.	Hellenistic Period in the Western Türkiye .....	29
1.5.1.	Historical Background .....	29
1.5.2.	Hellenistic Settlements .....	31
1.6.	Aim of the study .....	34
2.	MODEL DEVELOPMENT.....	35
2.1.	Archaeological Settlement: Spatial Phenomenon .....	37
2.2.	Characterization of Archaeological Sites .....	40
2.2.1.	Archaeological Sites as Polygonal Area .....	40
2.2.2.	Archaeological Sites as Network.....	48
2.2.3.	Computation of Potential Maps .....	51
2.3.	From Potential Maps into Predictive Map .....	54
2.3.1.	Reproducibility of Results with the Proposed Statistical Method .....	56
2.3.2.	Performance Assessment .....	60
2.4.	Combining the Potential Maps .....	62
2.5.	Evaluation of the Predictive Map .....	62
3.	CASE STUDY: HELLENISTIC SETTLEMENTS OF WESTERN TÜRKİYE.....	65
3.1.	Study Area Boundary .....	66
3.1.1.	Coastal Changes in the Study Area.....	67
3.2.	Archaeological Data .....	69
3.2.1.	Location and Period .....	70
3.2.2.	Typology and Size .....	71
3.2.3.	Sample Size.....	73

3.3.	Model Variables.....	74
3.3.1.	Topography .....	75
3.3.1.1.	Elevation .....	75
3.3.1.2.	Ruggedness .....	81
3.3.1.3.	Slope.....	92
3.3.1.4.	Aspect.....	102
3.4.	Natural Resources .....	112
3.4.1.	Arable Land Density .....	112
3.4.2.	Access to Water .....	122
3.4.3.	Rock Types Used in the City Walls .....	123
3.5.	Predictive Map.....	125
3.5.1.	Responses of Variables to the Proposed Statistical Method .....	125
3.5.2.	Independence of Variables.....	127
3.5.3.	Unification of Variables.....	128
3.6.	Performance of the Predictive Map .....	129
3.7.	Improvement of Predictive Map using a Socio-Cultural Feature: Road Network.....	134
3.8.	Evaluation of the Model .....	140
3.8.1.	General Evaluation.....	140
3.8.2.	Regional Evaluation.....	143
3.8.2.1.	Küçük Menderes and Büyük Menderes Valleys and their Southern Regions.....	143
3.8.2.2.	Gediz ve Bakırçay Valleys.....	145
3.8.2.3.	Northeastern Region of the Study Area .....	146

4. CONCLUSION.....	149
REFERENCES .....	153
APPENDICES	
A. ARCHAEOLOGICAL SETTLEMENT DATA .....	173
B. CHARACTERISTICS OF ARCHAEOLOGICAL SITE LOCATIONS .....	225
C. RESPONSE OF ARCHAEOLOGICAL SETTLEMENTS TO THE POTENTIAL MAPS .....	231
CURRICULUM VITAE .....	241

## LIST OF TABLES

### TABLES

Table 1-1 Example for judgmental weight assignment of variables for Neusius and Neusius (1989) in Harris (2013).....	10
Table 1-2 Other internal validation methods from Verhagen (2007).....	26
Table 1-3 The variables prepared for the model building and their presence in the equation produced by the logistic regression.....	28
Table 2-1 Example transformation of KDE values of slope to the final potential map having values between 0 and 1 for Gr80/20-Set2.....	54
Table 2-2 The correlation matrices between the slope potential maps having 80% of the known archaeological data for the training.....	56
Table 3-1. Comparison of sample size to the estimated population size.....	74
Table 3-2 Sample sizes of training and testing groups for the selected ratios for the archaeological dataset.....	74
Table 3-3 The correlation matrices between the ruggedness potential maps (value $\geq$ 0.8 is in light green and $0.8 > \text{value} \geq 0.65$ is in light gray).....	87
Table 3-4 The list of 5 archaeological settlements (from either training or testing data) of which locations are among the most potential area in each ruggedness potential maps (left) and the least potential area in each ruggedness potential maps (right) in alphabetical order.....	91
Table 3-5 The correlation matrices between the slope potential maps (value $\geq$ 0.8 is in light green and $0.8 > \text{value} \geq 0.65$ is in light gray).....	98
Table 3-6 The list of 5 archaeological settlements (from either training or testing data) of which locations are among the most potential area in each ruggedness potential maps (left) and the least potential area in each ruggedness potential maps (right) in alphabetical order.....	102
Table 3-7 The correlation matrices between the aspect potential maps (value $\geq$ 0.8 is in light green and $0.8 > \text{value} \geq 0.65$ is in light gray).....	108

Table 3-8 The list of 5 archaeological settlements (from either training or testing data) of which locations are among the least potential area in each ruggedness potential maps (left) and the most potential area in each aspect potential maps (right).....	112
Table 3-9 The correlation matrices between the arable land density potential maps (value $\geq$ 0.8 is in light green).....	119
Table 3-10 Rock types observed in the city walls and local geology (1:25.000 scale).....	124
Table 3-11 The summary of repeatability analysis for the groups.....	126
Table 3-12 The summary of gain statistics based on the testing data and the potential surface area percentages when the potential limit value is determined based on the 80% of training data successfully located for the groups having good repeatability.....	127
Table 3-13 Correlation matrices of four variables for the sets of Gr70/30.....	128
Table 3-14 Comparison of successfully located training, testing and overall data in each quantile for the predictive map PM70/30-Set1.....	131
Table 3-15 Kvamme's gain value for the predictive map PM70/30-Set1.....	132
Table 3-16 The number of settlements in each quantile at PMAll.....	133
Table 3-17 The number of settlements in each quantile and the name of settlements in these quantiles at the final predictive map.....	142
Table A-1 The list of archaeological settlements used in the study.....	171
Table B-1 Range of elevation values observed within the polygonal area and the median values with 95% confidence level for each archaeological site settled on in the study area in the Hellenistic Period.....	223
Table B-2 Range of TRI values observed within the polygonal area and the median values with 95% confidence level for each archaeological site settled on in the study area in the Hellenistic Period.....	224
Table B-3 Range of slope values observed within the polygonal area and the median values with 95% confidence level for each archaeological site settled on in the study area in the Hellenistic Period.....	226

Table B-4 Range of aspect values observed within the polygonal area and the median values with 95% confidence level for each archaeological site settled on in the study area in the Hellenistic Period.....	227
Table C-1 Sorted archaeological settlements with decreasing potentiality for ruggedness variable.....	231
Table C-2 Sorted archaeological settlements with decreasing potentiality for slope variable.....	233
Table C-3 Sorted archaeological settlements with decreasing potentiality for aspect variable.....	235
Table C-4 Sorted archaeological settlements with decreasing potentiality for arable land density variable.....	237

## LIST OF FIGURES

### FIGURES

Figure 1-1 Model building process (adjusted from Altschul (1988)).....	3
Figure 1-2 Model building steps of inductive and deductive approach.....	7
Figure 1-3 Example of histograms comparing distributions of slope for site location and background values from Harris (2013).....	10
Figure 1-4 Illustration of the contrast between accuracy and precision.....	13
Figure 1-5 The diagrammatic representation of the Romano-British settlement pattern based on the Christaller's transportation principle (from Ian Hodder (1972)).....	17
Figure 1-6 The application of elements of Figure 1-5 to the real distribution of Romano-British settlements (from Ian Hodder (1972)).....	18
Figure 1-7 The relative importance of natural and social environments in site location analysis with respect to the cultural complexity (from Kvamme (2006)).....	24
Figure 1-8 Distribution of various structures marking the borders of Klazomenian Territory (from Koparal (2011)).....	28
Figure 1-9 The extension of Seleucids in 281 BC (from Kosmin 2014).....	30
Figure 2-1 Flowchart of our archaeological predictive model.....	36
Figure 2-2 Raster data representing slope values for the study area as an example. Pixels forming the raster data can be seen as zoomed in a certain area.....	38
Figure 2-3 Examples of slope raster data and their histograms showing the variations in polygonal data (circle with a radius of 300 m) which belong to different archaeological sites.....	39
Figure 2-4 Statistical steps to derive the sites' characteristics for a variable while assessing the archaeological site as an area.....	40
Figure 2-5 Basic graphical representation of central tendency measures for unimodal and bimodal distributions (Sirkin 2019). $\bar{x}$ : Mean, Md: Median, Mo: Mode.....	42
Figure 2-6 Graphical representation of high and low variability (Ho 2017).....	43

Figure 2-7 Decompositioning of a multimodal distribution. Example shows the slope distribution of the archaeological site Akmonia.....	44
Figure 2-8 Flowchart for statistical analysis of aspect.....	45
Figure 2-9 An example showing circular mean (solid line) and the arithmetic mean (dashed line) from (Kalaylıoğlu 2020).....	46
Figure 2-10 Example aspect data of the archaeological sites Akmonia, Myrina and Teos together with their circular plots and linear histograms overlaid with fitted von Mises distributions (red line).....	48
Figure 2-11 Voronoi tessellation creation of a set of site points using midpoints between two sites.....	50
Figure 2-12 Voronoi tessellation creation of a set of site points using expanding circles around each site. The radius of circle expands from top left to right bottom...50	50
Figure 2-13 Steps to characterize the road network variable when assessing the archaeological site as point and related with its neighbours.....	51
Figure 2-14 Flowchart to compute potential map for a variable.....	52
Figure 2-15 Median slope values of archaeological sites with 95% CI for Gr80/20-Set2.....	52
Figure 2-16 Kernel density estimation curve overlaid the histogram of median slope distribution of archaeological sites available in the dataset of Gr80/20-Set2.....	53
Figure 2-17 Slope potential map of Gr80/20-Set2.....	54
Figure 2-18 Steps for the determination of potential maps of which variables will be used in the predictive map.....	55
Figure 2-19 Example potential map outputs.....	58
Figure 2-20 Sketch of the expected model performance responses with the changing sample sizes for training and testing.....	59
Figure 2-21 Boundary determined based on the cutting value at which 80% of the training data (PLAS-tr) observed within that high potential area (training data in black dots, testing data in black triangles).....	61
Figure 3-1 The boundary of study area. The inclined dashed areas at the coast indicates the current coastlines revised due to silting up.....	67

Figure 3-2 Paleogeographical evolution of the coastal plains of the western Türkiye (taken from Kayan (1999)).....	68
Figure 3-3 Hellenistic settlements in the study area.....	70
Figure 3-4. City size distribution of Archaic and Classical Poleis.....	73
Figure 3-5. Map (above) and frequency distribution (below) of the study area for elevation.....	77
Figure 3-6 Example elevation distributions at the archaeological sites Akmonia, Aphrodisias and Harpasa.....	77
Figure 3-7. Histogram of median elevation values together with KDE curve for all the known archaeological settlements in the dataset.....	78
Figure 3-8. Histograms of training data sets with changing percentages and overlaid KDE curves for elevation.....	79
Figure 3-9 Potential maps computed for the elevation variable based on the 3 sets of 5 groups that have different training and testing data ratio.....	80
Figure 3-10 Map (above) and frequency distribution (below) of the study area for Terrain Ruggedness Index.....	83
Figure 3-11 Example TRI distributions at the archaeological sites Aphrodisias, Priene and Sardis.....	83
Figure 3-12. Histogram of median TRI values together with KDE curve for all of the known archaeological settlements in the dataset .....	84
Figure 3-13. Histograms of training data sets with changing percentages and overlaid KDE curves for ruggedness.....	85
Figure 3-14 Potential maps computed for the ruggedness variable based on the 3 sets of 5 groups that have different training and testing data ratio.....	86
Figure 3-15 Comparison of ruggedness potential map outcomes colored based on successfully located archaeological sites of training data and overlaid with testing data locations.....	89
Figure 3-16 The effect of sample size on the potential surface area and the performance of testing data among the groups (A) and Kvamme’s gain values for the	

testing data (B) when 80% success rate is assumed in locating archaeological sites of training data for the ruggedness variable.....	90
Figure 3-17 Map (above) and frequency distribution (below) of the study area for slope.....	93
Figure 3-18 Example slope distributions at the archaeological sites Akmonia, Colossae, Pergamum.....	94
Figure 3-19. Histogram of median slope values together with KDE curve for all the known archaeological settlements in the dataset.....	94
Figure 3-20. Histograms of training data sets with changing percentages and overlaid KDE curves for slope.....	96
Figure 3-21 Potential maps computed for the slope variable based on the 3 sets of 5 groups that have different training and testing data ratio.....	97
Figure 3-22 Comparison of slope potential map outcomes colored based on successfully located archaeological sites of training data and overlaid with testing data locations.....	99
Figure 3-23 The effect of sample size on the potential surface area and the performance of testing data among the groups (A) and Kvamme's gain values for the testing data (B) when 80% success rate is assumed in locating archaeological sites of training data for the slope variable.....	100
Figure 3-24 Map (above) and frequency distribution (below) of the study area for aspect in degrees.....	104
Figure 3-25 Example aspect distributions at the archaeological sites Blaundos, Hierapolis and Hypaipa.....	104
Figure 3-26. Histogram of median aspect values together with density curve for all the known archaeological settlements in the dataset.....	105
Figure 3-27. Histograms of training data sets with changing percentages and overlaid KDE curves for aspec.....	106
Figure 3-28 Potential maps computed for the aspect variable based on the 3 sets of 5 groups that have different training and testing data ratio.....	107

Figure 3-29 Comparison of aspect potential map outcomes colored based on successfully located archaeological sites of training data and overlaid with testing data locations.....	109
Figure 3-30 The a effect of sample size on the potential surface area and the performance of testing data among the groups (A) and Kvamme’s gain values for the testing data (B) when 80% success rate is assumed in locating archaeological sites of training data for the aspect variable.....	110
Figure 3-31 Map (above) and frequency distribution (below) of the study area for arable land density.....	114
Figure 3-32 Example arable land density distributions at the archaeological sites Akmonia, Antiochia ad Maeandrum and Tripolis ad Maendrum.....	115
Figure 3-33. Histogram of median arable land density values together with density curve for all the known archaeological settlements in the dataset.....	116
Figure 3-34. Histograms of training data sets with changing percentages and overlaid KDE curves for arable land density.....	117
Figure 3-35 Potential maps computed for the arable land density variable based on the 3 sets of 5 groups that have different training and testing data ratio.....	118
Figure 3-36 Comparison of arable land density potential map outcomes colored based on successfully located archaeological sites of training data and overlaid with testing data locations.....	120
Figure 3-37 The effect of sample size on the potential surface area and the performance of testing data among the groups (A) and Kvamme’s gain values for the testing data (B) when 80% success rate is assumed in locating archaeological sites of training data for the arable land density variable.....	121
Figure 3-38 Predictive map (PM70/30-Set1) produced from Gr70/30-Set1.....	129
Figure 3-39 Example presentation of two buffer zones used in the statistical analysis of variables for the archaeological settlement Nysa (as a testing data over PM70/30-Set1).....	130
Figure 3-40 PMAI, the predictive map produced using all of the known archaeological settlements in the dataset.....	133

Figure 3-41 Example for travel-time raster map for Euphippe (No:19) and overlaid Voronoi polygons created using all of the known archaeological settlements.....	136
Figure 3-42. Histogram of travel-time away from all of the known archaeological sites to their neighbouring sites with the overlaid KDE curve.....	138
Figure 3-43 Potential map produced based on the travel-time between settlements.....	139
Figure 3-44 Comparison of KDE curves calculated based on the travel-time away from Gr70/30-Set1 and all of the known archaeological sites to their neighbouring sites.....	140
Figure 3-45 Predictive map showing the archaeological sites that are located at the highest potential zones (green dots) and that are at the lowest potential zones (red dots).....	141
Figure 3-46 Predictive map for Küçük Menderes and Büyük Menderes valleys and their southern regions.....	144
Figure 3-47 Predictive map for Gediz and Bakırçay valleys.....	146
Figure 3-48 Predictive map for the northeastern regions of the study area.....	148

# CHAPTER 1

## INTRODUCTION

Introduction of GIS has allowed spatial analysis for large regions. Archaeology has been one of the primary disciplines finding a place in such studies. The use of spatial analysis in archaeology started with map visualization of archaeological survey area and artefact distributions of survey results. It extended its use to the relationship between the settlement and its physiographic environment. Currently, GIS is being used in numerous archaeological research applications, e.g. remote sensing, geophysics, paleogeography, and predictive modelling. In this thesis, our interest lies in archaeological predictive modelling (APM). APM aims to support narrowing down of the possible locations on which an unknown archaeological site can be residing. When APM started to appear in 1970s, the motivation was to guide the cultural heritage management (Wheatley and Gillings 2002). Europe and USA were making use of predictive maps at governmental level. Nowadays, APM is being also used to gain insight about the former human behavior in site selection in the landscape.

On the other hand, the APMs are being criticized since their appearance (Wheatley and Gillings 2002, van Leusen 2002, Kamermans et al. 2009, Kamermans 2010, Verhagen et al. 2019). The quality and quantity of archaeological data (spatially and temporally), the types and weights of environmental, social and cultural inputs in the site selection, appropriateness of statistical analysis and missed testing/validation of model are the major areas of criticisms. This study aims to contribute suggesting solutions for the above listed common problematic areas of APMs. The problems are addressed and solutions are developed over a case study. The Hellenistic period

settlements of the western Türkiye are selected as a case study. Even though the region is well known with its rich ancient remains and archaeological settlements, there are still ancient major settlements mentioned in the texts (Kadoi, Magnesia ad Sipylum, Oroanna, Tisna/Titne etc.), but not located yet.

This study will be the first APM study used to identify the possible locations of unknown archaeological settlements in such a large scale in Türkiye. The APM resulting from this study is expected to (1) contribute to the understanding of site selection preferences of humans in the Hellenistic period in the western Türkiye, (2) assist the archaeologists with a spatial output displaying the areas where the likelihood of finding archaeological sites is high, and (3) be a start for the possible use of such models in the management of the rich cultural heritage of Türkiye.

### **1.1. Predictive Modelling Concept**

Predictive modelling is a process of predicting some desired outcomes by uncovering the relationships within the data (Kuhn and Johnson 2013). Finance, marketing, healthcare, and many other fields use predictive modeling to make informed decisions about future events and gain new insights from data.

The application of predictive model found its place in the archaeological field as well. Archaeological predictive models (APMs) are benefited in locating unknown archaeological sites based on the locational characteristics of known archaeological sites or on assumptions about human behavior (Kohler and Parker 1986). The idea behind the archaeological predictive modelling is that people who lived in the past did not randomly choose the places where they lived, as is the case today.

A predictive model is typically built from a sample collection, which represents the archaeological reality being studied, to test hypotheses derived from that sample. Preconditions are assumed during the modeling process. If the sample is similar to the model's prediction, this supports the hypotheses and provides more information about the sample. If the sample is different from the prediction, this suggests the need

for further investigation. This cycle of testing, modification, and cycling leads to continuous improvement in the model (Clarke 1972) (Figure 1-1).

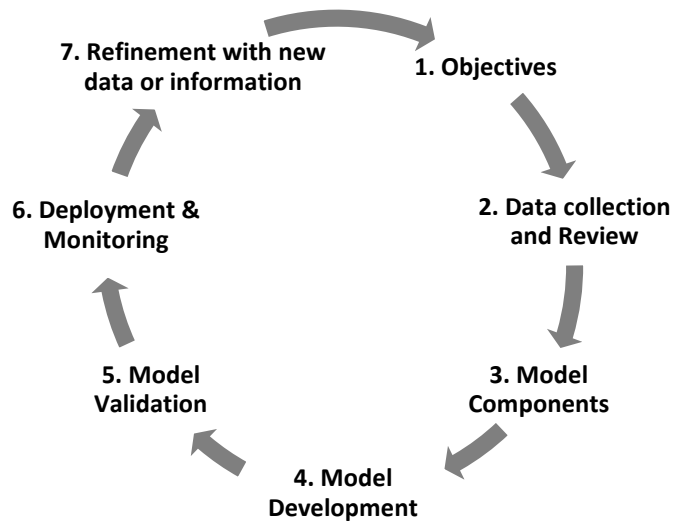


Figure 1-1 Model building process (adjusted from Altschul (1988)).

Building a predictive model follows a set of typical steps, regardless of what is being modeled or how it is being modeled. These steps include defining objectives, collecting and reviewing data, determining model components such as dependent and independent variables, developing the model method, and validating the model. The following sections describe these steps and other relevant concepts.

### **1.1.1. Model Objective(s)**

The major objective of archaeological predictive models is to identify the potential areas for archaeological sites in an investigated area within the context of cultural resource management (CRM) or academic research (Verhagen and Whitley 2020).

In CRM, predictive models are utilized during the planning stage of development projects to avoid disturbing archaeological remains. They assist planners in making

strategic decisions, such as rerouting the project or conducting salvage excavations, to preserve cultural heritage.

In an academic setting, predictive models provide insight into settlement patterns and human interactions with the environment and other societies. They can also be used as pre-survey research to reduce costs and increase efficiency (Ejstrud 2003).

Overall, the aim of archaeological predictive models is to provide a more comprehensive understanding of the past, and to guide conservation and management decisions in the present.

### **1.1.2. Model Components**

Model components are separated as dependent and independent variables (James et al. 2013). The dependent variable is the variable that is being predicted or explained by the independent variables. The independent variables are the variables used to predict or explain the dependent variable. The terms predictors, attributes, descriptors, and variables are also commonly used interchangeably with independent variables.

In archaeological predictive modelling, the location of archaeological sites is modelled. Based on ethnography and common sense, different cultural groups are expected to have different responses to the same environment because they have different norms, values, and ways of interacting with the world around them. This variation between cultures and over time forms the basis for predicting human locational behavior, which in turn helps inform the model (Kvamme 2006).

The archaeological data is recorded in a variety of forms (extensive/intensive surveys, excavations) and usually for a long period. Therefore, it is important to clean and organize the collected data properly for the analysis. When collecting archaeological data for the model, it is important to consider the following factors:

- Comparability in terms of types

- Comparability in term of period
- Locational accuracy
- Geometry of sites
- Number of sites
- Distribution of sites

The consistency and accuracy of archaeological data greatly influence the performance of the model.

The independent variables investigated for a possible relationship with the location of archaeological sites are commonly from physical environment (Wheatley and Gillings 2002). They are majorly derived from Digital Elevation Models (DEM) (e.g. slope, aspect). There are other environmental variables used in the models derived from geology, geomorphology, vegetation and hydrology. Environmental data is widely used in the predictive models because they are easy to obtain and use in GIS.

The socio-cultural variables are also used in predicting the location of archaeological sites. Kvamme (2006) refers the socio-cultural variables as human-created environment like markets, central places, political boundaries, and road network. In order to include such variables, the modelled area should be a well-studied archaeological region. Data availability is rather rare about the socio-cultural landscapes compared to the environmental data.

Altschul (1988) acknowledges that the selection of independent variables and their correlation with archaeological sites represents a formidable task in the process of model construction. These variables can be sourced from available data and prior knowledge, yet they may be identified through creative or intuitive approaches.

### **1.1.3. Modelling Method**

There are two main approaches employed in the archaeological predictive modelling studies: ‘inductive/data driven’ and ‘deductive/theory driven’. In the inductive approach, predictions rely on the data of a sample collection expected to characterize

settlement location preferences. In the deductive approach, the location preferences are hypothesized/formulated based on expert knowledge. The derived preferences in both approaches are used for a larger area to identify possible locations for archaeological settlements. On the other hand, Verhagen (2007) emphasizes that there is not much difference between inductive and deductive approaches in practice. In the data driven case, prior theories are considered during data and variable selection, and similarly, expert knowledge is based on the existing data when formulating the hypotheses. Both approaches are naturally intermingled in that sense.

The key differences in the employment of the two approaches are given within in Figure 1-2. In inductive approach, the research question is usually less well defined and shaped around the available data. The focus is on discovering patterns and relationships in the data, rather than testing predefined hypotheses. After data exploration and variables selection, the modelling technique is determined. There is training data, which is used to characterize the location of archaeological sites. After building the model, it is validated and deployed.

In the deductive approach, the research question is well-defined as it is formulated prior to model building. The relationships between the variables that should indicate the location of archaeological sites are determined based on existing theories and previous research in the field. The hypotheses are tested with the collected data. A suitable model is selected and evaluated. Finally, the model is deployed.

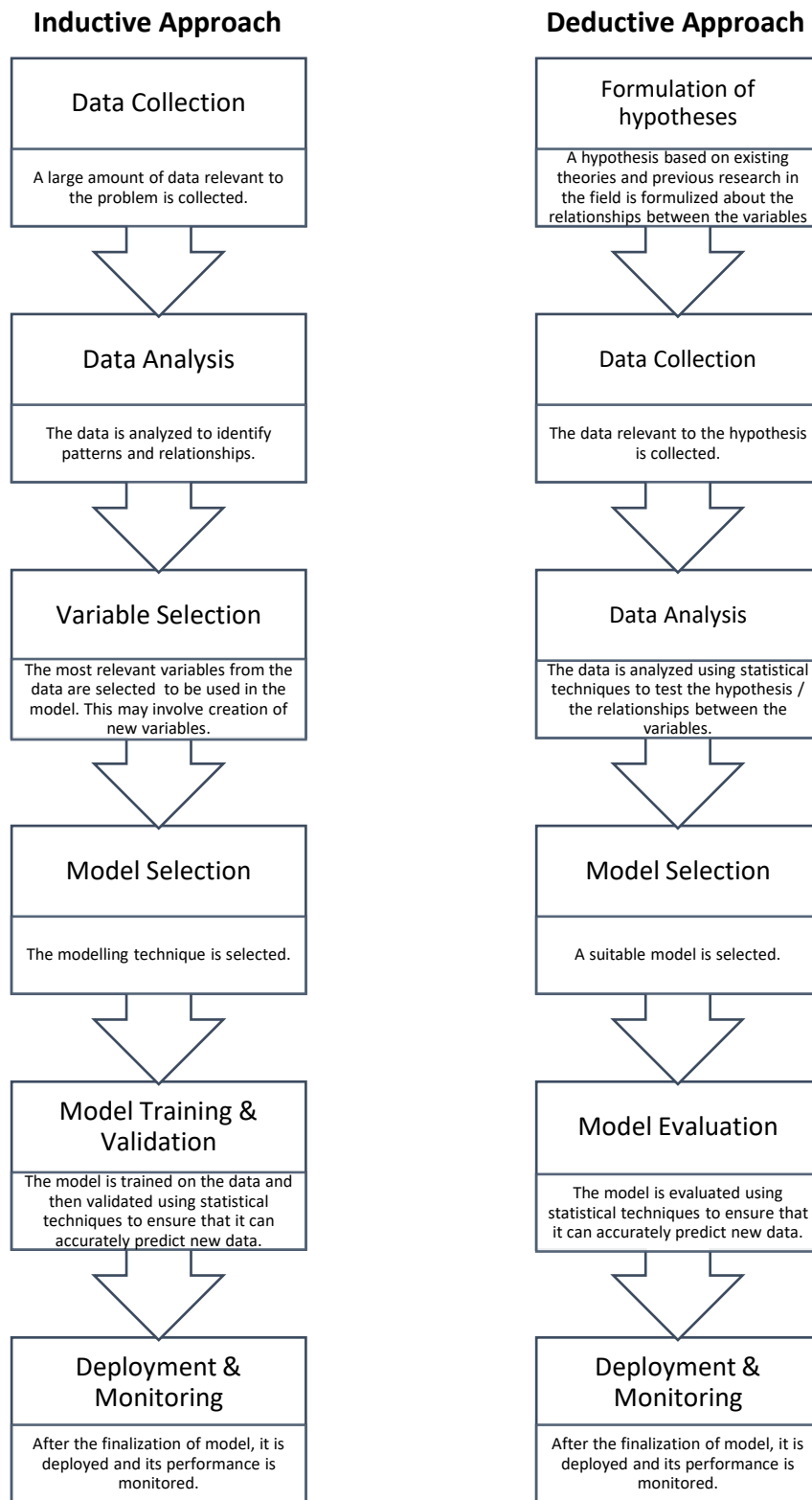


Figure 1-2 Model building steps of inductive and deductive approach

#### 1.1.4. Modelling Techniques

The statistical modelling techniques applied in archaeological predictive studies are varied very much including Boolean overlays, weighted additive layers, logistic regression, fuzzy logic, Bayesian statistics, machine learning based algorithms and more (e.g. Stančič and Kvamme 1998, Stančič et al. 2000, Hatzinikolaou et al. 2003, Kalaycı 2006, Finke et al. 2008, Balla et al. 2013, Diwan 2020, Yaworsky et al. 2020). Verhagen (2007) classifies the major statistical modelling techniques applied in APM into the following types:

- Expert judgment / intuitive models
- Deductive / expert judgment multi-criteria analysis models
- Correlative / inductive site density transfer models
- Correlative / inductive regression models
- Bayesian models

These techniques are primarily explained below, based on Verhagen's key characteristics summary.

**Expert judgement / intuitive models:** Expert intuition forms the basis for the construction of intuitive models, which may comprise of a single or multiple variables. An expert's statement, for instance, may dictate that lower-sloped areas are more suitable for archaeological site location than their higher-sloped counterparts. The model building process does not involve quantitative measurements and relies solely on subjective evaluation. The variables are then mapped and categorized into high, medium, or low classes on a base map. The absence of quantitative estimates and confidence intervals means that the model's performance can only be assessed through comparison with a test dataset.

**Deductive / expert judgement multi-criteria analysis models:** Deductive models are built from experts' knowledge, which is based on available data, past surveys and belief in the archaeological settlement choices. The expert selects the variables and

assigns scores/weights for the certain values of variables indicating relative importance of them in site location (Table 1-1). The map is then generated through the fusion of these variables in a Boolean overlay configuration. During this process, the weights are summed to show varying “attractiveness” of areas in the studied region. The areas having higher summed weights are interpreted as more attractive. Finally, the model is classified as high, medium, and low using the summed weights. The effectiveness of the model can only be determined by comparing it to a validated dataset or a trial survey program as the absence of quantitative estimates and confidence intervals prevents a more robust evaluation.

**Correlative / inductive site density transfer models:** The relationship between the archaeological site location and the variables are explored through data. First, whether there is a significant difference between the distribution of archaeological site locations and the variable values for the whole study area is compared using the Kolmogorov-Smirnov test (K-S test), the Chi-square test or similar tests. When such a difference is detected, it is assumed that there is a preference towards certain values of the variable. For example, the high concentration of sites at slopes less than 10% (as shown in Figure 1-3) suggests that these slopes are favoured for settlement. Weights to each range of variable values and among the variables are assigned based on the relative frequency of sites. Then, the variables are combined as Boolean overlays. The summed weights highlight the areas of relative appeal within the studied region. The quantification is in relative terms and no confidence limits are established. The use of performance measures and optimization of the model is an integral part of the modelling process.

This model type is powerful in statistically assessing the strength and nature of the correlation between archaeological site locations and variables (Harris 2013). The arbitrary decisions are reduced and more transparent, justifiable, and repeatable model is produced.

Table 1-1. Example for judgmental weight assignment of variables for Neusius and Neusius (1989) in Harris (2013)

Variable	Weight	Weight
Slope	0-3%	3
	4-9%	2
	10-15%	1
	>15%	0
Topographic Setting	terrace, floodplain, stream bench, river bluff	3
	saddle, hilltop, ridge top	2
	foot slope, toeslope	1
	hill slope, side slope	0
Aspect	south, southwest, east	3
	northeast, southwest, flat	2
	north, west, northwest	1
	no common direction	0
Proximity to Indian path	path located in block	3
	path in one or more adjacent blocks	2
	path one block distant	1
	no path in vicinity	0
Proximity to water source	water source located in block	3
	water source in adjacent blocks	2
	water source one block distant	1
	no water source in vicinity	0

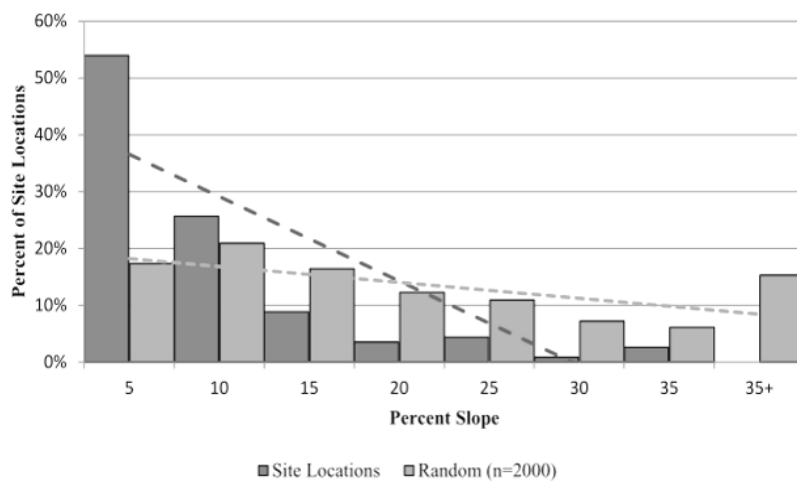


Figure 1-3 Example of histograms comparing distributions of slope for site location and background values from Harris 2013 (2013)

**Correlative / inductive regression models:** Regression analysis is a statistical technique that aims to examine the association between a dependent variable and one or more independent variables. Linear regression is the most commonly known regression analysis. In the most basic form a linear regression formula is:

$$y = \alpha + \beta x$$

where  $y$  is the dependent variable and  $x$  is the independent variable. The value of  $y$  is calculated from the value of  $x$ . However, in archaeological predictive modelling, the dependent variable is often binary (i.e. presence or absence) rather than continuous. Additionally, the relationship between the dependent variable and the independent variable is not linear (see Section 2.2). To handle such scenarios, logistic regression is used instead, which models the probability of the dependent variable belonging to a specific category (i.e. presence or absence):

$$y = \frac{1}{1 + e^{-(\alpha + \beta_1 x_1 + \beta_2 x_2 + \dots + \beta_p x_p)}}$$

where  $y$  is the predicted value of the dependent variable,  $x_p$  is the independent variable,  $B_p$  is the coefficient of the corresponding variable. Positive coefficients show a relationship between high values of the variable and the presence of the site, while negative coefficients signify that low values of the variable are associated with the presence of the site. An example logistic regression model outcome from an application in the prehistoric open-air sites of Pinon Canyon Archaeological Project, located in Las Animas County, southeastern Colorado (Kvamme 1992) is:

$$\begin{aligned} D = & -0.9425 + 0.00122(\textit{aspect}) - 0.0239(\textit{slope}) + 0.00277(\textit{relief}) \\ & + 0.00181(\textit{shelter}) - 0.00404(\textit{view}) \\ & - 0.00204(\textit{horizontal dist. to drainage}) \\ & - 0.000636(\textit{vertical dist. to drainage}) \end{aligned}$$

The positive coefficients of aspect, relief and shelter index indicate that the high values of these variables are related to the open-air site locations. The model also indicates that locations with low values of slope and close to drainages both horizontally and vertically were preferred as open-air sites in the studied region (see Kvamme (1992) for further detail). The calculated  $D$  value indicates how likely a location is open-air site with the entered variable values.

It should be noted that logistic regression, unlike the other modelling types mentioned in the previous sections, requires information on both the presence and absence of archaeological sites at the model development stage. The absence data is usually not readily available. To overcome this limitation, a common solution is to sample data randomly from the background data, as the majority of the study area is typically assumed to contain no archaeological sites. On the other hand, similarly no confidence limits are established and the model's performance can be measured, preferably based on a test dataset.

Logistic regression is the most commonly used predictive modelling technique in archaeology due to its robustness and easiness to understand its outcomes.

**Bayesian models:** Bayesian statistics is a method that can incorporate both deductive (based on prior knowledge and theories) and inductive (based on observed data) elements in a statistical modelling, including the archaeological predictive modelling (Verhagen 2007, Finke et al. 2008). The Bayes' theorem is as follows:

$$\text{posterior belief} = \text{conditional belief} * \text{prior belief}$$

Prior belief is the probability of an event based on expert knowledge or former studies outcomes (Hayes 2022). Conditional belief is the likelihood of an event occurring based on the occurrence of some other previous event. Posterior belief is the revised probability of an event after taking into consideration the new information. The method is applied in few archaeological predictive models (Finke et al. 2008). Verhagen (2007) notes that prior beliefs are generally assumed as uniform for all map

categories. This assumption actually turn the situation where no prior information is available. The main advantage of Bayesian models is inclusion of the prior knowledge. The accuracy of prior knowledge has a significant role in the improvement of estimates.

### 1.1.5. Model Performance

The success of a model in archaeological predictive modelling is evaluated based on its accuracy and precision. Accuracy refers to the degree to which the model correctly predicts the location of archaeological sites within the high potential zone. Precision, on the other hand, refers to the ability of the model to precisely define the boundaries of the high-probability zone, as compared to the total study area. The goal is to maximize both accuracy and precision, by correctly predicting as many site locations as possible within a well-defined high potential zone. Figure 1-4 portrays the differences between accuracy and precision.

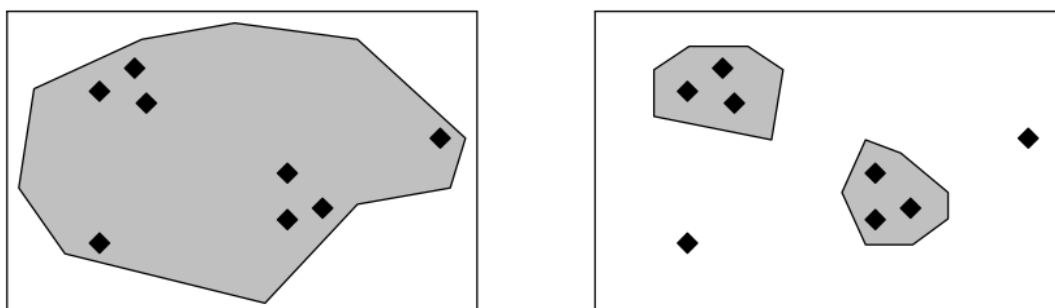


Figure 1-4 Illustration of the contrast between accuracy and precision. The model depicted on the left accurately identifies all sites, resulting in 100% accuracy. In contrast, the model on the right misses a few sites, resulting in lower accuracy, but higher precision (from Verhagen (2007)).

As the main aim of archaeological predictive model is to allocate the most likely locations for the archaeological settlements in the study area, the performance of the

model is measured by comparing the surface area percentage of high potential area and the percentage of observed archaeological settlements in this area. Related index is defined by Kvamme (1988) as followed:

$$G = 1 - \frac{p_a}{p_s}$$

where  $p_a$  is the percentage of area classified as high potential in the study area given by the predictive map,  $p_s$  is the percentage of observed archaeological sites within this area, and  $G$  is gain.

The gain ranges from -1 to 1: gain near 1 indicates the highest predictive utility, near 0 indicates low or no predictive utility, and near -1 indicates reverse predictive utility (Kvamme 1988). Negative values indicate that the sites are generally located outside of the model area classified as potential. The gain approach is easy to apply and enables comparison of models from different studies. It is the most widely used method for the model assessment.

#### **1.1.6. Model Validation**

The performance of a model can be evaluated using either a test dataset or an independent dataset. Verhagen (2007) separates testing and validation terms. According to his descriptions: testing the model should be carried out exclusively using an independent dataset in order to accept or reject the model, while validation of the model can be performed using either a test or independent dataset to determine the model's performance. The true testing of an archaeological predictive model requires collecting new data in the field, which can be time-consuming and costly. There are alternative validation techniques that can be considered first, the most common of which is the *validation set approach* (James et al. 2013). This involves randomly dividing the available data into two parts: a *training set* and a *validation set* (also known as a *hold-out set*). The training set is used to build the model, while the validation set is used to assess the model's performance by observing the model's

response to the validation set. When the available data is small in size, it should be used cautiously.

## **1.2. Overview of APM Studies**

The roots of APMs go back to the pioneering studies of Steward in 1938 and Wiley in 1953 on settlement patterns and on the relationship of settlement to environmental features (Kohler and Parker 1986). Predictive models are developed by subsequent analysis of settlement pattern studies and extrapolating them to a larger area. It can be said that APM studies developed in parallel with this trend in the 1960s when New Archaeology or Processual Archaeology was on the rise.

The term “predictive model” in archaeology appears in the publications in the early 1970s (Verhagen and Whitley 2012). With the ease in access of researchers to geographic information systems (GIS) software in the 1980s, APM studies gained momentum. From this period on, numerous modelling methods were developed and applied to archaeology.

When archaeological predictive modelling was initiated in the 1970s through United States Agencies such as the Bureau of Forestry and Land Management, the main purpose of them has been in the context of cultural heritage management (King 1978). The models created would be used to estimate the probability of an archaeological site being in the area of any project site planned by the government agencies in a region. This initiation had practical and economical reasons, but also had been the main impetus for the development of predictive methods (Wheatley and Gillings 2002).

The project of Minnesota Department of Transport, known as ‘MnModel’, is one of the well-known example developed at the governmental level among the APMs (Verhagen and Whitley 2020). The model aim was to predict prehistoric archaeological site locations for entire state of Minnesota in order to support the state transportation department at the planning stage of their transportation projects. The

model has been in use since 1998 (Minnesota Department of Transportation 2022). This is a rare project with its large scale and long-term scope.

Following USA, Canada and later Europe started to develop archaeological predictive models (e.g. Stančič et al. 2000, Ejstrud 2003). The increasing number of models had led to the discussions on their archaeological theory and methods (Ebert 2000, van Leusen et al. 2005). Even though the early models produced for the cultural heritage management were criticized for lacking explanation of human organizational systems, the valuable contribution of APMs could not be denied in understanding the distributions of archaeological sites, hence the human behaviour (Kvamme 2006).

David Clarke's book (1972), "Models in Archaeology," as its name suggests, was one of the earliest publications on the use of models in archaeology. He listed the main reasons why archaeologists should be concerned with models as follows:

- Personal opinions and approaches in archaeology are influenced by subconscious mind models accumulated over time.
- Conceptual models are used to interpret observations and should be made more explicit and testable.
- Testing and modifying models is crucial for empirical and scientific approaches.
- Models are simplified expressions of underlying theories.
- Models play an important role in hypothesis generation, testing, and explanation in archaeology.

The book also explores possible location models for archaeological settlements. An example demonstrating the predictive value of such models is given by Ian Hodder (1972) on the study of the Romano-British settlements. The central place theory, developed by Christaller (1933), forms the basis of one of the models analysed by him. According to this theory, even in simple agrarian societies, certain regions require goods or services they cannot produce themselves, leading to the creation of central service centers for the exchange of these products. The centralization of these

services minimizes the effort required to obtain them, making them more accessible to the surrounding tributary area. As a result, an idealized pattern of settlement is formed in a triangular/hexagonal lattice. He, first, justifies the applicability of this pattern to the Romano-British settlements. Then, he applies this idealized pattern as locational model between the major centers and the smaller walled towns (Figure 1-5) and compares with the real distribution of the Romano-British settlements (Figure 1-6) in order to predict major centers.

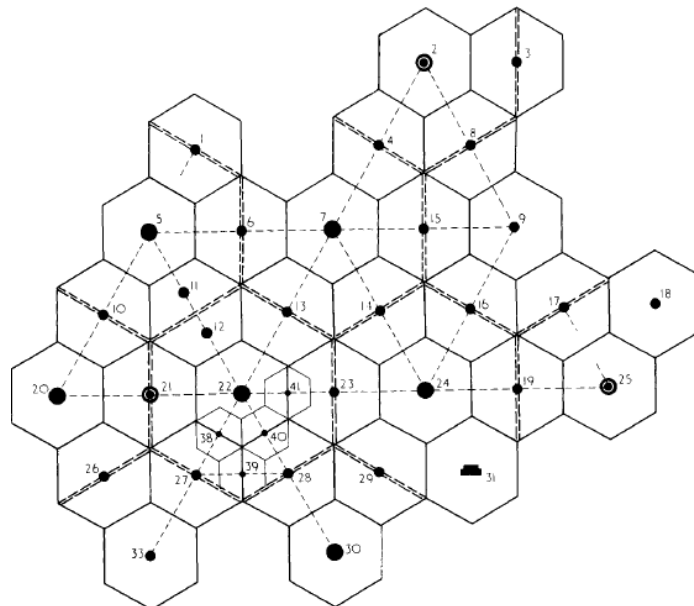


Figure 1-5 The diagrammatic representation of the Romano-British settlement pattern based on the Christaller's transportation principle (from Ian Hodder (1972))

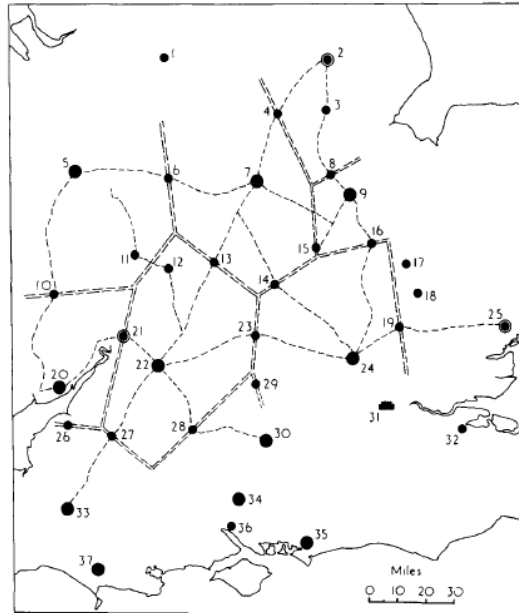


Figure 1-6 The application of elements of Figure 1-5 to the real distribution of Romano-British settlements (from Ian Hodder (1972))

After the appearance of early examples of predictive models especially for the prehistoric sites (e.g. Bettinger 1980, Jochim 1981, Parker 1982), Kohler and Parker wrote a chapter in 1986 in *Advances in Archaeological Method and Theory* that aimed to provide background information for policy discussions on the use of predictive models in cultural resource management (CRM) and to evaluate the potential of these models for research. This publication is often cited as the main source for the definition of archaeological predictive modelling:

*“Predictive locational models attempt to predict, at a minimum, the location of archaeological sites or materials in a region, based either on a sample of that region or on fundamental notions concerning human behavior.”*

The authors discuss various empiric correlative models for locational prediction used in both corporate and academic research, and contrasts them with models from a deductive tradition. The weaknesses of the empiric models, such as inappropriate

techniques, lack of consideration for validation, and low resolution, are noted. However, some of the models reviewed are accurate enough for planning purposes. The author notes that the underlying data could provide insight into settlement systems and locational processes, but this remains largely untapped. The surveys on which the models were based have produced a large amount of data and environmental information, and the models have emphasized the importance of environmental factors in site location. The models have also helped to understand the role of on-site and catchment variables and have addressed the challenge of incorporating non-subsistence variables.

In 1988, the US Department of the Interior Bureau of Land Management published a book entitled "Quantifying the Present and Predicting the Past: Theory, Method and Application of Archaeological Predictive Modeling" containing almost every aspect of predictive modelling in archaeology (Judge and Sebastian 1988). The authors of chapters were academic, federal and contract archaeologists. The book is about majorly prehistoric archaeology and correlative models, which are mainly or completely created through inductive methods. However, the book also includes information on the construction of explanatory models with deductively derived components. Model building process, statistical discussions and many other topics are covered.

The perception of archaeological remains underwent a change after the introduction of the National Historic Preservation Act in USA in 1966. They are now regarded as limited and non-renewable resources. This shift was first apparent in the United States and then Canada through the implementation of nationwide predictive modeling in archaeology. Similarly, European countries also began to adopt predictive modeling in archaeology, following the signing of the *European Convention on the Protection of the Archaeological Heritage* in 1992. The objective of the convention is to safeguard the archaeological legacy, which serves as both a resource for the shared history of Europe and a means of conducting historical and scientific research. The Netherlands developed their first nationwide predictive map, *Indicatieve Kaart van*

Archeologische Waarden, (IKAW<sup>1</sup>) in 1997 (Verhagen 2007). On the other hand, in the UK and France, full-scale prospection is typically carried out during the early stages of development planning to assess archaeological risks (Verhagen 2007). This limits the opportunity to shape planning decisions, apart from utilizing existing sites and monuments records. The development of predictive maps in other European countries were rather late.

At the same time, the effectiveness of predictive models in both management and research was being questioned by the archaeological community in Europe and the USA (Ebert 2000, van Leusen et al. 2005, Mehrer and Wescott 2005). The first version of the Dutch predictive map, which was developed using an inductive approach for cultural resource management, faced criticism for its suitability in the Dutch archaeological context where much of the remains are buried underground. To improve the methods for protecting the Netherlands' archaeological heritage, the Netherlands Organization for Scientific Research (NWO) established a research program. A team from academia and public archaeology was working together to advance predictive modeling. A baseline report, authored by Martijn van Leusen, Jos Deeben, Daan Hallewas, Paul Zoetbrood, Hans Kamermans, and Philip Verhagen, was published, providing a comprehensive overview of the relevant issues in predictive modelling (van Leusen et al. 2005, Verhagen 2007). The report, which also made international contributions, focussed on six improvement areas. These are:

- The quality of the archaeological input data
- Higher spatial and temporal resolution
- Environmental input factors
- The inclusion of socio-cultural factors
- (Spatial) statistics
- Testing

---

<sup>1</sup> Indicative Map of Archaeological Values of the Netherlands

Each theme is discussed in the following section.

Verhagen published another thorough study entitled “Case Studies in Archaeological Predictive Modelling in 2007 as part of his doctoral thesis. He focuses on the enhancement of archaeological predictive modelling, provides practical applications of methods and techniques and enquires alternative methods. He contributes the improvement areas mentioned above discussing sampling as a means to obtain the data to develop and test APMs, summarizing the main characteristics of the available statistical modelling techniques, and, in particular, reviewing the model evaluation and testing in depth.

Although there is still no resolution on these controversial issues, predictive modeling continue to advance (Finke et al. 2008, Carleton et al. 2012, Carleton et al. 2017) and remains a significant aspect in archaeological spatial analysis. As noted by Doran in 1972, the explanatory value of a model is just as important as its predictive ability. There are applications of APMs all around the world, making valuable contributions to the archaeological research (Wachtel et al. 2018, Diwan 2020).

### **1.3. Criticisms in APM**

The ongoing debates in APM theory and methods provides identification of and discussions on the major problems in the archaeological predictive modelling studies. The major problem areas mentioned in various sources (Verhagen 2007, Kamermans 2010, Carleton et al. 2017) are:

- Quality and quantity of archaeological input data
- Selection of variables
- Used statistical methods during the model development
- Testing of the developed model

The criticisms will be discussed within the scope of this study. The study is carried out with a data-driven approach on the Hellenistic period polis settlements in a wide area.

### **1.3.1. Archaeological input data**

Creating a comparable and accurate dataset for modelling studies is challenging due to the fragmentary nature of archaeological data and its collection using various methods. Data-driven predictive models heavily rely on the quality and quantity of archaeological data, which has received criticism for limitations (van Leusen 2002, Kamermans 2010). Bias in the data during surveys can stem from various factors, such as survey intensity, spatial layout, sampling unit size, visibility of archaeological remains, and recording practices (Verhagen 2007).

To enhance the quality of data for modelling purposes, a national digital database can be established, especially for large scale APMs. The focus should be on consistency, with clear descriptions of archaeological sites and identification of their periods. Examples of such databases are ARCHIS in the Netherlands and VIVRE in Luxembourg (Kamermans 2010). However, it is important to review the data to minimize bias and evaluate its accuracy in settlement location, period, and type before using it as model input.

In addition to quality, an appropriate sample size is vital for the validity of the model. To achieve consistency, subgroups of different site types can be created, such as administrative/economic/military centers, coastal/mountainous sites, or mixed types (Kohler and Parker 1986, van Leusen 2002). However, given the limited number of samples in many archaeological datasets, data quantity is often a concern.

Another criticism is the presentation of the archaeological sites as points in most of the APMs, rather than as areas. Such a representation fails to capture the diverse characteristics of the site's location (Mink et al. 2005, Carleton et al. 2012, Carleton et al. 2017). This can prove to be a statistically onerous task, particularly when the surrounding area boasts multiple distinctive landscape features. On the other hand, it is worth mentioning that while this approach may pose difficulties when examining the relationship between the site and certain variables, such as slope, it may not be as

relevant when studying the relationship between the site and other variables, such as proximity to a water source.

Finally, Ebert (2000) criticizes the dominance of the site-centered approach in inductive predictive modelling. He posits that archaeological sites are not discrete entities, but rather components of larger systems, and their locations are contingent upon the positions of other elements within that system, including other sites. Furthermore, travel between sites, which has been shown to play a significant role in shaping human systems, may in fact be even more crucial to consider than the sites themselves, as some studies suggest that the majority of human-environment interactions occur during such travel.

### **1.3.2. Variables**

The use of archaeological predictive models has been criticized for being overly focused on environmental factors, such as slope, soil type, and proximity to water (Wheatley 1993, Gaffney and van Leusen, 1995). However, human behavior is influenced not only by the environment, but also by social and cultural factors, which should be reflected in the archaeological record (Plog and Hill 1971). Kvamme (2006) suggests that as a society becomes more complex, the social variables become increasingly important compared to the environmental variables (Figure 1-7). However, incorporating these socio-cultural variables into models is challenging due to a lack of relevant data and quantifiable methods (Verhagen and Whitley 2020). Factors such as road networks, religious centers, and political boundaries are not easily accessible. Despite decades of study in some regions, the available information remains incomplete.

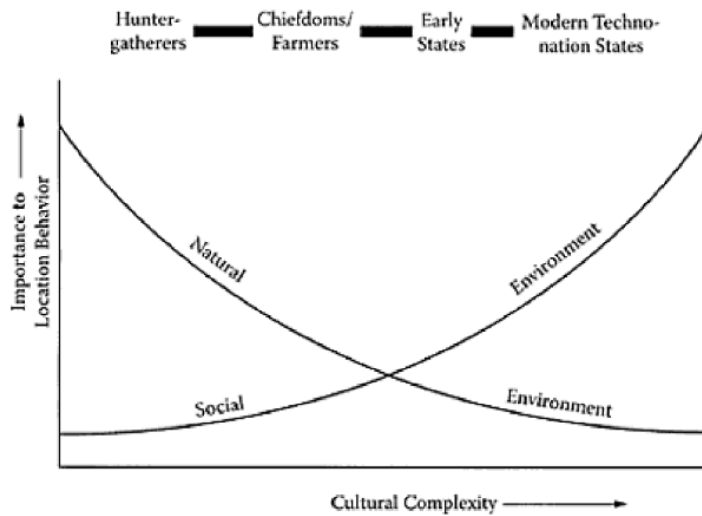


Figure 1-7 The relative importance of natural and social environments in site location analysis with respect to the cultural complexity (from Kvamme (2006))

According to Bintliff (2000), environmental determinism plays a crucial role in human adaptation to different landscapes. Understanding the topography and environment of a region can be instrumental in comprehending cultural development, making it a vital factor to consider.

Environmental variables are also being criticized. The input data used for these variables are from current landscape. The change of land since the period is commonly neglected as the geological processes occur much slowly compared to the human-life spans. However, there are geologically dynamic regions that this change can be intolerable. Besides, depositional processes in the studied regions are also important in the assessment of the quality of the archaeological data.

### 1.3.3. Statistical methods

As mentioned earlier, the practice of predictive modelling in archaeology is influenced by two major approaches: inductive and deductive. The inductive approach, also known as data-driven or correlative, is criticized for its potential for bias and lack of explanation. Such models require large datasets of previously known

archaeological sites to produce significant results. On the other hand, the deductive approach, which is theory-driven or explanatory, is criticized for its subjective nature. Van Leusen (2002) highlights that two other approaches of predictive modelling, possibilistic and probabilistic, are often overlooked.

According to the observations of Ebert (2000), in a possibilistic model, the gain is limited and can never exceed a certain level (i.e. 70%). This approach has sometimes been confused with the probabilistic approach, which expresses the likelihood of an area being used for a specific activity. Various statistical modelling techniques, including possibilistic and probabilistic approaches, are used in APMs, but most often the possibilistic one. Kvamme (1988) pointed out that archaeological predictive models do not predict the exact location of an unknown settlement, but instead indicate areas with similar characteristics based on known settlements and human behavior beliefs.

The regression statistical modelling techniques require both site-presence and site-absence data. However, site-absence data is often unavailable and collecting it can result in similar characteristics to site-presence data (Kvamme 1992). To overcome this, Kvamme proposed using pseudo-absence data by randomly sampling from the study area. Nevertheless, this argument was not convincing. Verhagen suggests using the site-presence to site-absence ratio. Alternatively, statistical modeling techniques that do not require site-absence data can be developed further.

Despite the increasing variety of statistical modelling techniques used in APMs, it is still challenging to determine which technique performs best for a given data set (Verhagen and Whitley 2020). Also it should be noted that as the models become more complex, it becomes increasingly difficult to interpret the results. It is important to consider that a particular data set may produce good results with one method, but poor results with another, making it crucial to determine the best method for any given data set (James et al. 2013).

### 1.3.4. Model Validation

As all in the predictive models, how accurate and how precise the archaeological predictive model developed is a concern. The common practice is to separate test data at the beginning of study from the dataset and use them to evaluate the model's performance. The ideal approach is to test/validate the model with new and independently collected data.

Verhagen (2007) mentions other techniques given in Table 1-2 indicating their rare use or wrong use.

Table 1-2 Other internal validation methods from Verhagen (2007)

split sampling (hold-out method)	<ul style="list-style-type: none"> <li>- keeps a test set apart, usually half of the data</li> <li>- determines error rate with the test set</li> <li>- error rate of test set and original data set are compared, not averaged</li> </ul>
cross validation	<ul style="list-style-type: none"> <li>- divides sample randomly into k subsets</li> <li>- withholds each subset from analysis in turn</li> <li>- constructs k models with remainder of data</li> <li>- and determines k error rates using withheld data</li> <li>- total error rate is estimated by averaging error rates across models</li> </ul>
leave-one-out (LOO)	<ul style="list-style-type: none"> <li>- same as cross-validation, but k = n (1 observation left out at a time)</li> </ul>
jackknife	<ul style="list-style-type: none"> <li>- same as LOO, but error rate determined differently</li> </ul>
bootstrap	<ul style="list-style-type: none"> <li>- takes a random sample with replacement of size n k times</li> <li>- determines the error rate using the original data set</li> <li>- total error rate is estimated by averaging error rates across models</li> <li>- extended error rate estimators have been developed</li> </ul>

### 1.4. Archaeological Predictive Modelling in Türkiye

One of the earliest and possibly the only archaeological predictive modelling study in Türkiye could be for the settlement mounds at the Lake District of Anatolia,

Konya, dating to the period of 9000 BCE – 5500 BCE with well defined archaeological settlement type and period (Kalaycı 2006). Kalaycı defines the average settlement sizes and match the pixel size of each site with the calculated size (i.e. 133 m x 133 m). Total number of 64 sites were presented as 95 pixel due to some larger sites. He employs logistic regression method to construct the predictive model. Since logistic regression method requires absence data, he randomly selects absence sites (120 pixels) for 20 times, which results 20 different predictive models. The final predictive model is acquired by taking averages of these obtained different predictive models. Table 1-3 shows the variables included to the logistic regression and found in the equation of which predictive model. At the end, he leaves out the PM6, PM7, PM8, PM13 and PM17 from the final predictive model based on their performances. During the development of the predictive model, many criticized topics were also considered. However, as Kalaycı states the testing data (10 pixels) were very few. The effect of sample size on the logistic regression models could be explored.

On the other hand, settlement pattern studies are more common in Türkiye (e.g. Yörükan 2009, Koparal 2011, Oğuz 2013, Hill 2016, Matessi et al. 2018). These studies provide a base information for the archaeological predictive modelling. An APM attempts to go a step further than settlement pattern analysis by extrapolating the information to a larger population (Kohler and Parker 1986). For example, forts, border marks and cult places found during the surveys of Klazomenai, are considered related to territory border of the polis (Koparal 2011; Figure 1-8) . When such structures are known for a larger area, they can be evaluated as a possible socio-cultural variable.

Table 1-3 The variables prepared for the model building and their presence in the equation produced by the logistic regression

	PM1	PM2	PM3	PM4	PM5	PM6	PM7	PM8	PM9	PM10	PM11	PM12	PM13	PM14	PM15	PM16	PM17	PM18	PM19	PM20
Distance to Lake	X	X	X					X												
Distance to River					X			X	X										X	
Distance to Major Class	X	X							X							X				
Soil Depth						X	X	X		X	X									
Erosion															X					
Soil Particle Size																				
Current Land Use		X	X	X	X	X			X	X	X		X							
Lithology				X	X	X					X	X		X	X					
Distance to Roughness Junc.																				
Roughness									X											X
Adjusted Distance to Ridges																	X		X	
Aspect		X	X		X	X	X	X	X	X	X		X		X	X	X	X	X	X
Slope	X	X					X	X						X						
Adjusted Elevation	X	X	X	X	X								X	X	X					
Elevation												X				X		X		

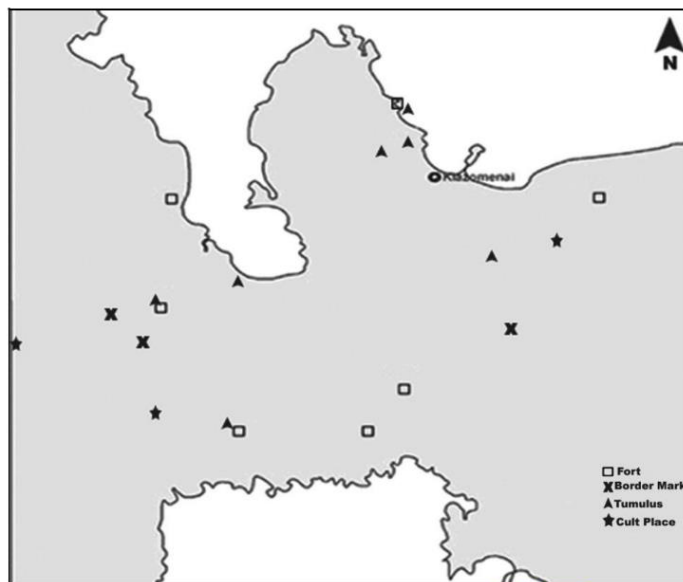


Figure 1-8 Distribution of various structures marking the borders of Klazomenian Territory (from Koparal (2011))

## **1.5. Hellenistic Period in the Western Türkiye**

### **1.5.1. Historical Background**

The Hellenistic period spans for some 300 years beginning with the reign of Alexander the Great (336–323 BCE) until the conquest of the last Hellenistic kingdom in Egypt by Rome in 30 BCE. Alexander the Great was crowned as a king at the age of 20 after the death of his father Philip II, who conquered and consolidated most of the Greece. Alexander expanded the Graeco-Macedonian world with his military campaigns through Asia Minor, Egypt, Persia and India and carried the Hellenic culture beyond the imagination of anyone in a very short time. His unexpected death in 323 BCE resulted in resolution of his kingdom into several kingdoms among his successors with years of invasions of each other's territories (Antigonid Macedonia, Ptolemaic Egypt, Seleucid Asia, as well as Attalid Pergamum, Mauryan India, the Anatolian kingdoms) (Kosmin 2014).

For over four decades, from 323 to 281 BCE, the successors of Alexander the Great, known as Diadochoi, engaged in battles across the empire (Horden et al. 2014). Asia Minor was under the control of Antigonos Monophthalmos in 321 BCE. He was considered as the most dominant of the Diadochoi. However, his ambition to conquer all of Macedonia led to his opponents forming an alliance against him. Eventually, Antigonos was defeated by the coalition in the Battle of Ipsus in 301 BCE. Afterwards, nearly all of Asia Minor, up to the Taurus Mountains, came under the rule of the Thracian ruler Lysimachos. However, after Lysimachos was killed in the Battle of Koroupedion in 281 BCE, the region was taken over by Seleucus I (Grabowski 2019). By 281 BCE, the Seleucid Empire had gained control over a vast territory that stretched from Bactria in the east to Asia Minor in the west (Figure 1-9). Syria and Mesopotamia, however, remained the epicenters of Seleucid power throughout the dynasty's long history.

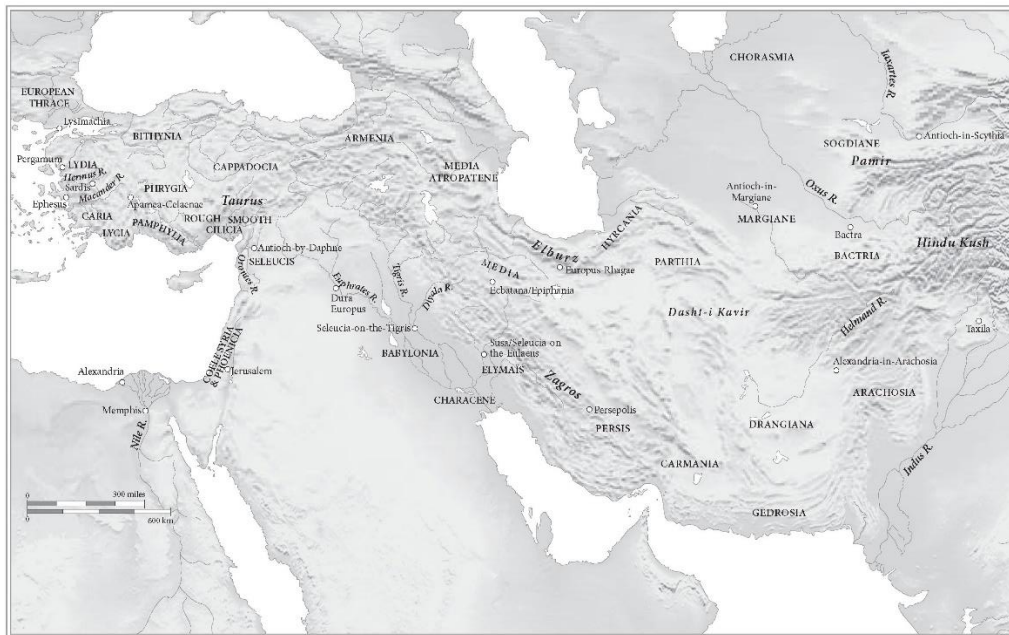


Figure 1-9 The extension of Seleucids in 281 BC (from Kosmin (2014))

Asia Minor, although situated remote, was not a peripheral area. Instead, it held a significant place in Seleucid politics. All Seleucid kings from Seleucus I to Antiochus III put in great effort and vast resources to control the western Asia Minor and the majority of the large and prosperous Hellenistic cities along the coast. For the dynasty with Macedonian origin and Hellenistic culture, the significance of this peninsula was not just the economic resources it provided, but also its importance as a transit region that directly linked the Seleucid Empire with the Aegean Sea (Schuler 2019b).

The Seleucid Empire was composed of a diverse collection of peoples and communities and had a complex structure. Its rulers struggled to strengthen their control and maintain stability, as internal conflicts and wars with outside forces constantly posed a challenge. In Asia Minor, there were independent kingdoms, smaller dynasties, and Hellenistic city-states of varying levels of power. The Seleucids faced opposition from the Attalid and Ptolemaic dynasties, among other issues in Asia Minor. Eventually, the Roman army invaded and defeated the

Seleucids in the Battle of Magnesia (190/189 BCE), signaling the end of Seleucid domination in the western Asia. Despite its challenges, the Seleucid rule in the western Asia lasted approximately a century.

Alexander the Great greatly expanded the reach of Hellenic culture by establishing, refounding, or renaming numerous cities. His successors, particularly the Seleucids, continued this practice. The Seleucid kings established many colonies in Lydia, the central region of their rule in Asia Minor, and surrounding areas (Schuler 2019b). These colonies were strategically placed along major roads (Kosmin 2014, Schuler 2019b) and while some were established as polis from the outset, many were initially rural communities (*katoikiai*). However, over time, during the Late Hellenistic and Roman Imperial periods, many of these rural communities grew into polis. In the region under study, the settlements founded, refounded, or renamed by the Seleucids included Hypaipa (refounded?), Tralleis (renamed and refounded), Nysa (newly founded?), and Thyateira (renamed) (Hill 2016). Kosmin (2014) also lists Antioch on the Maeander, Apamea Celaenae, and Laodicea on the Lycus as refoundation.

### **1.5.2. Hellenistic Settlements**

The Hellenistic period major settlements were called as *polis*. The term “*polis*” (plural: *poleis*) is commonly translated as “*city-state*” since a polis is only one city, but also politically, juristically, economically a self-governing state. Hansen (2006) identifies thirty-seven city-state culture around the world. There were many city-state clusters in antiquity in the Near East, Asia Minor, Greece and Italy: the Sumerian, Babylonian, Assyrian, Anatolian, Syrian, Phoenician, Neo-Hittite, Palestinian, Philistine, Lykian, Greek and Etruscan city-states. Greece and Asia Minor was the center of Greek city-states in Archaic period (c. 750 - 500 BCE). At that time, there may be local city-states in Asia Minor, but the whole region was Hellenized after the conquest of Persian Empire by Alexander the Great (Hansen 2006).

The poleis were comprised of relatively small citizen communities that shared a common language, religion, and social values. Despite their small size, these

communities engaged in a complex network of interactions and communications with one another, recognizing each other as equals (Hansen 2006, Schuler 2019a). They entered into agreements with both close neighbors and more distant partners. However, it is important to note that while these poleis may have been considered independent, this was limited to internal sovereignty, as they were frequently subject to the authority of larger regional powers. In spite of this challenging political reality, the Hellenistic period was not characterized by decline, but rather by resistance and prosperity among the poleis (Schuler 2019a).

The term "*polis*" can refer specifically to the urban center of a city-state, or to the city-state as a whole. The surrounding countryside of polis was called as *chora*. The polis was more of a focal point for civic life and governance, while chora was a vital component of the polis, providing food and resources for the city. The polis and chora were intimately connected, with each playing a crucial role in the success and survival of the city-state. The polis was also the center of political institutions, religious ceremonies, defense, production and trade, and education and entertainment. The monumental remains of civic structures from the period like agora, acropolis, temples, stoa, theaters, gymnasiums, baths, and city walls served as evidence of a settlement being a polis.

Self-sufficiency was crucial for any polis to prosper economically. However, achieving economic independence was challenging and complex. The role of chora in promoting economic self-reliance, was noticeable, as it was closely linked to land use, agriculture, and trade (Koparal 2011). Yet, self-sufficiency did not mean that a polis could survive in isolation. Instead, each polis had to establish networks and engage in trade with other poleis or communities to achieve autarchy, both economically and politically. The economic power of poleis varied significantly, with some relying more on trade and market economies, while others had a more agricultural and household-based economy. In addition to self-sufficiency, there were also alliances between poleis, including *synoikism*, where settlements combine to form a city, and *sympolity*, where two cities share a political system but not

necessarily unite physically (Difabio 2022). Although these alliances were not unique to the Hellenistic period, they were strongly concentrated in literary and epigraphic records of the Hellenistic period.

Difabio (2022) argues that while synoikisms were attempted in Asia Minor, they were often temporary or incomplete, and sympolities were not common in the region. One example of synoikism in the western Türkiye is the attempted unification of Lebedos and Teos, with Antigonos I seeking to bring the less significant city of Lebedos under the umbrella of the more important Teos. Some speculate that an earthquake in 304 BCE spurred the plan, while others suggest that Antigonos I simply wanted to establish a larger city. However, Lysimachos' takeover of the city in 302 BCE and the death of Antigonos I prevented the plan from being realized. In 288 BCE, Teos, Kolophon, and Lebedos attempted to relocate to Ephesus and form a larger city under the name of Lysimachos' wife, Arsinoe, but were unsuccessful too.

A sympolity in the western Türkiye suggested by Difabio (2022) was between Aphrodisias and its neighbor Plarasa dating back to the 2nd century BCE. The earliest evidence of this was an oath between the joint demos of Plarasa and Aphrodisias, as well as the demos of Kibyra in Kabalia and the demos of Tabenia, promising to protect one another and not act against each other or Rome. Later evidence of shared civic coinage bearing the names of the two communities dated to the late 1st century BCE supports this idea. The growth of Aphrodisias led to settlement movement that supported the city's expansion, while Plarasa remained inhabited. Ultimately, Aphrodisias became the main center of the area.

In conclusion, poleis underwent significant changes and developments during the Hellenistic period. One of the most notable characteristics of this time was the increase in urbanization, with many cities becoming more densely populated. These settlements were often diverse and cosmopolitan, reflecting the spread of Hellenic culture throughout the Mediterranean and Near East. Rulers sought to consolidate their power and control through a greater degree of centralization and bureaucracy. The economic growth of Hellenistic period poleis was driven by increased trade and commerce. Overall, the

Hellenistic period was a time of significant change and evolution for poleis, with many new and diverse cultural, intellectual, and social developments taking shape. This dynamic political, military, and economic conditions of the region during the Hellenistic period resulted in a distinct settlement pattern. In a rare regional study of the Hellenistic period in this area, Hill (2016) observed that urbanization was universal and homogeneous.

### **1.6. Aim of the study**

As described above, the archaeological predictive modelling studies have various problems that are debated for long period. Current study aims: producing a predictive map that displays the likelihood of discovering archaeological site at a location for a selected period and region; and contributing to the solutions of the problems of APMs. The problems focused in this thesis are:

- Quality of archaeological data
- Use of relevant variables
- Incorporation of socio-cultural variables
- Polygonal representation of archaeological settlements
- Use of out-of-box statistical methods
- Statistical method not requiring non-site data
- Testing/Evaluation of the model

Towards these aims, production of such a map will be illustrated over the case of “The urban centers (*polies*) of Hellenistic period western Türkiye”. The possible contribution of the resulting predictive map to the archaeological research will be explored with some examples. These studies can be extended by further studies.

## CHAPTER 2

### MODEL DEVELOPMENT

There are many criticisms for the usage of predictive modelling in locating archaeological sites. On the other hand, these criticisms also show the potential for improvement in the method. This thesis aims to concentrate on some of these problems and develops solutions. The subjects focused on are as follows:

- Use of archaeological data set depicting the meaningful picture of the period
- Determination of site selection criteria
- Representation of archaeological sites (point vs. polygon)
- Use of out-of-box statistical approaches
- Evaluation of the model output

In this thesis, we will develop a model for the Hellenistic period settlements of the western Türkiye and flowchart of the model framework is provided in Figure 2-1.

There are five major steps:

- 1- Database Creation:** Collection and review of archaeological data
- 2- Variable Selection:** Exploration of possible variables as site selection criteria
- 3- Data Characterization:** Statistical approach development and analysis to characterize the data for each selected variable
- 4- Method Assessment:** Exploration of prediction ability and reproducibility of the results generated from the selected variables
- 5- Model Evaluation:** Creation of predictive map and its performance assessment

This chapter gives the theoretical framework of model building steps and model evaluation steps. Application of these steps is given in the next chapter. The primary approach utilized is based on the identification of site location characteristics of known archaeological settlements within the study region, employing an inductive approach while making informed choices of variables based on the site type and period under investigation. Five steps given above are displayed in the model flowchart shown in Figure 2-1.

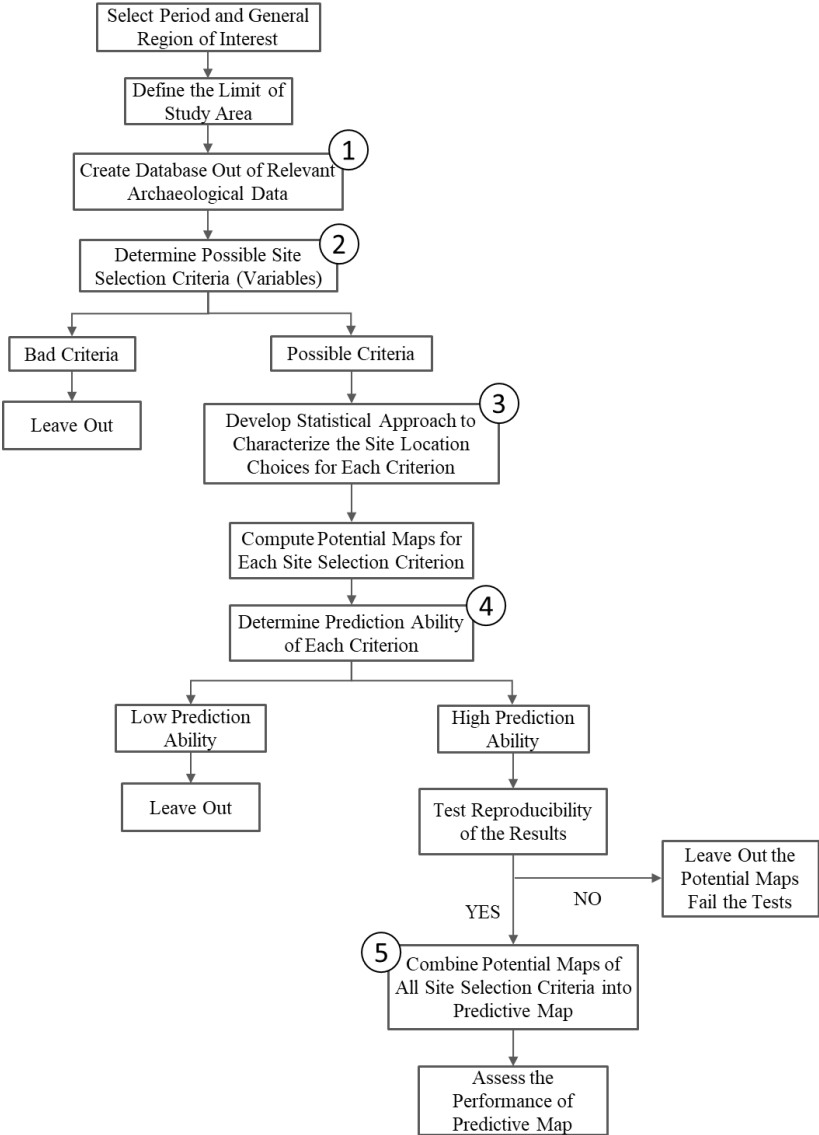


Figure 2-1 Flowchart of our archaeological predictive model

## **2.1. Archaeological Settlement: Spatial Phenomenon**

Archaeological settlement is a spatial phenomenon. An archaeological site either is located in an area due to some features of that site which motivate the people to live there or due to the interactions with its surrounding landscape or other archaeological sites in a larger area.

Raster data type is commonly used for the spatial analysis. Raster data is formed of pixels and each pixel has a value indicating an attribute of that location (e.g. elevation, slope, land status etc.). Location of an archaeological site can be represented as one pixel (point data) or a collection of pixels (polygonal data) (Figure 2-2). In this study, both cases are used depending on the site selection motivation criteria and the statistical approach developed.

The polygonal representation of archaeological site is used where the immediate surrounding of the archaeological site is the interest as in the topography. Without any hesitation, point data is expected to shade off the potentially diverse characteristics of topography that the site lies on. The point data usage for archaeological sites is one of the majorly criticized topics in the archaeological predictive modelling, especially when the environmental data is used (van Leusen 2002, Mink et al. 2005, Carleton et al. 2012). Despite the critics, point data is commonly used in the archaeological predictive models (Stančič et al. 2000, Vaughn and Crawford 2009), most probably since the use of this type of data is less labor intensive and relatively easy for basic statistical analysis. However, there are studies trying to include the size effect of archaeological site to their models. The authors of one recent study suggest a new model, which they call in short as LAMAP (locally-adaptive model for archaeological potential) (Carleton et al. 2012). They use a radius of 1 km around each known-site as a sample area for each variable in their model. They compare the density values of all known-sites to the density of the study area for the variables. For local adaptation, a distance decay function is used to give more

weight to each location of interest based on the nearby known sites' landscape characteristics.

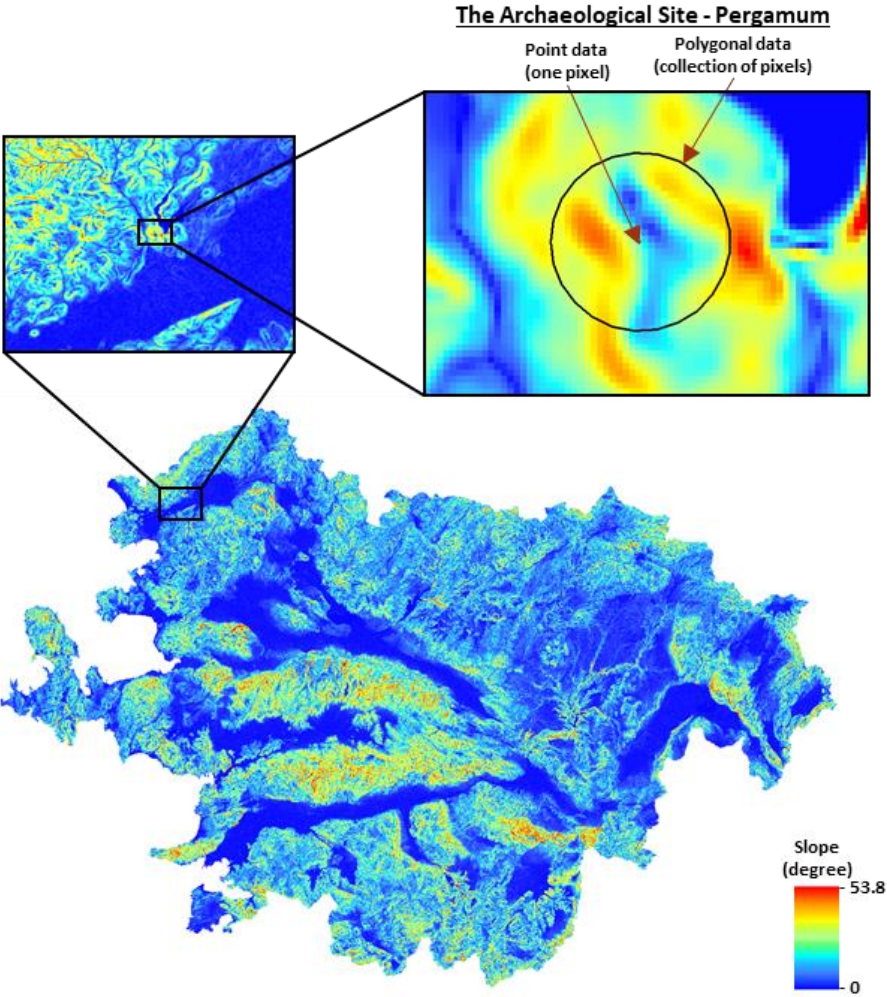


Figure 2-2 Raster data representing slope values for the study area as an example. Pixels forming the raster data can be seen as zoomed in a certain area. The color ramp shows the slope values stored as an attribute for each pixel. The location of archaeological site, Pergamum, is also shown as a point data and polygonal data.

Polygonal data clearly provides more information about the area under investigation. More information allows making use of elaborate statistical analysis, hence, better characterization of the site. Figure 2-3 shows how diversified can be polygonal data from settlement to settlement. Gradient of land (i.e. slope) is used as an example variable for a better understanding of the effect. It should be noted that, for polygonal data, an areal extent is required to define the archaeological site. This topic is discussed for the case evaluated in this study in Chapter 3.

The point representation of archaeological sites is also used in this study. Voronoi tessellation (Thiessen polygons) is employed to examine the relationship between archaeological sites and roads. Thiessen polygons enable the evaluation of potentially connected archaeological sites, as opposed to just relying on the distance between the sites and other features.

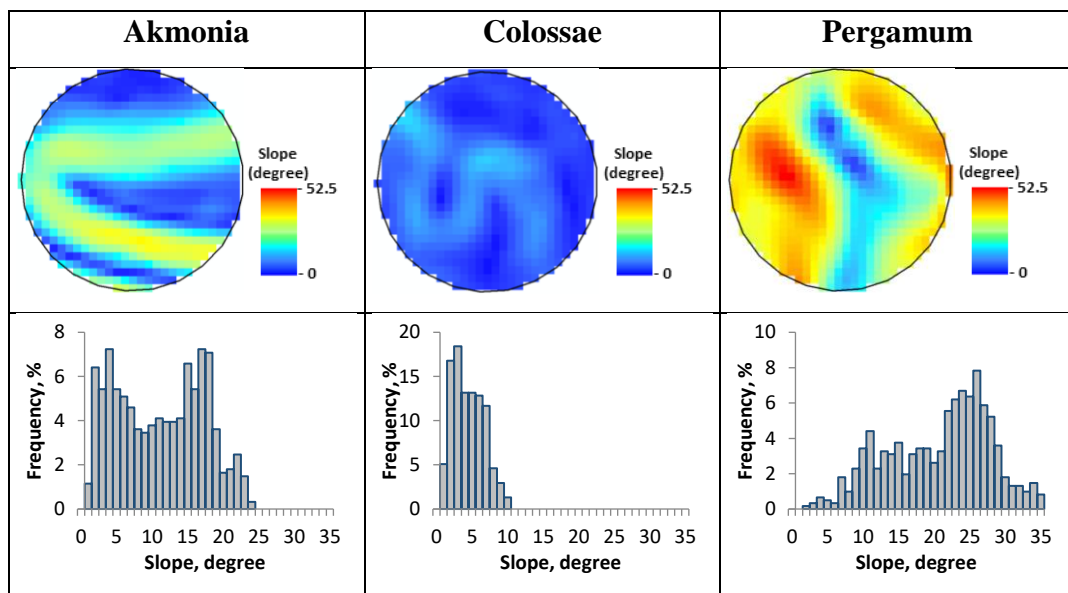


Figure 2-3 Examples of slope raster data and their histograms showing the variations in polygonal data (circle with a radius of 300 m) which belong to different archaeological sites.

## 2.2. Characterization of Archaeological Sites

The archaeological settlements are the primary input data to acquire the site selection preferences. Their presentation affects how well the preferences are reflected in the model.

### 2.2.1. Archaeological Sites as Polygonal Area

Converting polygonal data of a variable to a value representing the archaeological site requires particular statistical concentration. In this study, the polygonal area is used when the topographic variables (i.e. elevation, slope, ruggedness and aspect) and arable land density are investigated as the site selection criteria. However, the approach can be used for any type of variable that is considered better to be analyzed for a polygonal area. Flowchart of the statistical analysis developed to achieve sites' characteristics is given in Figure 2-4.

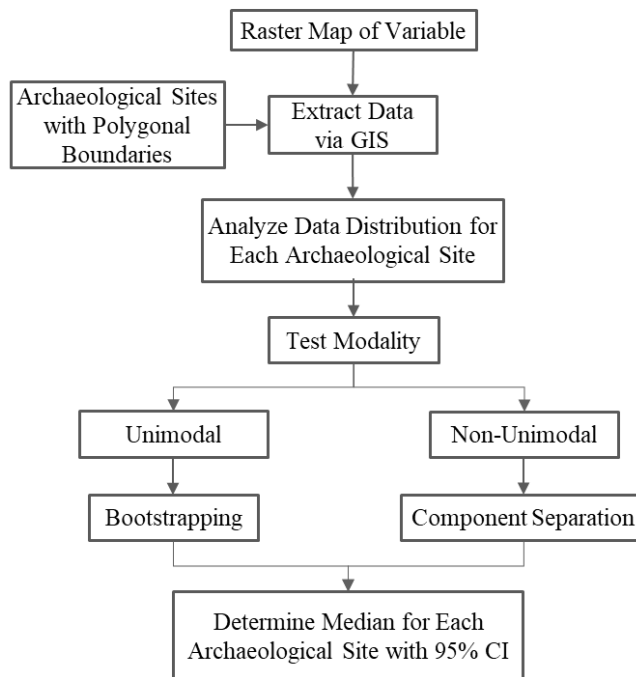


Figure 2-4 Statistical steps to derive the sites' characteristics for a variable while assessing the archaeological site as an area.

The raster of variable in examination is clipped out for the polygon defined for each archaeological site. The values of each pixel in these polygons are exported from GIS environment to data sheets. Afterwards, their histograms are produced for each settlement and some statistical analyses are conducted.

Statistical tools used are: *histogram, mean, mode, median, modality test, dispersion, and confidence interval*. These tools and how they were used are reviewed below for readers' convenience.

**Histograms:** Histograms are one of the common ways of data visualization and show the frequencies of data such that the visualized distribution let us to observe which values more commonly occur in the data set, how widely or narrowly spread the values are, whether the data is skewed and/or have multiple modes. Even if the individual distributions for a variable are illustrated for each archaeological site, the challenging part is to cope with various types of distributions when all archaeological sites in the data set is evaluated and determining the statistical parameters that will represent the distributions.

**Mean, Mode, Median:** In this study, since the values appearing more often in the data set are expected to indicate the site preference for the settlement, mode, mean and median (i.e. measures of central tendency) of the data are given special attention (Figure 2-5). Distribution with one mode is called as unimodal, with two modes called as bimodal and more than two modes called as multimodal. *Hartigan's Dip Test for Unimodality* is used to determine whether the distribution is significantly non-unimodal, in other words, bi- or multimodal. Test measures the difference between empirical distribution and the best fitting unimodal distribution (Hartigan J. A. 1985). Package "*dip test*" in R<sup>2</sup> is used for the unimodality assessment (Maechler 2016). It is considered that each mode observed in the histograms should contribute to the decision of settlement location.

---

<sup>2</sup> R is a programming language and open-source software environment for statistical computing and graphics.

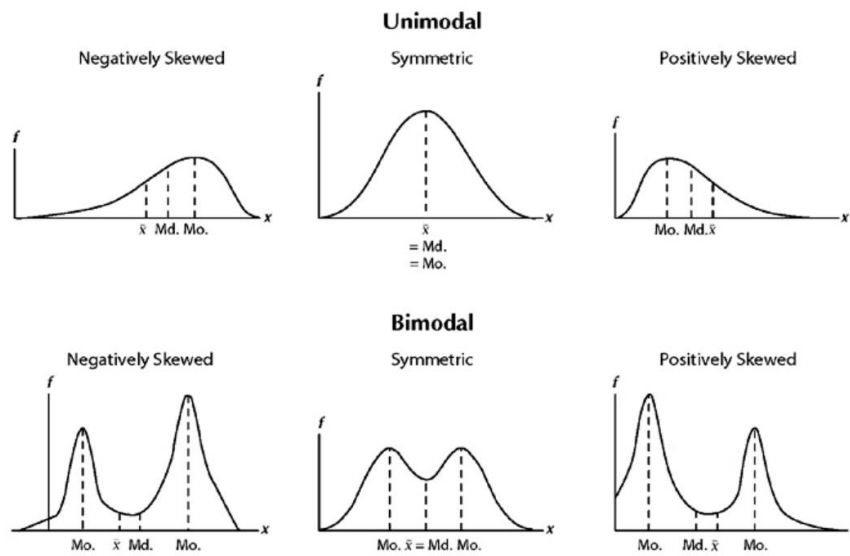


Figure 2-5 Basic graphical representation of central tendency measures for unimodal and bimodal distributions (Sirkin 2011).  $\bar{x}$ : Mean, Md: Median, Mo: Mode.

Mean and median are among the most commonly used values indicating the center of a distribution. When a distribution is normal (symmetrical) and unimodal, its mean and median values are identical and shows the typical value in the data. Instead, if the distribution is skewed, mean is affected by extreme values in the data and is dragged away from the typical value while median is not affected by extreme values (Ho 2017). Therefore, median is used while moving forward to the next step of the statistical analysis.

**Dispersion:** Dispersion, which describes how closely or widely distributed the values are in a data set, is another important property of a distribution that should be considered. Figure 2-6 shows two distributions having same median, but exhibiting different variability. This results in different ranges of plausible values for the estimated statistics from observed data like median. The estimation range, which is called as confidence interval, is determined based on the probability of containing the true value of the investigated statistical parameter. The most commonly used confidence intervals are 95% and 99%. In this study, 95% is selected as the

confidence interval for median to be used at the further steps of the statistical analysis. When a distribution is significantly dispersed then the median estimated with 95% confidence interval should have a larger range compared to a distribution having less variability.

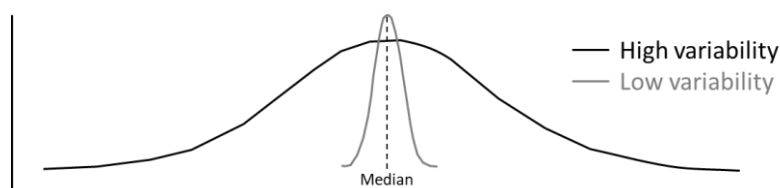


Figure 2-6 Graphical representation of high and low variability (Ho 2017)

**Determination of Median:** The final step involves estimating median values for archaeological sites, which often have non-parametric distributions that do not follow a specific distribution for the evaluated variable. This presents a challenge in determining a typical or representative value. (e.g. Figure 2-3). The median values of unimodal distributions are calculated using *Bootstrapping* method. With this method, it is possible to estimate the median without prior knowledge of the population distribution type. The technique involves making inferences about the sample data population, assuming that the data can be modeled by resampling itself (Efron and Tibshirani 1993, Mooney and Duval 1993). This technique allows assigning measures of accuracy like confidence interval. Combination of “*replicate*” and “*sample*” functions in R is used for the application of Bootstrapping method (Clapham 2020).

When there are multiple modes in the distribution, they are separated into components using the “*mixtools*” package in R (Benaglia et al. 2009). Each component is assumed to follow a normal distribution, and the median values for each component along with a 95% confidence interval are calculated. As the mean and median of a normal

distribution are equal, the confidence interval for each component is computed as follows:

$$\text{Confidence interval} = \bar{x} \pm Z \frac{s}{\sqrt{n}}$$

$\bar{x}$  = sample mean (equals median too since the distribution is normal)

Z = standard z score for the confidence level (here is 1.96 for 95%)

s = standard deviation

n = sample size

As an example, Figure 2.7 shows the decomposed normal distributions of slope values for the Akmonia archeological settlement.

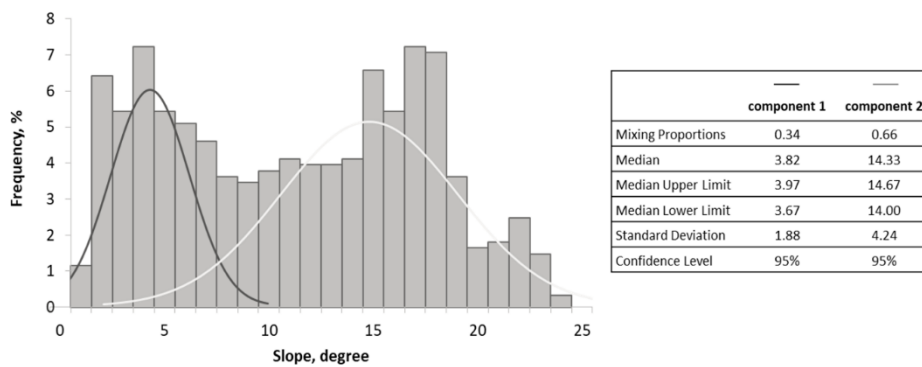


Figure 2-7 Decompositioning of a multimodal distribution. Example shows the slope distribution of the archaeological site Akmonia.

After following these steps for each archaeological site and evaluating the variable as a potential site selection criterion, a set of median values with varying frequencies will be obtained. These frequencies can indicate the potential for the existence of sites with those values in the entire study area.

**Analysis of Circular Data:** Among the topographical variables, aspect differs from the others due to its data type. Aspect is the direction of slope faces and measured in

degrees clockwise from north. Such data is called circular data and requires special statistical methods. Although aspect is a continuous data, most of the predictive modelling studies often treat it as a categorical variable (i.e. N, NE, E, SE, S, SW, W, and NW).

In this study, a parallel methodology to the other variables represented as a polygonal area (elevation, slope, ruggedness and arable land density) is developed for aspect, but employing circular data statistics (Figure 2-8). Why use of circular data statistics is important shown via an example displaying two data points with the directions of  $330^\circ$  and  $30^\circ$  and mean of them (Figure 2-9). For the example, arithmetic mean would result in  $180^\circ$  instead of  $0^\circ$ , although the latter value clearly makes more sense.

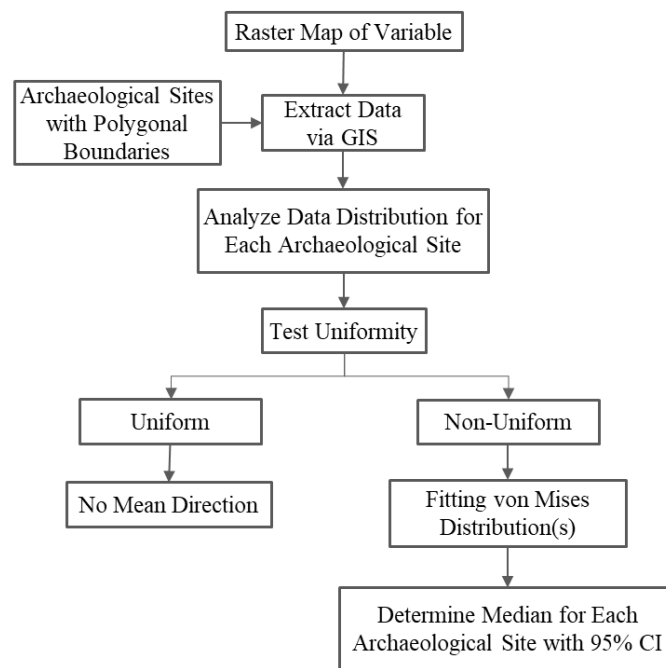


Figure 2-8 Flowchart for statistical analysis of aspect

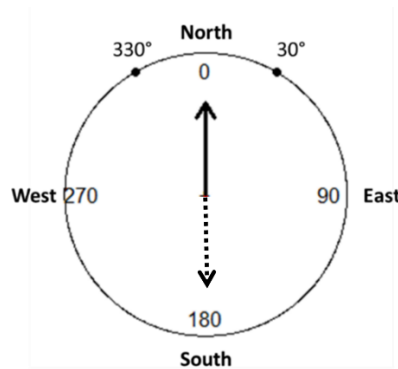


Figure 2-9 An example showing circular mean (solid line) and the arithmetic mean (dashed line) from (Kalaylıoğlu 2020)

For the statistical analysis, first the aspect values clipped out from the polygonal area of each archaeological site. Later, each of them is explored for their frequencies, spread and type of distribution. The aspect data of archaeological sites Akmonia, Myrina and Teos are shown to better visualize circular data (Figure 2-10). As seen in Figure 2-8, the foremost step should be testing the distribution's uniformity, in other words, checking whether there is any significant directionality in the distribution. There are several uniformity tests having different methodologies, namely Rao's spacing test, Kuiper's test and Watson's test. Package "circular" is used in R for the uniformity assessment (Lund et al. 2017). Only one site out of 51, namely Myrina, has shown no significant directionality. Other sites' distributions have either one peak (unimodal) or more peaks (multimodal). From the linear data distributions with multiple modes, it will be recalled that the distributions were separated into components (i.e. sub-distributions of a heterogeneous population), where each component has a normal distribution. In circular statistics, von Mises distribution takes the role of normal distribution.

Probability density function (f) of mixture of N number of distribution is given by:

$$\begin{aligned}
 f(x; \theta_1, \theta_2, \theta_3, \dots, \theta_N) \\
 &= p_1 \times f_1(x; \theta_1) + p_2 \times f_2(x; \theta_2) + \dots + (1 - p_1 - p_2 - \dots \\
 &\quad - p_{(N-1)}) \times f_N(x; \theta_N)
 \end{aligned}$$

where  $f_1, f_2, \dots$  and  $f_N$  are the probability density functions of von Mises distributions, with parameters of  $\theta_1=(\mu_1, \kappa_1), \theta_2=(\mu_2, \kappa_2), \dots$  and  $\theta_N=(\mu_N, \kappa_N)$  and membership probabilities of  $p_1, p_2, \dots$  and  $p_N$ .

The von Mises probability density function for the angle  $x$  is given by:

$$f(x/\mu, \kappa) = \frac{e^{\kappa \cos(x/\mu)}}{2\pi I_0(\kappa)}$$

where  $I_0(\kappa)$  is the modified Bessel function of order 0.

The parameters  $\mu$  and  $1/\kappa$  are analogous to  $\mu$  and  $\sigma^2$  (mean and variance) in the normal distribution. In circular data,  $\mu$  is the mean direction of sample angles and the parameter  $\kappa$  is the concentration parameter indicating how concentrated the data around the mean. The greater the value of  $\kappa$  is the higher the concentration of the distribution around the mean direction.

Package ‘‘BAMBI’’ is used in R for fitting the aspect values of known archaeological site’s distributions to the mixture of von Mises distributions (Chakraborty and Wong 2017). The fitted density estimations of Akmonia and Teos are shown in Figure 2-10 as examples. The mean values of each component with 95% confidence interval are calculated for each archaeological settlement.

As in linear data, when all of these steps are followed for each archaeological site for aspect, a set of median values will be obtained having different frequencies, which should indicate the potential of site existence on those values in the whole study area.

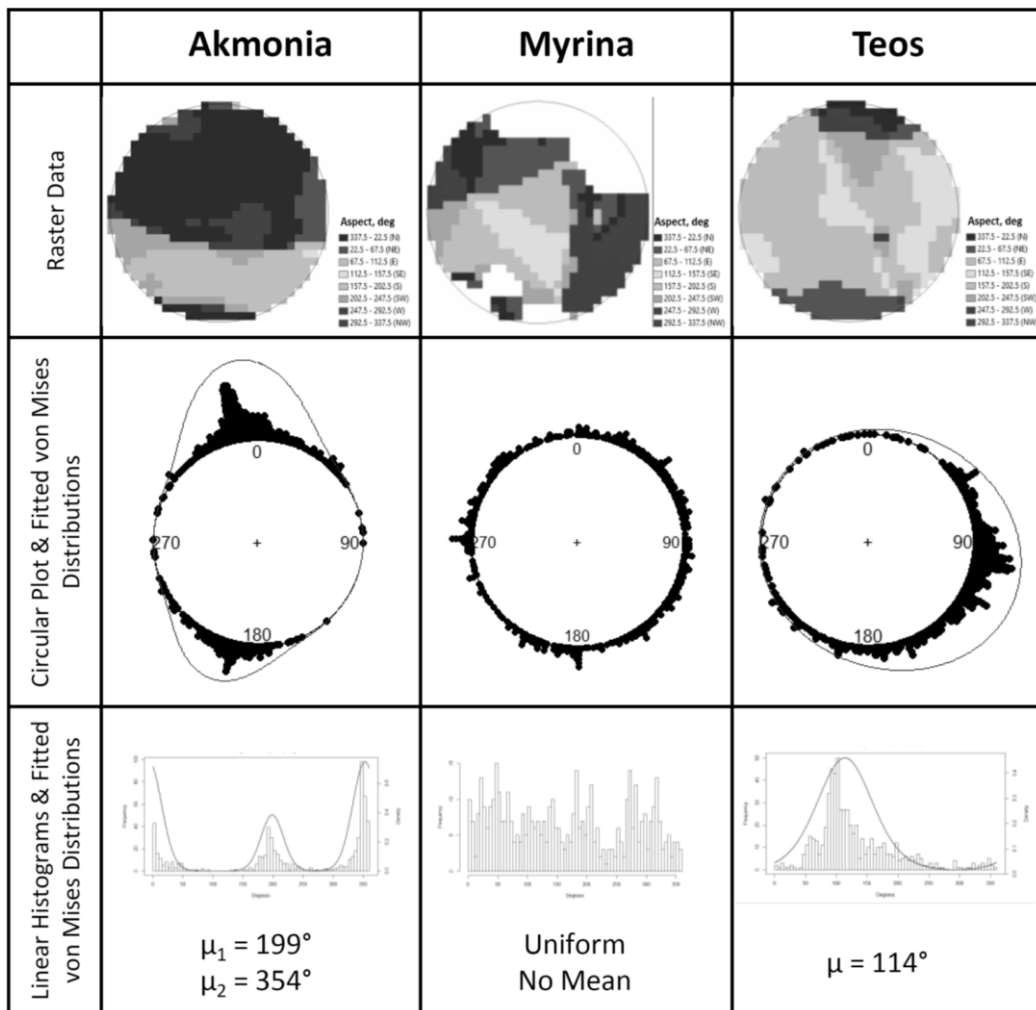


Figure 2-10 Example aspect data of the archaeological sites Akmonia, Myrina and Teos together with their circular plots and linear histograms overlaid with fitted von Mises distributions (gray line).

### 2.2.2. Archaeological Sites as Network

The extent of territory of an archaeological site, its neighbours and relationship among them and its surrounding are import to understand the period of interest on a regional scale. In order to define possible “territories” of a site in archaeology, a spatial partition method called as Voronoi diagram is commonly used (Wheatley and

Gillings 2002). With this method, a surface is divided into regions using geometric properties of a point distribution and the method has a very wide application area.

The Voronoi diagrams help to examine the point patterns (here archaeological sites) in a region. The study of point patterns are expected to provide explanatory insight about the process responsible for creating it (Okabe et al. 2000). The model of John Bintliff can be given as an example in archaeology, which explains the development of prehistoric and historic settlement by defining territory size through time with Voronoi polygons based on the twenty years of fieldwork data in Boeotia, Greece (Bintliff 2000).

A Voronoi diagram can be created by drawing perpendicular line between the midpoints of each two sites and intersecting these perpendicular lines to define the polygon around every site (Figure 2-11). The same Voronoi diagram can also be created by drawing circles around each point with an increasing radius. As the radius of circles is expanded, the neighbouring circles touches to each other and starts squishing each other forming a line which defines the boundary between the two nearest neighbouring sites (Figure 2-12). The region defined for each point is called as Voronoi cells or Voronoi polygons, also known as Thiessen polygons. The latter method provides better visualization of how the territory of an archaeological site and Voronoi cells area related.

In this study, Voronoi polygons are used when road network variable is investigated for its possible contribution in locating the archaeological settlements. The road network variable includes the travel time between the archaeological settlements (see Section 3.7). The Voronoi polygons are used as an indicative of possible neighbours of a settlement. The travel-time extracted for the settlement and its neighbours are simply collected as the characteristic travel-time (Figure 2-13)

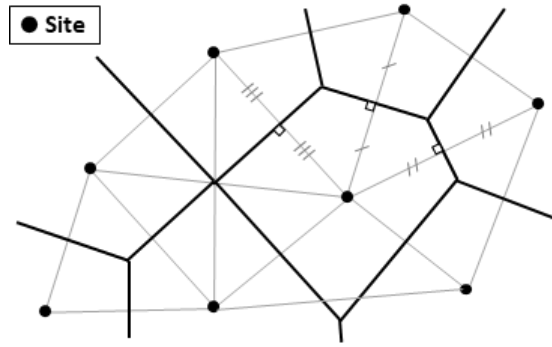


Figure 2-11 Voronoi tessellation creation of a set of site points using midpoints between two sites

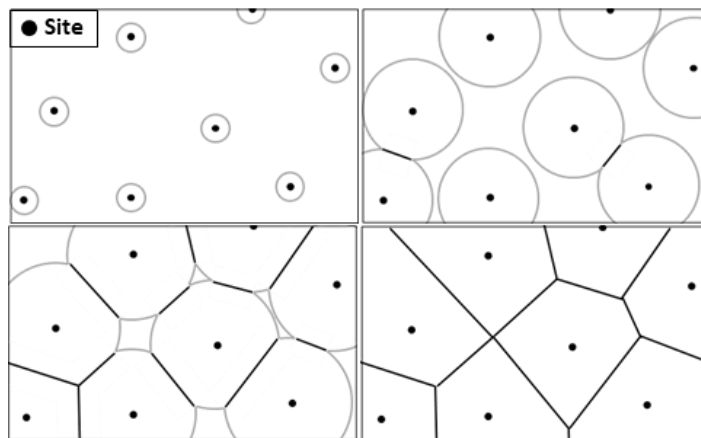


Figure 2-12 Voronoi tessellation creation of a set of site points using expanding circles around each site. The radius of circle expands from top left to right bottom.

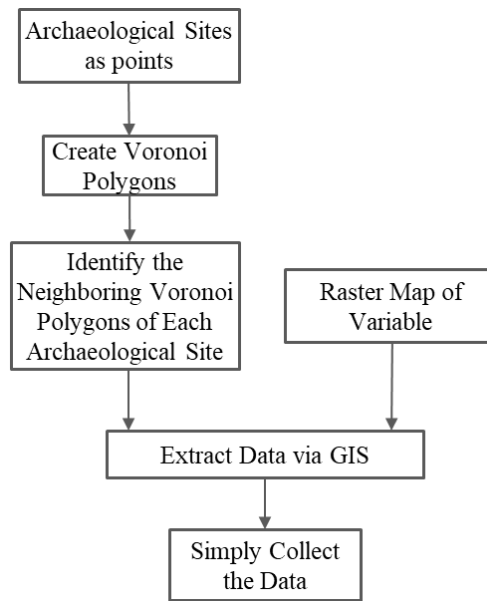


Figure 2-13 Steps to characterize the road network variable when assessing the archaeological site as point and related with its neighbours

### 2.2.3. Computation of Potential Maps

In previous section, the method to collect the values characterizing the archaeological sites are given. Even though all the values are observed ones, they have different frequencies indicating that the potential of site existence chance differs from location to location. Steps followed to compute the potential map for a variable is given in Figure 2-14.

**Distribution of Data Characterizing the Archaeological Site Locations:** In order to classify the archaeological site existence potential, first the histogram of each variable is obtained. However, this was not straightforward when the archaeological sites represented as polygon, since the median of each archaeological site with 95% CI is actually an interval as a result of their changing dispersion and modality. For example, Priene's median slope is between 18.8 and 20.1 with 95% confidence. This range is displayed with many closely valued points as in Figure 2-15 for the archaeological sites. The histogram of medians of archaeological sites in the dataset

is built bringing these points together (Figure 2-16). In the figures, the archaeological data of Gr80/20-Set2 (for detail of naming see Section 2.3.1) is used from the case study to show the steps for the computation of potential map as an example. The slope around 5 degrees and between 15-20 degrees seem to be occurring more often compared to the other values in Figure 2-15, which is in compliance with the histogram in Figure 2-16.

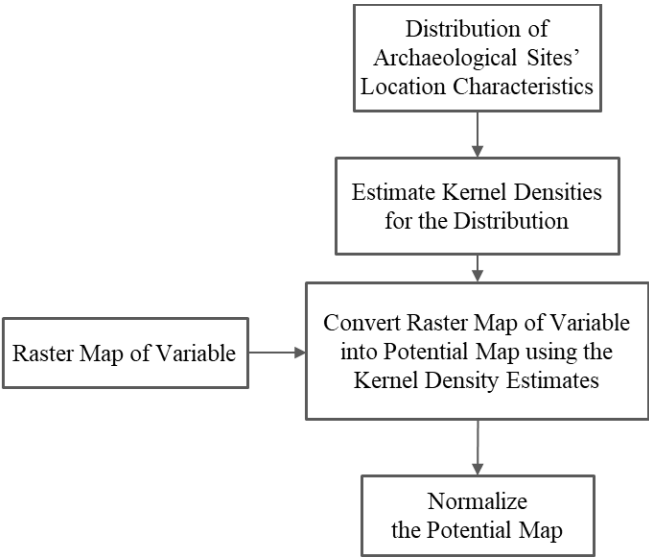


Figure 2-14 Flowchart to compute potential map for a variable



Figure 2-15 Median slope values of archaeological sites with 95% CI for Gr80/20-Set2

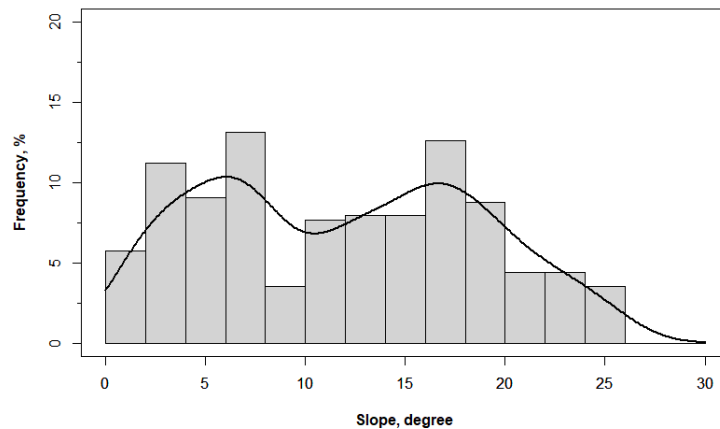


Figure 2-16 Kernel density estimation curve overlaid the histogram of median slope distribution of archaeological sites available in the dataset of Gr80/20-Set2.

**Kernel Density Estimation of Distribution:** The probability density curve for the distribution of each variable is obtained using *kernel density estimation (KDE)* in R software (Figure 2-16). KDE is calculated by weighting the distances of all the data points (Conlen 2018). The kernel density estimate is higher at a value if there are more data points nearby. Higher kernel density estimates indicate a higher probability of occurrence of corresponding values in the dataset.

**Conversion from Raster Map to Potential Map:** The resulting kernel density values are divided into small bins and the average values are assigned to the corresponding range of the variable, allowing for continuous potential value assignment across the study area (Table 2-1).

**Normalization of the Potential Map:** Finally, the density values are normalized to a range between 0 and 1 to improve interpretability.

An example calculation for the transformation of KDE values to slope potential values is provided in Table 2-1. The resulting map presents a continuous assessment of the site potential based on the evaluated variable (see Figure 2.17), with higher values indicating higher potential areas compared to lower values.

Table 2-1 Example transformation of KDE values of slope to the final potential map having values between 0 and 1 for Gr80/20-Set2.

Slope Value, degree	KDE Value	Bin Size in Slope, degree	Range of Slope Value, degree	Average of KDE Value in the Range	Normalized Value btw 0 - 1
0.0000	0.01648				
0.0587	0.01701	0.0587	0 - 0.06	0.01675	0.321
0.1174	0.01755	0.0587	0.06 - 0.12	0.01729	0.332
0.1761	0.01810	0.0587	0.12 - 0.18	0.01783	0.342
0.2348	0.01865	0.0587	0.18 - 0.23	0.01838	0.353
cont.					
cont.					

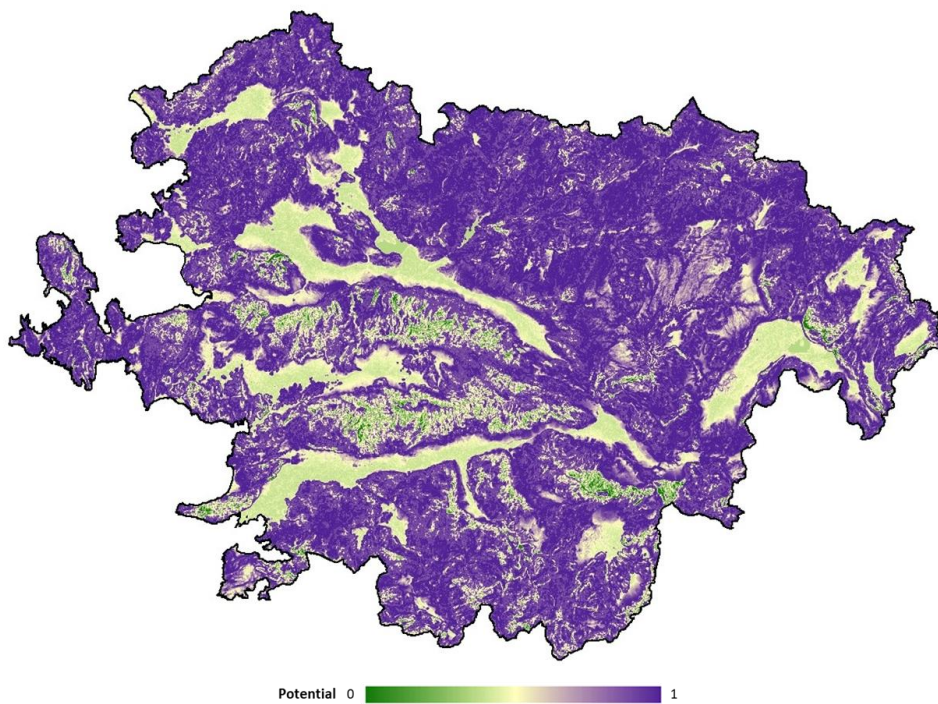


Figure 2-17 Slope potential map of Gr80/20-Set2

### 2.3. From Potential Maps into Predictive Map

In this study, the outcome maps of statistical methodology described until this section were called as *potential maps*. After the data analysis regarding each variable a

potential map was created. The potential maps out of several variables are unified into a *predictive map*.

Towards the predictive map, two issues were concerned:

1. Reproducibility of the results
2. Performance of the potential maps

Figure 2-18 provides the flowchart for the determination of potential maps to be used in the predictive map. The steps are detailed in the following subsections.

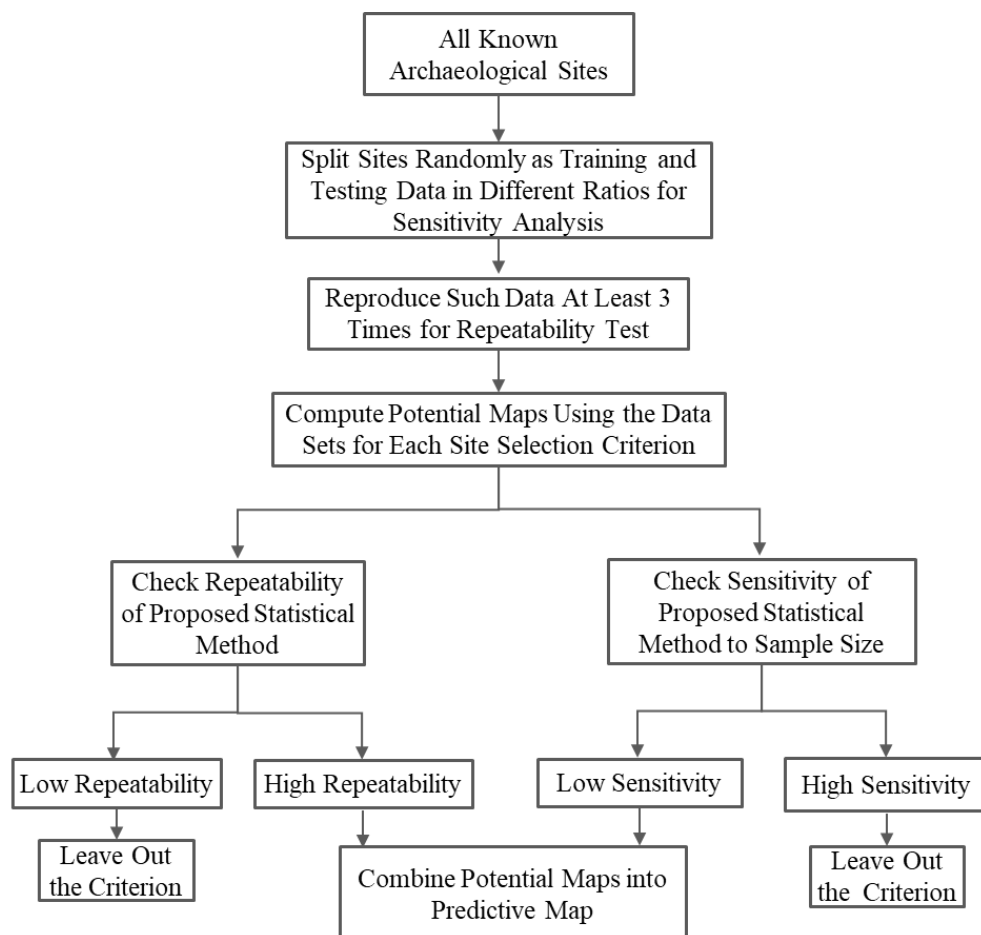


Figure 2-18 Steps for the determination of potential maps of which variables will be used in the predictive map.

**2.3.1. Reproducibility of Results with the Proposed Statistical Method**

The performance of proposed statistical method is investigated by evaluating its repeatability and its sensitivity to the sample size. We will first describe repeatability and sensitivity in our context.

**Repeatability:** Repeatability tests how successfully the proposed methodology gives similar results with a different dataset. Actually, this test can also provide insight about how comparable the archaeological sites in the dataset are. The correlation between the potential maps are computed using the Band Collection Statistics tool in ArcGIS<sup>3</sup>. The correlation coefficient can take values between +1 and -1, indicating the strength and direction of the relationship between two variables. When there is a positive correlation, an increase in one variable corresponds to an increase in the other variable. Conversely, a negative correlation suggests that as one variable increases, the other variable decreases. A correlation of zero implies that there is no association between the two variables, and they are independent of each other. Higher correlation is expected between the three data sets, when the proposed statistical method produces similar results. Table 2-2 shows the correlation matrices for the resulting potential maps for Gr80/20 as an example.

Table 2-2 The correlation matrices between the slope potential maps having 80% of the known archaeological data for the training.

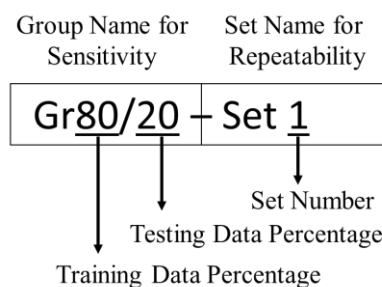
Groups	Sets	Gr80/20		
		Set1	Set2	Set3
Gr80/20	Set1	1	0.95	0.98
	Set2	0.95	1	0.95
	Set3	0.98	0.95	1

---

<sup>3</sup> ArcGIS is a commercial, geographic information system software developed and maintained by Esri.

**Sensitivity analysis:** Sensitivity analysis tests how the statistical method responds to the different number of sample input. The studies from earth sciences frequently utilize sensitivity analysis because this analysis can help to understand where an uncertainty was introduced to the model (Burg et al. 2016). The major approach employed in this study is data-driven and it is important to observe the effect of training and testing data counts during the model development. In order to observe the effect of sample size, the performance of each potential map is compared among the datasets. Performance is a function of percentage of successfully located archaeological sites and the percentage surface area of where they were located in the study area (see Section 1.1.5).

When potential map of any variable is calculated, three sets of data is created by selecting randomly having same number of samples for the examined variable for repeatability analysis. For sensitivity to the sample size, the input data (i.e. training data) having 90%, 80%, 70%, 60% and 50% of the all known archaeological sites are included to the statistical analysis. The remaining known archaeological sites from the each ratio are used for testing the potential maps and the predictive map. At the end, 15 potential maps (i.e. 3 sets from repeatability x 5 groups from sensitivity) are evaluated for any examined variable to assess the applicability of the method and the effect of sample input number. Figure 2-19 shows the resulting potential maps for the slope variable as an example. Names of each potential map is given according to the following structure:



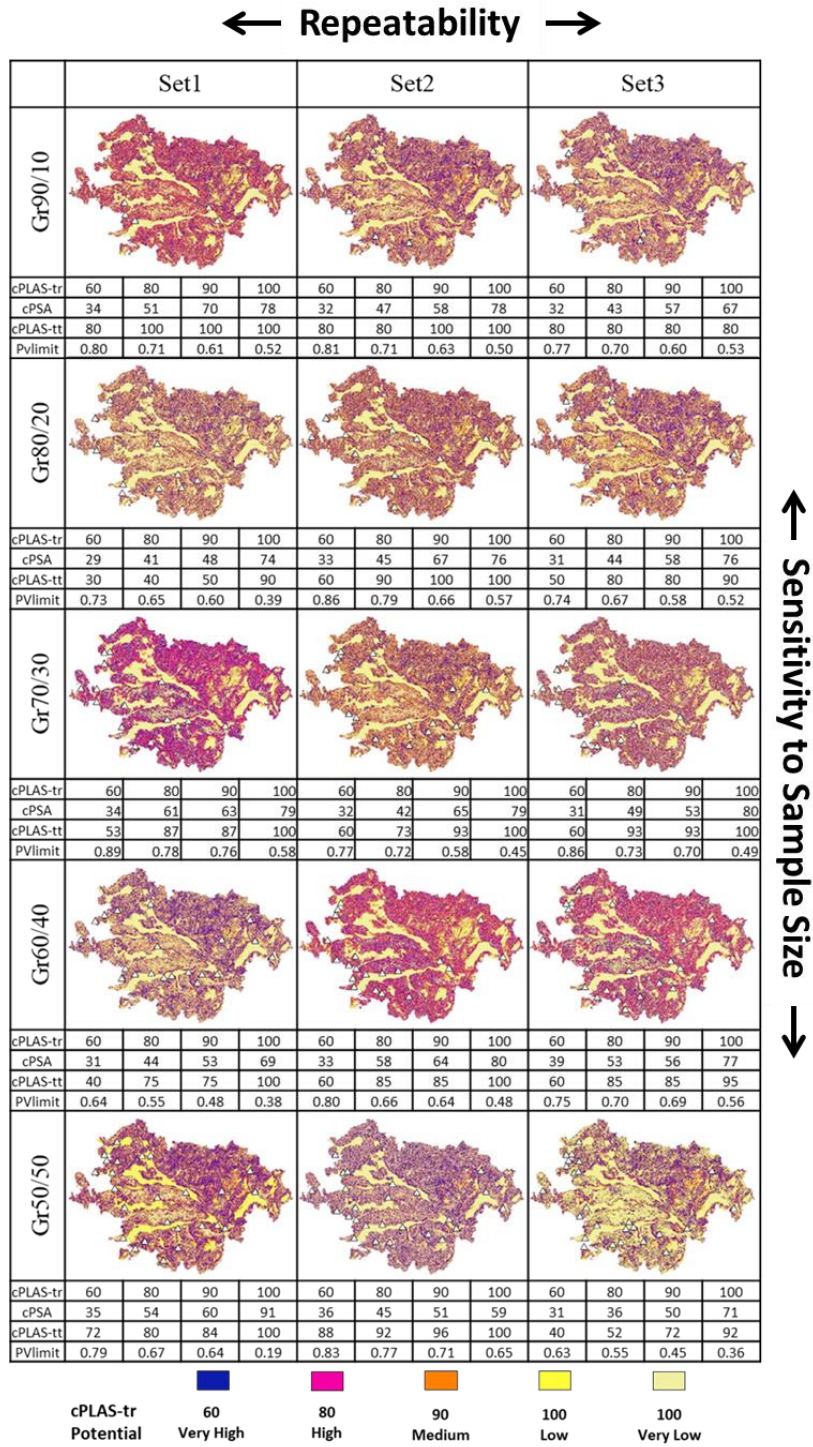


Figure 2-19 Example potential map outputs. Each column shows training data with same sample size, but having different archaeological settlements for the repeatability analysis. Each row shows training and testing data ratios used in the statistical analysis out of the known archaeological dataset for the sensitivity to sample size analysis.

What would be expected at the performance of the model with changing training and testing data is tried to be illustrated in Figure 2-20. The performance of training data and testing data are compared to each other. When the training data is too few, then its representativeness for the settlement locations could be low. Therefore, high variation is expected at the performance of output model as the sample size of training data fed to the model decreases. When the testing data is too few, then their respond to the model could not be seen properly. The model might have good results, but due to the variation at the performance of testing data, its evaluation would not be possible. When the testing data is not few, it seems hard to know what to expect for the performance of testing data because of the high variation in the produced potential maps. These variations are expected to stabilize around at certain training and testing data ratio indicating that the investigated variable can be used at the predictive map production and that the output model can be assessed properly for its performance.

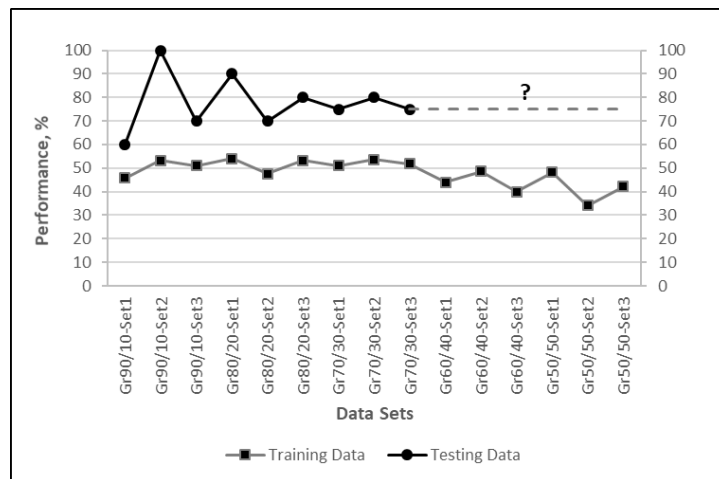


Figure 2-20 Sketch of the expected model performance responses with the changing sample sizes for training and testing

### 2.3.2. Performance Assessment

In APMs, the model performance is typically evaluated for the predictive map. However, in this study, we also assessed the performance of each variable's potential map.

First, a cutting value (PVlimit) that classifies the study area as having high potential should be determined. We calculated this value at which 80% of the training data (PLAS-tr) observed within that high potential area. Figure 2-21 provides an example to clarify the cutting value. In this case, the cutting value of 0.79 (PVlimit) was calculated from the potential map, indicating that areas with values higher than 0.79 are more likely to contain archaeological sites. This value is determined such that if we control for training data performance in this area, we would find 80% of the training data (PLAS-tr) in this high-potential area. Afterwards, we can look for the performance of testing data in this area. The analysis shows that 90% of the testing data (PLAS-tt) is in this high-potential area, which accounts for 45% of the entire study area (PSA). The cutting value for any percentage of the training data can be calculated if further exploration is desired. Additionally, Kvamme's gain value can be easily calculated using these values. The long version of abbreviations used in the paragraph are as follows:

**PVlimit:** The value of potential map defining the boundary at which 80% of the training data (PLAS-tr) is observed

**PLAS-tr:** Percentage of archaeological sites observed within the limited study area from training dataset

**PLAS-tt:** Percentage of archaeological sites observed within the limited study area from testing dataset

**PSA:** Percentage of surface area at which 80% of the training data (PLAS-tr) is observed

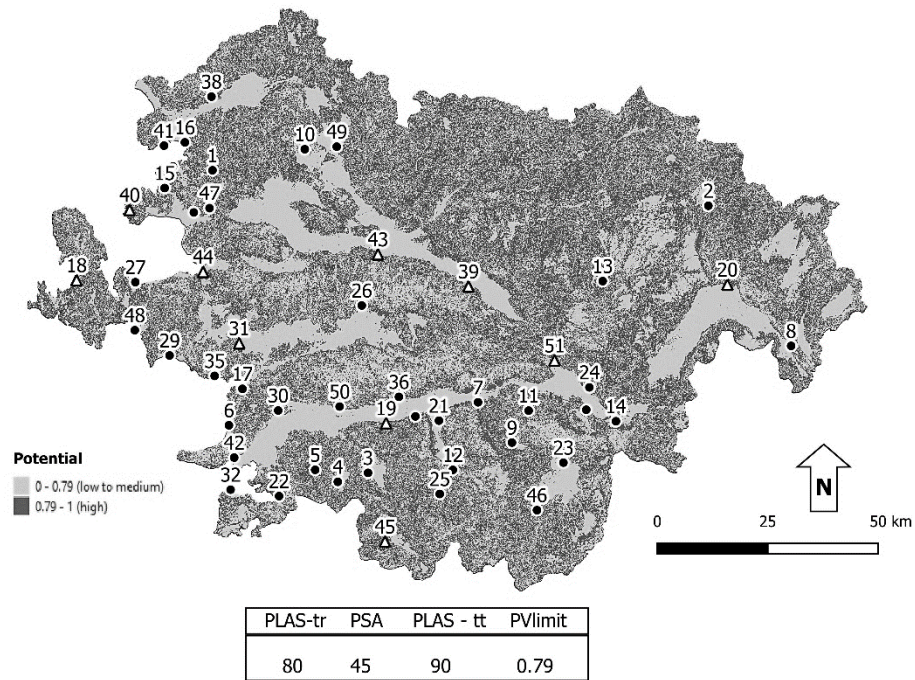


Figure 2-21 Boundary determined based on the cutting value at which 80% of the training data (PLAS-tr) observed within that high potential area (training data in black dots, testing data in black triangles).

In cases where an archaeological settlement is represented as a point, its potential value can be easily obtained by collecting the pixel value from the corresponding location in the potential raster map of the variable being investigated. However, in this study, there are variables of which the archaeological settlements are represented as polygons meaning that an archaeological settlement has a range of potential values inside the polygon. In order to determine whether an archaeological site is successfully located on a potential map, the highest 30% of potential values within the polygon are compared with the PVlimit values. For example, as shown in Figure 2-21, at least 30% of the potential values within the buffer zone of each testing data should be higher than the PVlimit value of 0.79 to be considered successfully located in the potential map. The successfully located archaeological settlements can be ranked in descending order based on the potential values within the 30% area of the

polygon. The higher the potential values filling 30% of the polygonal area, the higher the ranking of the archaeological settlement.

#### **2.4. Combining the Potential Maps**

After the evaluation of potential maps as in the flowchart in Figure 2-18, which variable can be used in the predictive map is determined. The variables that give repeatable results are included in the predictive map. The appropriate sample size that can be used for each variable are identified based on the response of model. If the sample size is not sufficient for any variable, this variable is excluded. The selected variables are added together to produce the final predictive map. Each potential map has potential values between 0 and 1, providing a relative probability for site preference.

It is expected that the controlled progress of the model starting from the variables level should have significant contribution in improvement of the quality of final model and in understanding of the influence of each variable (or interpretation of outcomes) into the final model.

#### **2.5. Evaluation of the Predictive Map**

The word of “evaluation” is used instead of the terms of “validation” and “testing” of the predictive map to broaden the sense of performance analysis of the output model.

The ideal way of evaluating an APM is to conduct a field survey to test the model. While this may be feasible for predictive models produced by government resources, it is often challenging to find such resources for studies like this thesis. Therefore, this study employs a commonly practiced method, which is to use the data itself for testing the model. The data is divided into training and testing sets. The training set is used as input for statistical analysis, while the testing set is used to assess the performance of the APM (i.e. Kvamme’s gain value).

To prospect for archaeological sites using the predictive map, we will employ two methods:

- **Comparison with ancient texts:** The study area contains archaeological sites mentioned in historical texts. Although some of these sites have approximate locations described in the texts, their exact locations are unknown. We will compare the high-potential zones identified in the predictive map with these sites to see if they match.
- **Desktop research:** The predictive map may also suggest high-potential areas where sites could exist. In these cases, we will conduct desktop research to find supporting evidence for the possible existence of sites in these areas.



## CHAPTER 3

### CASE STUDY:

#### HELLENISTIC SETTLEMENTS OF WESTERN TÜRKİYE

Türkiye has a rich and dynamic settlement history dating back to approximately 10,000 BCE. The country is home to numerous renowned archaeological sites such as Çatalhöyük, Troy, Ephesus, Hattuşa, Zeugma, and Göbekli Tepe, which showcase the diverse civilizations that have thrived in the region throughout history.

In this study, the Hellenistic *poleis* (i.e. urban centers) located in the western Türkiye has been selected for the archaeological predictive modelling because:

- They are distinguishable by their common civic structures and are numerous in the area.
- There are still undiscovered settlements from this period that are mentioned in ancient texts.
- Previous studies have mainly focused on the *polis* level, making it possible to make a significant contribution to the regional studies.

The aim of this study is to develop a predictive map displaying the preferred polis settlement locations for the Hellenistic period using a data-driven approach. The Hellenistic poleis were typically established on low-lying, easily defensible hilltops for security and near fertile alluvial plains for agricultural purposes. The road network also played a crucial role in ensuring mobility. Through quantifiable methods, this study hopes to support archaeologists in the explanation of the natural and socio-cultural relationships that influenced the locations of Hellenistic poleis in the region. The predictive map produced will serve as a complementary tool for archaeologists

in their desktop research alongside other resources such as ancient texts, aerial photography, and remote sensing.

At the end of the study, some potential applications will be explored for the predictive map. However, it is hoped that the findings of this study will have a broader impact on the field of archaeology.

### **3.1. Study Area Boundary**

For regional studies, the area could be either physiographic or behavioral as defined by Kowalewski (2008). The physiographic region is described by places like drainage basin, coastal plain, mountain chains etc. The behavioral region is identified by the interaction of settlements or central places forming an integrated social entity.

In this study, the physiographic region was used to delimit the study area, particularly the drainage basins of Büyük Menderes (anc. Meander), Küçük Menderes (anc. Cayster), Gediz (anc. Hermos) and Bakırçay (anc. Caicus) covering 53,590 km<sup>2</sup> of an area (Figure 3-1). The region is characterized by a horst-graben system. The topography shaped by grabens (valleys) and horsts (mountain ridges) formed due to the lowering and raising of fault blocks respectively. The rivers of Büyük Menderes, Küçük Menderes, Gediz and Bakırçay flow at the valleys separated by the mountains of Aydın, Bozdağ, Yunt and Madra.

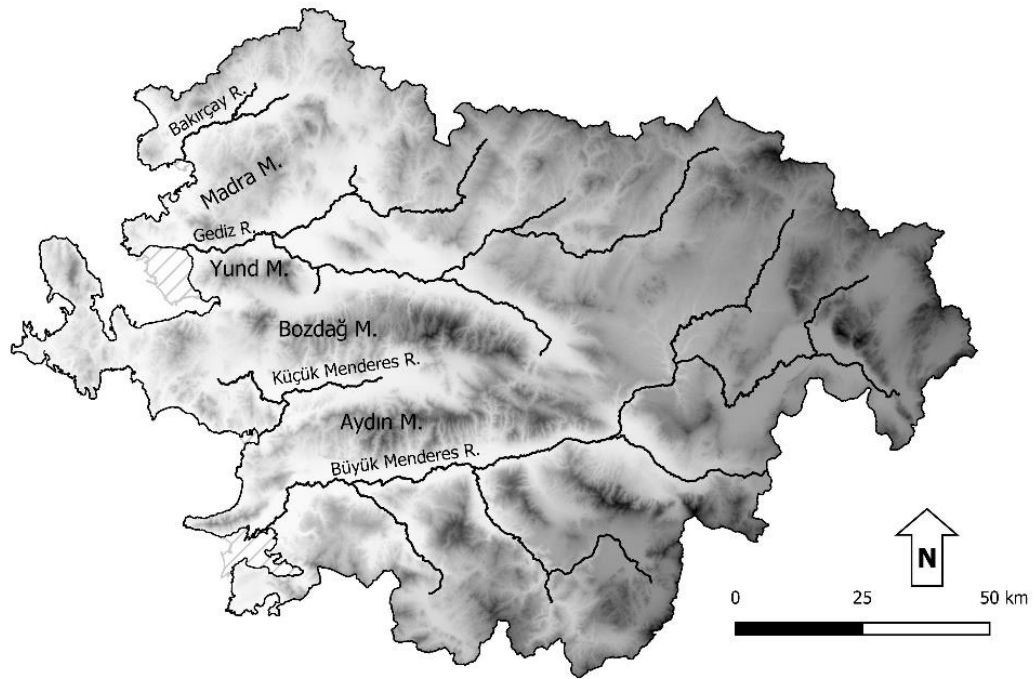


Figure 3-1 The boundary of study area. The inclined dashed areas at the coast indicates the current coastlines revised due to silting up.

### 3.1.1. Coastal Changes in the Study Area

The western coast of Türkiye has shown extensive and rapid changes at its river mouths. Kayan (1999) defines three main stages explaining the sedimentary development and geomorphological formation of the present delta plains in the Aegean coast of Türkiye (Figure 3-2):

“(1) The Early Holocene is characterized by post-glacial transgression and dependent sedimentation. (2) The Middle Holocene was the period when sea level reached the present level, and apart from small fluctuations, stopped rising. Alluviation and deltaic progradation were prevalent during this transition period from marine to terrestrial environments. (3) The Late Holocene, deltaic progradation slowed down and delta plains were covered by floodplain sediments.”

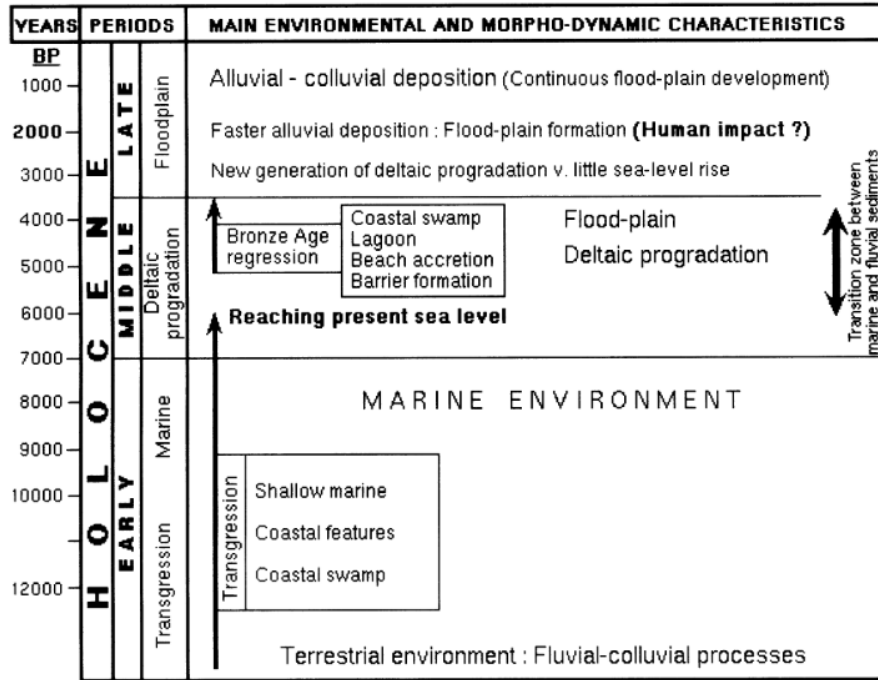


Figure 3-2 Paleogeographical evolution of the coastal plains of the western Türkiye (taken from Kayan (1999)).

The same sequence characterized by these three stages can be seen throughout the western coasts of Türkiye. The coastal changes in the Hellenistic period occurred in the last stage landlacking the major port cities like Ephesus, Miletus and Priene by the high sediment loads of the rivers.

The studies benefited for the change of coastal plains in the study area are as follows:

- Büyük Menderes (Müllenhoff et al. 2005, Knipping et al. 2008)
- Küçük Menderes (Brückner 1996, Brückner et al. 2017)
- Gediz (Yavuz Hakyemez et al. 1999, Kayan and Öner 2015)
- Bakırçay (Seeliger et al. 2013, Pint et al. 2015, Seeliger et al. 2019)

The final study area is given in Figure 3-1.

### 3.2. Archaeological Data

The major data for naming and locating the poleis (i.e. urban centers) in the Hellenistic period in the study area was collected from Pleiades<sup>4</sup>, a joint project incorporating the contents of following works:

- Richard J. A. Talbert (ed.), *Barrington Atlas of the Greek and Roman World*, Princeton, 2000.
- Michael McCormick, Guoping Huang, Kelly Gibson et al. (ed.) *Digital Atlas of Roman and Medieval Civilizations (DARMC)*, Harvard University Center for Geographic Analysis, 2007.

The inputs of which feature type is described as settlement and dated to Hellenistic period within the study area, 119 in numbers, were filtered out from the Pleiades dataset. After detailed examination of them, 51 sites out of 119 were considered as suitable for the predictive modelling analysis (Figure 3-3, Appendix A). The aspects of evaluation are given in the following subsections.

A profound evaluation of dataset provides consistent input for the model, expectedly resulting comparable settlements (i.e. settlements having similar site selection criteria). This should allow eventually comprehensive model interpretation too.

However, there are still some uncertainties in the final dataset. Even for a polis settlement, it was very difficult to confirm the dataset. In order to assess the dataset consistency, the results of each settlement will be examined separately for each variable during the model development.

---

<sup>4</sup> Pleiades is an online database for places of ancient world. Current content quality is continuously upgraded. New content is also added by individual Pleiades users. Each record in the database undergoes some level of scholarly peer review. The records include, for example, alternative names of the place, chronological information, and relevant ancient and modern citations. Last access to the site for data retrieval was April 2020.

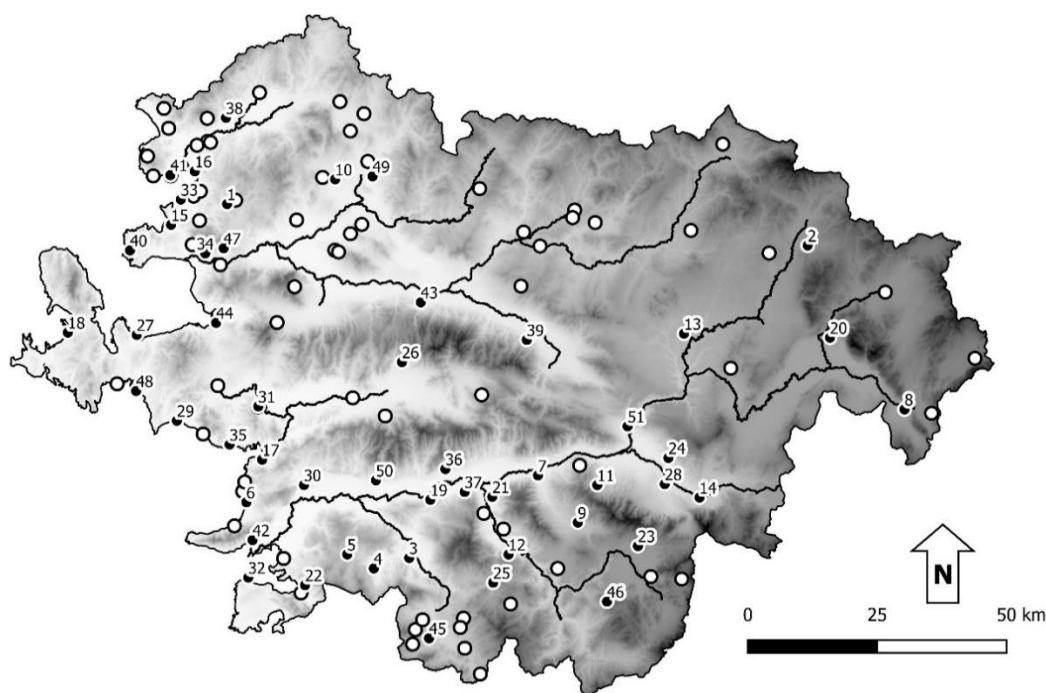


Figure 3-3 Hellenistic settlements in the study area: selected archaeological settlements (chosen as poleis) for the study (numbered, black dots) and remaining archaeological settlements (white dots).

### 3.2.1. Location and Period

The quality of dataset was improved by reviewing additional literature, inspecting the sites at another digital platform named ToposText<sup>5</sup> and checking the archaeological remains visually on the Google Earth Imageries for each site in the list of 119 settlements. The key literature reviewed for the sites' type, period and locational confirmation included:

- Individual articles for the city plan or any basic sketch of each settlement for the assessment of accurate location (Appendix A)

---

<sup>5</sup> ToposText is an indexed collection of ancient Greek texts and provides also locations of those places mentioned in the texts from the Neolithic period up through the 2nd century CE. Last access to the site for data retrieval was April 2020.

- The annual meeting reports of excavation and survey results published by the General Directorate of Cultural Assets and Museums of the Republic of Türkiye
- An Inventory of Archaic and Classical Poleis edited by Hansen and Nielsen (2004)
- The recently published book of The Geography of Urbanism in Roman Asia Minor by Willet (2020)
- Archaeology and the "Twenty Cities" of Byzantine Asia by Foss (1977)

Additionally, in order to ensure the location of a polis in the defined period, the sites having at least one public building dated to the period (e.g. a theater, an agora, a gymnasium, a stadium, and/or city walls) was included to the study. The point indicating the settlement was placed in the central part of archaeological remains, as much as possible, paying attention to the distribution of Hellenistic period remains.

### **3.2.2. Typology and Size**

The settlements are often hierarchically classified as: 1st order (town or city); 2nd order (village or hamlet); 3rd order (farmsteads and homesteads). They can be also classified functionally like economic center, administrative center, and military garrison etc. The functional characteristics can be a mixed type as well.

The source dataset has tags of major ancient settlement and ancient settlement, but for the Roman period. After the locational and periodical evaluation, 36 out of 51 selected settlements were found categorized as major ancient settlements, and 15 of them as ancient settlements. This categorization can be considered as equivalent of cities and towns indicating that their physical sizes were most likely different, but all of them hierarchically were in the 1st order settlement type.

The source data did not include any information indicative of the functional characteristics of the settlements. However, Hill (2016) describes the universality of polis in the region so that founding a polis could be considered as a package, which

can be scaled up and down, exported and reproduced in numerous locations. During this study, in which aspects the settlements were similar to each other or different from each other would be explored for a possible contribution too.

As outlined in Section 2.1, during the statistical analysis, archaeological sites will be regarded as having a distinct spatial extent if it is more appropriate to treat the investigated variable as an area. The ideal case would be to determine the true settlement boundary for each settlement in the dataset for the selected period. Unfortunately, the sources to reach such boundaries were problematic:

- The city walls enclosing the settlements were rarely fully preserved.
- The preserved city walls were usually lacking of temporal details.
- City plans with detailed temporal resolution were missing for most of the settlements.

Therefore, the literature was reviewed to identify a representative area for the extent of a polis in the Hellenistic period in the western Türkiye. The most relevant data was considered as the Copenhagen Polis Centre's inventory for Archaic and Classical Poleis (Hansen and Nielsen 2004), which was the first thorough study of poleis. Hansen (2006), later, looked into the data collected further and calculated the sizes of polis for 232 of the 1,035 poleis in the Polis Centre's Inventory (Figure 3-4). He strictly selected the cities whose walls enclosed the entire city and he found that almost all poleis had an area of more than 5 ha; the average size is 65 ha and the median size as 40 ha.

The median size of 40 ha was selected as the representative area for the archaeological sites used in the predictive modelling. This area was presented with a circle having 350 m of radius around each sites.



Figure 3-4. City size distribution of Archaic and Classical Poleis

### 3.2.3. Sample Size

The sample size, or the number of settlements used in the study, can impact the representativeness of the population being studied. A larger sample size typically provides a more accurate representation.

The ratio of sample size to the total population size was explored using the study of Hansen and Nielsen (2004) on Archaic and Classical period polis territories. They found that, in their statistical analysis of 635 communities spread across a wide geography, the poleis had territories encompassing an area of 150 km<sup>2</sup> in average. The study area covers a total of 53,590 km<sup>2</sup>. Table 3-1 shows the sample sizes used as training data and the percentage of these sample sizes to the estimated population size in this study, with satisfying the two rules of thumb often used for sample size determination as a starting point: a minimum of 30 samples (Khan 2023, Sirkin 2011) or 10% of the population size (Jeff 2017, Ben 2022). Additionally, throughout the study, sensitivity of the model to the sample size was assessed.

Table 3-1. Comparison of sample size to the estimated population size

Study Area, km <sup>2</sup>	Mean territory size of poleis, km <sup>2</sup>	Expected # of poleis in the study area	Sample sizes used as training data	The ratio of sample size to estimated population size, %
53,590	150	357	46	13
			41	11
			36	10
			31	9
			26	7

### 3.3. Model Variables

There is a general notion of that early eastern Greek settlements were lying on low hills and closely located to natural harbors and arable lands (Hill 2019). During the variable selection, the knowledge available about the Hellenistic period and the general site location preferences were considered. The arguments for each variable is given in the relevant subsection.

For the statistical analysis, the archaeological dataset separated into training and testing groups with changing percent ratios of 90/10, 80/20, 70/30, 60/40 and 50/50 respectively in order to investigate the effect of sample size in the analysis in Table 3-2. Each ratio group was also created three times selecting the archaeological sites randomly among all known archaeological sites for repeatability analysis. At the end, out of 5 groups and 3 sets, 15 datasets were analyzed for each variable.

Table 3-2 Sample sizes of training and testing groups for the selected ratios for the archaeological dataset

Groups	Number of Settlements	
	Training	Testing
<b>Gr90/10</b>	46	5
<b>Gr80/20</b>	41	10
<b>Gr70/30</b>	36	15
<b>Gr60/40</b>	31	20
<b>Gr50/50</b>	26	25

### **3.3.1. Topography**

Topography is the physical description of a land and is one of the most commonly used environmental factors in archaeological predictive modelling studies (Argyriou et al. 2017, Kalaycı 2006, Vaughn and Crawford 2009). Topography as an environmental factor has significant effect on the climate, landforms, soil types etc. in return it is expected to have influence on the site selection of humans to settle (Huggett and Cheesman 2002). Bintliff et al. (2000) based on his ca. twenty-year of intensive archaeological field survey in Boeotia in Greece, he interprets that the settlement pattern of standard network of nucleated sites are more significantly related to the territory and its limitations/opportunities compared to the conscious “sense of place”.

Elevation, ruggedness, slope and aspect are the most common attributes used for characterizing the topography of a place. In this study, these attributes were explored to define a set of criteria for the local topography on which the Hellenistic settlements were located. Digital Elevation Model (DEM) of the study area was obtained from EU-DEM elevation model provided by European Environmental Agency. The EU-DEM is a 3D raster dataset with elevations captured at 1 arc second postings (2.78E-4 degrees) or about every 30 meters. It is a hybrid product based on SRTM and ASTER GDEM data fused by a weighted averaging approach. Other variables (slope, ruggedness and aspect) are derived from DEM.

Topographical analyses were carried out on polygonal data obtained from circular area having 350 m of radius (from now on, mentioned as buffer zone) for each settlement. The results of these analyses are discussed in the following subsections.

#### **3.3.1.1. Elevation**

Elevation is one of the elements defining the terrain and has effects on the climate and existing animal and plant species in a region. It is commonly used in archaeological predictive modelling. However, in this study, due to the large size of

the study area, it was considered that relative elevation (ruggedness, later discussed in Section 3.3.1.2) of a settlement to its surrounding area seems to be a more plausible criterion in site selection. There are few studies discussing the limitations of use of elevation in the APM (Revert 2017, Malaperdas and Zacharias 2019). In this study, the variable was still investigated in order to control its possible contribution.

### **Distribution of Elevation in the Study Area**

Elevation map and histogram prepared for the study area are given in Figure 3-5. Elevation in the study area ranges from 0 to 2600 m, but the levels above 1500 m are rarely observed. The low levels occur more often towards the coastal area and at the valley bottoms. There is a second peak in the distribution around 800 m appearing usually at the eastern and south-eastern part of the study area.

### **Characteristic Elevation Values for Archaeological Sites**

First, the elevation values clipped out from the polygonal area of each archaeological site were explored for their frequencies, spread and type of distribution. The raster maps and histograms of the archaeological sites of Akmonia, Aphrodisias and Harpasa are shown as examples for a better visualization of elevation data in Figure 3-6. The change of elevation values is rather low in an archaeological site, but it is notably high between the settlements. The medians of Akmonia, Aphrodisias and Harpasa are ca. 1000 m, 500 m and 170 m respectively. After this step, the data for each site was examined for their modality. Based on their modality test results, they were processed accordingly to achieve median values with 95% confidence level considering the statistical evaluation steps in Figure 2-4. The results are summarized in Appendix B. Most of the settlements are lying on low elevation values and generally have low diversity. Using these results, histogram of elevation changes for all settlements is plotted (Figure 3-7). There is a significant clustering between 0 m and 400 m indicating a tendency towards these elevations. Similarly, some preference towards the elevation values between 400 m and 1300 m can be considered, but relatively low.

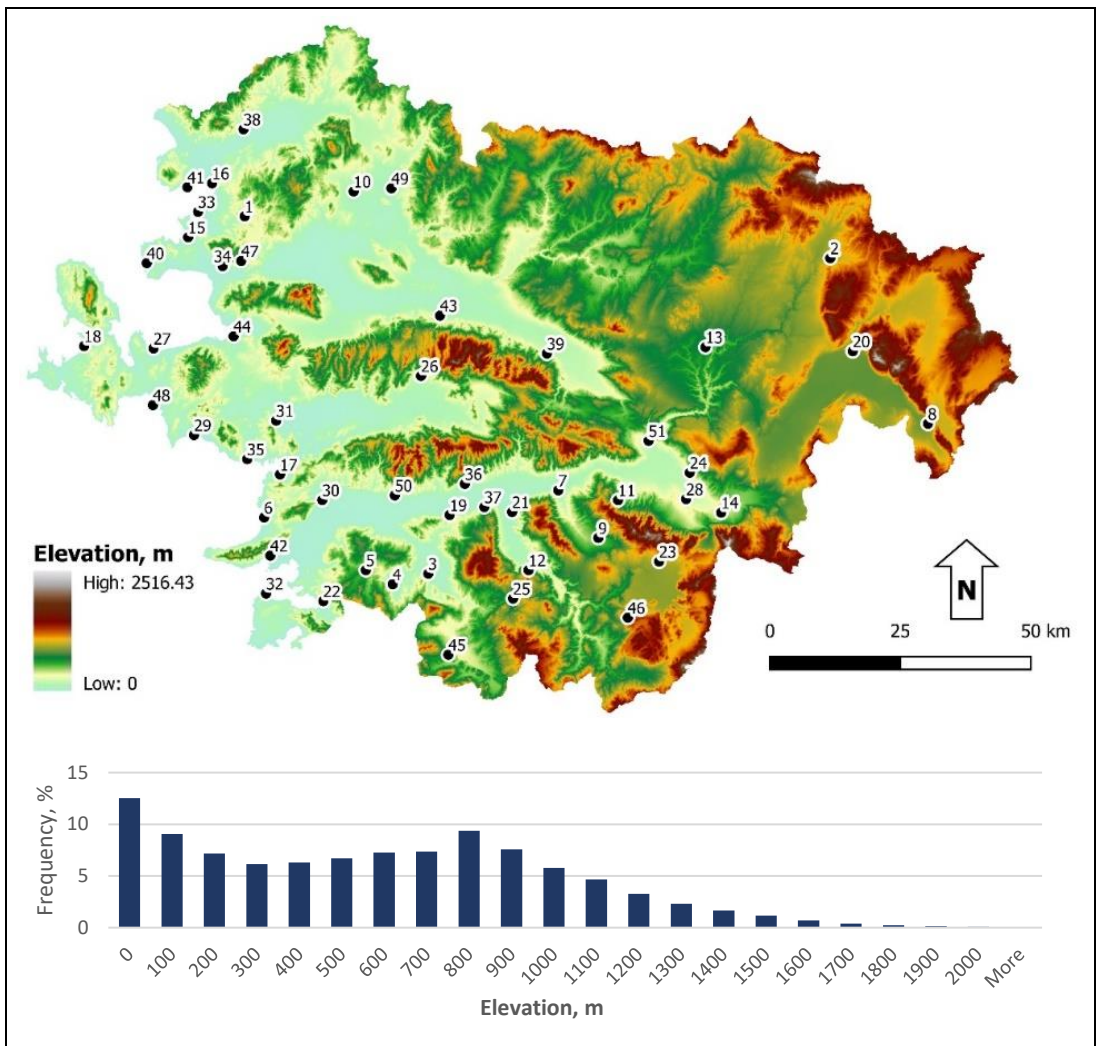


Figure 3-5. Map (above) and frequency distribution (below) of the study area for elevation

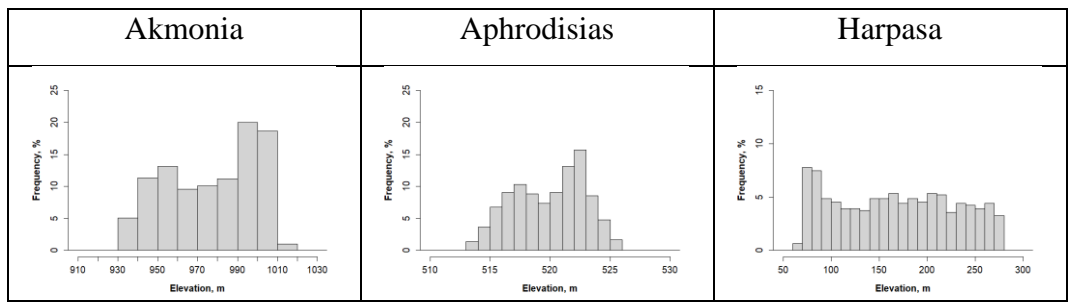


Figure 3-6 Example elevation distributions at the archaeological sites Akmonia, Aphrodisias and Harpasa

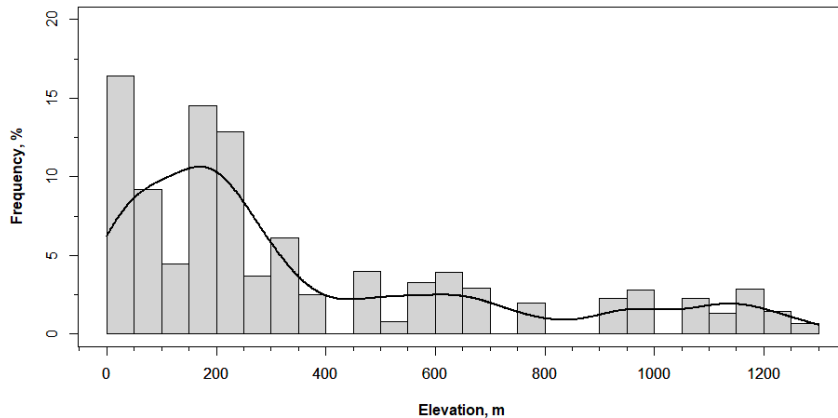


Figure 3-7. Histogram of median elevation values together with KDE curve for all the known archaeological settlements in the dataset

### Potential Map of Elevation

The histograms based on the median elevation values of archaeological sites were plotted as described in Section 2.2. for each of the 15 datasets (Figure 3-8). Later, the probability density curves for the distributions were obtained using kernel density estimation in R.

Estimated density values were transferred to the original elevation map with a very small bin size (i.e. 1.27 m) such that the data could be assumed continuous. Lastly, the density values were normalized between 0 and 1 for a better understanding. Final potential maps for each group were obtained by reclassifying the original elevation map using the normalized values for each bin interval. There are 15 elevation potential maps produced for 5 groups and 3 sets for each group. The elevation potential maps computed based on these groups and sets are shown in Figure 3-14. In general, the potential maps indicate that the coastal areas and along the valley bottoms are more likely places to locate an archaeological site for the studied period. The east and south-eastern part of the study area possess hardly any potential for settlement. However, the archaeological data already includes 13 out of 51 settlements (25%) in this area. Their presence produce relatively low KDE values around 600 m and 1100 m. It was considered that the gradual and large change in

elevation in the whole study area and therefore rather low diversity in each archaeological site are not good indicators for deriving the preferred settlement location. This problem had been mentioned as spatial autocorrelation in the paper of Kohler and Parker (1986). The authors point out that for variables like elevation or soil type whose values change more slowly with distance may exhibit severe spatial autocorrelation. They propose discarding the variable from the analysis. Same approach was applied and further processing of the variable was stopped to avoid the misleading conclusions.

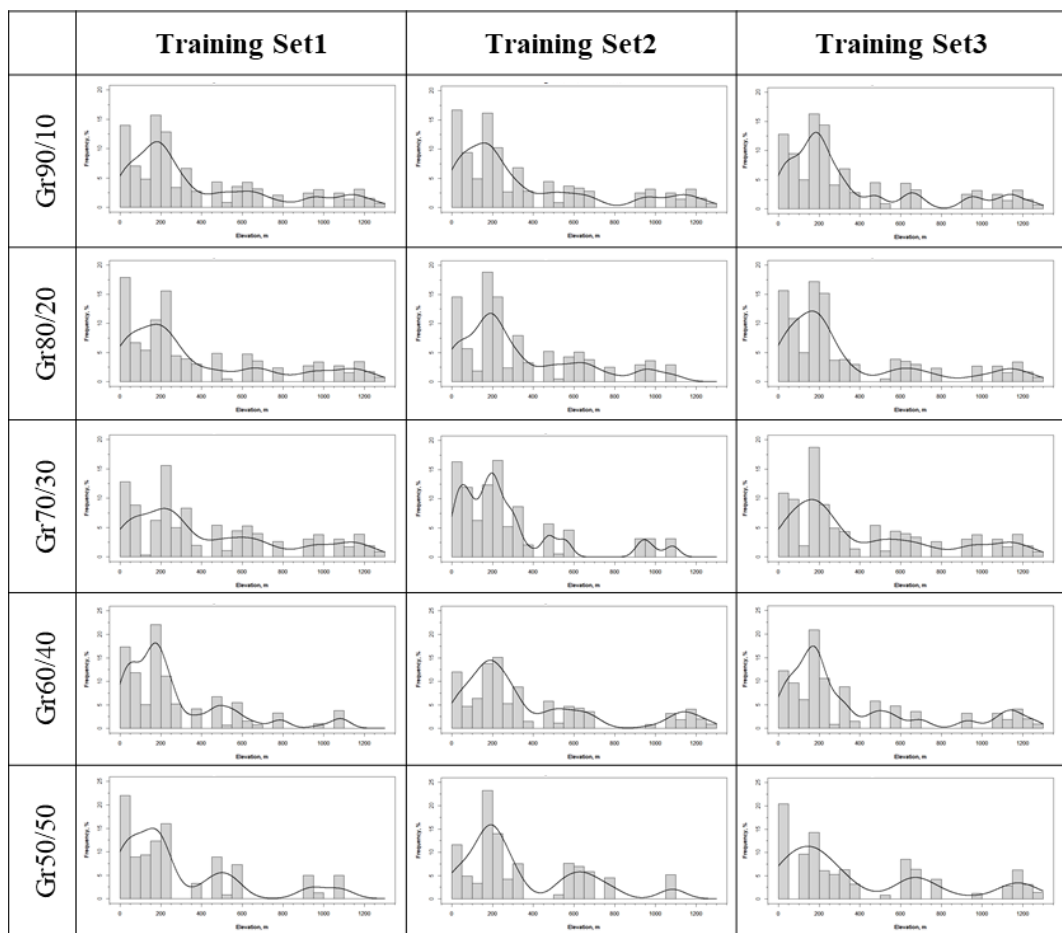


Figure 3-8. Histograms of training data sets with changing percentages and overlaid KDE curves for elevation

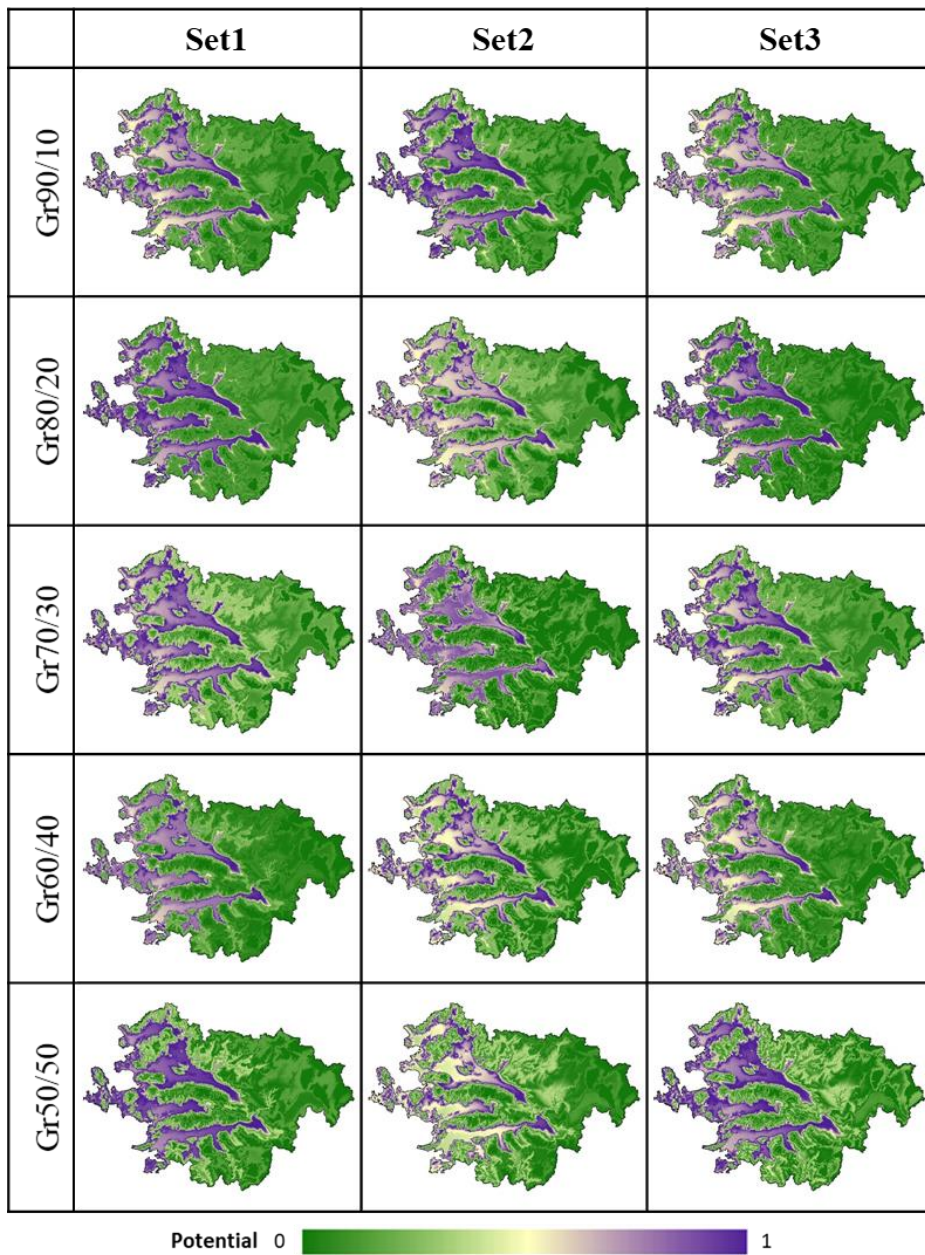


Figure 3-9 Potential maps computed for the elevation variable based on the 3 sets of 5 groups that have different training and testing data ratio

### 3.3.1.2. Ruggedness

Ruggedness expresses the topographical unevenness of a land. Riley et al. (1999) developed a measurement method to quantify this heterogeneity. Terrain ruggedness index (TRI) lets us to track the elevation changes in a predefined area in an objective way. The formula for TRI of a grid cell surrounded by immediate cells is as follows:

-1,1	0,1	1,1
-1,0	0,0	1,0
-1,-1	0,-1	1,-1

If each square represents a grid cell of digital elevation model,

$$TRI = \sqrt{\sum(x_{ij} - x_{00})^2}$$

where  $x_{ij}$  is elevation of neighbour cell to cell  $x_{00}$ .

The size of predefined area requires caution when ruggedness is examined, because it should be determined depending on the question investigated. In this study, TRI was calculated for the circular area having a radius of 350 m (i.e. map resolution of 25 m x 14 grid cells), which was same as the buffer zone for each archaeological site. Such size was expected to provide information about the local accessibility and defense (Huggett and Cheesman 2002).

The city walls can be considered as the most important characteristics of the poleis (Hansen and Nielsen 2004). They were built only for defense purposes. They had towers and gates. The gates were guarded during the wartime. The topography was used in favour while constructing the city walls. The city walls of Priene, Pergamum and Ephesus are among the well-known examples in the western Türkiye.

The planners made also use of steep slope and terrain irregularities to create monumental townscapes in the Hellenistic period (Owens 1992). For example, theaters were built against hillside. A polis was beyond spreading the Greek way of

life, it was a mean of propaganda. The Hellenistic kings had become benefactors of poleis to show their power by supporting construction of great and stunning buildings.

It was assumed reasonable to expect a relationship between terrain ruggedness and location of a polis when defense system and town planning were concerned. The more rugged the terrain was the more cutting of surface would be needed, or the least rugged the terrain was the more construction block would be carried to the site.

### **Distribution of Ruggedness in the Study Area**

Ruggedness map and histogram prepared for the study area are given in Figure 3-10. TRI values in the region ranges from 0 to 225. Valleys and mountainous areas are clearly seen with the changing TRI values. The higher TRI value is, the more rugged the land is. TRI is observed at similar percentages (ca. 10-15%) up to the value of 30. The TRI values greater than 30 covers almost 40% of the study area.

### **Characteristic Ruggedness Values for Archaeological Sites**

First, the TRI values clipped out from the polygonal area of each archaeological site were explored for their frequencies, spread and type of distribution. The raster maps and histograms of the archaeological sites of Priene, Sardis and Aphrodisias are shown as examples for a better visualization of change of TRI data in Figure 3-11. Later, the data for each site was examined for their modality. After their modality tests, they were processed accordingly to achieve median values with 95% confidence level considering the statistical evaluation steps in Figure 2-4. The results are summarized in Appendix B. In general, the archaeological sites are lying on low to medium rugged landscape. Priene, Eumeneia and Aegae are seen among the settlements found on the highly rugged landscape. While the terrains of Aphrodisias and Herakleia Salbakes show the lowest diversity for ruggedness, the terrains of Ephesus and Priene show the highest variability. Using these results, histogram of TRI changes for all settlements were plotted (Figure 3-12). A significant peak around TRI value of 30 is observed. The TRI values between 5 and 45 seem to be occurring more often than the remaining values.

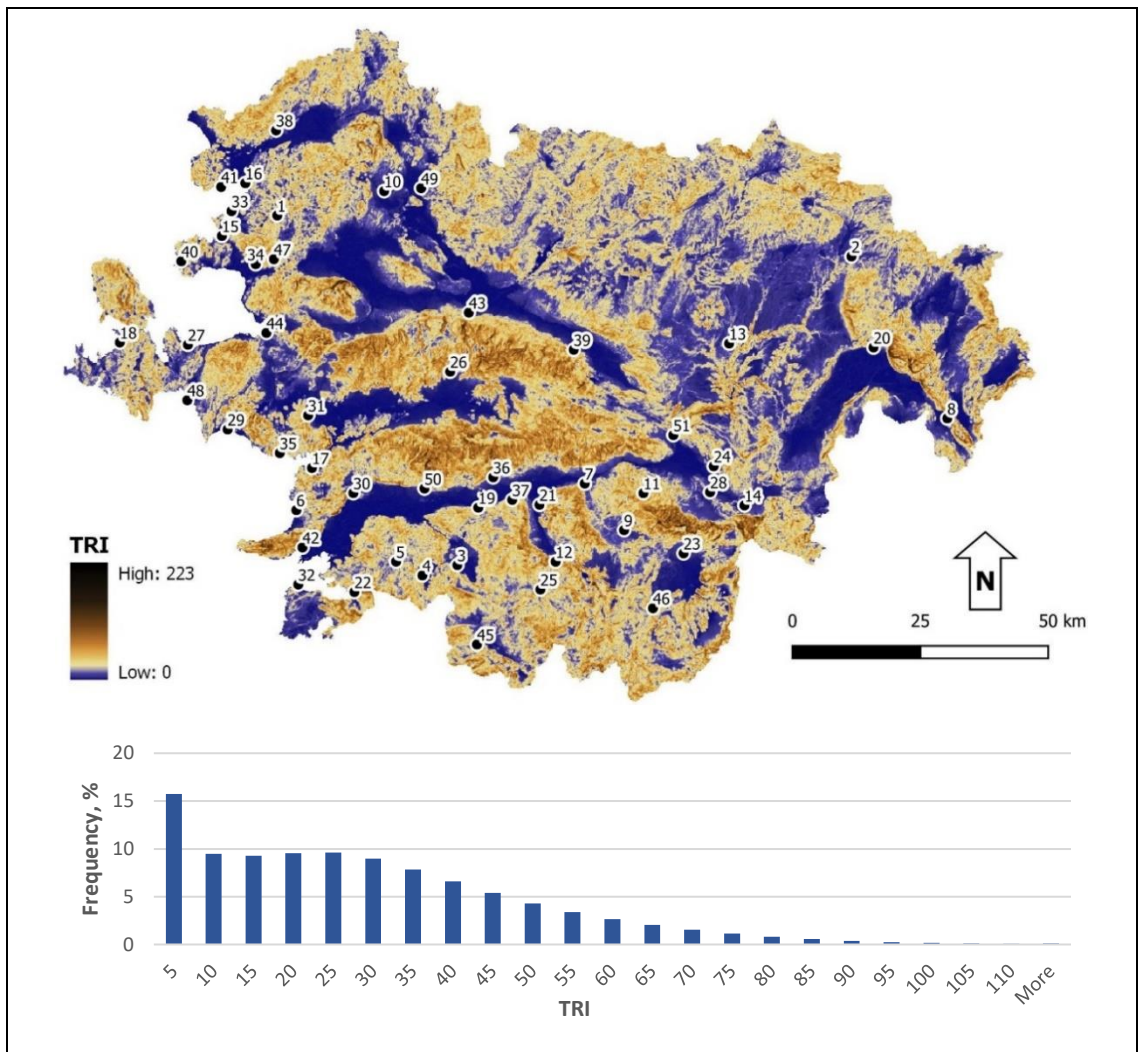


Figure 3-10 Map (above) and frequency distribution (below) of the study area for Terrain Ruggedness Index

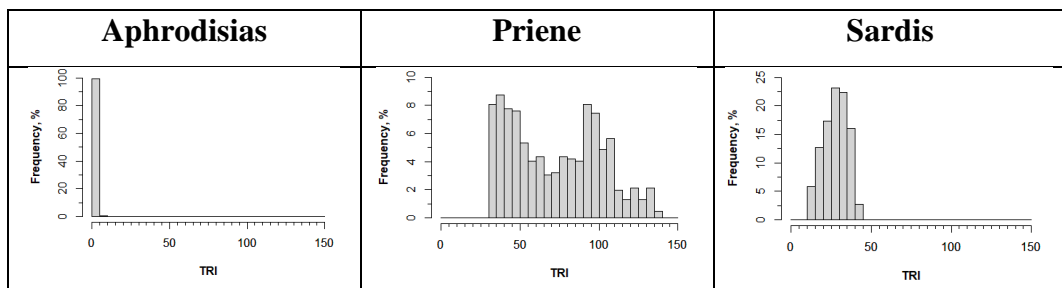


Figure 3-11 Example TRI distributions at the archaeological sites Aphrodisias, Priene and Sardis

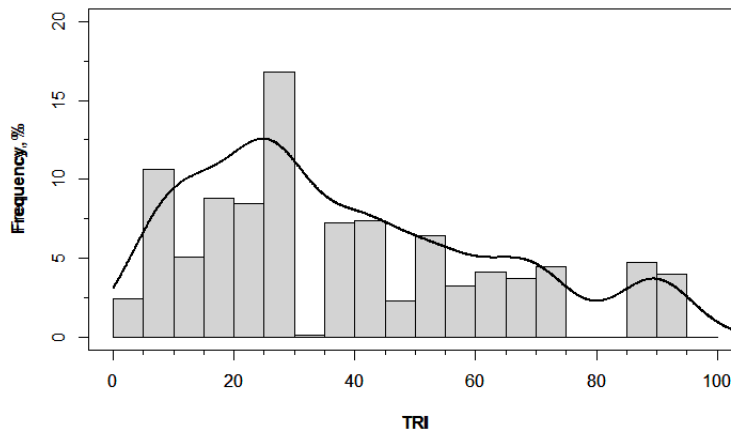


Figure 3-12. Histogram of median TRI values together with KDE curve for all the known archaeological settlements in the dataset

### Potential Map of Ruggedness

The histograms based on the median ruggedness values of archaeological sites were plotted as described in Section 2.2. for each of the 15 datasets (Figure 3-13). Later, the probability density curves for the distributions were obtained using kernel density estimation in R.

When transferring these estimated density values to the original ruggedness map, the bin size of 0.107 TRI was used. Later, the density values were normalized between 0 and 1 for a better understanding. Final potential maps for each group were obtained by reclassifying the original ruggedness map using the normalized values for each bin interval. The ruggedness potential maps for 15 datasets are shown in Figure 3-14. In general, the potential maps indicate that the valley bottoms and mountain ridges are less likely places to locate an archaeological site for the studied period.

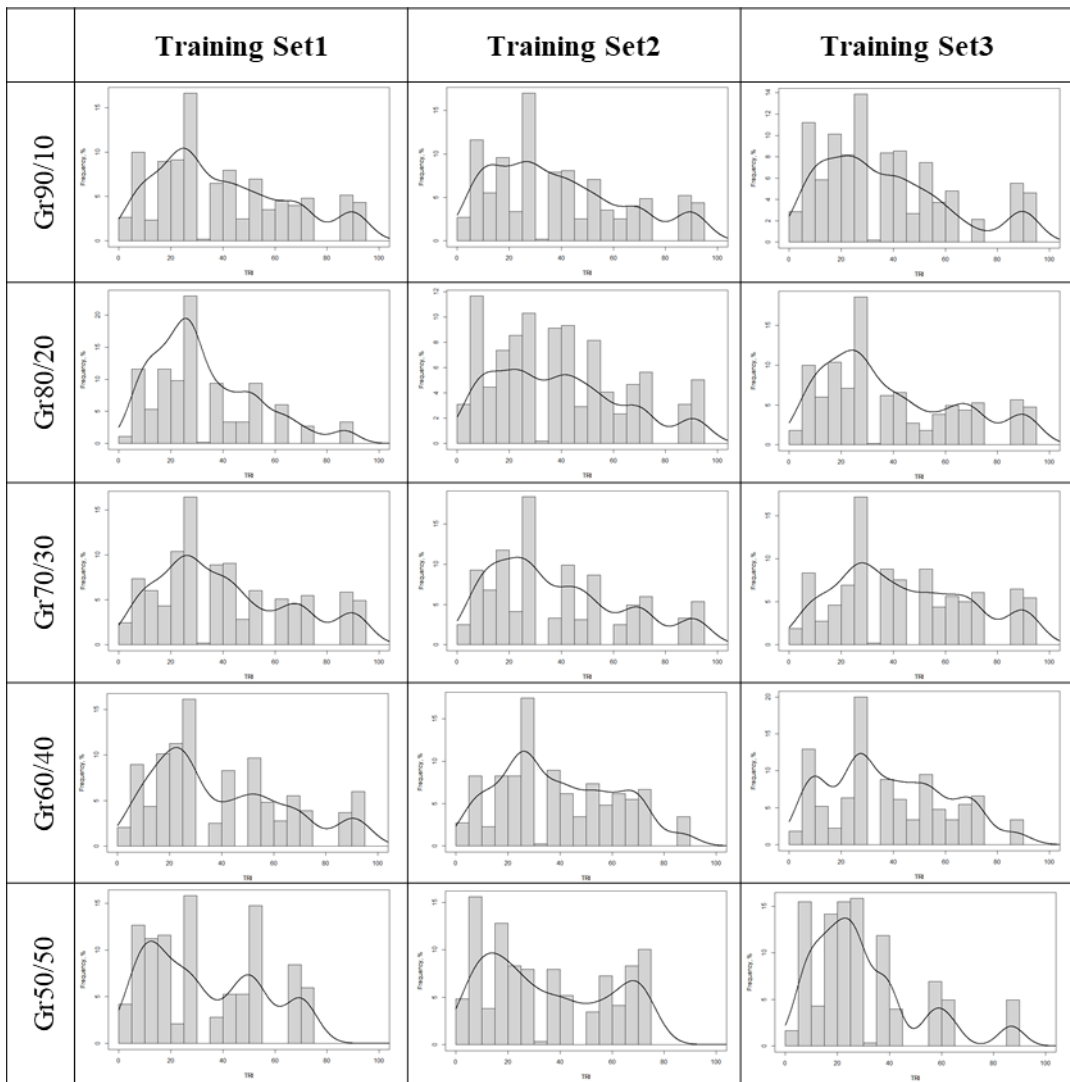


Figure 3-13. Histograms of training data sets with changing percentages and overlaid KDE curves for ruggedness

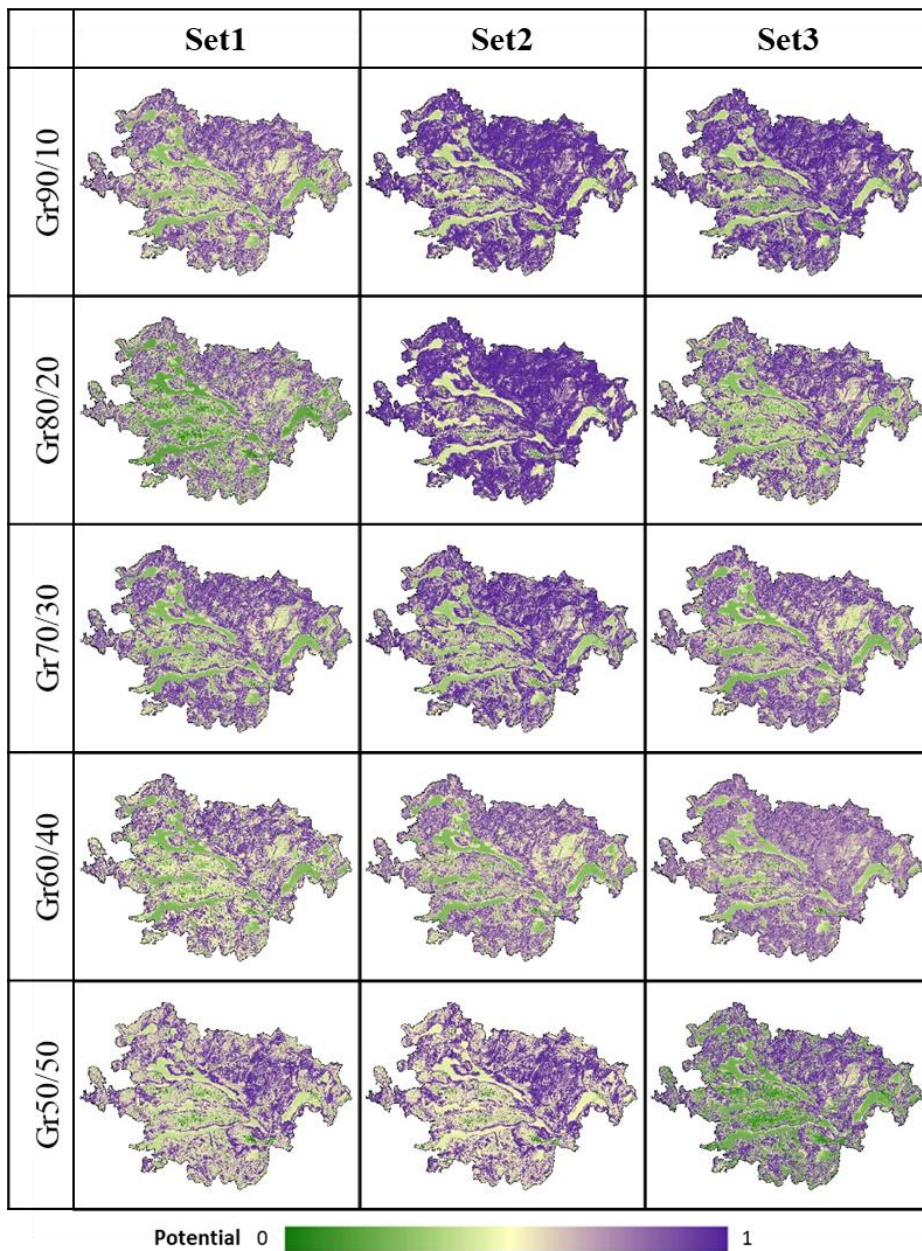


Figure 3-14 Potential maps computed for the ruggedness variable based on the 3 sets of 5 groups that have different training and testing data ratio

### Repeatability of Statistical Analysis

The correlation matrices between the 15 potential maps were computed (Table 3-3). The subsets of Gr90/10 and Gr80/20 were found strongly correlated having greater

than 0.8  $R^2$  value. In general, the results indicate that the higher the training data ratio is, the higher the correlation between each set. This means that the repeatability gets better with the increasing number of sample. On the other hand, even the three sets of training data of Gr50/50 (trained with 26 known archaeological sites) have shown good correlation with values greater than 0.70  $R^2$ .

Table 3-3 The correlation matrices between the ruggedness potential maps (value  $\geq 0.8$  is in light green and  $0.8 > \text{value} \geq 0.65$  is in light gray)

Groups	Sets	Gr90/10			Gr80/20			Gr70/30			Gr60/40			Gr50/50		
		Set1	Set2	Set3	Set1	Set2	Set3	Set1	Set2	Set3	Set1	Set2	Set3	Set1	Set2	Set3
Gr90/10	Set1	1	0.93	0.93	0.98	0.89	0.96	0.97	0.96	0.90	0.95	0.95	0.89	0.58	0.60	0.89
	Set2	0.93	1	0.98	0.94	0.96	0.94	0.92	0.97	0.80	0.87	0.84	0.88	0.73	0.71	0.91
	Set3	0.93	0.98	1	0.94	0.96	0.93	0.89	0.97	0.75	0.90	0.81	0.82	0.76	0.72	0.92
Gr80/20	Set1	0.98	0.94	0.94	1	0.86	0.98	0.93	0.97	0.83	0.96	0.90	0.86	0.66	0.67	0.94
	Set2	0.89	0.96	0.96	0.86	1	0.86	0.87	0.94	0.76	0.83	0.81	0.84	0.74	0.68	0.82
	Set3	0.96	0.94	0.93	0.98	0.86	1	0.91	0.98	0.78	0.96	0.86	0.80	0.69	0.75	0.97
Gr70/30	Set1	0.97	0.92	0.89	0.93	0.87	0.91	1	0.91	0.94	0.85	0.95	0.91	0.45	0.48	0.82
	Set2	0.96	0.97	0.97	0.97	0.94	0.98	0.91	1	0.77	0.95	0.84	0.82	0.77	0.77	0.94
	Set3	0.90	0.80	0.75	0.83	0.76	0.78	0.94	0.77	1	0.76	0.97	0.91	0.26	0.29	0.65
Gr60/40	Set1	0.95	0.87	0.90	0.96	0.83	0.96	0.85	0.95	0.76	1	0.85	0.76	0.72	0.73	0.92
	Set2	0.95	0.84	0.81	0.90	0.81	0.86	0.95	0.84	0.97	0.85	1	0.93	0.40	0.43	0.75
	Set3	0.89	0.88	0.82	0.86	0.84	0.80	0.91	0.82	0.91	0.76	0.93	1	0.49	0.45	0.71
Gr50/50	Set1	0.58	0.73	0.76	0.66	0.74	0.69	0.45	0.77	0.26	0.72	0.40	0.49	1	0.92	0.74
	Set2	0.60	0.71	0.72	0.67	0.68	0.75	0.48	0.77	0.29	0.73	0.43	0.45	0.92	1	0.81
	Set3	0.89	0.91	0.92	0.94	0.82	0.97	0.82	0.94	0.65	0.92	0.75	0.71	0.74	0.81	1

### Sensitivity to the Sample Size

Figure 3-15 shows the potential maps colored based on the cumulative percentages of successfully located archaeological settlements for the training data, particularly 60%, 80%, 90%, 100%. The corresponding cumulative percentage of surface area, cumulative percentage of testing data and the determined limiting potential value are also summarized under the each map. cPLAS-tr of 80% is converted to graphs to compare the potential map outcomes (Figure 3-16). While Figure 3-15 provides a better visualization, the graph in Figure 3-16 provides a better understanding of the

response of training and testing data and the influence of sample size on the performance of variable.

Figure 3-15, in general, shows valley bottoms and mountain ridges were less preferred to the rest of the study area. This general trend is hard to be observed at the northeastern part of the study area due to its different topography. Although the outcomes of maps are similar in trend, they present some differences.

Figure 3-16 (A) shows the performance of testing data within the area where the training data is successfully located. The best average gain is at Gr90/10 (0.42). Unexpectedly, Gr80/20-Set1 has the lowest gain. It has high cPSA (75%) and low performance for the testing data (cPLAS-tt, 40%). On the other hand, interestingly, Gr80/20-Set2 has the lowest cPSA (33%) and a high cPLAS-tt (90%) resulting a gain of 0.63. Its gain is calculated as an example in the below:

$$\text{Gain} = 1 - \text{cPSA} / \text{cPLAS-tt}$$

$$\text{Gain} = 1 - 33 / 90 = 0.63$$

High variation in Gr80/20 seems extraordinary and could be related how the model's respond was sensitive to the combination of spatial distribution of training and testing samples. The other groups show somewhat similar performances. Only the testing data of Gr50/50-Set3 has low performance (52%).

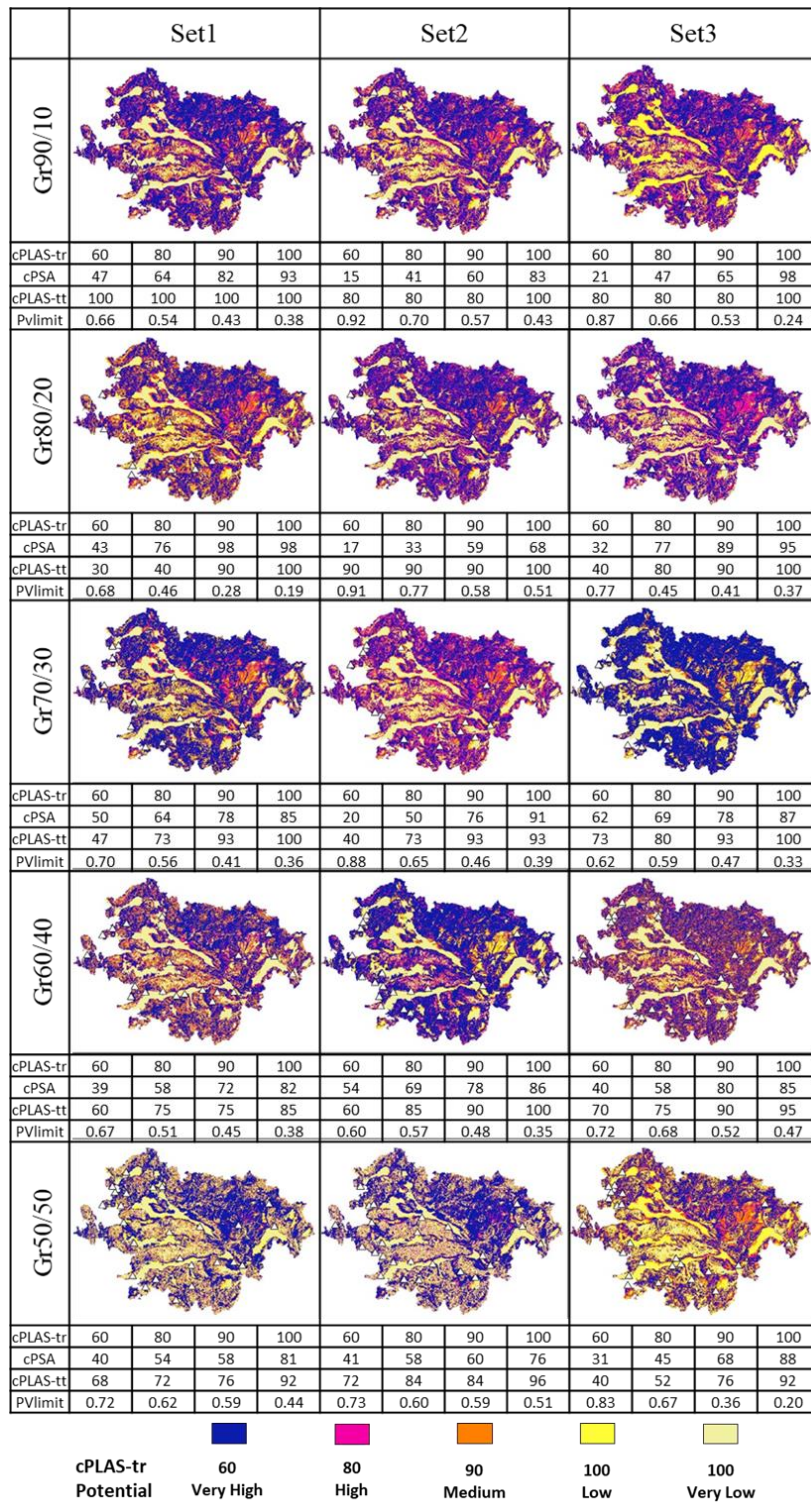


Figure 3-15 Comparison of ruggedness potential map outcomes colored based on successfully located archaeological sites of training data and overlaid with testing data locations.

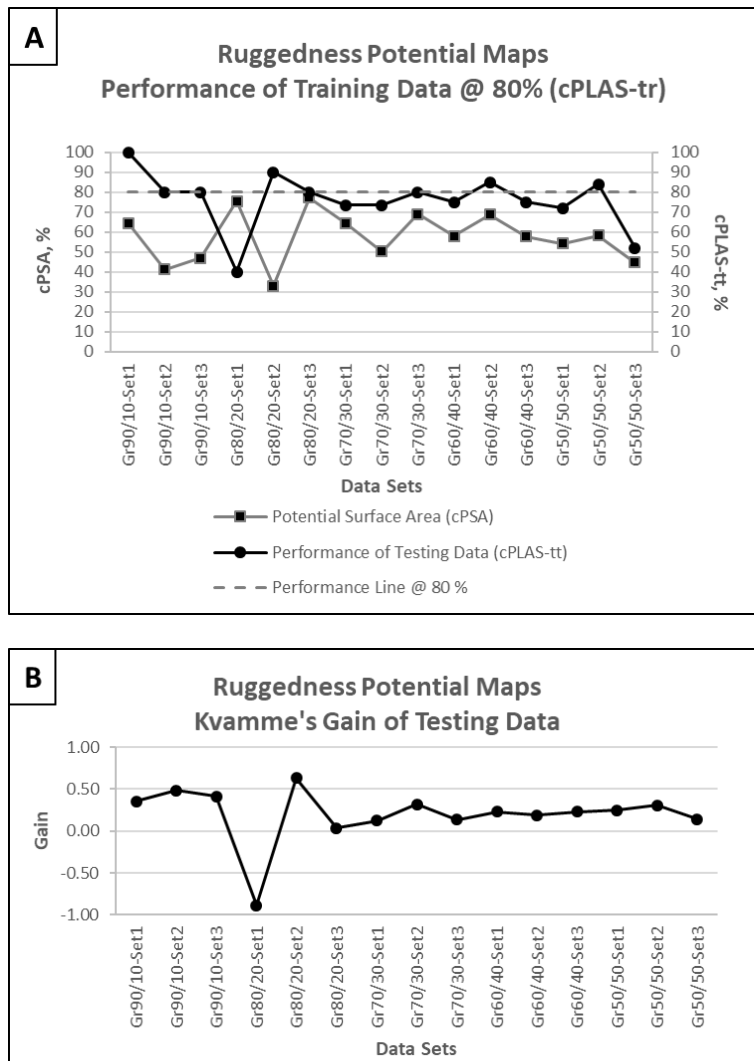


Figure 3-16 The effect of sample size on the potential surface area and the performance of testing data among the groups (A) and Kvamme's gain values for the testing data (B) when 80% success rate is assumed in locating archaeological sites of training data for the ruggedness variable.

### Basic Archaeological Results from Ruggedness Potential Map

The results of ruggedness potential maps were further looked for the archaeological sites. All of the archaeological settlements available in the datasets were ordered with decreasing potential as explained in Section 2.3.2. (Appendix C). The top 5 and bottom 5 of them are listed for each ruggedness potential maps in Table 3-4.

The top 5 includes often the archaeological settlements of Hyllarima, Notion and Philadelpheia. These settlements' locations can be the most characteristic places when terrain ruggedness is considered. The bottom 5 includes often the archaeological settlements of Aegae, Eumeneia and Thyateira. Some of the possible reasons of their low potential values can be as follows:

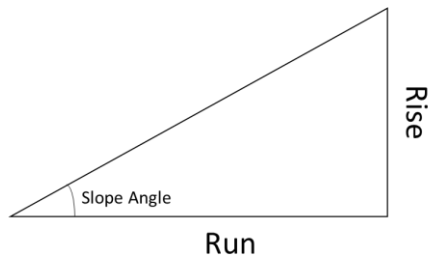
- These settlements' locations can be not as accurate as it was thought.
- Their polygonal area may not be representative.
- These settlements' locations can be outliers. In other words, they may have different characteristics (e.g, cult center, early period settlements) than their contemporary settlements.
- Even though the locations were not preferred for the investigated variable, there might be other more important reasons for settling at that location.

Table 3-4 The list of 5 archaeological settlements (from either training or testing data) of which locations are among the most potential area in each ruggedness potential maps (left) and the least potential area in each ruggedness potential maps (right) in alphabetical order

	Most Potential			Least Potential		
	Set1	Set2	Set3	Set1	Set2	Set3
Gr90/10	Blaundos Hyllarima Hypaipa Notion Philadelpheia	Akmonia Euhippe Hyllarima Notion Philadelpheia	Hyllarima Amyzon Notion Nysa Philadelpheia	Aegae Anaia Aphrodisias Miletus Thyateira	Aegae Bargasa Eumeneia Pergamum Thyateira	Aegae Bargasa Eumeneia Pergamum Thyateira
Gr80/20	Akmonia Euhippe Hyllarima Notion Philadelpheia	Amyzon Erythrai Hyllarima Notion Nysa	Blaundos Hyllarima Hypaipa Notion Philadelpheia	Aegae Bargasa Eumeneia Pergamum Thyateira	Aegae Bargasa Eumeneia Pergamum Thyateira	Aegae Anaia Bargasa Eumeneia Thyateira
Gr70/30	Akmonia Euhippe Hyllarima Notion Philadelpheia	Amyzon Hyllarima Notion Nysa Philadelpheia	Akmonia Apamea Euhippe Metropolis Philadelpheia	Anaia Aphrodisias Eumeneia Miletus Thyateira	Aegae Bargasa Eumeneia Pergamum Thyateira	Elaea Anaia Aphrodisias Miletus Thyateira
Gr60/40	Amyzon Hyllarima Notion Nysa Philadelpheia	Hyllarima Akmonia Euhippe Notion Philadelpheia	Euhippe Akmonia Apamea Metropolis Philadelpheia	Aegae Anaia Aphrodisias Miletus Thyateira	Anaia Aphrodisias Elaea Miletus Thyateira	Aegae Anaia Aphrodisias Eumeneia Thyateira
Gr50/50	Colossae Cyme Hierapolis Myrina Tripolis adM.	Antiochia adM. Erythrai Hierapolis Stratonikeia Tripolis adM.	Amyzon Hyllarima Notion Nysa Philadelpheia	Aegae Bargasa Eumeneia Pergamum Priene	Alinda Eumeneia Orthosia Priene Tabai	Harpasa Aegae Bargasa Eumeneia Priene

### 3.3.1.3. Slope

Slope is the angle of a surface relative to the horizontal. The slope of terrain may change from flat to steep. The formula of slope is as follows:



$$\text{Slope Angle} = \arctan\left(\frac{\text{Rise}}{\text{Run}}\right)$$

where *Slope Angle* is in degrees.

Slope is among the most commonly used environmental variables in APM (Stančič et al. 2000, Vaughn and Crawford 2009, Carleton et al. 2012, Diwan 2020). It can be related to land use, political stability, transportation and more. In Hellenistic period, the region was politically unstable, and mobility of people was high (Kosmin 2014). The settlements then must have needed some protection but also be located a place not difficult to access.

#### **Slope Map of the Study Area**

Slope map and histogram prepared for the study area are given in Figure 3-17. The slope values in the study area shows a right-skewed distribution. In other words, the lower the slope values are the more common they occur in the study area or vice versa. More than 50 % of study area has slope less than 8 degrees and the values greater than 20 degrees are hardly observed.

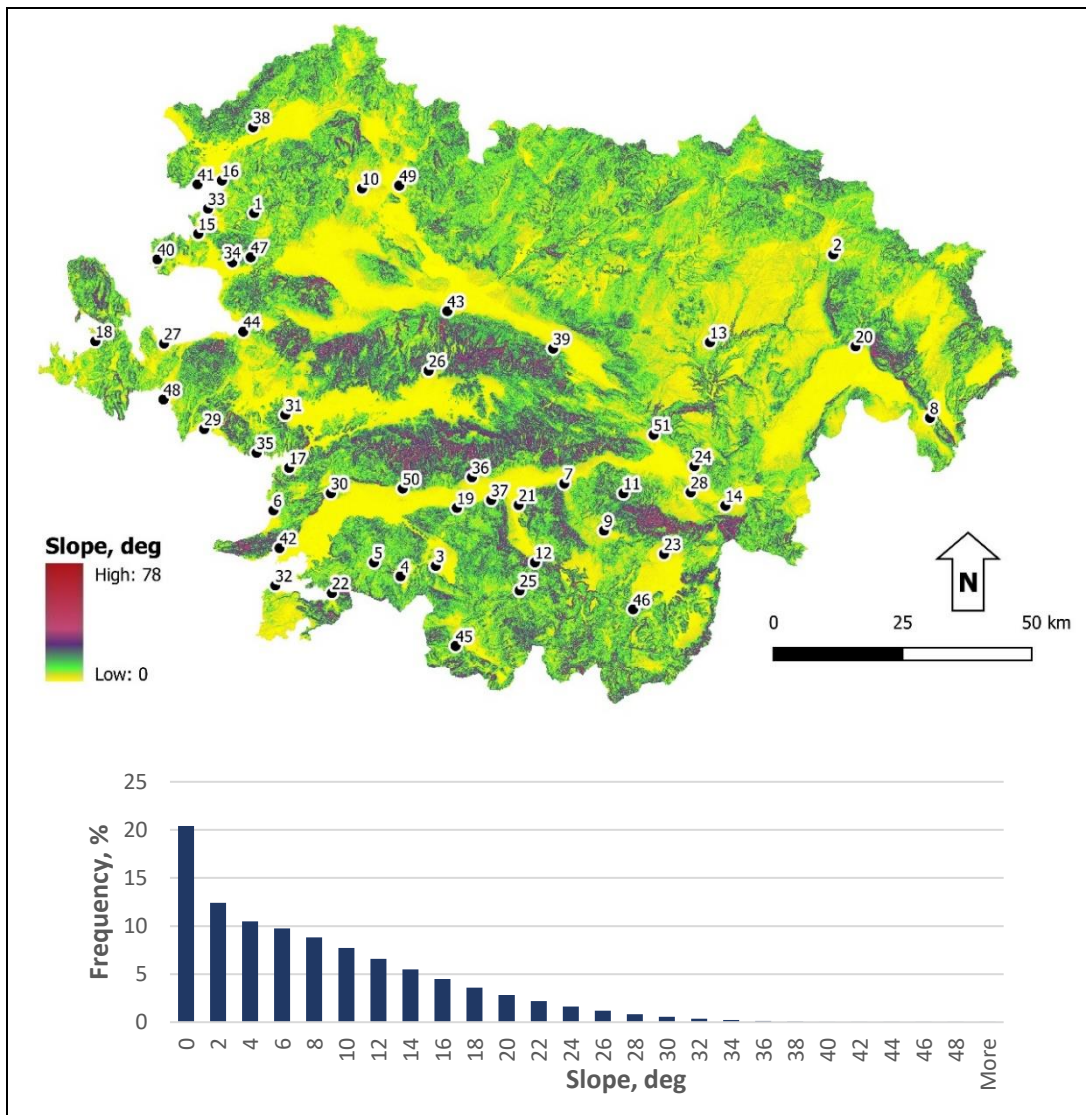


Figure 3-17 Map (above) and frequency distribution (below) of the study area for slope

### Characteristic Slope Values for Archaeological Sites

The slope values clipped out from the polygonal area of each archaeological site were explored for their frequencies, spread and type of distribution. The raster maps and histograms of the archaeological sites of Akmonia, Colossae and Pergamum are shown as examples for a better visualization of change of slope data in Figure 3-18. Later, the data for each site was examined for their modality. After their modality

tests, they were processed accordingly to achieve median values with 95% confidence level considering the statistical evaluation steps in Figure 2-4. The results are given in Appendix B. In general, the location of archaeological sites have low to medium slope. While the locations of Aphrodisias, Elaea, and Herakleia Salbakes have the lowest variation in slope, the locations of Priene, Bargasa, and Aegae have the highest variation. Using these results, histogram of slope changes for all settlements was plotted (Figure 3-19). The slope values are more often observed around 7 and 16 degrees compared to the remaining ones.

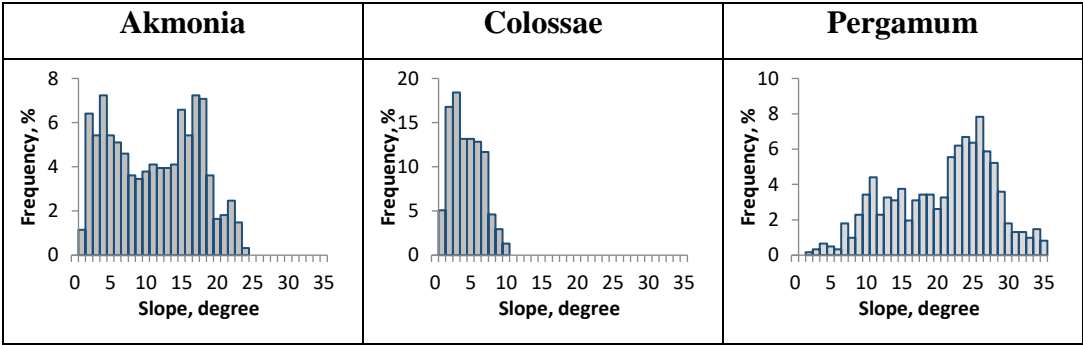


Figure 3-18 Example slope distributions at the archaeological sites Akmonia, Colossae, Pergamum

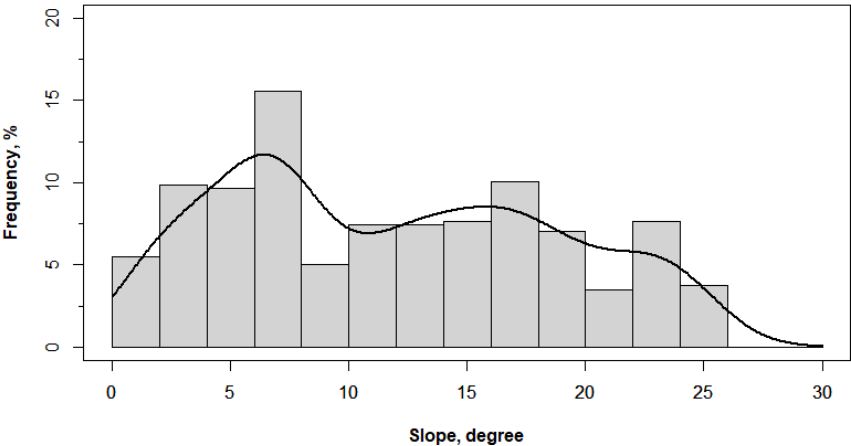


Figure 3-19. Histogram of median slope values together with KDE curve for all the known archaeological settlements in the dataset

### **Potential Map of Slope**

The histograms based on the median slope values of archaeological sites were plotted as described in Section 2.2. for each of the 15 datasets (Figure 3-20). Later, the probability density curves for the distributions were obtained using kernel density estimation in R.

When transferring these estimated density values to the original slope map, the bin size of 0.058 degree was used. Later, the density values were normalized between 0 and 1 for a better understanding. Final potential maps for each group were obtained by reclassifying the original slope map using the normalized values for each bin interval. The slope potential maps for 15 datasets are shown in Figure 3-21. In general, the potential maps indicate that the valley bottoms and mountain ridges are less likely places to locate an archaeological site for the studied period.

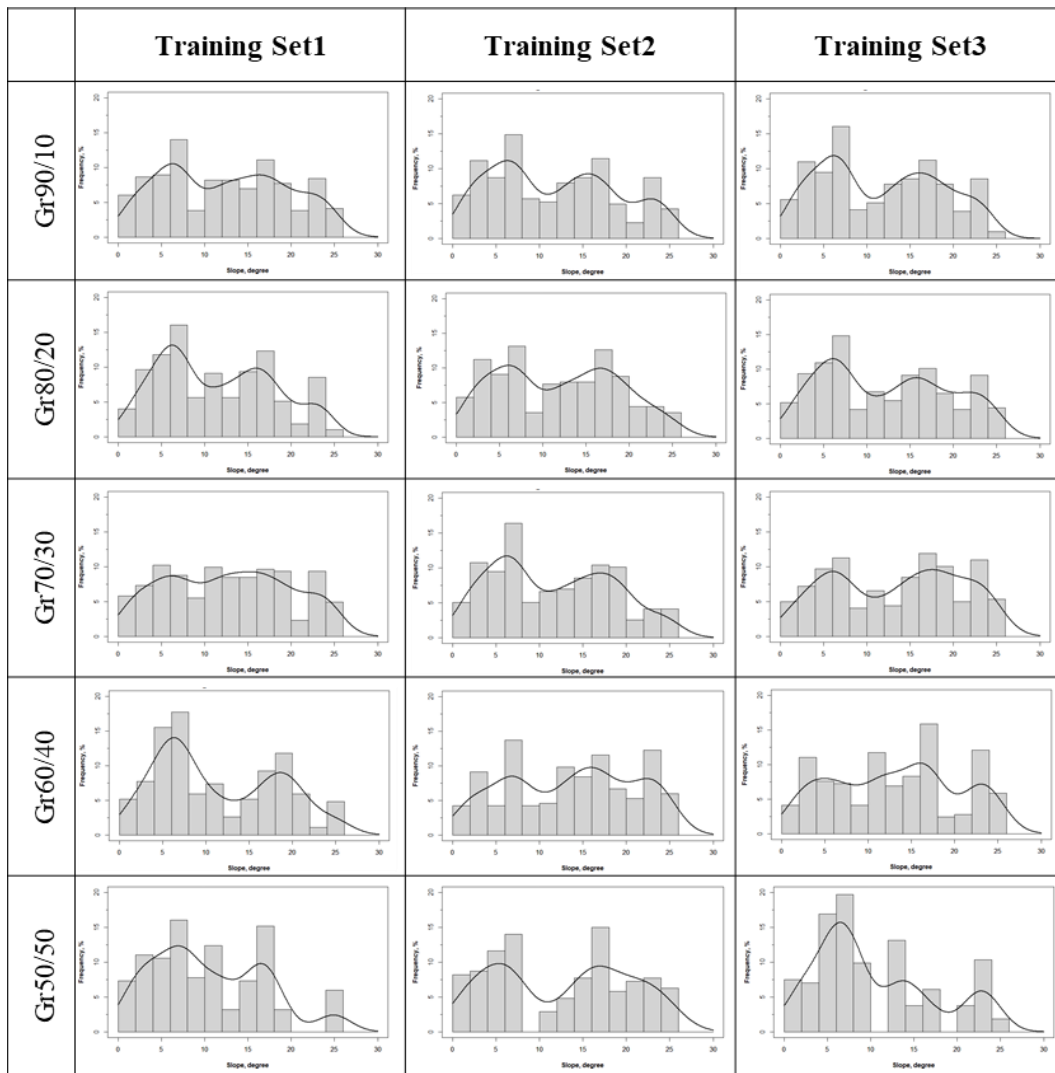


Figure 3-20. Histograms of training data sets with changing percentages and overlaid KDE curves for slope

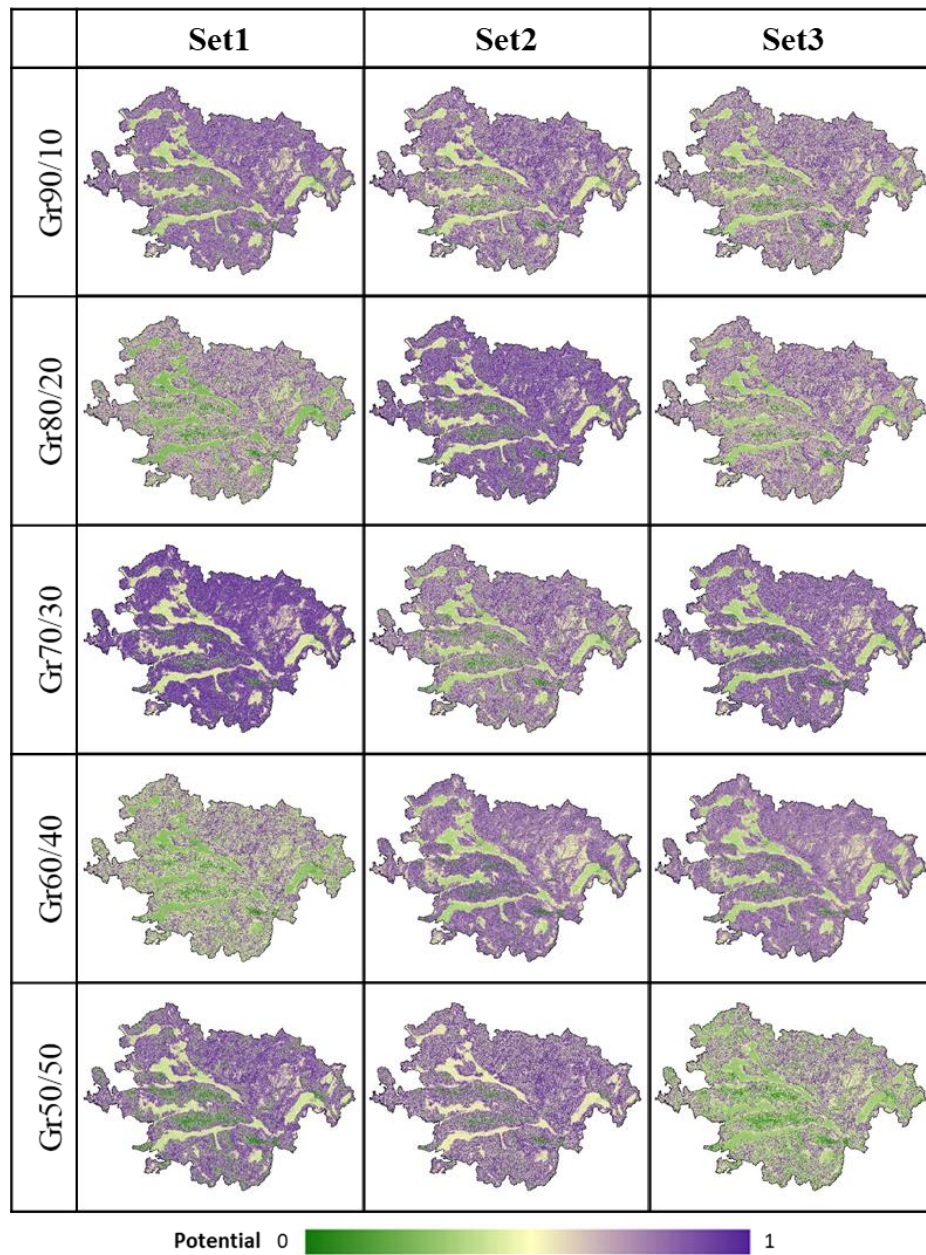


Figure 3-21 Potential maps computed for the slope variable based on the 3 sets of 5 groups that have different training and testing data ratio

### Repeatability of Statistical Analysis for Slope

The correlation matrices between the 15 potential maps were computed (Table 3-5). The subsets of Gr90/10, Gr80/20 and Gr70/30 were found strongly correlated having

greater than 0.8  $R^2$  value. In general, the results indicate that the higher the training data ratio is, the higher the correlation between each set. This means that the repeatability gets better with the increasing sample size. The low correlation between the subsets Gr60/40 and Gr50/50 should indicate high variation in the results.

Table 3-5 The correlation matrices between the slope potential maps (value $\geq$ 0.8 is in light green and 0.8>value  $\geq$ 0.65 is in light gray)

Groups	Sets	Gr90/10			Gr80/20			Gr70/30			Gr60/40			Gr50/50		
		Set1	Set2	Set3	Set1	Set2	Set3	Set1	Set2	Set3	Set1	Set2	Set3	Set1	Set2	Set3
Gr90/10	Set1	1	0.95	0.96	0.97	0.97	0.97	0.94	0.97	0.92	0.86	0.89	0.86	0.85	0.81	0.78
	Set2	0.95	1	0.98	0.97	0.95	0.98	0.83	0.98	0.83	0.88	0.77	0.76	0.92	0.84	0.87
	Set3	0.96	0.98	1	0.96	0.97	0.98	0.82	0.98	0.88	0.91	0.79	0.74	0.87	0.90	0.83
Gr80/20	Set1	0.97	0.97	0.96	1	0.95	0.98	0.86	0.98	0.84	0.91	0.79	0.77	0.92	0.77	0.87
	Set2	0.97	0.95	0.97	0.95	1	0.95	0.91	0.98	0.90	0.84	0.85	0.85	0.87	0.86	0.72
	Set3	0.97	0.98	0.98	0.98	0.95	1	0.84	0.98	0.90	0.92	0.82	0.76	0.86	0.86	0.86
Gr70/30	Set1	0.94	0.83	0.82	0.86	0.91	0.84	1	0.85	0.87	0.66	0.93	0.97	0.75	0.66	0.57
	Set2	0.97	0.98	0.98	0.98	0.98	0.98	0.85	1	0.86	0.93	0.78	0.75	0.92	0.84	0.84
	Set3	0.92	0.83	0.88	0.84	0.90	0.90	0.87	0.86	1	0.78	0.95	0.82	0.63	0.87	0.57
Gr60/40	Set1	0.86	0.88	0.91	0.91	0.84	0.92	0.66	0.93	0.78	1	0.62	0.51	0.86	0.76	0.90
	Set2	0.89	0.77	0.79	0.79	0.85	0.82	0.93	0.78	0.95	0.62	1	0.91	0.59	0.74	0.47
	Set3	0.86	0.76	0.74	0.77	0.85	0.76	0.97	0.75	0.82	0.51	0.91	1	0.65	0.63	0.43
Gr50/50	Set1	0.85	0.92	0.87	0.92	0.87	0.86	0.75	0.92	0.63	0.86	0.59	0.65	1	0.63	0.86
	Set2	0.81	0.84	0.90	0.77	0.86	0.86	0.66	0.84	0.87	0.76	0.74	0.63	0.63	1	0.60
	Set3	0.78	0.87	0.83	0.87	0.72	0.86	0.57	0.84	0.57	0.90	0.47	0.43	0.86	0.60	1

### Sensitivity of Performance of Slope Potential Map

Figure 3-22 shows the potential maps colored based on the cumulative percentages of successfully located archaeological settlements for the training data, particularly 60%, 80%, 90%, 100%. The corresponding cumulative percentage of surface area, cumulative percentage of testing data and the determined limiting potential value are also summarized under the each map. cPLAS-tr of 80% is converted to graphs to compare the potential map outcomes (Figure 3-23). While Figure 3-22 provides a better visualization, the graph in Figure 3-23 provides a better understanding of the response of training and testing data and the influence of sample size on the performance of variable.

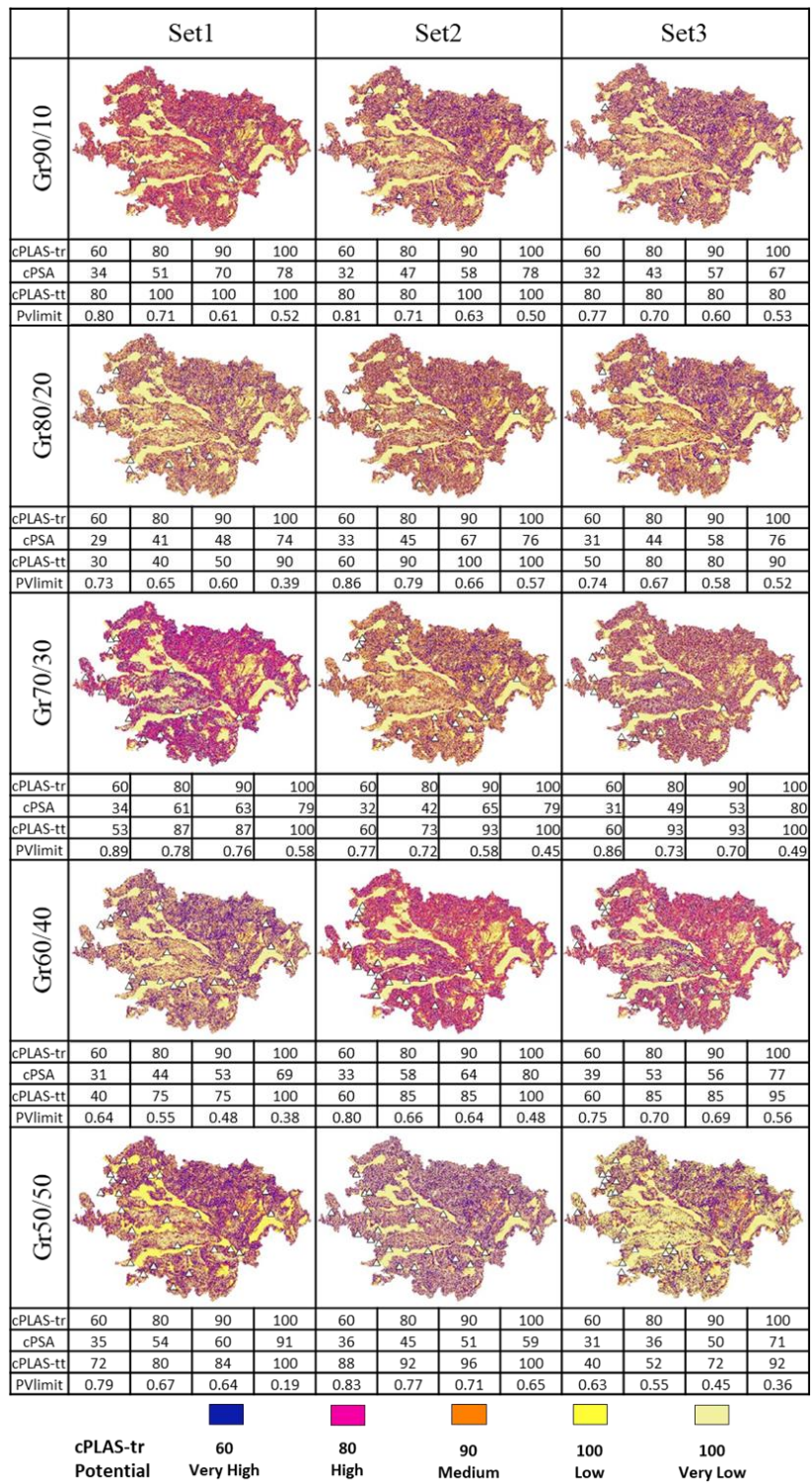


Figure 3-22 Comparison of slope potential map outcomes colored based on successfully located archaeological sites of training data and overlaid with testing data locations.

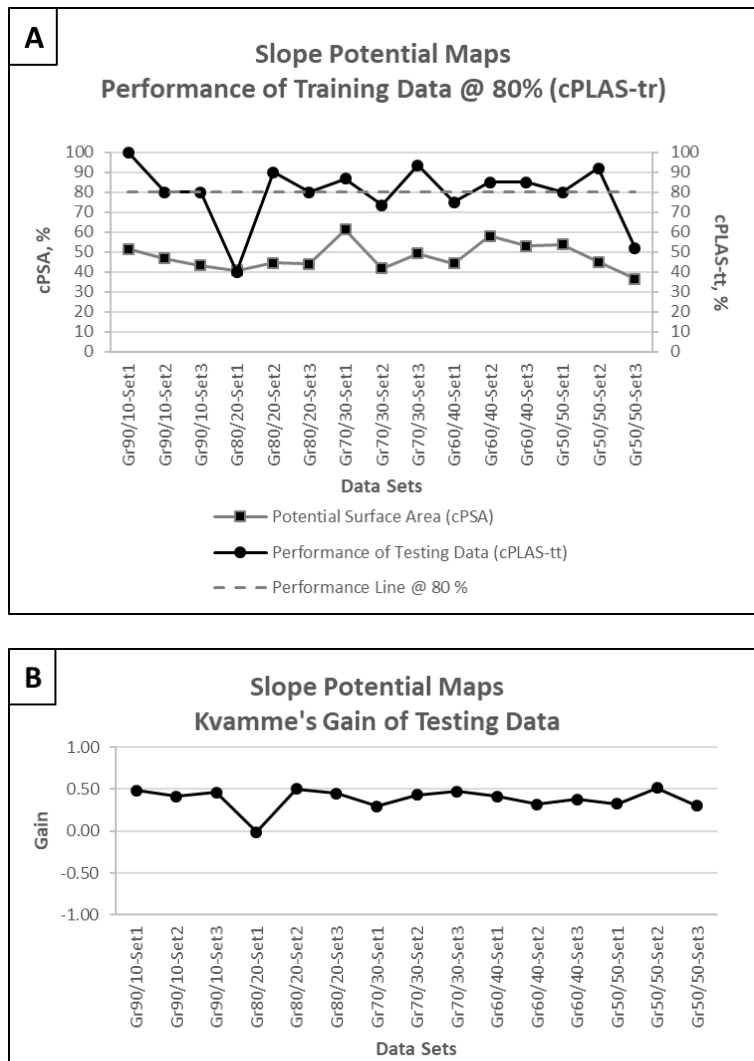


Figure 3-23 The effect of sample size on the potential surface area and the performance of testing data among the groups (A) and Kvamme's gain values for the testing data (B) when 80% success rate is assumed in locating archaeological sites of training data for the slope variable.

Figure 3-22 shows that the valley bottoms distinctively were less preferred to the rest of the study area. The mountain ridges were also less preferred, but it was not as distinctive as valley bottoms in the most of slope potential maps. Although the outcomes of maps are similar in trend, they present some differences. In general, the reduction rates of surface area and the performance of potential maps seems good.

Figure 3-23 (A) shows the percent of surface area at which 80% of training data were successfully located for the groups. The percent of potential surface area becomes more stable as the sample size input increase. The testing data in general performs near 80% except Gr80/20-Set1 (40%) and Gr50/50-Set3 (52%).

Figure 3-23 (B) illustrates the Kvamme's gain values for each dataset. In general, the values are between 0.3 and 0.5 except Gr80/20-Set1. This dataset seems to require a special attention.

### **Basic Archaeological Results from Slope Potential Map**

The results of slope potential maps were further looked for the archaeological sites. All of the archaeological settlements available in the datasets were ordered with decreasing potential as explained in Section 2.3.2. (Appendix C). The top 5 and bottom 5 of them are listed for each slope potential maps in Table 3-6.

The top 5 includes often the archaeological settlements of Antiochia ad Maeandrum., Heraclea ad Latmum, Hyllarima and Klazomenai. These settlements' locations can be the most characteristic places when slope of the land is considered. The bottom 5 includes often the archaeological settlements of Aphrodisias, Miletus and Thyateira. Some of the possible reasons of their low potential values were given in the Section 3.3.1.2 and not repeated here.

Table 3-6 The list of 5 archaeological settlements (from either training or testing data) of which locations are among the most potential area in each ruggedness potential maps (left) and the least potential area in each ruggedness potential maps (right) in alphabetical order

	Most Potential			Least Potential		
	Set1	Set2	Set3	Set1	Set2	Set3
Gr90/10	Antiochia adM. Apollonis Heraclea adLa. Hyllarima Klazomenai	Antiochia adM. Apollonis Heraclea adLa. Hyllarima Klazomenai	Antiochia adM. Apollonis Heraclea adLa. Hyllarima Klazomenai	Anaia Aphrodisias Elaea Miletus Thyateira	Aegae Bargasa Eumeneia Harpasa Thyateira	Aegae Aphrodisias Bargasa Miletus Thyateira
Gr80/20	Antiochia adM. Apollonis Heraclea adLa. Hyllarima Klazomenai	Antiochia adM. Apollonis Heraclea adLa. Hyllarima Klazomenai	Antiochia adM. Apollonis Heraclea adLa. Hyllarima Klazomenai	Aegae Aphrodisias Bargasa Miletus Thyateira	Anaia Aphrodisias Bargasa Miletus Thyateira	Anaia Aphrodisias Bargasa Miletus Thyateira
Gr70/30	Akmonia Euhippe Hyllarima Notion Philadelphieia	Antiochia adM. Apollonis Heraclea adLa. Hyllarima Klazomenai	Heraclea adLa. Hypaipa Metropolis Notion Tabai	Anaia Aphrodisias Eumeneia Miletus Thyateira	Aegae Aphrodisias Bargasa Miletus Thyateira	Anaia Aphrodisias Elaea Miletus Thyateira
Gr60/40	Antiochia adM. Heraclea adLa. Hyllarima Klazomenai Myrina	Alinda Apamea Hypaipa Metropolis Notion	Alinda Apamea Metropolis Neonteichos Notion	Aphrodisias Bargasa Eumeneia Miletus Thyateira	Anaia Aphrodisias Elaea Miletus Thyateira	Anaia Aphrodisias Elaea Miletus Thyateira
Gr50/50	Amyzon Antiochia adM. Heraclea adLa. Hyllarima Klazomenai	Antiochia adM. Apollonis Colossae Heraclea adLa. Klazomenai	Antiochia adM. Apollonis Heraclea adLa. Hyllarima Klazomenai	Aegae Bargasa Eumeneia Harpasa Thyateira	Anaia Aphrodisias Bargasa Miletus Thyateira	Aegae Bargasa Eumeneia Harpasa Priene

### 3.3.1.4. Aspect

Aspect is the direction of slope faces and is commonly among the variables used in archaeological predictive modeling to define the local topography (Espa et al. 2006, Vaughn and Crawford 2009, Carleton et al. 2012, Gümüş et al. 2017). Aspect can be important due to its relation to solar radiation at a site. Huggett and Cheesman (2002) discuss its effect on local climate, agriculture, animal and plant distributions and soil types.

As mentioned in Section 2.2.1., aspect is measured in degrees clockwise from north and such data is called circular data. However, most of the predictive modelling studies using aspect (Vaughn and Crawford 2009, Revert 2017, Diwan 2020) treat it as a categorical variable (i.e. N, NE, E, SE, S, SW, W, NW and flat). Since the

archaeological sites were represented as polygonal area instead of a point in this study, the investigation of aspect using circular data statistics becomes more critical.

### **Aspect Map of the Study Area**

Aspect map and histogram prepared for the study area are given in Figure 3-24. Aspect values in the region ranges from  $0.4^{\circ}$  to  $360^{\circ}$ . When a surface does not have any slope, there would be no aspect as well. In such cases, aspect value is assumed as -1. There are no zero aspect values in the study area.

The histogram of aspect values show similar frequencies in each interval. The aspect map shows that the mountains in the study area commonly elongate in the west - east directions with facing north and south slopes.

### **Characteristic Aspect Values for Archaeological Sites**

First, the aspect values clipped out from the polygonal area of each archaeological site were explored for their frequencies and spread. For a better visualization of change of aspect data in an archaeological site, the raster maps and histograms of the archaeological sites Blaundos, Hierapolis and Hypaipa are shown in Figure 3-25. Later, the data for each site was examined for their uniformity. After their uniformity tests, they have been processed accordingly to achieve median values with 95% confidence level considering the statistical evaluation steps in Figure 2-8.

The results for each archaeological settlement are summarized in Appendix B. The settlements were usually lying on more than one dominant direction. Based on the median values of each settlements, histogram of aspect changes for all settlements was also plotted (Figure 3-26). The archaeological sites are found to be located at the west-northwest and southeast slopes.

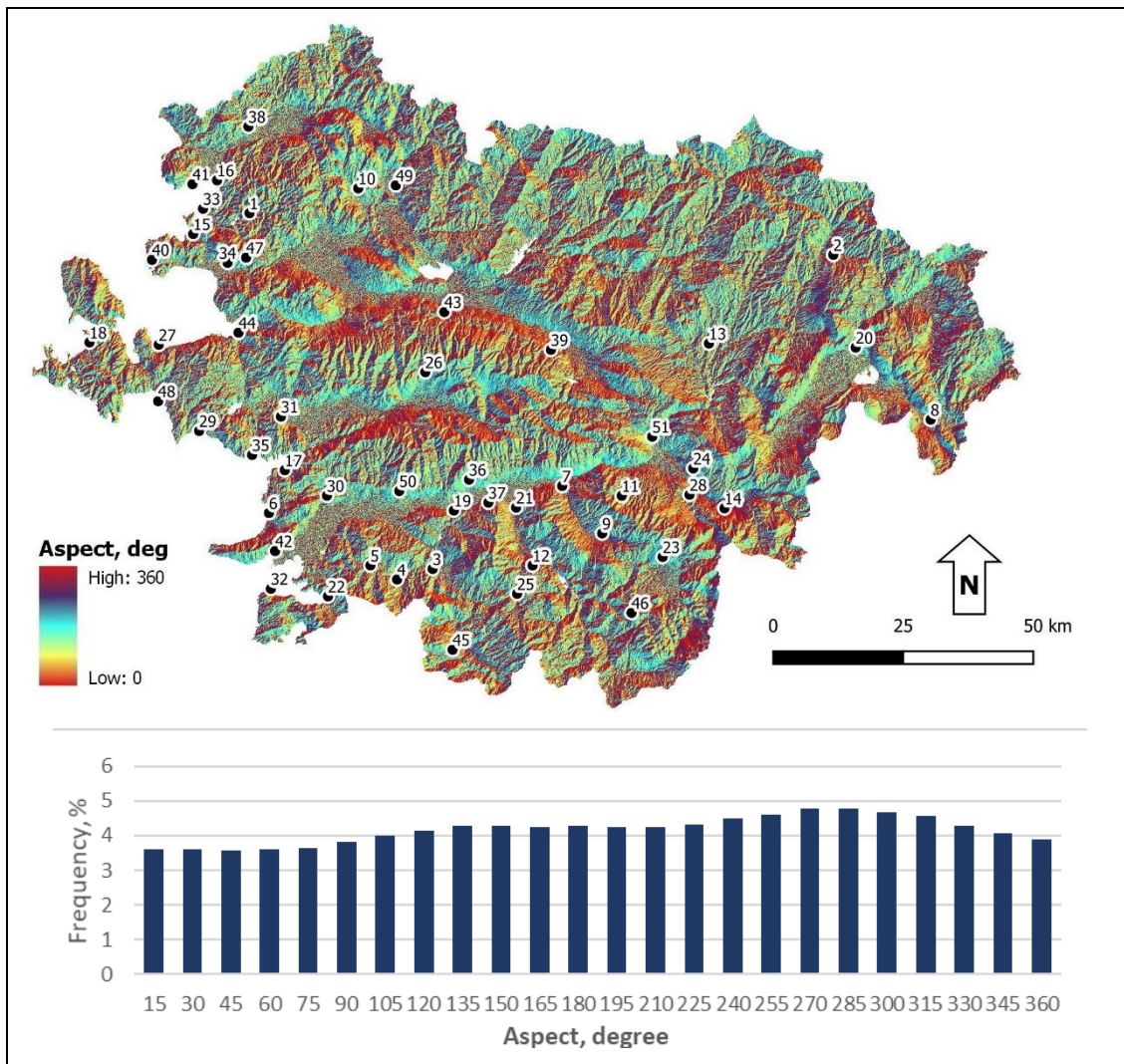


Figure 3-24 Map (above) and frequency distribution (below) of the study area for aspect in degrees

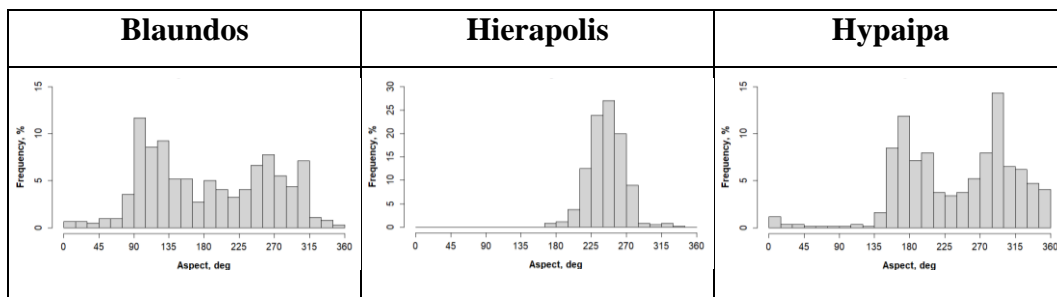


Figure 3-25 Example aspect distributions at the archaeological sites Blaundos, Hierapolis and Hypaipa

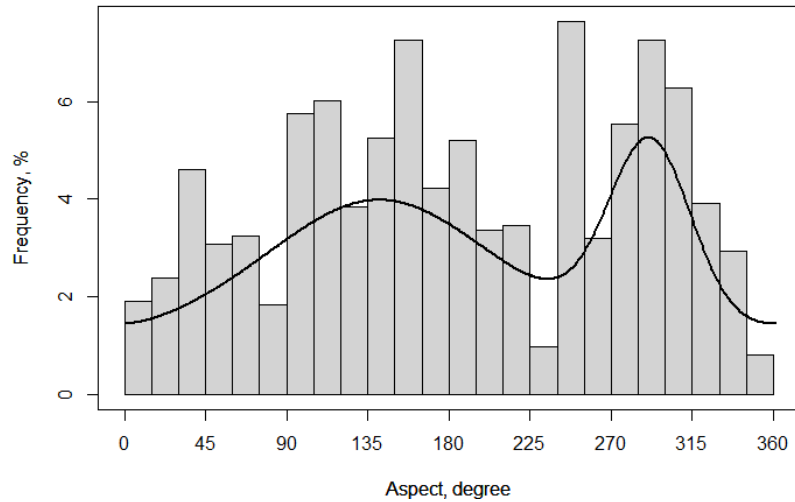


Figure 3-26. Histogram of median aspect values together with density curve for all the known archaeological settlements in the dataset

### Potential Map of Aspect

The histograms based on the median aspect values of archaeological sites were plotted as described in Section 2.2. for each of the 15 datasets (Figure 3-27). Later, the probability density curves for the distributions were obtained using kernel density estimation in R.

When transferring these estimated density values to the original aspect map, the bin size of 0.01 radian (or 0.57 degrees) was used. Later, the density values were normalized between 0 and 1 for a better understanding. Final potential maps for each group were obtained by reclassifying the original aspect map using the normalized values for each bin interval. The aspect potential maps for 15 datasets are shown in Figure 3-28. In general, the potential maps indicate that the valley bottoms and mountain ridges are less likely places to locate an archaeological site for the studied period.

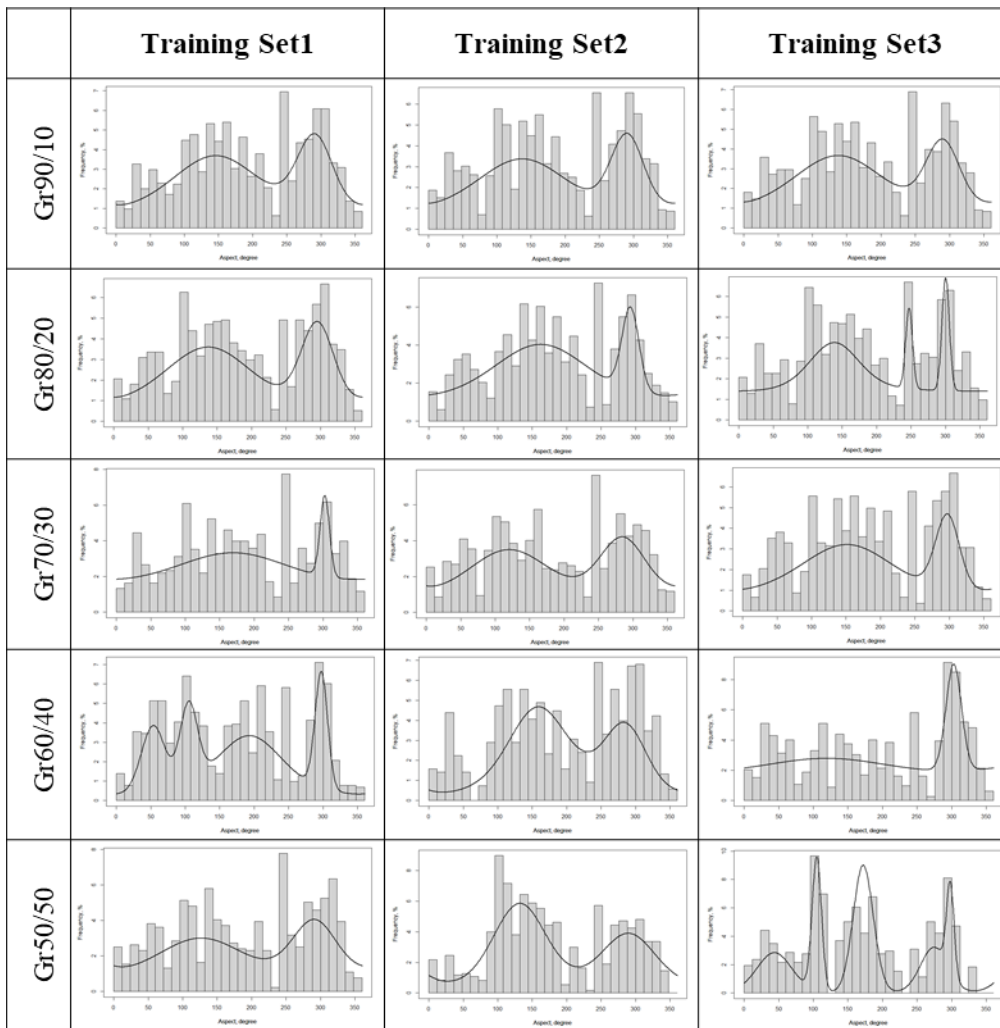


Figure 3-27. Histograms of training data sets with changing percentages and overlaid KDE curves for aspect

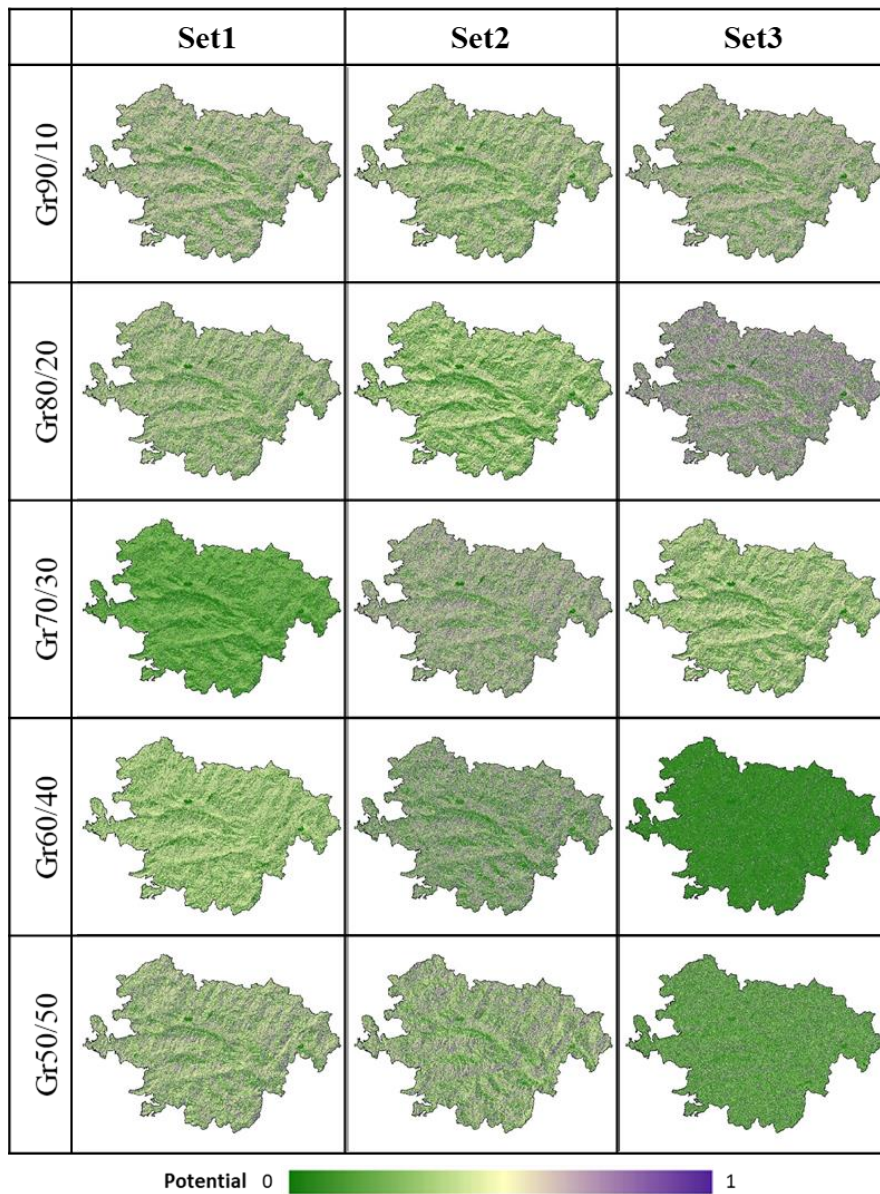


Figure 3-28 Potential maps computed for the aspect variable based on the 3 sets of 5 groups that have different training and testing data ratio

### Repeatability of Statistical Analysis for Aspect

The correlation matrices between the 15 potential maps were computed (Table 3-7). The subsets of Gr90/10 and Gr80/20 were found strongly correlated having greater than 0.8  $R^2$  value. The subsets of Gr70/30 was also demonstrated some level of

correlation. Gr70/20-Set1 and Gr70/20-Set2 were found significantly correlated with Gr70/20-Set3 while having low correlation between each other. In general, the results indicate that the higher the training data ratio is, the higher the correlation between each set. This means that repeatability gets better with the increasing sample size. In the other groups, low  $R^2$  values indicate low repeatability for these groups.

Table 3-7 The correlation matrices between the aspect potential maps (value $\geq$ 0.8 is in light green and  $0.8 > \text{value} \geq 0.65$  is in light gray)

Groups	Sets	Gr90/10			Gr80/20			Gr70/30			Gr60/40			Gr50/50		
		Set1	Set2	Set3	Set1	Set2	Set3	Set1	Set2	Set3	Set1	Set2	Set3	Set1	Set2	Set3
Gr90/10	Set1	1	0.98	0.98	0.96	0.88	0.96	0.63	0.91	0.93	0.51	0.93	0.54	0.93	0.79	0.45
	Set2	0.98	1	0.99	0.98	0.86	0.96	0.61	0.93	0.93	0.55	0.91	0.58	0.95	0.78	0.46
	Set3	0.98	0.99	1	0.97	0.87	0.98	0.61	0.93	0.92	0.57	0.89	0.50	0.92	0.83	0.49
Gr80/20	Set1	0.96	0.98	0.97	1	0.84	0.96	0.66	0.88	0.96	0.57	0.87	0.67	0.93	0.80	0.46
	Set2	0.88	0.86	0.87	0.84	1	0.83	0.71	0.68	0.93	0.70	0.71	0.48	0.70	0.65	0.52
	Set3	0.96	0.96	0.98	0.96	0.83	1	0.60	0.91	0.90	0.54	0.88	0.47	0.90	0.91	0.47
Gr70/30	Set1	0.63	0.61	0.61	0.66	0.71	0.60	1	0.45	0.79	0.69	0.49	0.76	0.51	0.45	0.42
	Set2	0.91	0.93	0.93	0.88	0.68	0.91	0.45	1	0.76	0.44	0.91	0.46	0.96	0.79	0.34
	Set3	0.93	0.93	0.92	0.96	0.93	0.90	0.79	0.76	1	0.67	0.78	0.70	0.82	0.72	0.49
Gr60/40	Set1	0.51	0.55	0.57	0.57	0.70	0.54	0.69	0.44	0.67	1	0.26	0.52	0.41	0.34	0.61
	Set2	0.93	0.91	0.89	0.87	0.71	0.88	0.49	0.91	0.78	0.26	1	0.47	0.94	0.81	0.29
	Set3	0.54	0.58	0.50	0.67	0.48	0.47	0.76	0.46	0.70	0.52	0.47	1	0.61	0.26	0.25
Gr50/50	Set1	0.93	0.95	0.92	0.93	0.70	0.90	0.51	0.96	0.82	0.41	0.94	0.61	1	0.74	0.34
	Set2	0.79	0.78	0.83	0.80	0.65	0.91	0.45	0.79	0.72	0.34	0.81	0.26	0.74	1	0.33
	Set3	0.45	0.46	0.49	0.46	0.52	0.47	0.42	0.34	0.49	0.61	0.29	0.25	0.34	0.33	1

### Sensitivity of Performance of Aspect Potential Map

Figure 3-29 shows the potential maps colored based on the cumulative percentages of successfully located archaeological settlements for the training data, particularly 60%, 80%, 90%, 100%. The corresponding cumulative percentage of surface area, cumulative percentage of testing data and the determined limiting potential value are also summarized under the each map. cPLAS-tr of 80% was converted to graphs to compare the potential map outcomes (Figure 3-30). While Figure 3-29 provides a better visualization, the graph in Figure 3-30 provides a better understanding of the response of training and testing data and the influence of sample size on the performance of variable.

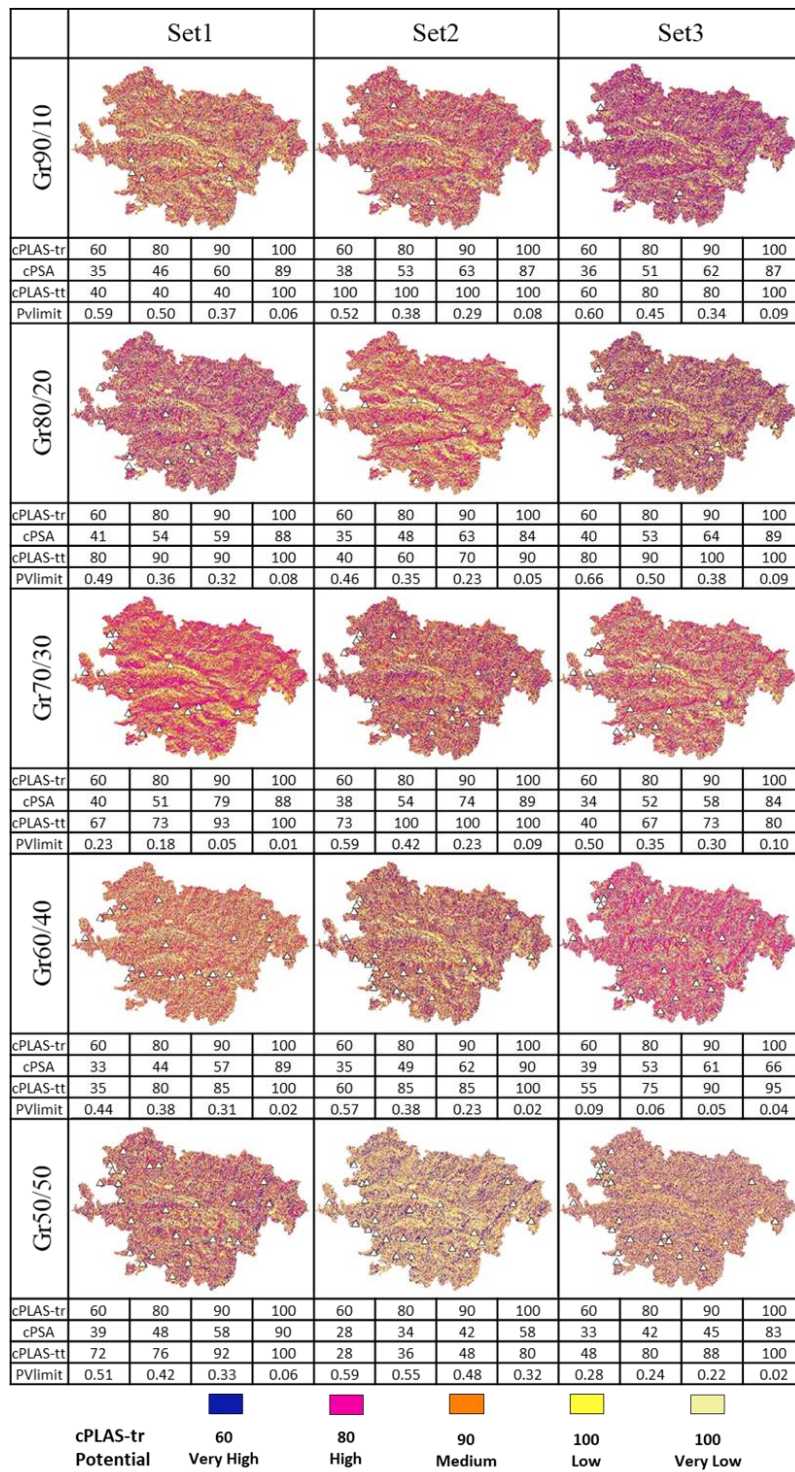


Figure 3-29 Comparison of aspect potential map outcomes colored based on successfully located archaeological sites of training data and overlaid with testing data locations.

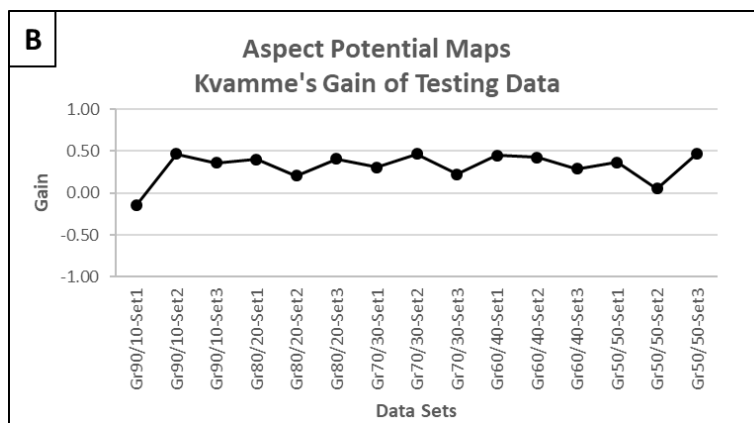
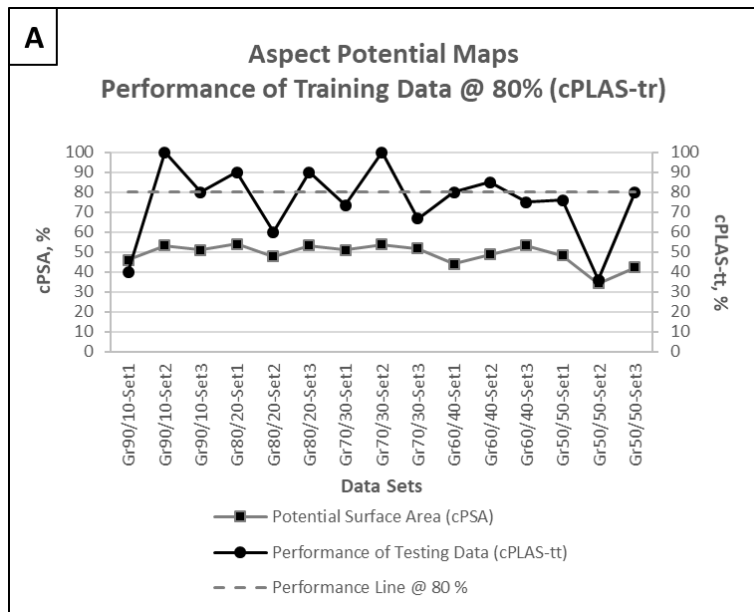


Figure 3-30 The a effect of sample size on the potential surface area and the performance of testing data among the groups (A) and Kvamme's gain values for the testing data (B) when 80% success rate is assumed in locating archaeological sites of training data for the aspect variable.

Figure 3-29 shows that the western and southwestern skirts of mountains were more preferred for settling to the rest of the study area. This differentiation becomes harder to be observed towards the Gr50/50. On the other hand, they seem generally successful in reducing the potential surface area.

Figure 3-30 (A) shows the percent of surface area at which 80% of training data were successfully located for the groups. The variation in cPSA is very small for the groups Gr90/10, Gr80/20 and Gr70/30. The variation in cPSA increases from Gr60/40 to Gr50/50. The potential maps of Gr90/10-Set1, Gr80/20-Set2 and Gr50/50-Set2 show very low performances during the testing (40%, 60% and 36% respectively). The remaining potential maps have around 80% performance for the testing data. The calculated gain values for the testing data is given in Figure 3-30 (B). The values changes from 0.2 to 0.47 except Gr90/10-Set1 and Gr50/50-Set2.

### **Basic Archaeological Results from Aspect Potential Map**

The results of aspect potential maps were further looked for the archaeological sites. All of the archaeological settlements available in the datasets were ordered with decreasing potential as explained in Section 2.3.2. (Appendix C). The top 5 and bottom 5 of them are listed for each aspect potential maps in Table 3-8.

The top 5 includes often the archaeological settlements of Anaia, Apamea, Harpasa, Hyllarima and Tabai. These settlements' locations can be the most characteristic places when aspect of the land is considered. The bottom 5 includes often the archaeological settlements of Alabanda, Magnesia ad Maeandrum, Philadelpheia and Sardis. Some of the possible reasons of their low potential values were given in the Section 3.3.1.2 and not repeated here.

Table 3-8 The list of 5 archaeological settlements (from either training or testing data) of which locations are among the least potential area in each ruggedness potential maps (left) and the most potential area in each aspect potential maps (right)

	Most Potential			Least Potential		
	Set1	Set2	Set3	Set1	Set2	Set3
Gr90/10	Anaia Apamea Harpasa Hyllarima Tabai	Anaia Apamea Harpasa Hyllarima Tabai	Anaia Apamea Harpasa Hyllarima Tabai	Alabanda Magnesia adM. Philadelpheia Sardis Smyrna	Alabanda Magnesia adM. Philadelpheia Sardis Smyrna	Alabanda Magnesia adM. Philadelpheia Sardis Smyrna
Gr80/20	Anaia Apamea Harpasa Hyllarima Tabai	Anaia Apamea Harpasa Hypaipa Tabai	Alinda Apamea Eumeneia Harpasa Tabai	Akmonia Alabanda Magnesia adM. Philadelpheia Sardis	Alabanda Magnesia adM. Philadelpheia Sardis Smyrna	Akmonia Alabanda Magnesia adM. Philadelpheia Sardis
Gr70/30	Akmonia Euhippe Hyllarima Notion Philadelpheia	Anaia Apamea Harpasa Hyllarima Tabai	Anaia Apamea Harpasa Hyllarima Tabai	Anaia Aphrodisias Eumeneia Miletus Thyateira	Akmonia Alabanda Magnesia adM. Philadelpheia Sardis	Alabanda Magnesia adM. Philadelpheia Sardis Smyrna
Gr60/40	Amyzon Erythrai Euhippe Tabai Teos	Anaia Apamea Harpasa Hyllarima Tabai	Anaia Euhippe Harpasa Hyllarima Tabai	Alabanda Magnesia adM. Orthosia Sardis Smyrna	Akmonia Alabanda Magnesia adM. Philadelpheia Sardis	Alabanda Ephesus Hierapolis Sardis Tralles
Gr50/50	Anaia Apamea Harpasa Hyllarima Tabai	Alinda Attouda Erythrai Eumeneia Stratonikeia	Apollonis Hypaipa Priene Teos Tripolis adM.	Akmonia Alabanda Magnesia adM. Philadelpheia Sardis	Akmonia Alabanda Magnesia adM. Philadelpheia Sardis	Akmonia Antiochia adM. Magnesia adM. Orthosia Smyrna

### 3.4. Natural Resources

Available natural resources is an important proxy for site location preferences. In this study, arable land, access to water and rock sources for city wall building blocks are evaluated.

#### 3.4.1. Arable Land Density

The economic prosperity of a polis depended heavily on its self-sufficiency. As discussed in Section 1.5.2, the surrounding territory was crucial for providing land for agricultural use. According to Bintliff's (2000) analysis of the evolution of poleis, the Dark Ages saw only a few small and widely dispersed settlements. However, as the population grew, villages became more interconnected, and their territories expanded to roughly a 2.5 km radius each. Some villages grew into larger towns, and

many claimed to be independent city-states. Eventually, the most powerful village-states took over the smaller city-states, leading to the formation of larger city-states with expanded territories.

In this study, we assumed that each settlement had a core territory of approximately 2.5 km radius, which was about a one-hour walking distance from the settlement. This buffer zone of one-hour walking distance was used in the arable land analysis. The calculation steps for the time required travelling from one location to another is explained in Section 3.7.

Arable land data was acquired from the national 1:25,000 scaled soil classification map. The arable land boundary was defined based on the land use capability classification. Later, we created a density map of arable areas, rather than simply noting the availability of arable land. A circular area of 5 km radius was scanned for the whole study area. Total count of pixels categorized as arable was assigned to the central pixel of the circular area as the density value. As a result, the higher the value of a pixel became, the higher the arable land density became in the map.

#### **Arable Land Density Map of the Study Area**

Arable land density map and histogram prepared for the study area are given in Figure 3-31. The values observed in the study area range between 0 and 125,527. The distribution is right-skewed. Lower arable land density values occur more often in the study area. Around 50% of the study area has 35,000 density values. Higher arable land density values are observed through the valleys as expected.

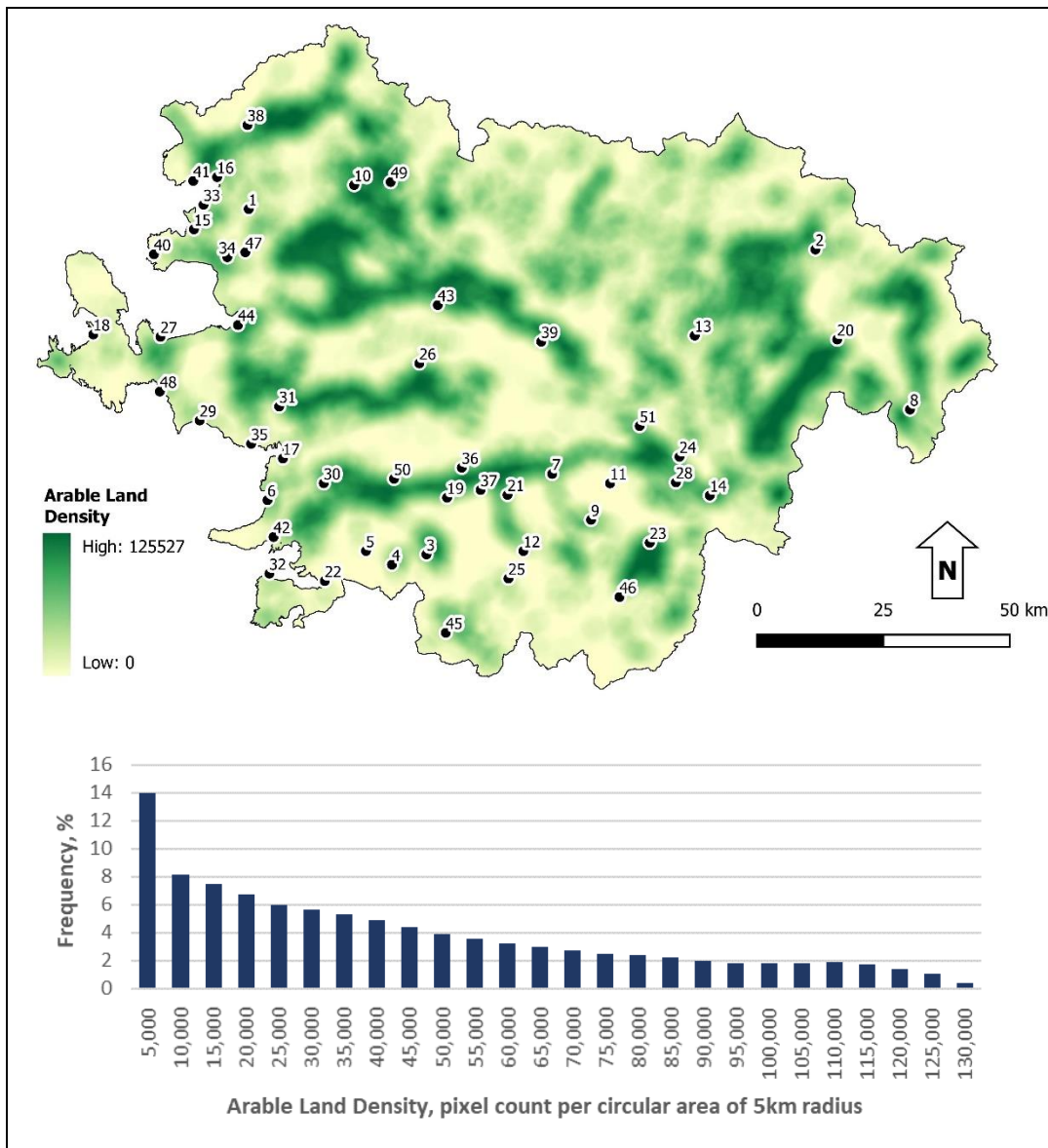


Figure 3-31 Map (above) and frequency distribution (below) of the study area for arable land density

### Characteristic Arable Land Density Values for Archaeological Sites

First, the arable land density values clipped out from the polygonal area of each archaeological site were explored for their frequencies and spread. For a better visualization of change of arable land density in an archaeological site, the raster

maps and histograms of the archaeological sites Akmonia, Antiochia ad Maeandrum and Tripolis ad Maeandrum are shown in Figure 3-32. Later, the data for each site was examined for their modality. After their modality tests, they were processed accordingly to achieve median values with 95% confidence level considering the statistical evaluation steps in Figure 2-4.

The results for each archaeological settlement are summarized in Appendix B. Almost half of the settlements have non-unimodal distribution. Based on the median values of each settlements, histogram of arable land density changes for all settlements was also plotted (Figure 3-33). The peak is observed around the value of 70,000. Although there are few settlements having higher density values, it was assumed that this decrease not necessarily meaning that the values lower than the peak value was preferred for settling. They could only be few in numbers. Therefore, the value of highest frequency was maintained in the later analysis. It should also be noted that there could be some reason not to settle on high arable land density values (drainage problems etc.). However, for this study, the approach will be kept simpler.

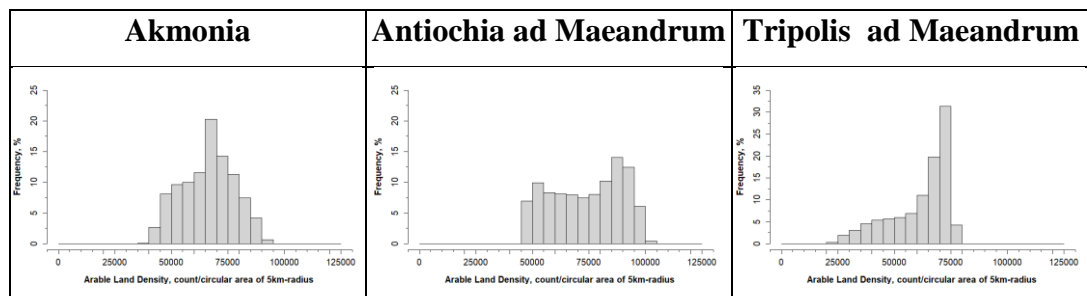


Figure 3-32 Example arable land density distributions at the archaeological sites Akmonia, Antiochia ad Maeandrum and Tripolis ad Maendrum

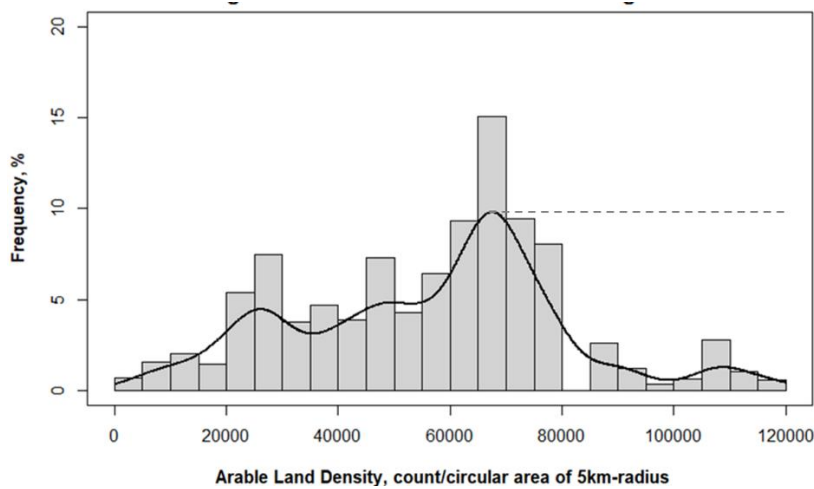


Figure 3-33. Histogram of median arable land density values together with density curve for all the known archaeological settlements in the dataset. The dashed line indicates the arable land density with the highest frequency. It is assumed that the highest frequency value should be maintained while the arable density value increases.

### Potential Map of Arable Land Density

The histograms based on the median arable land density values of archaeological sites were plotted as described in Section 2.2 for each of the 15 datasets (Figure 3-34). Later, the probability density curves for the distributions were obtained using kernel density estimation in R. As mentioned before, in this variable, the value of highest kernel density estimate was maintained as the arable land density value increases (Figure 3-34). In general, the peak value was observed around 70,000.

When transferring these estimated density values to the original arable land density map, the bin size of 117 was used. Later, the density values were normalized between 0 and 1 for a better understanding. Final potential maps for each group were obtained by reclassifying the original arable land density map using the normalized values for each bin interval. The arable land density potential maps for 15 datasets are shown in Figure 3-35. In general, the potential maps indicate that the valleys are more likely places to locate an archaeological site for the studied period.

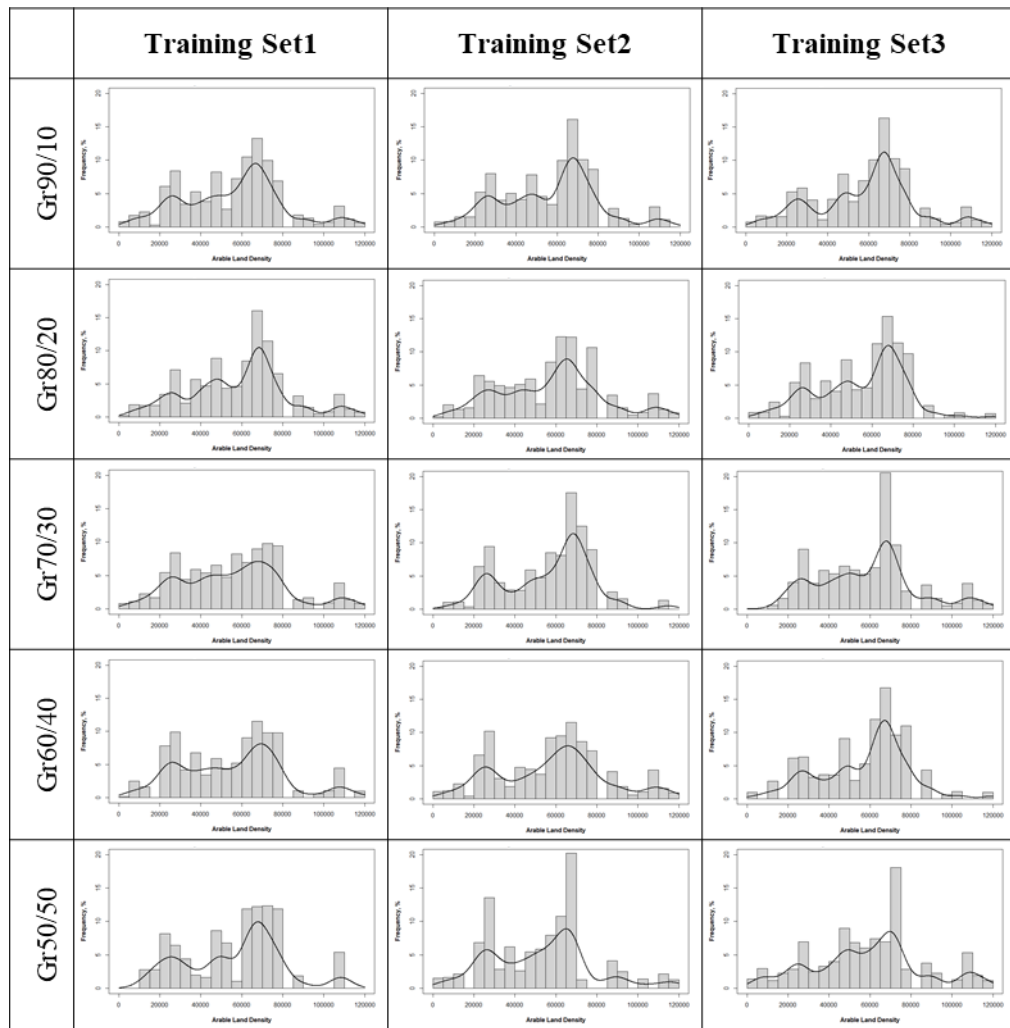


Figure 3-34. Histograms of training data sets with changing percentages and overlaid KDE curves for arable land density

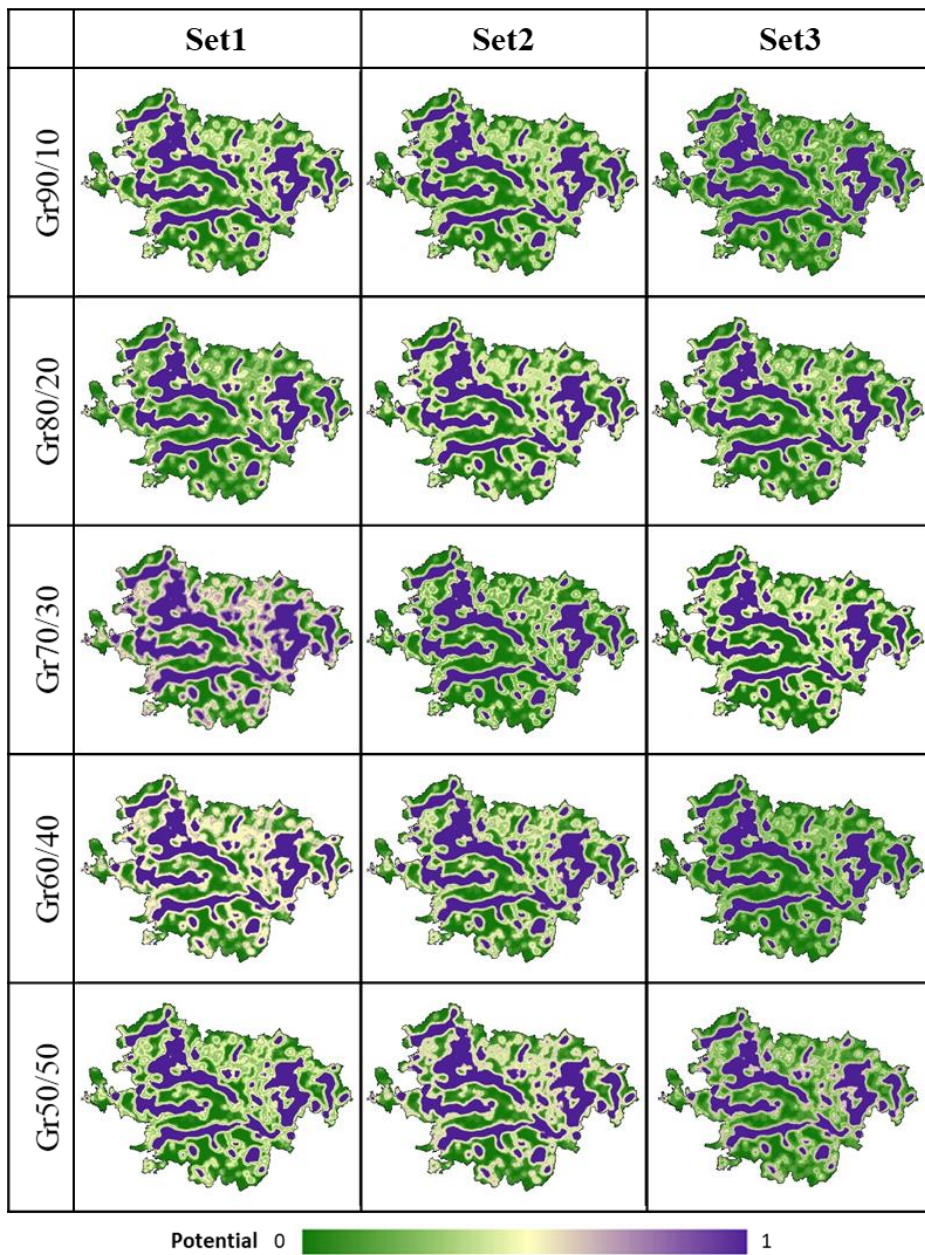


Figure 3-35 Potential maps computed for the arable land density variable based on the 3 sets of 5 groups that have different training and testing data ratio

### Repeatability of Statistical Analysis for Arable Land Density

The correlation matrices between the 15 potential maps were computed (Table 3-9). All groups and sets showed very strong correlation. Even though the arable land was

converted to a continuous map as a density map, it stems from a categorical map. This might be causing the high correlation values. How this situation affects the results is expected to be seen in the next section.

Table 3-9 The correlation matrices between the arable land density potential maps (value $\geq$ 0.8 is in light green)

Groups	Sets	Gr90/10			Gr80/20			Gr70/30			Gr60/40			Gr50/50		
		Set1	Set2	Set3	Set1	Set2	Set3	Set1	Set2	Set3	Set1	Set2	Set3	Set1	Set2	Set3
Gr90/10	Set1	1	1.00	0.99	0.99	1.00	0.99	0.97	0.99	0.99	0.98	0.99	0.99	0.99	0.99	0.98
	Set2	1.00	1	0.99	0.99	0.99	1.00	0.96	0.99	1.00	0.98	0.97	0.99	0.99	0.97	0.98
	Set3	0.99	0.99	1	0.99	0.98	0.99	0.92	0.99	0.98	0.95	0.97	1.00	0.99	0.96	0.98
Gr80/20	Set1	0.99	0.99	0.99	1	0.98	1.00	0.94	0.98	0.99	0.96	0.95	0.99	0.98	0.95	0.99
	Set2	1.00	0.99	0.98	0.98	1	0.99	0.97	0.99	0.99	0.98	0.99	0.98	0.99	0.99	0.98
	Set3	0.99	1.00	0.99	1.00	0.99	1	0.95	0.99	0.99	0.97	0.97	1.00	0.99	0.97	0.99
Gr70/30	Set1	0.97	0.96	0.92	0.94	0.97	0.95	1	0.94	0.97	0.99	0.97	0.93	0.95	0.98	0.95
	Set2	0.99	0.99	0.99	0.98	0.99	0.99	0.94	1	0.99	0.97	0.98	0.99	0.99	0.98	0.97
	Set3	0.99	1.00	0.98	0.99	0.99	0.99	0.97	0.99	1	0.99	0.98	0.99	0.99	0.98	0.98
Gr60/40	Set1	0.98	0.98	0.95	0.96	0.98	0.97	0.99	0.97	0.99	1	0.98	0.95	0.98	0.99	0.95
	Set2	0.99	0.97	0.97	0.95	0.99	0.97	0.97	0.98	0.98	0.98	1	0.97	0.98	1.00	0.96
	Set3	0.99	0.99	1.00	0.99	0.98	1.00	0.93	0.99	0.99	0.95	0.97	1	0.99	0.96	0.98
Gr50/50	Set1	0.99	0.99	0.99	0.98	0.99	0.99	0.95	0.99	0.99	0.98	0.98	0.99	1	0.98	0.97
	Set2	0.99	0.97	0.96	0.95	0.99	0.97	0.98	0.98	0.98	0.99	1.00	0.96	0.98	1	0.96
	Set3	0.98	0.98	0.98	0.99	0.98	0.99	0.95	0.97	0.98	0.95	0.96	0.98	0.97	0.96	1

### Sensitivity of Performance of Arable Land Density

Figure 3-36 shows the potential maps colored based on the cumulative percentages of successfully located archaeological settlements for the training data, particularly 60%, 80%, 90%, 100%. The corresponding cumulative percentage of surface area, cumulative percentage of testing data and the determined limiting potential value are also summarized under the each map. cPLAS-tr of 80% was converted to graphs to compare the potential map outcomes (Figure 3-37). While Figure 3-36 provides a better visualization, the graph in Figure 3-37 provides better understanding of the response of training and testing data and the influence of sample size on the performance of variable.

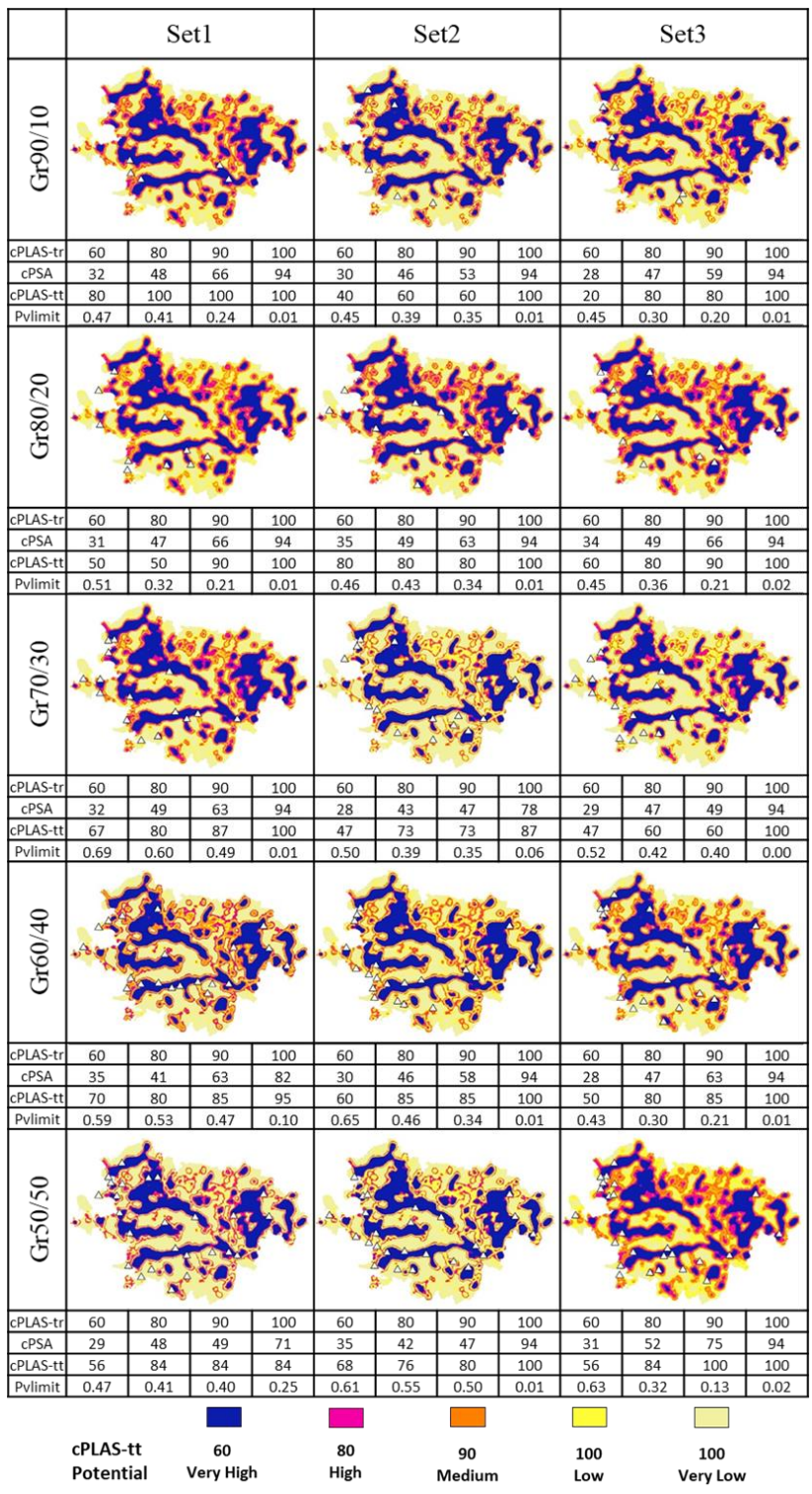


Figure 3-36 Comparison of arable land density potential map outcomes colored based on successfully located archaeological sites of training data and overlaid with testing data locations.

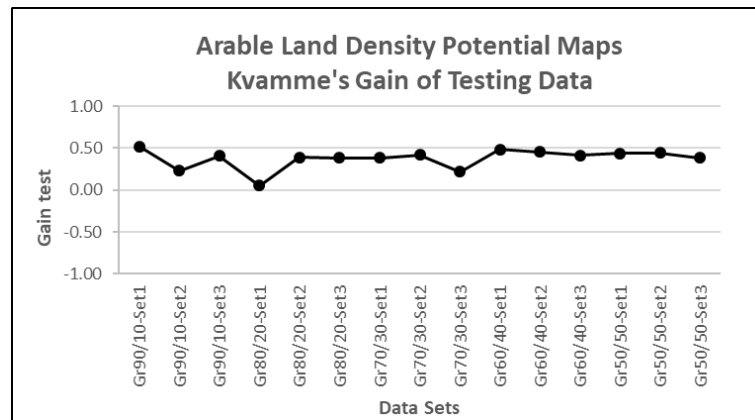
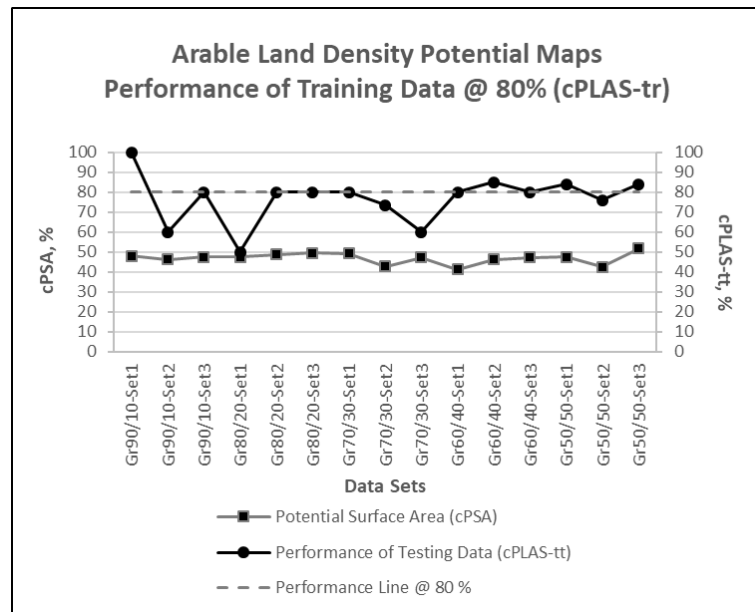


Figure 3-37 The effect of sample size on the potential surface area and the performance of testing data among the groups (A) and Kvamme's gain values for the testing data (B) when 80% success rate is assumed in locating archaeological sites of training data for the arable land density variable.

Figure 3-36 shows that the transition zone from arable land to the mountainous area was more preferred for settling. There are minor differences among the potential maps of the groups. On the other hand, they seem generally successful in reducing the potential surface area.

Figure 3-37 (A) shows the percent of surface area at which 80% of training data were successfully located for the groups. The variation in cPSA (in average 47%) is very small for the groups. The variation in cPSA slightly increases towards Gr50/50. The performance variation is high in the groups with few testing data as expected. The calculated gain values for the testing data is given in Figure 3-37 (B). The values changes from 0.22 to 0.52 except Gr80/20-Set1.

### **Basic Archaeological Results from Arable Land Density**

The results of arable land density potential maps were further looked for the archaeological sites. All of the archaeological settlements available in the datasets were ordered with decreasing potential as explained in Section 2.3.2. (Appendix C).

The top 5 and the bottom 5 of the archaeological settlements are same for all of the datasets. The top 5 includes the archaeological settlements of Akmonia, Alabanda, Antiochia ad Maeandrum, Apamea and Apollonis. The bottom 5 includes the archaeological settlements of Notion, Phocaea, Heraclea ad Latmum, Amyzon and Attouda. Due to high similarity of the potential maps, the order of archaeological settlements' potentials have minor differences among the datasets. 3 out of 5 archaeological settlements listed at the bottom area coastal settlements (i.e. Notion, Phocaea and Heraclea ad Latmum) and other 2 (Amyzon and Attouda) are located at mountainous area. This might indicate that arable land presence was less important for these sites compared to the other variables. They might have other natural resources or economical input to compensate the absence of arable land.

#### **3.4.2. Access to Water**

Access to water is crucial, therefore various water-related variables (e.g. distance to stream, distance to spring, and ground water table) are incorporated into archaeological predictive models. However, the integration of these variables is often limited and not well-considered (Church et al. 2000). Topographic features like depressions and drainages are considered as indicators of water resources, without

considering the duration (short and long term) of water availability, its quality, or other factors that could affect its availability such as geomorphological and geological influences. Water availability is also directly influenced by climatic change (Hay et al. 1993). Kvamme (1992) warns on the use of hydrological factors like water table at the predictive modelling for the prehistoric settlements at Pinon Canyon Archaeological Project in Las Animas County, southeastern Colorado due to the possible effect of climatic changes on the variable.

The water supply systems like dams, cisterns, aqueducts and wells have been used since prehistoric times to access water (Mays et al. 2012). As a result, the ways in which water was supplied to the poleis during the Hellenistic period were diverse. For instance, the drinking water in Hierapolis was delivered through pipes and channels, sourced from springs located between 6.3 km to 13.5 km away (Scardozzi 2020). Metropolis had limited evidence of rainwater cisterns. The city was clearly relied on piped water. There are two springs on the slopes behind Metropolis that may have served as possible water sources (Hill 2016). In Ephesus, a deep layer of weathered mica schist between the Bülbül and Panayır mountains where the city was located acted as an aquifer, collecting both surface and underground water from the hills and draining under the agora. Houses on the hills had wells that accessed this underground flow (Crouch 2003).

When developing a map of water availability for predictive modeling, it was crucial to include all possible water sources used during the studied period and region as a single variable to prevent bias. However, this could not be possible for this study.

### **3.4.3. Rock Types Used in the City Walls**

As discussed in Section 1.5.1., during the Hellenistic period in Asia Minor, maintaining stability was a challenge due to internal conflicts and wars with outside forces. The Hellenistic kings relied on the cities of Asia Minor to maintain power and generate income through the management of resources such as land. Therefore, these cities were often protected by fortifications (McNicoll and Milner 1997).

Since city walls were a defining feature of poleis (Hansen and Nielsen 2004), the rock types used in their construction were considered as a possible variable for identifying locations of unknown archaeological sites. Table 3-10 lists the rock types used in the city walls of some known settlements and compares them to the local geology using geological maps of Türkiye at 1:500,000 and 1:25,000 scales (published by Mineral Research Institute of Türkiye (MTA)). It was found that the rock types used in the walls were typically from the immediate surrounding area, in other words, there were no preference towards certain rock types. Therefore, no further analysis was performed.

On the other hand, a possible use could be eliminating unused rock type/lithology as a building material in city walls, but the detail of the existing maps was not sufficient for such analysis.

Table 3-10 Rock types observed in the city walls and local geology (1:25.000 scale)

City	City Wall Stones (McNicoll and Milner 1997)	Lithology	Description
<b>Alabanda</b>	Mainly gneiss, but blocks of granite also exist	Alluvial Sandstone-Mudstone-Limestone Migmatite-Gneiss	Undifferentiated Quaternary
<b>Alinda</b>	Gneiss	Alluvial Conglomerate	Metagranitoids Continental clastic rocks
<b>Ephesus</b>	Built of the limestone which forms the Bülbüldağı massif	Marble Alluvial Schist Conglomerate-Sandstone-Mudstone	Alluvial fan, slope debris, moraine etc. Marble Undifferentiated Quaternary
<b>Heraclea ad Latmum</b>	Granite	Alluvial Augen Gneiss-Metagranitoid	Metagranitoids
<b>Miletus</b>	Limestone, some marble and rarely gneiss are used	Alluvial Conglomerate-Sandstone-Mudstone Limestone	Undifferentiated Quaternary Lacustrine carbonate rocks Continental clastic rocks
<b>Priene</b>	Blue-grey marble	Alluvial Marble	Undifferentiated Quaternary, Marble, Schists

### **3.5. Predictive Map**

For this study, several variables were considered including elevation, ruggedness, slope, aspect, arable land density, access to water, and rock types used in the city walls. However, rock type was eliminated as it did not provide significant information for the characterization of archaeological site locations. Elevation was also eliminated due to the low prediction ability caused by spatial autocorrelation, and access to water was eliminated due to the difficulty in producing a representative base map of water sources.

The remaining variables are first tested for the reproducibility of the proposed statistical method. The potential maps of variables that pass the tests having the most appropriate sample size are used to produce the predictive map. Later, the predictive map is assessed for its performance using the testing dataset. If the performance of output is considered satisfactory, the predictive map is reproduced with the full dataset (i.e. all of the known archaeological sites).

During the investigation of variables, incorporation of a socio-cultural feature to the predictive map had also been explored. A new way of inclusion of road network as a socio-cultural variable was developed, which we believe will improve the predictive map. This improvement is discussed in the Section 3.7.

With this improvement, the final predictive map was produced, which we will evaluate in Section 3.8.

#### **3.5.1. Responses of Variables to the Proposed Statistical Method**

Until now, 15 (5 groups x 3 sets) potential maps for each variable were calculated in order to control reproducibility of the statistical analyses suggested and the effect of sample size on the model response. The performances of each potential map were also evaluated with the Kvamme's gain statistics.

The results of repeatability analyses for each variable and for each group is summarized in Table 3-11. The groups having R<sup>2</sup> values greater than 0.7 for all their sets were considered producing repeatable results for all variables.

For these remaining groups, Table 3-12 shows the Kvamme’s gain statistics calculated for the testing data and the potential surface area percentages of which the limiting values were determined based on the 80% of successfully located training data. Gr90/10 and Gr70/30 had comparable results. Only once, set1 of Gr90/10 shows negative gain probably as a result of low sample size of the testing data (5 out 51). Gr80/20 (except ruggedness) showed comparable results too. All of the gain values of Gr70/30 were found as positive.

The results have shown increased stability at Gr70/30, indicating that the proposed method can reliably establish relationships with a sample size of at least 35, and can be tested with a test data size of at least 15.

Table 3-11 The summary of repeatability analysis for the groups.

	Ruggedness	Slope	Aspect	Arable Land Density
Gr90/10	✓	✓	✓	✓
Gr80/20	✓	✓	✓	✓
Gr70/30	✓	✓	✓	✓
Gr60/40	✓	X	X	✓
Gr50/50	✓	X	X	✓

Table 3-12 The summary of gain statistics based on the testing data and the potential surface area percentages when the potential limit value is determined based on the 80% of training data successfully located for the groups having good repeatability

		Ruggedness		Slope		Aspect		Arable Land Density	
		Gain	cPSA	Gain	cPSA	Gain	cPSA	Gain	cPSA
Gr90/10	Set 1	0.36	64.43	0.49	51.46	-0.15	45.81	0.52	47.98
	Set 2	0.48	41.28	0.42	46.71	0.47	53.15	0.23	46.13
	Set 3	0.41	46.87	0.46	43.20	0.36	51.04	0.41	47.46
Gr80/20	Set 1	-0.89	75.52	-0.01	40.56	0.40	54.01	0.05	47.43
	Set 2	0.63	32.96	0.51	44.54	0.21	47.62	0.39	48.70
	Set 3	0.04	77.18	0.45	43.84	0.41	53.19	0.38	49.29
Gr70/30	Set 1	0.12	64.40	0.29	61.24	0.31	50.92	0.38	49.27
	Set 2	0.32	50.10	0.43	41.62	0.46	53.55	0.42	42.57
	Set 3	0.14	68.99	0.47	49.09	0.22	51.76	0.22	47.05

### 3.5.2. Independence of Variables

The variables analyzed for the settlement location preferences in this study are derivatives of or to some extent related to the topography of study area. Therefore, the independence of variables were checked before moving forward. Since the processed maps (i.e. potential maps) will be unified as the predictive map, their correlation matrices were calculated (Table 3-13). The  $R^2$  values between Set1 and Set2 were very close to each other while Set3 had slightly different values. There is a positive correlation between ruggedness and slope variables. These variables are negatively correlated with arable land density. Aspect has very low correlation with any variables. The higher the correlation is, than there is more possibility to have dependency between the variables. The threshold value for  $R^2$  is selected as 0.75 based on the similar studies. As a result, all of the variables are used in the predictive map.

Table 3-13 Correlation matrices of four variables for the sets of Gr70/30

<b>Gr70/30-Set1</b>	<b>Ruggedness</b>	<b>Slope</b>	<b>Aspect</b>	<b>Arable Land Density</b>
<b>Ruggedness</b>	1.00	0.66	0.02	-0.29
<b>Slope</b>	0.66	1.00	0.01	-0.26
<b>Aspect</b>	0.02	0.01	1.00	0.00
<b>Arable Land Density</b>	-0.29	-0.26	0.00	1.00
<b>Gr70/30-Set2</b>	<b>Ruggedness</b>	<b>Slope</b>	<b>Aspect</b>	<b>Arable Land Density</b>
<b>Ruggedness</b>	1.00	0.66	0.01	-0.22
<b>Slope</b>	0.66	1.00	0.01	-0.16
<b>Aspect</b>	0.01	0.01	1.00	0.00
<b>Arable Land Density</b>	-0.22	-0.16	0.00	1.00
<b>Gr70/30-Set3</b>	<b>Ruggedness</b>	<b>Slope</b>	<b>Aspect</b>	<b>Arable Land Density</b>
<b>Ruggedness</b>	1.00	0.55	0.02	-0.50
<b>Slope</b>	0.55	1.00	0.02	-0.32
<b>Aspect</b>	0.02	0.02	1.00	0.00
<b>Arable Land Density</b>	-0.50	-0.32	0.00	1.00

### 3.5.3. Unification of Variables

The addition method was used to produce the predictive map out of the potential maps of each variable. No extra weighting procedure was used. Each map was continuous and normalized. The process of addition done was simply as follows:

$$\text{Predictive Map} = (\text{Ruggedness} + \text{Slope} + \text{Aspect} + \text{Arable Land Density}) / 4$$

Since the repeatability of results were shown, for the sake of practicality, only the predictive map based on Gr70/30-Set1 was calculated and named as PM70/30-Set1 (Figure 3-38). The predictive map was colored in 10% quantile. Each quantile has same number of pixels; hence each color range presents 10% of the study area. The higher the quantile percent range is, the more likely is to come across an archaeological settlement.

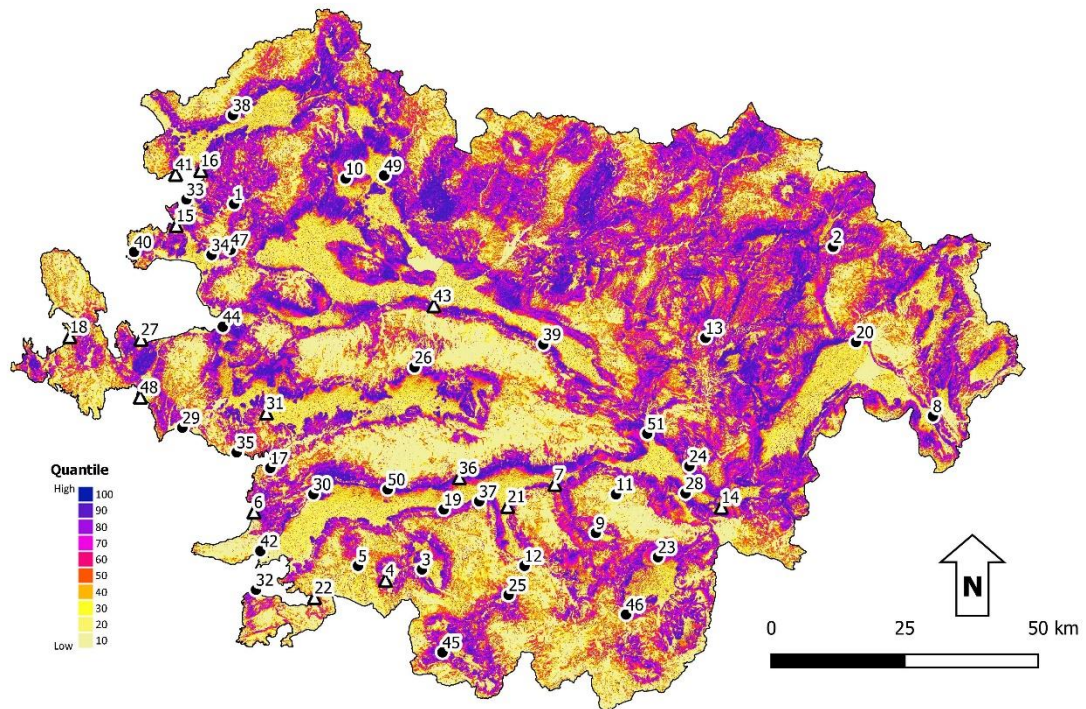


Figure 3-38 Predictive map (PM70/30-Set1) produced from Gr70/30-Set1 (training data in black dots, testing data in white triangles).

### 3.6. Performance of the Predictive Map

During the analysis of many variables, the archaeological settlements had been represented as polygonal areas. Two different sized areas were used for the representation:

- 1 - Circular area with a 350 m of radius for topographical variables
- 2 - One-hour of walking distance away from the settlement for arable land density variable

Figure 3-39 shows the polygonal areas used for the archaeological settlement of Nysa, which was a testing data for the predictive map of PM70/30-Set1. When determining whether a testing data was successfully located in a certain area, the buffer zone of one-hour walking distance was used because it covers other polygonal areas as well.

The pixels within the one-hour walking distance away from each testing data were split with the same range values of the quantiles of the corresponding predictive map. At which quantile range that 30 % of the total count of pixel values in this buffer zone was reached was determined. Then, the testing data was considered as successfully located at this quantile range.

As an example, the number of successfully located training, testing and overall data in each quantile for PM70/30-Set1 is shown in Table 3-14. In general, they showed similar trends as expected. 80% and above of the archaeological settlements were found as located at ca. 50 % of the study area. There was no known archaeological settlements at 30% of the study area.

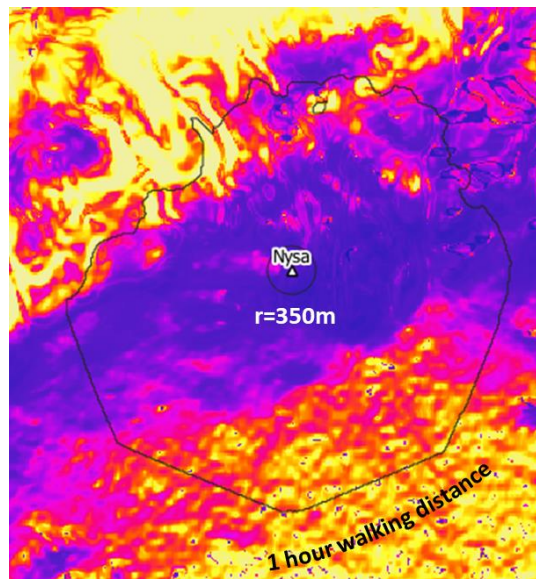


Figure 3-39 Example presentation of two buffer zones used in the statistical analysis of variables for the archaeological settlement Nysa (as a testing data over PM70/30-Set1).

Table 3-14 Comparison of successfully located training, testing and overall data in each quantile for the predictive map PM70/30-Set1

PM70/30-Set1									
	Training data			Testing data			Overall		
quantile	#	cum. #	cum.%	#	cum. #	cum.%	#	cum. #	cum.%
100 - 90	2	2	6	1	1	7	3	3	6
90 - 80	12	14	39	2	3	20	14	17	33
80 - 70	11	25	69	6	9	60	17	34	67
70 - 60	3	28	78	2	11	73	5	39	76
60 - 50	2	30	83	3	14	93	5	44	86
50 - 40	4	34	94	1	15	100	5	49	96
40 - 30	2	36	100	0	15	100	2	51	100
30 - 20	0	36	100	0	15	100	0	51	100
20 - 10	0	36	100	0	15	100	0	51	100
10 - 0	0	36	100	0	15	100	0	51	100

There is no clear range of gain values that can be suggested for a “good model”. This depends on the contribution seek during the study. A review of gain values and its interpretation, which is rare to observe in the literature, is done by Verhagen (2007). He draws attention to the significance of the accuracy of predictive modelling. He asks whether a model with 60% of archaeological sites in a 30% of surface area or a model with 80% of archaeological sites in a 40% of surface area is better. Both models have 0.5 Kvamme’s gain. He emphasizes on the higher risk of coming across an archaeological settlement at the first model because the remaining surface area for low potential (70%) is greater than the second model’s remaining low potential surface area.

As seen in Table 3-15, the model developed has a performance of 0.49 Kvamme’s gain. The proposed method produced significant results from the used variables for

the studied period and region. Now, using all of the known archaeological settlements, the predictive map was built and named as PMAII (Figure 3-40).

Table 3-15 Kvamme’s gain value for the predictive map PM70/30-Set1

	<b>PM70/30-Set1</b>
<b>Surface area, %</b>	41
<b>Testing data within that area, %</b>	80
<b>Kvamme’s Gain</b>	<b>0.49</b>

The distribution of high and low potential values in the study area creates distinct zones on the predictive map, but without sharp boundaries due to the use of continuous data analysis instead of classification into zones during the model development. The majority of the poleis is situated in valleys alongside major rivers such as Büyük Menderes, Küçük Menderes, Gediz, and Bakırçay, particularly at the base of nearby mountains. The sites in the southern and northeastern parts of the study area share also somehow similar characteristics, only the plains formed by the tributaries of rivers are less developed in these regions. Table 3-16 displays the distribution of settlements across the predictive map's 10% quantiles, including the names of each settlement within those quantiles. 78% (40 out of 51) of poleis in the dataset are located at 40% of the study area. In addition, ca. 30% of the study area might hardly have an unknown archaeological settlement from this period in this region.

The Kvamme’s gain values for both predictive maps (PM70/30-Set-1 and PMAII) were found as 0.49. While the input sample size for the PM70/30 was 36 during the model building, the input sample size of PMAII was 51, indicating that the predictive map was strongly indicative of the studied settlements and region. It was not affected significantly with the addition of new settlement.

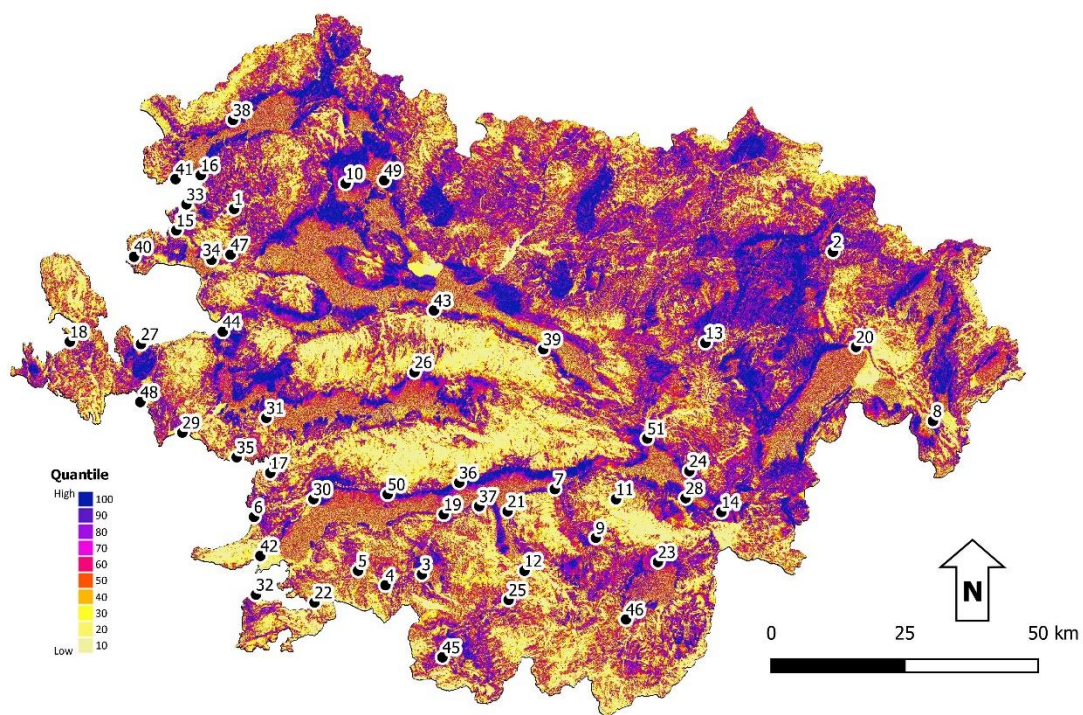


Figure 3-40 PMAI, the predictive map produced using all of the known archaeological settlements in the dataset.

Table 3-16 The number of settlements in each quantile at PMAI

PMAI				
quantile	PVlimit	#	cum. #	cum.%
100 - 90	1 - 0.72	5	5	10
90 - 80	0.72 - 0.66	12	17	33
80 - 70	0.66 - 0.62	10	27	53
70 - 60	0.62 - 0.58	13	40	78
60 - 50	0.58 - 0.55	5	45	88
50 - 40	0.55 - 0.52	4	49	96
40 - 30	0.52 - 0.48	2	51	100
30 - 20	0.48 - 0.44	0	51	100
20 - 10	0.44 - 0.37	0	51	100
10 - 0	0.37 - 0	0	51	100

### **3.7. Improvement of Predictive Map using a Socio-Cultural Feature: Road Network**

The mobility across the poleis was high in the Hellenistic period (Oliver 2015). Available manpower was critical in defense of the poleis and also in the commercial activities. The poleis needed to demonstrate and advertise their qualities to attract manpower to their cities. The new Hellenistic poleis in the western Türkiye were founded along strategic long distance communication routes from the late 4th and 3rd centuries (Hill 2016). For example, Nysa, Seleucia-Tralleis (a refoundation) and Antioch-on-the-Maeander were newly founded poleis along the key artery between the Aegean and northern Syria (Kosmin 2014). The major difficulty for this variable was to achieve the correct road map without missing any routes for the interested period. It was sure that a settlement was located along the road.

The GIS based modelling of road networks have been studied in archaeology since 1990s and distance to road lines were one of the most commonly used variables in archaeological predictive modelling (e.g. Balla et al. 2013, Revert 2017). Later, different studies started to appear focusing on the network nature of the road lines and finding the “optimal” path between the cities. Verhagen et al. (2019) provided an overview for the current approaches available in this topic. The common attitude appears as to reconstruct the roadlines existed during the interested period.

In this study, also firstly, the reconstruction of road network of Hellenistic period had been attempted. The overlaps of ancient road network of Barrington Atlas, milestones of David French<sup>6</sup> and main roads of the modern road network without highways were used to reach the road network of the period as accurate as possible and as complete as possible. However, the resulting road network for the studied period was either obviously missing some routes or having additional extra routes of which existence could not be sure.

---

<sup>6</sup> Digitized copy of milestones from the book of Roman Roads and Milestones of Asia Minor by David French (courtesy of Michele Massa).

Later, the travel-time between settlements were focused. The distance between settlements are expected to change based on the travelling conditions, but the travel time or the effort spent should be approximately same. The optimum travel time between locations was determined using the least cost path analysis (LCP). LCP methodologies and its use in archaeology is well discussed by Herzog (2014). As the name of analysis implied, the algorithm aims to find the cheapest route between two targets based on the defined cost components. There are various cost components like slope, wetlands, vegetation cover, altitude etc. Slope is the most commonly used one in the archaeological LCP studies (Herzog 2014) and it is the only cost used in this study as well.

The cost of varied slope was estimated based on the human movement model developed experimentally by Irmischer and Clarke (2018) on-road. The model gives the walking speed of a person at the different terrains as follows:

$$Speed(m/s) = 0.11 + e^{\frac{-(Slope+5)^2}{2 \times 30^2}} \quad \text{where: } Slope = \frac{\Delta \text{elevation}}{\Delta \text{distance}} \times 100$$

The reciprocal of the equation provides the time required travelling from one location to another.

Esri's ArcGIS Path distance tool was used for the cost calculations. Slope is anisotropic, in other words, the direction of movement over a raster cell for example having 10 degrees slope will affect the walking speed of the traveler. If the traveler is walking uphill, the cost will be higher compared to when walking downhill. This effect was included to the cost calculations using vertical friction factor in the Path distance tool (Tripcevich 2009). The tool outputs the least accumulated cost away from source cell(s) to any other cell in the given area.

The least accumulated cost was calculated from each archaeological settlement to each cell in the study area considering them as a starting point. Thus, the necessary time to reach any cell away from the archaeological settlement became known. The

travel-time raster map away from the settlement of Euphippe is given as an example in Figure 3-41. The nearest settlement to Euphippe, namely Nysa, requires 4 hr 7 min of travelling. These individual maps were used to estimate the travel-time between the settlements for the study area.

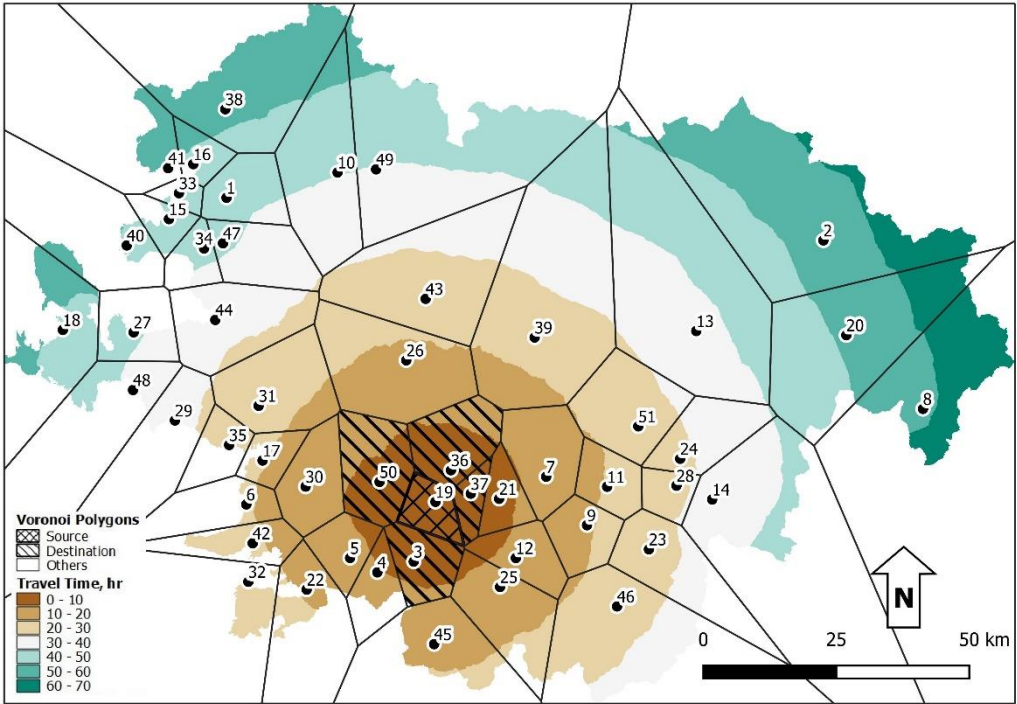


Figure 3-41 Example for travel-time raster map for Euphippe (No:19) and overlaid Voronoi polygons created using all of the known archaeological settlements

The raster maps showing the travel time away from each archaeological site were calculated. Then, the steps were followed given in Section 2.2.2. to determine the travel-time between all of the known archaeological sites.

First, the Voronoi polygons were created using the archaeological sites. Figure 3-41 shows the travel-time map of the archaeological settlement of Euphippe (No:19) and the Voronoi polygons created using the archaeological sites as an example. Next, The travel-time information was collected from the raster map for the source settlement

(No:19) and the destination settlements which were located at the neighbouring Voronoi polygons (No:3, 36, 37 and 50). This approach smoothed the travel-time between the settlements due to the unknown roads in the region and provides more general and characteristic value. Four settlements (i.e. Nysa, Orthosia, Tralles and Alabanda) were located at the neighbouring Voronoi polygons of Euphippe. Nysa had the shortest travel-time (4 hr 7 min) from Euphippe. Orthosia, Tralles and Alabanda had the travel-times of 4 hr 12 min, 7 hr 21 min, and 6 hr 54 min respectively. In the following calculations, all of these four values were used as characteristic travel-time from Euphippe to the neighbouring settlements.

Using the travel-time for all archaeological settlements between the settlements and the settlements located at the neighbouring Voronoi polygons were collected. This data is presented as a histogram in Figure 3-42. The travel-time between settlements was found as around 7.5 hours at maximum. Later, the probability density curve for the distribution was obtained using kernel density estimation in R. If the archaeological sites in the study area were fully known, there should not be any decrease in the graph after a certain travel-time. Therefore, in the calculation of potential map, after the highest kernel density estimate, the value was maintained even if the travel-time continue to increase (Figure 3-42).

The estimated density values were transferred to the travel-time map using the bin size of 0.058 hr (or 3.5 minutes) as described in Section 2.2. Finally, the density values are normalized between 0 and 1 for a better understanding and the resulting map was displayed with 10% of quantile change in Figure 3-43. Since the highest kernel density value was maintained, a large and continuous area became high potential for locating the unknown archaeological settlements at the northeast of the study area due to the low data availability there. On the other hand, while during the statistical approach development, the travel-time variable was considered such that the chance of being any settlement close by to the known settlements would be low, and the potential values increase away from the known settlements indicating that it gets more likely to come across a/an new/unknown archaeological settlement.

To incorporate this input into the existing predictive map, the raster map was transformed into two categories: site likely and site not likely, with a threshold potential value of 0.5 (as shown in Figure 3-43). This approach aims to eliminate locations that share similar site characteristics with known archaeological sites, but where site occurrence is unlikely due to the presence of other sites nearby. This strategy addresses the limitations of the following arguments:

- APMs can identify locations with similar site characteristics; it does not guarantee the presence of archaeological sites at all such locations (Kvamme 1988).
- Sites are not independent entities but rather components of a system, whose locations depend on the locations of other system components, including other sites (Ebert 2000).

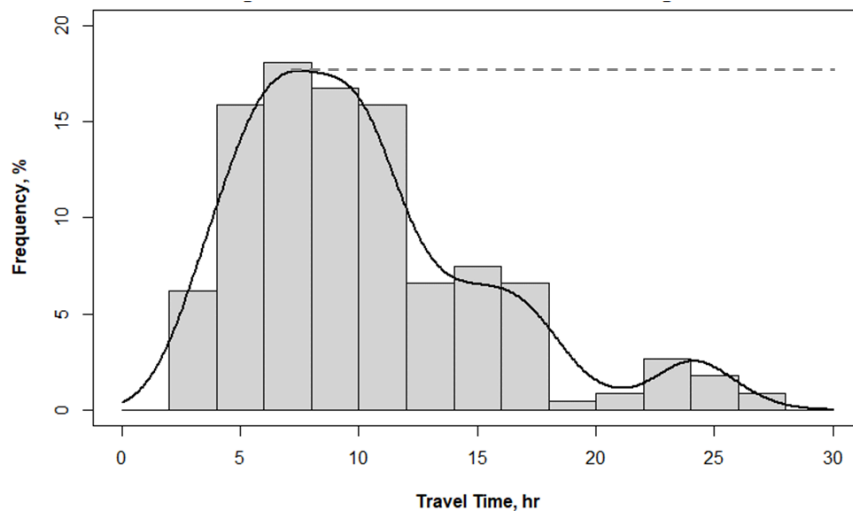


Figure 3-42. Histogram of travel-time away from all of the known archaeological sites to their neighbouring sites with the overlaid KDE curve. The dashed line indicates the travel-time having the highest frequency, which is evaluated as the maximum possible travel-time in the study area for the dataset used.

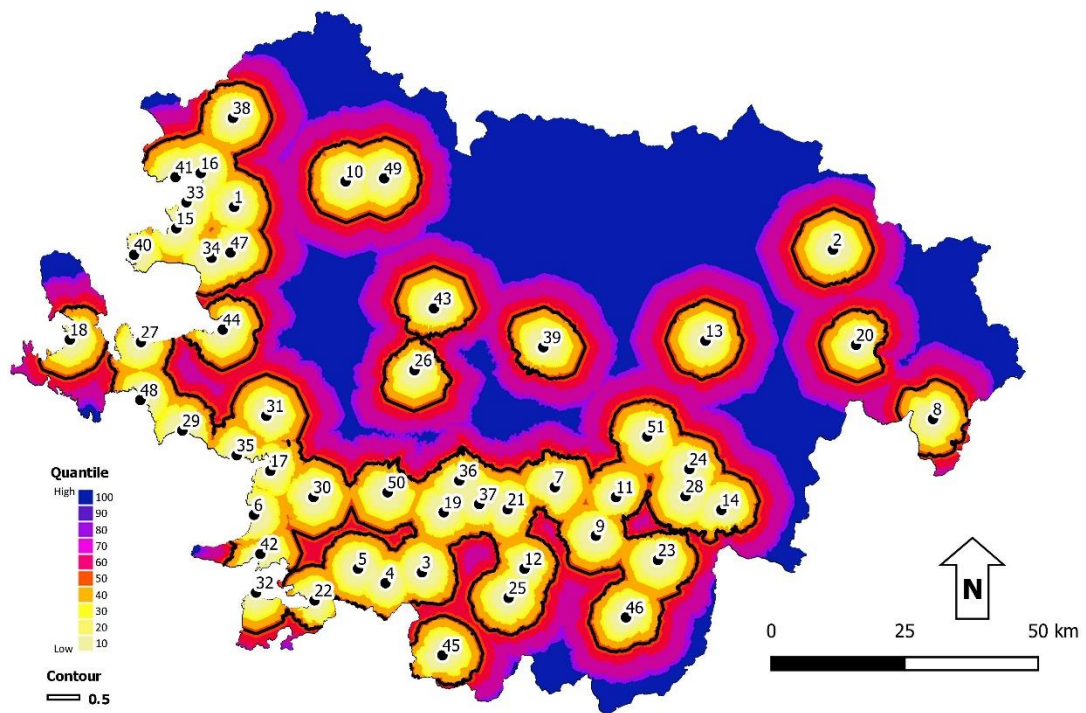


Figure 3-43 Potential map produced based on the travel-time between settlements. The contour value of 0.5 (black line) indicates the boundary between site-likely and site-not-likely areas.

Lastly, the sensitivity of this analysis to the sample size was also investigated using the sample input data of Gr70/30-Set1. The travel-times between the training settlements (36 out of 51) and the settlements located at their neighbouring Voronoi polygons were collected. The KDE curve calculated from Gr70/30-Set1 was compared to the KDE curve produced based on all of the known archaeological settlements (Figure 3-44). There is a very slight difference that can result in a small effect at the site-likely and site-not-likely boundary around each settlement. On the other hand, we should be aware of that any addition of new site will have significant contribution to the evaluation of the predictive map.

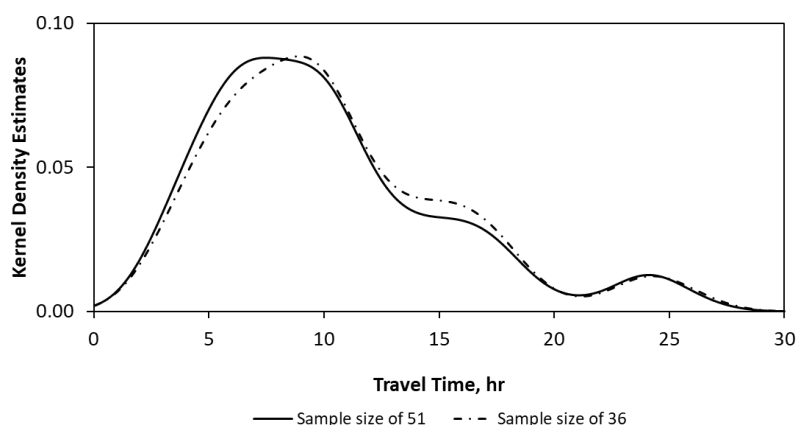


Figure 3-44 Comparison of KDE curves calculated based on the travel-time away from Gr70/30-Set1 and all of the known archaeological sites to their neighbouring sites.

### 3.8. Evaluation of the Model

The final predictive map is shown in Figure 3-45, which was formed of PMAll and the overlay of the contour line showing the boundary between site-likely and site-not-likely areas.

#### 3.8.1. General Evaluation

This study explored where ancient Greek city-states (called poleis) preferred to settle during the Hellenistic period in the western Türkiye. The factors elevation, terrain, slope, aspect, arable land density, access to water, and the type of rock used for building city walls were examined. The results indicated that the poleis tended to settle in low to medium rugged terrain, with moderate slopes and access to arable land within an hour's walk. The predictive map created narrowed down potential settlement areas to 41%, within which 80% of known archaeological settlements were located. The map identified approximately 26 high-potential zones for settlements in the study area (see Section 3.8.2 for details). However, more data and variables are needed for the northeastern region of the study area to better identify potential settlement locations.

Table 3.17 shows how settlements are distributed across the predictive map's 10% quantiles, including the names of each settlement within those quantiles. In the top 10%, Smyrna, Akmonia, Nysa, Elaea, and Laodicea ad Lycum were found, but no clustering was observed among them (Figure 3-45). At the bottom 20%, Alinda, Notion, Miletus, Attouda, Priene, and Bargasa were found. These settlements are located in the Büyük Menderes valley and its southern regions, with Notion, Miletus, and Priene situated on the coast, and Alinda, Bargasa, and Attouda located at relatively higher hilltops compared to others. However, after reviewing the input data following the results, it was suspected that the location of Bargasa may not be as accurate as initially thought. Additionally, these settlements may be less comparable to other sites. Further archaeological research may shed light on this.

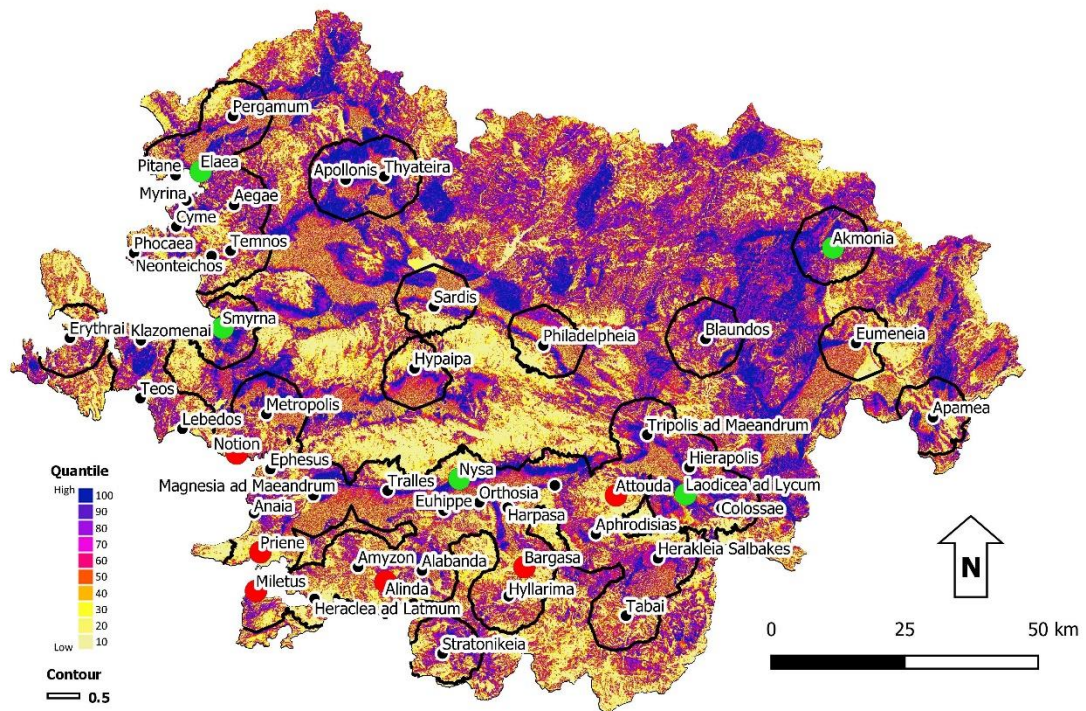


Figure 3-45 Predictive map showing the archaeological sites that are located at the highest potential zones (green dots) and that are at the lowest potential zones (red dots)

Table 3-17 The number of settlements in each quantile and the name of settlements in these quantiles at the final predictive map

<b>Final Predictive Map</b>						
quantile	PVlimit	#	cum. #	cum.%	Name of the Settlements	
100 - 90	1 - 0.72	5	5	10	Smyrna Akmonia Nysa	Elaea Laodicea adLy.
90 - 80	0.72 - 0.66	12	17	33	Herakleia Salbakes Tralles Apamea Apollonis Magnesia adM. Hierapolis	Tripolis adM. Pergamum Hypaipa Colossae Eumeneia Anaia
80 - 70	0.66 - 0.62	10	27	53	Blaundos Antiochia adM. Hyllarima Harpasa Aphrodisias	Stratonikeia Sardis Pitane Cyme Alabanda
70 - 60	0.62 - 0.58	13	40	78	Myrina Thyateira Orthosia Neonteichos Tabai Aegae Euhippe	Temnos Philadelpheia Metropolis Erythrai Lebedos Teos
60 - 50	0.58 - 0.55	5	45	88	Klazomenai Phocaea Heraclea adLa.	Amyzon Ephesus
50 - 40	0.55 - 0.52	4	49	96	Alinda Notion	Miletus Attouda
40 - 30	0.52 - 0.48	2	51	100	Priene	Bargasa
30 - 20	0.48 - 0.44	0	51	100	None	
20 - 10	0.44 - 0.37	0	51	100	None	
10 - 0	0.37 - 0	0	51	100	None	

### **3.8.2. Regional Evaluation**

#### **3.8.2.1. Küçük Menderes and Büyük Menderes Valleys and their Southern Regions**

The map shows the high potential and site likely locations for archaeological sites in the Küçük Menderes and Büyük Menderes river regions, and their southern areas (Figure 3-46). The polis settlements were located along the transition zone between the valleys and mountains. The ones located along the valleys formed by the tributaries of the Büyük Menderes River in the south have shown also similar characteristics. On the other hand, the high potential zones became less clear towards the south as the plains formed by rivers get narrower in size.

After examining the high potential zones and likely site areas, it was estimated that approximately 11 or more archaeological sites could be located in this region, with four around the Küçük Menderes River, three around the Büyük Menderes River, and eight in the south of the Büyük Menderes River (Figure 3-46). Some of these locations have been looked into more closely.

For example, a high potential and likely site area (P04) was observed at the east of Nysa. After researching this zone, the Roman settlement of Mastaura was found in the high potential zone (Willet 2020). Mastaura, did not exist in the Pleiades Project database or any other major sources controlled from the literature for the Hellenistic polis settlements. On the other hand, one study states that there are reasons to suggest that Mastaura might have had the status of a town during the Hellenistic period (Nollé 2016).

Another high potential and site-likely area observed (P06) was the location of Burunköy village near Söke, Aydın. After a further research, it was found that 12 rock tombs were discovered in the area and were taken under government protection (Aydın Kültür Varlıklarını Koruma Bölge Kurulu 2017). The dates of the tombs were

not precisely known, but they were believed to be from the late Hellenistic or Roman period.

Near the other high potential and site-likely zones, there are sites that their approximate locations overlap with these particular areas (P01, P02, P03, P05, P07, P08, P09, P10). These sites were often digitized from the Barrington Atlas of the Greek and Roman World as part of the Pleiades Project. Some of the sites have additional references from ancient texts and/or surveys, which were used to assess the site's name, location, and period with confidence. The names of the sites listed in these particular areas for the Hellenistic period include Oroanna, Larisa, Kaira, Gevele, Syneta, Kavaklı, Neapolis, Görle, Astragon, and Apollonia Salbakes. The information from the Pleiades Project and the predictive map complement each other, increasing the site potential in these particular areas.

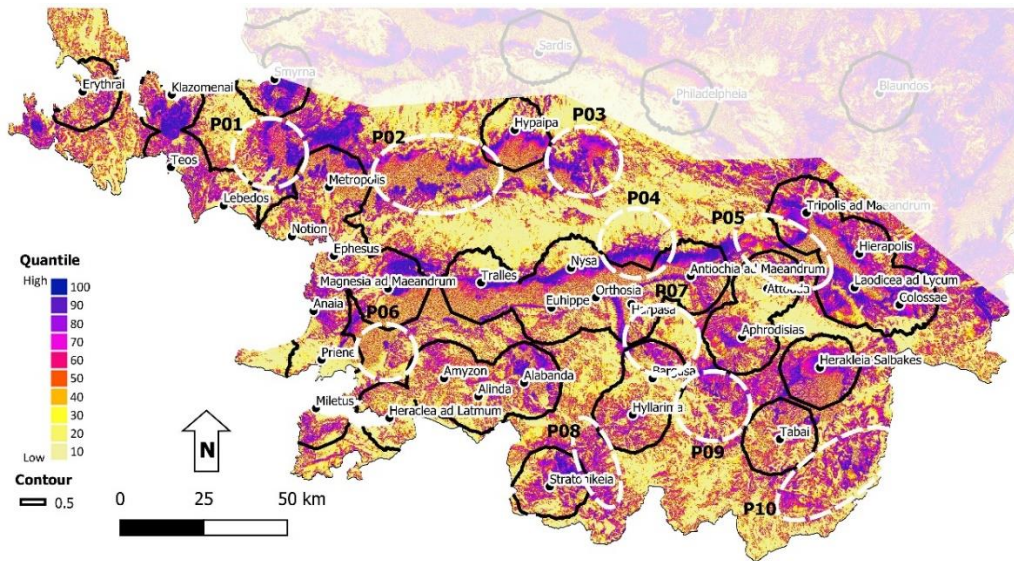


Figure 3-46 Predictive map for Küçük Menderes and Büyük Menderes valleys and their southern regions. The overlaid black contour line shows the boundary between site-likely and site-not-likely areas. The dashed white circles are potential zones where site-likely areas and the locations indicated by ancient texts overlap.

### 3.8.2.2. Gediz ve Bakırçay Valleys

The predictive map for the Gediz and Bakırçay valleys is shown in Figure 3-47, together with the boundary drawn based on travel-time between settlements. The high potential zones and site-likely areas were found located along the transition zone between the valleys and the mountains, similar to the Büyük Menderes and Küçük Menderes valleys. Based on this analysis, it was estimated that there may be eight or more archaeological sites in the region, with around five located in the Gediz valley and three in the Bakırçay valley (Figure 3-47). Some of these locations have been further investigated.

For instance, the Maionia (Atetta?) archaeological settlement was located in the northeast of the high potential and site-likely area (P17) between Sardis and Philadelpheia, according to the Pleiades Project database. The true location of the settlement is not known, but Gökçeören/Menye was suggested based on observations made by G. Keppel in 1831 and Hamilton in 1837 (Akar Tanrıver 2006). Currently, no archaeological remains have been recorded in the area. The settlement was also known in the Roman period (Willet 2020).

Magnesia ad Sipylum is another archaeological site with an unknown location. Some statues, small finds, and fragments of ancient buildings have been found on Mount Sipylos (references in Pleiades Project). The modern city of Manisa is a possible location for the ancient city. However, the predictive map developed in this study suggests that the site is more likely located on the eastern flanks of Mount Sipylos and the western flanks of Bozdağ Mountain, where both mountains get closest to each other (P16).

Other archaeological settlements from the Hellenistic period, such as Parthenion?, Pityaia, Sarıçam, Stratonicea/Hadrianopolis, Tyanollos, Hermokapeleia/Thyessos?, Hierakome/Hierokaisareia, Hyrkanis, Nakrason, Nymphaion, Agatheira, and Gergitha? that have approximate locations in the Pleiades Project database overlap with the high potential and site likely areas in the predictive map (P11, P12, P13, P14,

P15, and P18). The information from the Pleiades Project and the predictive map complement each other, increasing the potential for archaeological sites in these areas.

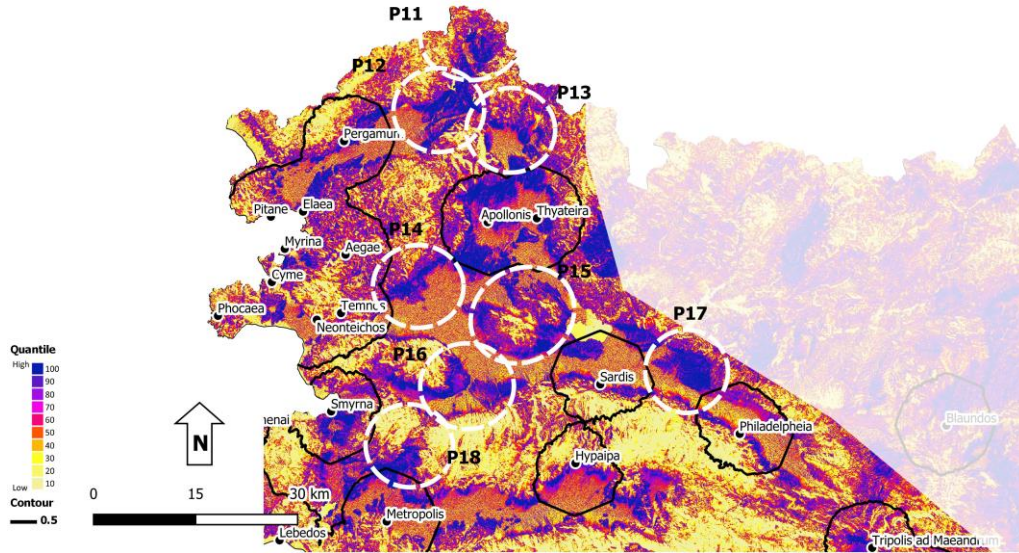


Figure 3-47 Predictive map for Gediz and Bakırçay valleys. The overlaid black contour line shows the boundary between site-likely and site-not-likely areas. The dashed white circles are potential zones where site-likely areas and the locations indicated by ancient texts overlap.

### 3.8.2.3. Northeastern Region of the Study Area

Although the high potential zones in the northeastern part of the study area are not as distinct as in other regions due to the absence of a clear boundary between valleys and mountains, there are still smaller zones that deserve attention (Figure 3-48). These areas are located at the transition zone of the flanks of hilly regions and smaller plains formed by the tributaries of major rivers.

The study identified seven high potential zones based on information derived from travel-time between settlements and known approximate locations of settlements, but there is a significant potential for the existence of more polis settlements in the area.

Of the high potential zones, P19 seems to be associated with the Kadoi archaeological settlement. The true location of the settlement is not known. However, several locations in the area are under government protection such as statue fragments and small finds in Eskigediz (Türktüzün et al. 2016), a necropolis in Gökler (Kütahya Kültür Varlıklarını Koruma Bölge Kurulu 2017), wall remains of a chapel and small surface finds dating back to the Hellenistic period to Late Byzantine period around 2.5 km southwest of Güzüngülü (Kütahya Kültür Varlıklarını Koruma Bölge Kurulu 2015b), small finds on the surface possibly related to a Roman settlement around 2.2 km northwest of Yaylaköy (Kütahya Kültür Varlıklarını Koruma Bölge Kurulu 2015d), small finds and wall remains of some buildings in Uğurluca (Kütahya Kültür Varlıklarını Koruma Bölge Kurulu 2015c), probably a settlement from the Late Byzantine period, and a hoyuk called Hoyratkaşı in Çeltikçi (Kütahya Kültür Varlıklarını Koruma Bölge Kurulu 2015a), probably from the Early Bronze Age. The area seems dynamic in terms of settlement history based on these finds, strengthening the possibility of the existence of a Hellenistic polis settlement in the area. On the other hand, due to the large area of this study, another study more focused on the interested area should be considered for further narrowing down the potential area for the polis settlement. In such a study, besides the topographic variables, the relationship, if any, from different period settlements and polis settlements can be used.

The Pleiades Project database lists other archaeological settlements from the Hellenistic period, such as Tamasis, Tarsis?, Silandos, Emoddi, Lyendos, Dioskome, Eukarpia, and Dionysoupolis, which have approximate locations that overlap with the high potential and site likely areas in the predictive map (P20, P21, P22, P23, P24, and P25). The information from the Pleiades Project and the predictive map complement each other, further increasing the potential for archaeological sites in these areas.

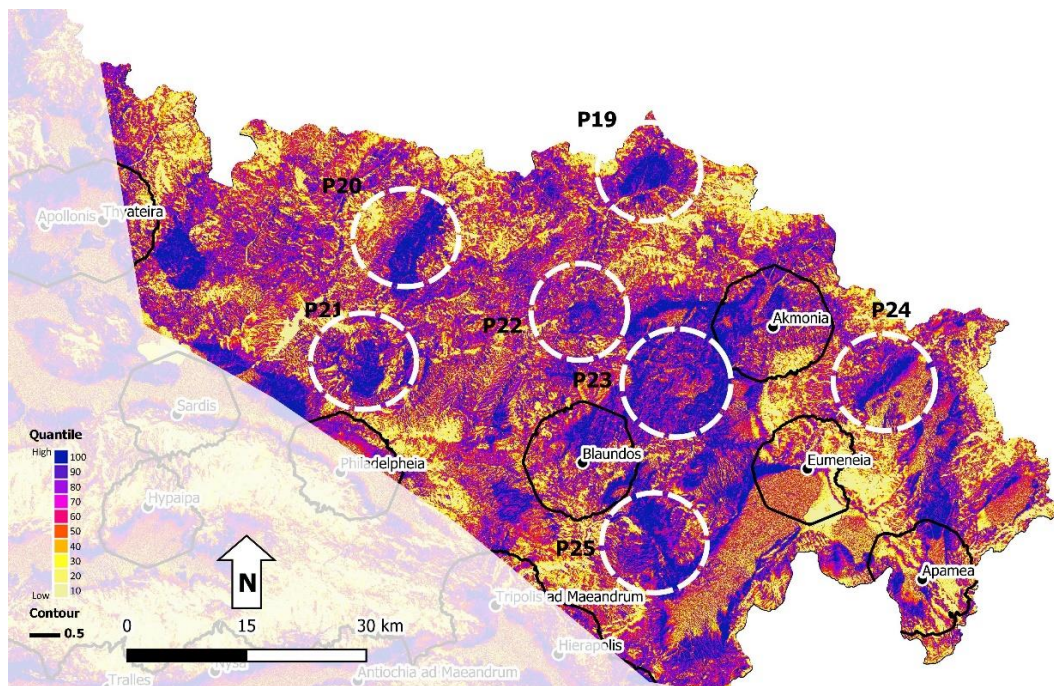


Figure 3-48 Predictive map for the northeastern regions of the study area. The overlaid black contour line shows the boundary between site-likely and site-not-likely areas. The dashed white circles are potential zones where site-likely areas and the locations indicated by ancient texts overlap.

## CHAPTER 4

### CONCLUSION

The study aimed contributions in two major areas: archaeological predictive modelling studies and a predictive map development for the Hellenistic period settlements of the western Türkiye.

Actions taken to improve archaeological predictive model quality:

- Accuracy and compatibility of the archaeological settlement dataset for model input was tried to be justified to a great degree.
- In the evaluation of a variable, polygonal areas were used in cases where it was thought that displaying an archaeological settlement as an area will contribute significantly.
- The main statistical approach was determined as data-driven, but during the variable selection, former knowledge from settlement pattern analyses or other researches in the region regarding the Hellenistic period was considered.
- New statistical methods were developed considering the ways of possible contribution from each variable.
- A continuous map, to a certain degree, showing the relative potential of pixels for each variable was created.
- A new way of use of road network, a socio-cultural variable, in conjunction with APMs to support the detection of likely site locations in a study area was introduced. Travel times between known settlements were utilized for this purpose.

- By repeating the statistical analysis on randomly selected samples and on different sample sizes, the reproducibility of results was ascertained.
- The enquiries on possible outcomes and success in performance was started at the variable level.
- A list of how settlements' responses were to the model was prepared in order to create a medium for the discussion of the variables and the predictive map at the archaeological settlement level. It was considered that a new value might emerge by increasing the connection between the archaeologists and the predictive model produced.
- In addition to gain statistics, at evaluation of the model, the locations of independent settlements were used, and candidate high potential zones were explored at desktop.

Limitations encountered during the model development:

- It was very difficult to be sure whether the location of some of the archaeological settlement is known from solely literature, or from any in situ remains.
- The collaboratively formed database served significantly for the collection of known archaeological settlements in the region. However, for the locational, temporal and site type refinement, finding and reviewing the individual papers, majorly national ones, were critical and time consuming.
- Defining representative polygonal area(s) was problematic due to different levels of spatial relationship of an archaeological settlement with its surrounding area,
- The statistical methods suggested were basic/understandable in concept, but challenging in employing. Assessment of the polygonal data for each archaeological settlement and production/evaluation of many potential maps for repeatability and sensitivity analyses were required use of R and Python codes besides main GIS tools in order to accelerate the process.

The outcomes of archaeological predictive model for the Hellenistic period settlements of the western Türkiye:

- During the Hellenistic period, there was a prevailing belief that the poleis favored settling in low-lying, defensible hilltops and cultivating alluvial plains. Mobility was also facilitated by a well-developed road network. This study provides a quantified and spatially identified basis for this intuition, transforming it into a verifiable statement.
- The variables examined in this study included elevation, ruggedness, slope, aspect, arable land density, access to water, and rock types used in constructing the city walls. However, the elevation variable was discarded due to spatial autocorrelation. Additionally, access to water was excluded due to the challenge of producing a water availability map that account the diverse water sources used in the period. Finally, rock type was eliminated because the available rock types at immediate location of the archaeological sites were exploited for the city wall construction.
- During the evaluation, the model was observed producing consistent and comparable results. Specifically, using a sample size of 36 for training yielded repeatable outcomes. Moreover, performance tests were conducted using 15 testing data points, which were deemed sufficient for the purpose.
- Aspect was the most sensitive variable to the sample size.
- Based on the period under study, the poleis in the region generally preferred locations with low to medium rugged terrain, moderate slopes (approximately 5-15°), and a southeastern and/or west-northwestern orientation, as well as access to arable land within an hour's walking distance. The road network analysis indicated that travel time between settlements was approximately 7.5 hours.
- The predictive map effectively narrowed down the potential settlement area to 41%, within which 80% of the known archaeological settlements were

located. Furthermore, the study suggested that 30% of the remaining study area is unlikely to accommodate any significant polis settlements.

- The predictive map, combined with the road network analysis results, identified approximately 26 high-potential zones for settlements in the study area. Specifically, eleven potential sites were located in the Küçük Menderes and Büyük Menderes valleys and their southern regions, eight sites were located in the Gediz and Bakırçay valleys, and seven sites were located in the northeastern part of the study area.
- The northeastern region of the study area appears to have fewer known archaeological settlements. Consequently, additional data and/or variables seem to be required to differentiate potential settlement locations better in this particular area.

## REFERENCES

- Akar Tanrıver, D. S., 2006, Kula Yakınlarında Bir Antik Kent: Maionia (Gökçeören/Menye), In *Geçmişten Geleceğe Köprü Yanık Ülke Kula Sempozyumu*, 197–209, Kula Belediyesi, İzmir.
- Akdeniz, E., Erön, A., and Akıllı, N., 2018, 2017 Yılı Thyateira ve Hastane Höyüğü Kazıları, In *Kazı Sonuçları Toplantısı 40(1)*, Kültür Varlıkları ve Müzeler Genel Müdürlüğü.
- Akkan, Y., Tavukçu, A. Y., Temür, A., Tavukçu, Z. A., Ceylan, M., Coşkun, S., and Atalay, A., 2016, Alabanda 2015, In *Kazı Sonuçları Toplantısı 38(1)*, 305–28, Kültür Varlıkları ve Müzeler Genel Müdürlüğü, Edirne.
- Altschul, J. A., 1988, Models and the Modeling Process, In *Quantifying the Present and Predicting the Past: Theory, Method and Application of Archaeological Predictive Modeling* (eds. W. J. Judge, and S. Lynne), 61–96, U.S. Department of the Interior, Bureau of Land Management Service Center.
- Argyriou, A. V., Teeuw, R. M., and Sarris, A., 2017, GIS-based landform classification of Bronze Age archaeological sites on Crete Island, *PLoS ONE*, **12**(2).
- Aydın Kültür Varlıklarını Koruma Bölge Kurulu, 2017, 09.02.2017 Tarihli 6066 Nolu Karar.
- Balla, A., Pavlogeorgatos, G., Tsiafakis, D., and Pavlidis, G., 2013, Modelling archaeological and geospatial information for burial site prediction, identification and management, *International Journal of Heritage in the Digital Era*, **2**(4), 585–609.

Ben (user:173082), 2022, 10% rule for sample sizes, URL:  
<https://stats.stackexchange.com/q/401940>.

Benaglia, T., Chauveau, D., Hunter, D. R., and Young, D. S., 2009, Mixtools: An R package for analyzing finite mixture models, *Journal of Statistical Software*, **32**(6), 1–29.

Bettinger, R. L., 1980, Explanatory/Predictive models of hunter-gatherer adaptation, *Advances in Archaeological Method and Theory*, **3**, 189–255.

Bintliff, J., Dickinson, O., Howard, P., and Snodgrass, A., 2000, Deconstructing ‘The Sense of Place’? Settlement Systems, Field Survey, and the Historic Record: A Case-study from Central Greece, *Proceedings of the Prehistoric Society*, **66**, 123–49.

Bintliff, J., 2000, Settlement and Territory: A socio-ecological approach to the evolution of settlement systems, In *Human Ecodynamics* (eds. G. Bailey, R. Charles, and N. Winder), 21–30, Oxford: Oxbow books.

Brückner, H., 1996, Coastal Changes in Western Turkey: Rapid delta progradation in historical times, *Transformations and Evolution of the Mediterranean Coastline*, **18**(CIESM Science Series 3. Bulletin de l’Institut Océanographique, Monaco 18), 107–38.

Brückner, H., Herda, A., Kerschner, M., Müllenhoff, M., and Stock, F., 2017, Life cycle of estuarine islands — From the formation to the landlocking of former islands in the environs of Miletos and Ephesos in western Asia Minor (Turkey), *Journal of Archaeological Science: Reports*, **12**, 876–94.

Burg, M. B., Peeters, H., and William, A. L., 2016, Introduction to Uncertainty and Sensitivity Analysis in Archaeological Computational Modeling, In *Uncertainty and Sensitivity Analysis in Archaeological Computational Modeling* (eds. M. B. Burg, H. Peeters, and A. L. William), 1–20, Springer International Publishing.

- Cahill, N., 2018, The city of Sardis, *The Archaeological Exploration of Sardis*, URL: <https://sardisexpedition.org/en/essays/latw-cahill-city-of-sardis>.
- Carleton, W. C., Conolly, J., and Ianonne, G., 2012, A locally-adaptive model of archaeological potential (LAMAP), *Journal of Archaeological Science*, **39**(11), 3371–85.
- Carleton, W. C., Cheong, K. F., Savage, D., Barry, J., Conolly, J., and Iannone, G., 2017, A comprehensive test of the Locally-Adaptive Model of Archaeological Potential (LAMAP), *Journal of Archaeological Science: Reports*, **11**, 59–68.
- Chakraborty, S., and Wong, S. W. K., 2019, Bambi: an R package for Fitting Bivariate Angular Mixture Models, *arXiv:1708.07804v3*.
- Church, T., Brandon, R. J., and Burgett, G. R., 2000, GIS Applications in Archaeology: Method in Search of Theory, In *Practical Applications of GIS for Archaeologists: A Predictive Modelling Toolkit* (eds. K. L. Wescott, and R. J. Brandon), 144–66, Taylor & Francis.
- Clapham, M., 2020, Resampling Methods (Bootstrapping), URL: <https://websites.pmc.ucsc.edu/~mclapham/Rtips/resampling.htm>.
- Clarke, D. L., 1972, Models and Paradigms In Contemporary Archaeology, In *Models in Archaeology* (ed. D. L. Clarke), 1–61, Routledge.
- Conlen, M., 2018, Kernel density estimation explainer, URL: <https://mathisonian.github.io/kde/>.
- Conze, A., and Schuchhardt, C., 1899, Die Arbeiten Zu Pergamon 1886-1889 (Tafel IX), *Mitteilungen des Deutschen Archäologischen Instituts, Athenische Abteilung* 24.

Coşkun, G., 2018, Lebedos ve Territoryumu Arkeolojik Yüzey Araştırması, 2017, In *Araştırma Sonuçları Toplantısı 36(2)*, Kültür Varlıkları ve Müzeler Genel Müdürlüğü.

Crouch, D. P., 2003, Eastern Greco-Roman Cities, In *Geology and Settlement: Greco-Roman Patterns*.

Çekilmez, M., Dereboylu Poulain, E., Erön, A., Erdan, E., Akbulut, N., and Özdemir, E., 2016, 2015 Yılı Myrina ve Gryneion Antik Kentleri Yüzey Araştırması, In *Araştırma Sonuçlar Toplantısı 34(1)*, Kültür Varlıkları ve Müzeler Genel Müdürlüğü, Edirne.

Debord, P., and Varinlioğlu, E., 2010, *Cités de Carie: Harpasa, Bargasa, Orthosia dans l'Antiquité*, Presses Universitaires de Rennes, Rennes.

Debord, P., and Varinlioğlu, E., 2018, *Hyllarima da Carie, état de la question*, Ausonius, Bordeaux.

Denizli İl Kültür ve Turizm Müdürlüğü, 2020a, Colossae Antik Kenti, URL: <https://denizli.ktb.gov.tr/TR-211757/colossae-antik-kenti.html>.

Denizli İl Kültür ve Turizm Müdürlüğü, 2020b, Heraklia Salbace Antik Kenti, URL: <https://denizli.ktb.gov.tr/TR-211759/heraklia-salbace-antik-kenti.html>.

Denizli İl Kültür ve Turizm Müdürlüğü, 2020c, Laodikeia Antik Kenti Yerleşim Planı, URL: <https://denizli.ktb.gov.tr/TR-211744/laodikeia.html>.

Difabio, C., 2022, Synoikism, Sympolity, and Urbanization: A regional approach in Hellenistic Anatolia, University of Michigan.

- Diwan, G. A., 2020, GIS-based comparative archaeological predictive models: A first application to iron age sites in the bekaa (Lebanon), *Mediterranean Archaeology and Archaeometry*, **20**(2), 143–58.
- Doran, J., 1972, Computer models as tools for archaeological hypothesis formation, In *Models in Archaeology* (ed. D. L. Clarke), 425–51, Routledge.
- Duman, B., 2020, Tripolis Gezi Güzergahları, *Tripolis Kazı Arşivi*, URL: <https://www.pau.edu.tr/tripolis/tr/sayfa/tur-guzergahlari>.
- Durmuşlar, F., 2018, Structural Conservation of Cevher Paşa Bath in Kale, Denizli, İzmir Institute of Technology.
- Ebert, J. I., 2000, The state of the art in “inductive” predictive modeling: Seven big mistakes (and lots of smaller ones), In *Practical Applications of GIS for Archaeologists: A Predictive Modelling Toolkit* (eds. K. L. Wescott, and R. J. Brandon), 137–43, Taylor & Francis.
- Efron, B., and Tibshirani, R. J., 1993, *An Introduction to the Bootstrap*, Chapman & Hall, New York.
- Ejstrud, B., 2003, Indicative Models in Landscape Management: Testing the methods, In *Symposium The Archaeology of Landscapes and Geographic Information Systems. Predictive Maps, Settlement Dynamics and Space and Territory in Prehistory.*, 119–34.
- Erkanal Öktü, A., Akalın, A. G., İren, K., and Lichter, C., 2002, 2001 Kuzey İzmir-Menemen Ovası Yüzey Araştırması, In *Araştırma Sonuçları Toplantısı 20(1)*, 301–14, Anıtlar ve Müzeler Genel Müdürlüğü, Ankara.
- Erskine, A., 2005, *A Companion to the Hellenistic World*, Blackwell Publishing Ltd.

- Ersoy, Y. E., Hasdađlı, İ., Uzun, K., and Çetin, C., 2015, Urla-Klazomenai Kazıları, In *Kazı Sonuçları Toplantısı 37(2)*, Kùltür Varlıkları ve Müzeler Genel Müdürlüğü, Erzurum.
- Espa, G., Benedetti, R., De Meo, a., Ricci, U., and Espa, S., 2006, GIS based models and estimation methods for the probability of archaeological site location, *Journal of Cultural Heritage*, **7(3)**, 147–55.
- Filges, A., 2006, *Blaundos: Berichte zur Erforschung einer Kleinstadt im lydisch-phrygischen Grenzgebiet*, Istanbuler Forschungen, Bd. 48, Ernst Wasmuth Verlag, Tübingen.
- Finke, P. a., Meylemans, E., and van de Wauw, J., 2008, Mapping the possible occurrence of archaeological sites by Bayesian inference, *Journal of Archaeological Science*, **35(10)**, 2786–96.
- Foss, C., 1977, Archaeology and the “Twenty Cities” of Byzantine Asia, *American Journal of Archaeology*, **81(4)**, 469–86.
- Gaffney, V., and van Leusen, P. M., 1995, Postscript - GIS, environmental determinism and archaeology: A parallel text, In *Archaeology and geographical information systems: A European perspective* (eds. G. R. Lock, and Z. Stančič), 367–82, Taylor & Francis, London.
- Grabowski, T., 2019, Küçük Asya’da Ptolemaioslar Hanedanı, In *Hellenistik ve Roma Dönemlerinde Anadolu: Krallar, İmparatorluklar, Kent Devletleri* (ed. O. Tekin), 22–44, Yapıkredi Yayınları.
- Gümüş, M. G., Durduran, S. S., Bozdağ, A., and Gümüş, K., 2017, GIS Investigation of Site Selection of Historical Structures : The Case of Knidos (Datça, Turkey ), **17(2)**, 149–57.

- Hansen, M., and Nielsen, T., 2004, *An Inventory of Archaic and Classical Poleis*, Oxford University Press.
- Hansen, M. H., 2006, *Polis: An Introduction to the Ancient Greek City-State*, OUP Oxford.
- Harris, M. D., 2013, Task 1 Literature Review, *Pennsylvania Department of Transportation Archaeological Predictive Model Set*, URA Corporation.
- Hartigan, J. A., and Hartigan, P. M., 1985, The dip test for bimodality, *The Annals of Statistics*, **13**(1), 70–84.
- Hatzinikolaou, E., Hatzichristos, T., Siolas, A., and Mantzourani, E., 2003, Predicting Archaeological Site Locations Using G.I.S. and Fuzzy Logic, In *The Digital Heritage of Archaeology. CAA2002. Computer Applications and Quantitative Methods in Archaeology. Proceedings of the 30th CAA Conference* (eds. D. Martin, and A. Sarris), 169–78, Hellenic Ministry of Culture, Athen.
- Hay, L. E., Battaglin, W. A., Parker, R. S., and Leavesley, G. H., 1993, Modeling the effects of climate change on water resources in the Gunnison River Basin, Colorado, In *Environmental modeling with GIS* (eds. M. F. Goodchild, B. O. Parks, and L. T. Steyaert), 173–81, Oxford University Press, New York.
- Hayes, A., 2022, Bayes' Theorem: What It Is, the Formula, and Examples, URL: <https://www.investopedia.com/terms/b/bayes-theorem.asp>.
- Herzog, I., 2014, Least-cost Paths - Some Methodological Issues, *Internet Archaeology*(36).
- Hill, D., 2016, Urbanisation and settlement in western Asia Minor: Ionia and Metropolis in the Torbalı Plain , a GIS approach, University of Oslo.

Hill, D., 2019, The Formation and Development of Political Territory and Borders in Ionia from the Archaic to the Hellenistic Periods: A GIS Analysis of Regional Space, *Journal of Greek Archaeology*, **4**, 96–129.

Ho, R., 2017, *Understanding Statistics for the Social Sciences with IBM SPSS*, Chapman and Hall/CRC.

Hodder, I., 1972, Locational models and the study of Romano-British settlement, In *Models in Archaeology* (ed. D. L. Clarke), 871–85, Routledge.

Horden, P., and Kinoshita, S., 2014, *A Companion to Mediterranean History*, John Wiley & Sons, Ltd.

Huggett, R. J., and Cheesman, J., 2002, *Topography and the Environment*, Prentice Hall.

Humann, C., and Dörpfeld, W., 1893, Ausgrabungen in Tralles (Tafel XII-XIII), In *Athener Mitteilungen* 18.

Irmischer, I. J., and Clarke, K. C., 2018, Measuring and modeling the speed of human navigation, *Cartography and Geographic Information Science*, **45**(2), 177–86.

James, G., Witten, D., Hastie, T., and Tibshirani, R., 2013, *An Introduction to Statistical Learning*, Vol. 103, Springer Texts in Statistics, Springer New York, New York, NY.

Jeff, 2017, 10% Rule of Assuming “Independence” Between Trials, URL: <https://www.khanacademy.org>.

Jochim, M. A., 1981, *Strategies for survival: Cultural behavior in an ecological*

context, Academic Press.

Judge, W. J., and Sebastian, L., 1988, *Quantifying the Present and Predicting the Past: Theory, Method and Application of Archaeological Predictive Modeling*, U.S. Department of the Interior, Bureau of Land Management Service Center, Denver.

Kadıođlu, M., 2018, *Teos Rehber Kitap 2 / Teos Guide Book II*, Teos Antik Kenti Kazı Başkanlığı.

Kalaycı, T., 2006, Predictive Modeling of Settlement Mounds (9000-5500 BC) in The Lake District Region And Its Immediate Environs, Middle East Technical University.

Kalaylıođlu, Z., 2020, Directional Data Analysis, *Statistics for Archaeometry*, Department of Statistics, Middle East Technical University.

Kalkan, H., and Koçak Yaldır, A., 2013, Antik Hypaipa Kenti ve Çevresi Yüzey Araştırması - 2012, In *Araştırma Sonuçlar Toplantısı 31(2)*, Kültür Varlıkları ve Müzeler Genel Müdürlüğü, Muđla.

Kamermans, H., van Leusen, M., and Verhagen, P., 2009, Archaeological prediction and risk management, In *Archaeological Prediction and Risk Management: Alternatives to Current Practice*, 9–19, Leiden University Press.

Kamermans, H., 2010, The Application of Predictive Modelling in Archaeology: Problems and Possibilities, *Beyond the Artifact. Digital Interpretation of the Past. Proceedings of CAA2004. Prato 13–17 April 2004*, 273–7.

Kayan, İ., 1999, Holocene stratigraphy and geomorphological evolution of the Aegean coastal plains of Anatolia, *Quaternary Science Reviews*, **18**(4–5), 541–8.

Kayan, İ., and Öner, E., 2015, Research on the Alluvial Geomorphology of the Gediz Delta Plain (İzmir) Based on Sedimentological and Paleontological Evidence, *Aegean Geographical Journal*, **24**(2), 1–27.

Khan, S., 2023, Small Sample Size Confidence Intervals, URL: <https://www.khanacademy.org>.

von Kienlin, A., 2011, Stadtopografie und Architektur, In *Kelainai 1: Kelainai-Apameia Kibotos: Développement urbain dans le contexte anatolien/Stadtentwicklung im anatolischen Kontext* (ed. L. Summerer), Ausonius Editions, Bordeaux.

King, T. F., 1978, *The archeological survey: Methods and uses*, Washington, D.C. : Heritage Conservation and Recreation Service, U.S. Dept. of the Interior, 1978., Washington, D.C.

Knipping, M., Müllenhoff, M., and Brückner, H., 2008, Human induced landscape changes around Bafa Gölü (western Turkey), *Vegetation History and Archaeobotany*, **17**(4), 365–80.

Kohler, T. A., and Parker, S. C., 1986, Predictive Models for Archaeological Resource Location, *Advances in Archaeological Method and Theory*, **9**, 397–452.

Koparal, E., 2011, Urbanization Process and Spatial Organization in Klazomenian Khora from Early Iron Age to Roman Period, Middle East Technical University.

Kosmin, P. J., 2014, *The Land of the Elephant Kings: Space, Territory, and Ideology in the Seleucid Empire*, Harvard University Press.

Kowalewski, S. a., 2008, Regional settlement pattern studies, *Journal of Archaeological Research*, **16**(3), 225–85.

Kuhn, M., and Johnson, K., 2013, *Applied predictive modeling*.

Kütahya Kültür Varlıklarını Koruma Bölge Kurulu, 2015a, 24.06.2015 Tarihli 2478 Nolu Karar.

Kütahya Kültür Varlıklarını Koruma Bölge Kurulu, 2015b, 26.11.2015 Tarihli 2855 Nolu Karar.

Kütahya Kültür Varlıklarını Koruma Bölge Kurulu, 2015c, 27.01.2015 Tarihli 2179 Nolu Karar.

Kütahya Kültür Varlıklarını Koruma Bölge Kurulu, 2015d, 27.01.2015 Tarihli 2180 Nolu Karar.

Kütahya Kültür Varlıklarını Koruma Bölge Kurulu, 2017, 08.04.2017 Tarihli 3983 Nolu Karar.

Kvamme, K. L., 1988, Development and Testing of Quantitative Models, In *Quantifying the Present and Predicting the Past: Theory, Method and Application of Archaeological Predictive Modeling* (eds. W. J. Judge, and S. Lynne), 325–418, U.S. Department of the Interior, Bureau of Land Management Service Center.

Kvamme, K. L., 1992, A Predictive Site Location Model on the High Plains: An Example with an Independent Test, *Plains Anthropologist*, **37**(138), 19–40.

Kvamme, K. L., 2006, There and Back Again: Revisiting Archaeological Locational Modeling, In *GIS and Archaeological Site Modeling* (eds. M. W. Mehrer, and K. L. Wescott), 4–37, London.

La Marca, A., 2013, Kyme Hellenistik Sur Duvarı, In *A Festschrift for Orhan Bingöl*

*on the occasion of his 67th Birthday* (ed. G. Kökdemir), 301–15, Bilgin Kültür Sanat Yayıncılık, Ankara.

van Leusen, M., 2002, *Pattern to Process: Methodological investigations into the formation and interpretation of spatial patterns in archaeological landscapes*, Rijksuniversiteit Groningen.

van Leusen, M., Deeben, J., Hallewas, D., Zoetbrood, P., Kamermans, H., and Verhagen, P., 2005, A Baseline for Predictive Modelling in the Netherlands, *Predictive Modelling for Archaeological Heritage Management: A research agenda*, 25–92.

Lund, U., Agostinelli, C., Arai, H., Gagliardi, A., Portugues, E. G., Giunchi, D., Irisson, J. O., Pocernich, M., and Rotolo, F., 2017, R package “circular”: Circular Statistics (version 0.4-93).

Maechler, M., 2016, Hartigan’s dip test statistic for unimodality (version 0.75-7).

Malaperdas, G., and Zacharias, N., 2019, The habitation Model Trend Calculation (MTC): A new effective tool for predictive modeling in archaeology, *Geo-Spatial Information Science*, **22**(4), 314–31.

Mark, H., 2010, Aphrodisias State Plan with City Grid, URL: <http://aphrodisias.classics.ox.ac.uk/images/Aphrodisias-Map-1.gif>.

Matessi, A., Dalkılıç, E., and D’Alfonso, L., 2018, Settlement Patterns, Ancient Routes and Environmental Change in South Cappadocia (Turkey), During the Holocene, *Ömer Halisdemir Üniversitesi Mühendislik Bilimleri Dergisi*, **7**(3), 1107–12.

Mays, L. W., Sklivaniotis, M., and Angelakis, A. N., 2012, Water for human

- consumption through history, In *Evolution of Water Supply Through the Millennia* (eds. A. N. Angelakis, L. W. Mays, D. Koutsoyiannis, and N. Mamassis), 19–42, IWA Publishing.
- McNicoll, A. W., and Milner, N. P., 1997, Hellenistic fortifications from the Aegean to the Euphrates, *Oxford monographs on classical archaeology*, Clarendon Press.
- Mehrer, M. W., and Wescott, K. L. (eds.), 2005, *GIS and Archaeological Site Location Modeling*.
- Mercangöz, Z., 2005, 4. Yılında Kuşadası, Kadikalesi/Anaia Kazısı, *Sanat Tarihi Dergisi*, **14**(1), 205–23.
- Mercangöz, Z., 2007, Kuşadası, Kadikalesi Kazısı 2006 Yılı Çalışmaları, In *Kazı Sonuçları Toplantısı 29(3)*, Kültür Varlıkları ve Müzeler Genel Müdürlüğü.
- Meriç, R., 1986, 1985 Yılı Alaşehir Kazı Çalışmaları I, In *Kazı Sonuçları Toplantısı 8(2)*, 263–75, Eski Eserler ve Müzeler Genel Müdürlüğü, Ankara.
- Metropolis Kazı ve Araştırmaları, 2017, Metropolis Kent Planı, URL: <http://metropolis.web.tr/>.
- Mink, P., Pollack, D., and Jo Stokes, B., 2005, Points vs. Polygons, In *GIS and Archaeological Site Location Modeling*, 219–39, CRC Press.
- Minnesota Department of Transportation, 2022, About MnModel, *Minnesota Statewide Archaeological Predictive Model*, URL: <https://www.dot.state.mn.us/mnmodel/index.html>.
- Mooney, C. Z., and Duval, R. D., 1993, *Bootstrapping : A nonparametric approach*

*to statistical inference*, Sage Publications, Newbury Park, Calif.

Müllenhoff, M., Brückner, H., and Handl, M., 2005, Geoarchaeological evidence for rapid landscape change in western Turkey – the example of the Maeander ( Büyük Menderes ) delta, *Most*(2005), 35032.

Naumann, R., and Kantar, S., 1950, Die Agora von Smyrna, *Istanbuler Forschungen*, **17**, 69–114.

Nollé, J., 2016, Beiträge zur kleinasiatischen Münzkunde und Geschichte: 12. Mastaura am Fuße der Mesogis – Überlegungen zu den Patriatraditionen einer wenig bekannten antiken Polis, *Gephyra*, **13**, 49–82.

Oğuz, E. D., 2013, The Rural Settlement Pattern of Bozburun Peninsula During Classical and Hellenistic Periods, Middle East Technical University.

Okabe, A., Boots, B., Sugihara, K., Chiu, S. N., and Kendall, D. G., 2000, *Spatial Tessellations: Concepts and Applications of Voronoi Diagrams*.

Oliver, G. J., 2015, Mobility, Society, and Economy in the Hellenistic Period, In *The Economies of Hellenistic Societies, Third to First Centuries BC*, 345–67.

Owens, E. J., 1992, *The City in the Greek and Roman World*, Routledge.

Özkaya, V., and San, O., 2001, Alinda and Amyzon: Two Ancient Cities in Caria, In *Araştırma Sonuçlar Toplantısı 19(1)*, Anıtlar ve Müzeler Genel Müdürlüğü, Ankara.

Öztaner, 2018, Nysa Antik Kenti Şehir Planlaması, In *Future Cities, II. International Urban, Environment and Health Congress*, Cappadocia.

- Özyiğit, Ö., 2003, Recent Work At Phokaia in the Light of Akurgal'S Excavations, *Anatolia*, **25**, 109–28.
- Parker, S., 1982, *Predictive Modeling of Site Settlement Systems Using Multivariate Logistics*.
- Pint, A., Seeliger, M., Frenzel, P., Feuser, S., Erkul, E., Berndt, C., Klein, C., Pirson, F., and Brückner, H., 2015, The environs of Elaia's ancient open harbour - a reconstruction based on microfaunal evidence, *Journal of Archaeological Science*, **54**, 340–55.
- Pirson, F., 2007, Pergamon - Bericht über die Arbeiten in der Kampagne 2006: Mit Beiträgen von Martin Bachmann, Ralf von den Hoff und Martin Zimmermann, *Archäologischer Anzeiger*, **2**, 13–70.
- Pirson, F., 2008, Pergamon-2007 Kampanyasında Yakın Çevrede Yapılan Çalışmalar, In *Araştırma Sonuçları Toplantısı 26 (2)*, 283–302, Kültür Varlıkları ve Müzeler Genel Müdürlüğü, Ankara.
- Plog, F., and Hill, J. ., 1971, Explaining variability in the distribution of sites. In The distribution of prehistoric population aggregates, In *Proceedings of the Southwestern Anthropological Research Group, Anthropological Reports 1* (ed. G. J. Gumerman), 17–36.
- Ragone, G., 2007, Temnos (Görece Kale - Southern Aeolis) Research Project: 2006 Report, In *Araştırma Sonuçlar Toplantısı 25(3)*, Kültür Varlıkları ve Müzeler Genel Müdürlüğü, Kocaeli.
- Ratté, C., Rojas, F., and Commito, A., 2016, Notion Archaeological Survey, 2014-2015, In *Araştırma Sonuçları Toplantısı 34(2)*, Kültür Varlıkları ve Müzeler Genel Müdürlüğü, Edirne.

Revert, N. P. A., 2017, The Roman Settlement Pattern of the Somme: Site Location analysis and Predictive Modelling.

Riley, S., Stephen, D., and Robert, E., 1999, A Terrain Ruggedness Index that quantifies topographic heterogeneity, *Intermountain Journal of Sciences*, **5**(1–4), 23–7.

Ruggendorfer, P., 2011, Ergebnisse der Städtebaulichen Untersuchungen in Alinda 2010, In *29. Araştırma Sonuçları Toplantısı 2. Cilt*, 67–81, Kültür Varlıkları ve Müzeler Genel Müdürlüğü, Malatya.

Saldaña, M., 2018, The City Plan, *Procedural Magnesia: Reconstructing the Urban Topography of Magnesia on the Maeander in 3D*, URL: <http://proceduralmagnesia.com/>.

Scardozi, G., 2020, *The Territory of Hierapolis in Phrygia: Archaeological Guide*, Ege Yayınları.

Schuler, C., 2019a, Kırılgenlık ve Direnç: Hellenistic Küçük Asya’da Hellen Kent Devletleri (Polies), In *Hellenistik ve Roma Dönemlerinde Anadolu: Krallar, İmparatorluklar, Kent Devletleri* (ed. O. Tekin), 188–201, Yapıkredi Yayınları.

Schuler, C., 2019b, Küçük Asya’da Seleukoslar Egemenliđi, In *Hellenistik ve Roma Dönemlerinde Anadolu: Krallar, İmparatorluklar, Kent Devletleri* (ed. O. Tekin), 9–21, Yapıkredi Yayınları.

Sear, F., 2006, *Roman Theatres. An Architectural Study*, Oxford University Press.

Seeliger, M., Bartz, M., Erkul, E., Feuser, S., Kelterbaum, D., Klein, C., Pirson, F., Vött, A., and Brückner, H., 2013, Taken from the sea, reclaimed by the sea: The fate of the closed harbour of Elaia, the maritime satellite city of Pergamum

- (Turkey), *Quaternary International*, **312**, 70–83.
- Seeliger, M., Pint, A., Feuser, S., Riedesel, S., Marriner, N., Frenzel, P., Pirson, F., Bolten, A., and Brückner, H., 2019, Elaia, Pergamon's maritime satellite: the rise and fall of an ancient harbour city shaped by shoreline migration, *Journal of Quaternary Science*, **34**(3), 228–44.
- Sezgin, T., and Taşkiran, M., 2011, Eumeneia Kent Planı ve Savunması, In *Eumeneia, Şeyhli ve Işıklı* (ed. B. Söğüt), 61–71, Ege Yayınları.
- Sezgin, Y., 2018, Aiolis'te Bir Dağ Kent: Aigai, In *Arkeoloji, Tarih, Coğrafya, Turizm ve Kültürüyle Geçmişten Günümüze I . Aliğa Sempozyumu Bildirileri* (eds. M. Çekilmez, and S. Vardar), 71–95, İzmir.
- Sirkin, R. M., 2011, *Statistics fo the Scoial Sciences* 3rd ed., SAGE Publications, Inc., Thousand Oaks.
- Smith, R. R. R. R., and Ratté, C., 1996, Archaeological research at Aphrodisias in Caria, 1994, *American journal of archaeology*, **100**(1), 5–33.
- Söğüt, B., 2015, Stratonikeia'nın Yerleşim Tarihi ve Yapılan Çalışmalar, In *Stratonikeia Çalışmaları I Stratonikeia ve Çevresi Araştırmaları* (ed. B. Söğüt), 1–8, Ege Yayınları.
- Söğüt, B., 2016, Attouda (Hisar) Antik Kenti, *Cedrus*(5), 241–60.
- Stančič, Z., and Kvamme, K. L., 1998, Settlement patterns modelling through Boolean overlays of social and environmental variables, *New Techniques for Old Times, Computer Applications and Quantitative Methods in Archaeology. Proceedings of the 26th conference, Barcelona March 1998.*, 231–7.

Stančič, Z., Veljanovski, T., and Podobnikar, T., 2000, Understanding Roman Settlement Patterns through Multivariate Statistics and Predictive Modelling, In *Beyond the map: Archaeology and spatial technologies* (ed. G. R. Lock), 147–56, IOS Press.

Taştemür, E., and Dinç, M., 2018, Akmonia Yüzey Araştırmalarında Ele Geçen Terra Sigillata ve Geç Roma Kırmızı Astarlı Seramikleri, *Hitit Üniversitesi Sosyal Bilimler Enstitüsü Dergisi*, **11**(3), 2606–20.

Topaloğlu, S., 2017, Discussions on Integration of Rural and Archaeological Landscapes in Ildır/ Erythrai, Middle East Technical University.

Tripcevich, N., 2009, Working with Archaeological data in Arcmap 9.2: A brief tour of Viewshed and Cost distance functions, UC Berkeley Anthropology.

Türktüzün, M., Aybek, S., and Ünan, S., 2016, Debboy Köprüsü Heykelleri ve Phrigia’da Bir Roma Kenti; Kadonhon, In *Kütahya Müzesi 2015 Yıllığı “50. Yıl Anısına,”* 107–31, Bilgin Kültür Sanat Yayıncılık.

University of Salento, 2013, Pianta di Hierapolis in epoca ellenistica e primo-imperiale, URL: <https://www.hierapolis.unisalento.it/15?articolo=4>.

Vaughn, S., and Crawford, T., 2009, A predictive model of archaeological potential: An example from northwestern Belize, *Applied Geography*, **29**(4), 542–55.

Verhagen, P., 2007, *Case Studies in Archaeological Predictive Modelling*, LUP Dissertations, Amsterdam University Press, Amsterdam.

Verhagen, P., and Whitley, T. G., 2012, *Integrating Archaeological Theory and Predictive Modeling: A Live Report from the Scene*, Vol. 19.

- Verhagen, P., Kamermans, H., van Leusen, M., and Ducke, B., 2019, 5. New developments in archaeological predictive modelling, *The Cultural Landscape and Heritage Paradox*, Landscape & Heritage Studies, 431–44.
- Verhagen, P., and Whitley, T. G., 2020, Predictive Spatial Modelling, In *Archaeological Spatial Analysis* (eds. M. Gillings, P. Hacıgüzeller, and G. Lock), 231–46, Routledge.
- Wachtel, I., Zidon, R., Garti, S., and Shelach-Lavi, G., 2018, Predictive modeling for archaeological site locations: Comparing logistic regression and maximal entropy in north Israel and north-east China, *Journal of Archaeological Science*, **92**, 28–36.
- Weber, B. F., 2002, Ausgrabungen in Milet, URL: <https://www.ruhr-uni-bochum.de/milet/in/stadtplan.htm>.
- Wheatley, D., 1993, Going over old ground: GIS, archaeological theory and the act of perception, In *Computing the past: Computer applications and quantitative methods in archaeology - CAA 92* (eds. J. Andresen, T. Madsen, and I. Scollar), 133–8, Aarhus University Press.
- Wheatley, D., and Gillings, M., 2002, *Spatial Technology and Archaeology: The Archaeological Applications of GIS*, Taylor & Francis Inc.
- Willet, R., 2020, *The Geography of Urbanism in Roman Asia Minor*, Equinox Publishing.
- Yavuz Hakyemez, H., Erkal, T., Göktas, F., Hakyemez, H. Y., Erkal, T., and Go, F., 1999, Late Quaternary evolution of the Gediz and Büyük Menderes grabens, Western Anatolia, Turkey, *Quaternary Science Reviews*, **18**(4–5), 549–54.

Yaworsky, P. M., Vernon, K. B., Spangler, J. D., Brewer, S. C., and Coddling, B. F., 2020, Advancing predictive modeling in archaeology: An evaluation of regression and machine learning methods on the Grand Staircase-Escalante National Monument, *PLoS ONE*, **15**(10 October), 1–22.

Yörükan, G., 2009, A study on Celtic/Galatian impacts on the settlement pattern in Anatolia before the Roman era, Middle East Technical University.

## APPENDICES

### A. ARCHAEOLOGICAL SETTLEMENT DATA

The archeological settlement data used in this study is given in Table A-1. Details regarding these settlements (name, period, coordinates, site plan (if possible) and Google Earth plan view) are provided in the following pages. In addition to latitude and longitude, the sites' coordinates are given in UTM ED50 refrence system.

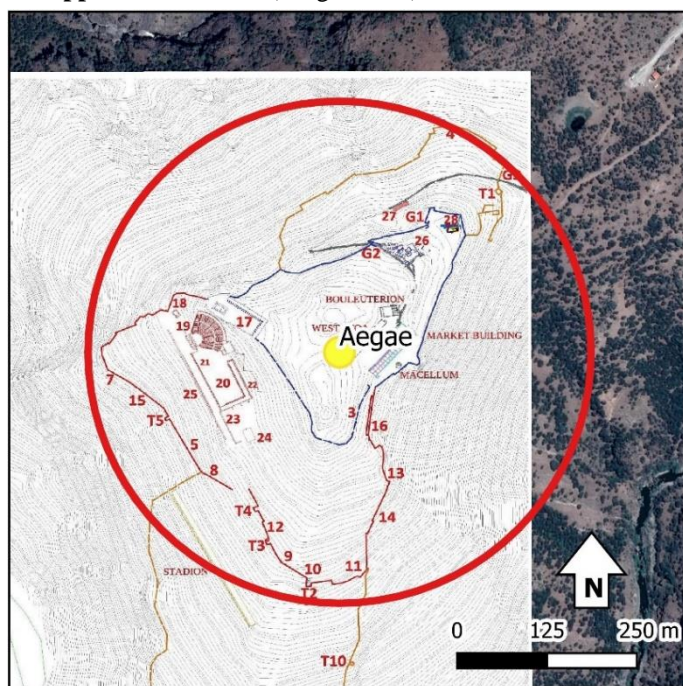
Table A-1 The list of archaeological settlements used in the study.

IDNo	Name	IDNo	Name
1	Aegae	27	Klazomenai
2	Akmonia	28	Laodicea ad Lycum
3	Alabanda	29	Lebedos
4	Alinda	30	Magnesia ad Maeandrum
5	Amyzon	31	Metropolis
6	Anaia	32	Miletus
7	Antiochia ad Maeandrum	33	Myrina
8	Apamea	34	Neonteichos
9	Aphrodisias	35	Notion
10	Apollonis	36	Nysa
11	Attouda	37	Orthosia
12	Bargasa	38	Pergamum
13	Blaundos	39	Philadelpheia
14	Colossae	40	Phocaea
15	Cyme	41	Pitane
16	Elaea	42	Priene
17	Ephesus	43	Sardis
18	Erythrai	44	Smyrna
19	Euhippe	45	Stratonikeia
20	Eumeneia	46	Tabai
21	Harpasa	47	Temnos
22	Heraclea ad Latmum	48	Teos
23	Herakleia Salbakes	49	Thyateira
24	Hierapolis	50	Tralles
25	Hyllarima	51	Tripolis ad Maeandrum
26	Hypaipa		

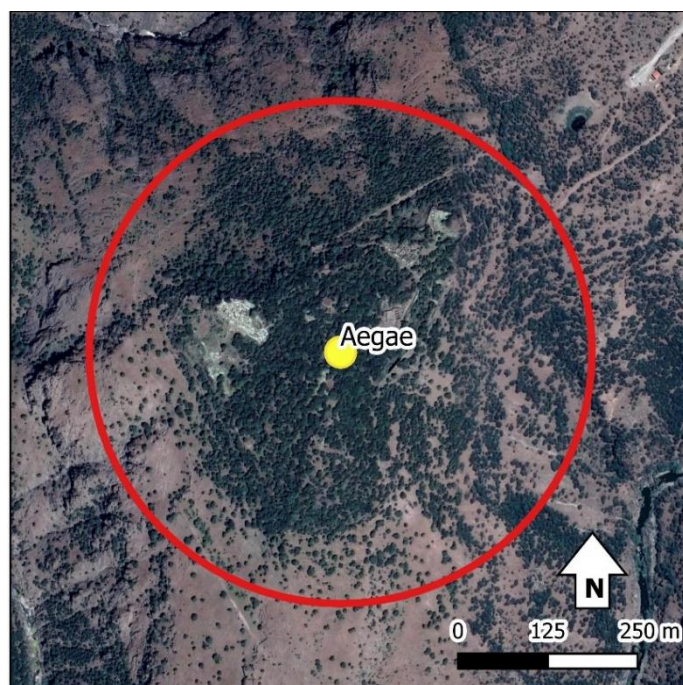
## 1. Aegae (Aigai)

<b>Province</b> Manisa / Merkez	<b>Period</b> 750 BC	<b>Coord.</b> UTME, N 516422 4298159
<b>GeoCont.</b> Nemrut Kale	AD 640	Lat, Long 38.83039 27.18872

Site plan or other supportive material (Sezgin 2018)



Google Earth View



## 2. Akmonia

<b>Province</b> Uşak/ Banaz	<b>Period</b> 330 BC	<b>Coord.</b> UTME, N 740890 4282132
<b>GeoCont.</b> Ahat	AD 640	Lat, Long 38.65336 29.76772

**Site plan or other supportive material** (Taştemür and Dinç 2018)



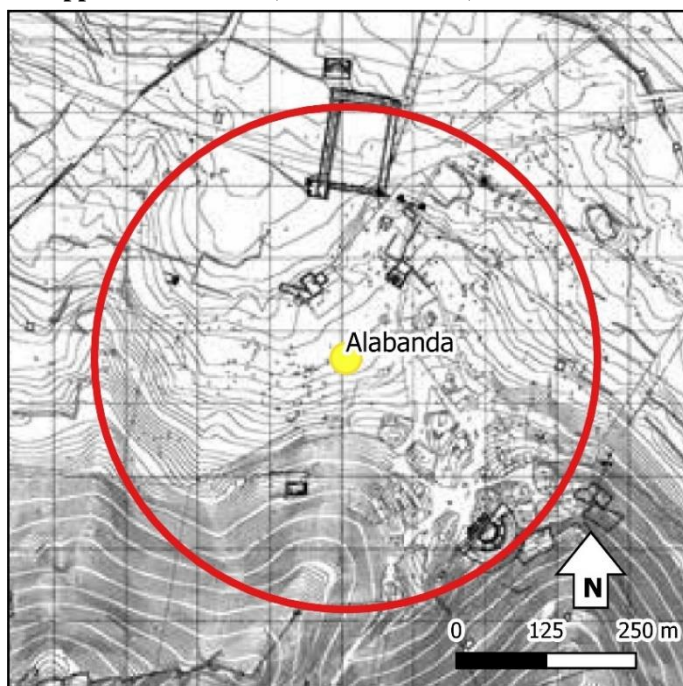
**Google Earth View**



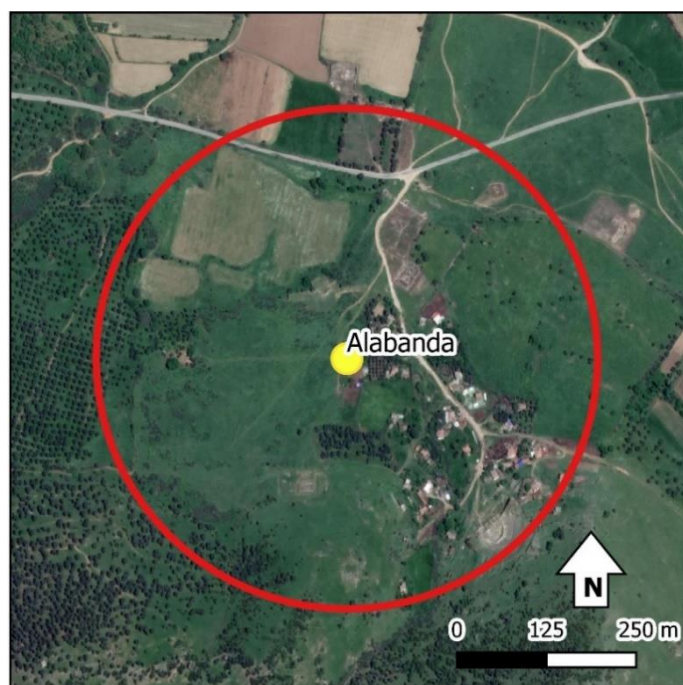
### 3. Alabanda/Antiocheia Chrysaoron

<b>Province</b> Aydın / Çine	<b>Period</b> 550 BC	<b>Coord.</b> UTME, N 586822 4161388
<b>GeoCont.</b> Doğanyurt	AD 640	Lat, Long 37.59381 27.98301

Site plan or other supportive material (Akkan et al. 2016)



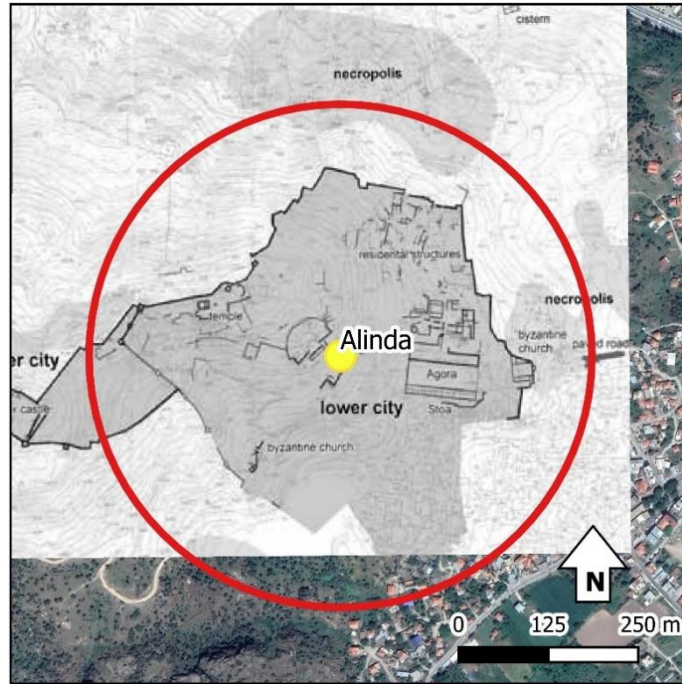
Google Earth View



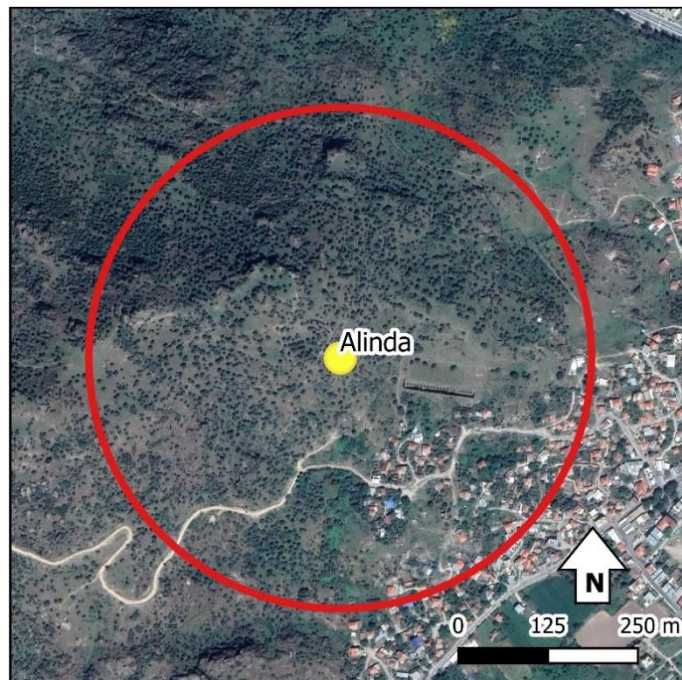
#### 4. Alinda/Alexandria ad Latmum

<b>Province</b> Aydın / Karpuzlu	<b>Period</b> 550 BC	<b>Coord.</b> UTME, N 573151 4157330
<b>GeoCont.</b> Karpuzlu	AD 640	Lat, Long 37.55842 27.82776

Site plan or other supportive material (Ruggendorfer 2011)



Google Earth View



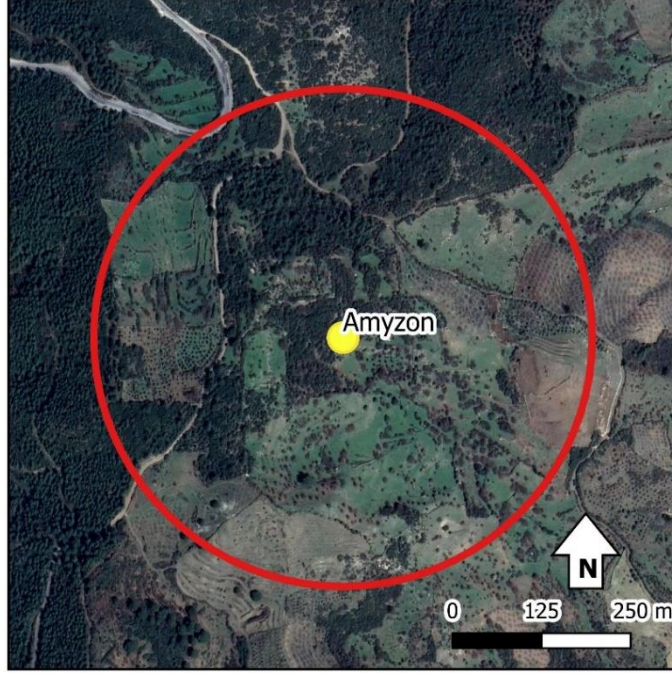
## 5. Amyzon/Mydon

<b>Province</b> Aydın / Koçarlı	<b>Period</b> 550 BC	<b>Coord.</b> UTME, N 562877 4162747
<b>GeoCont.</b> Mazın Kalesi	AD 640	Lat, Long 37.60800 27.71191

### Site plan or other supportive material

The location of site is adjusted observing the architectural remains, especially the city walls that were mentioned in Özkaya and San (2001).

### Google Earth View



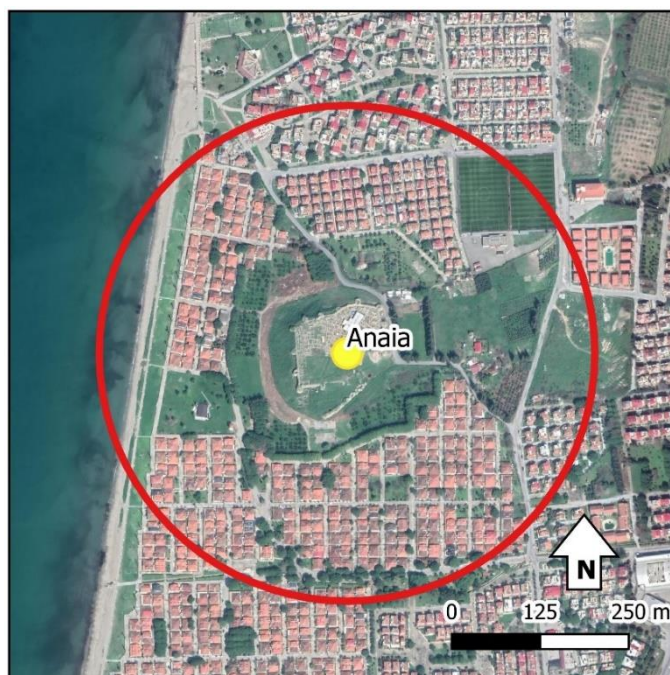
## 6. Anaia

<b>Province</b> Aydın / Kuşadası	<b>Period</b> 330 BC	<b>Coord.</b> UTME, N 523873 4182882
<b>GeoCont.</b> Kadikalesi	AD 2100	Lat, Long 37.79132 27.27067

### Site plan or other supportive material

The city, known as Anaia in antiquity and in the Middle Ages, was located right near the mound on which the Byzantine fortress, today called as Kadikalesi, was built to protect the harbor of the city (Mercangöz 2007). Even though not much known about the Hellenistic Period in Anaia, stone inscriptions and artefacts used in the construction of later buildings and ceramic finds dating the period were found during the excavations (Mercangöz 2005).

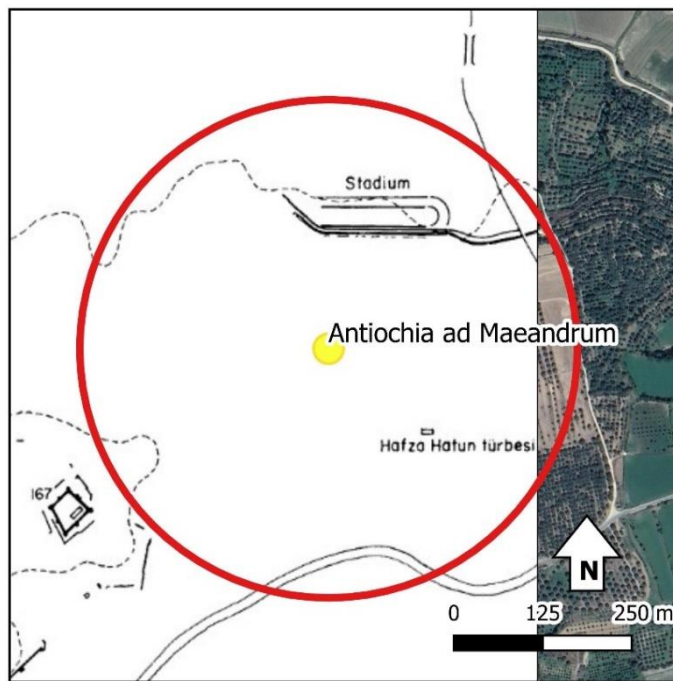
### Google Earth View



## 7. Antiochia ad Maeandrum

<b>Province</b> Aydın / Kuyucak	<b>Period</b> 330 BC	<b>Coord.</b> UTME, N 636621 4193276
<b>GeoCont.</b> Başaran	AD 640	Lat, Long 37.87507 28.55293

Site plan or other supportive material (Smith and Ratté 1996)



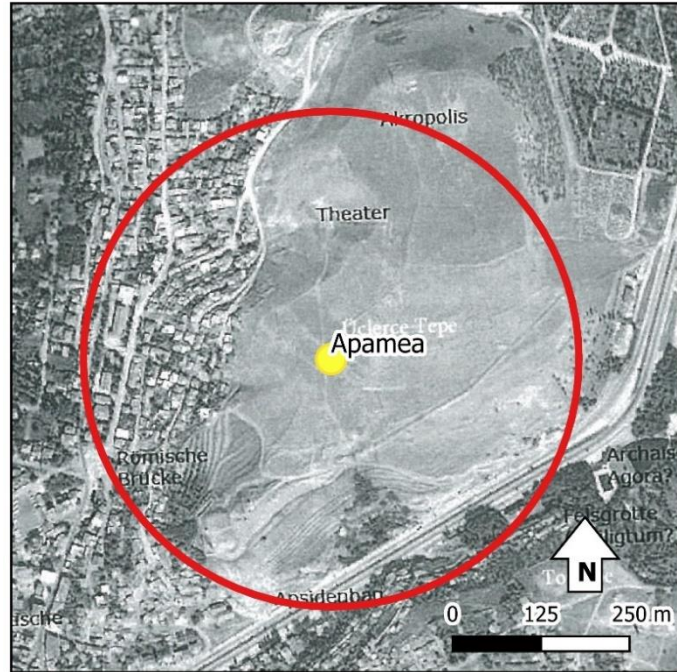
Google Earth View



## 8. Apamea/Kelainai/Kibotos (Apameia)

<b>Province</b> Afyonkarahisar / Dinar	<b>Period</b> 550 BC	<b>Coord.</b> UTME, N 778346 4218774
<b>GeoCont.</b> Dinar	AD 2100	Lat, Long 38.07227 30.17256

Site plan or other supportive material (Von Kienlin 2011)



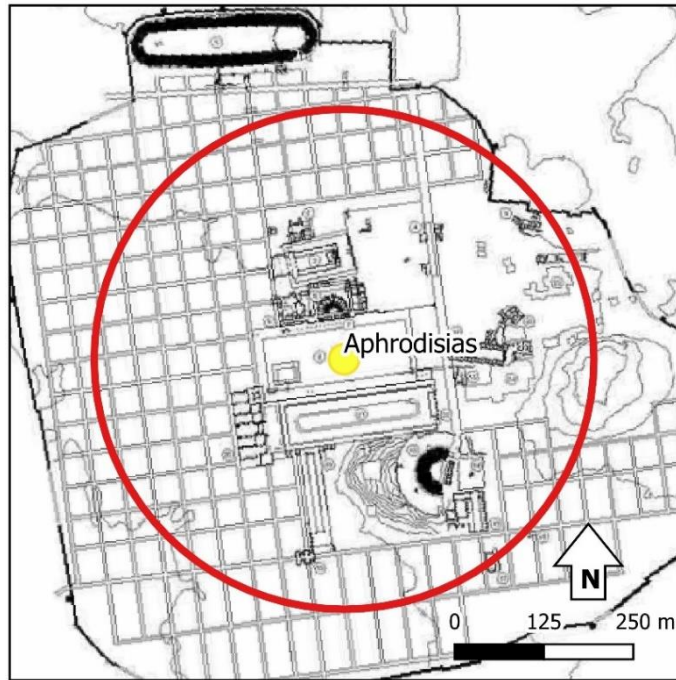
Google Earth View



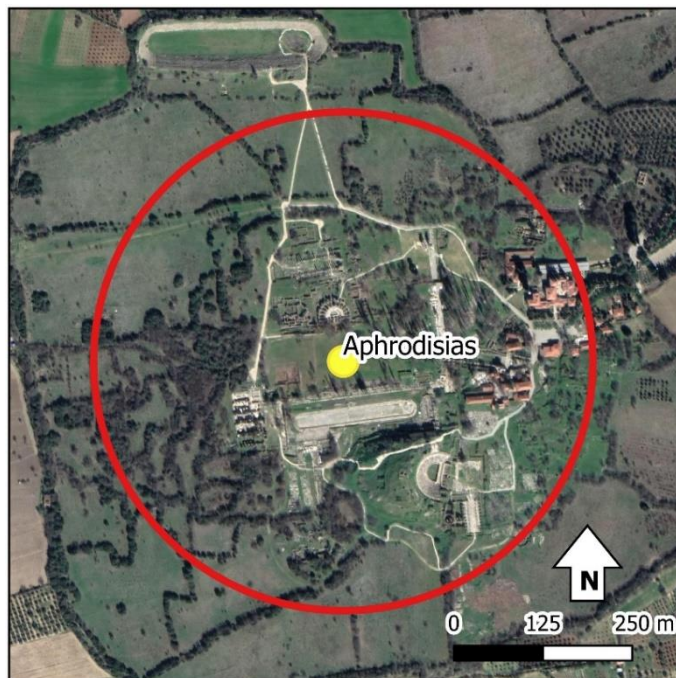
## 9. Aphrodisias

<b>Province</b> Aydın / Karacasu	<b>Period</b> 550 BC	<b>Coord.</b> UTME, N 651995 4175059
<b>GeoCont.</b> Geyre	AD 640	Lat, Long 37.70852 28.72386

Site plan or other supportive material (Mark 2010)



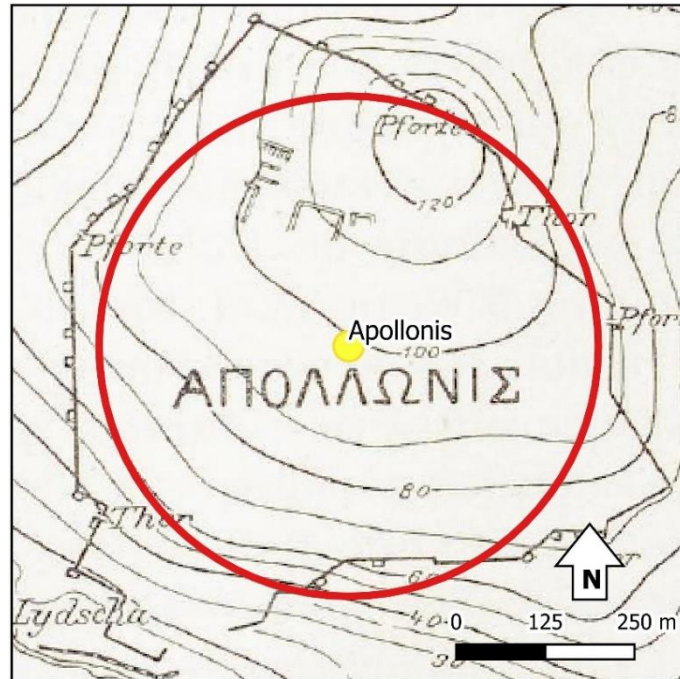
Google Earth View



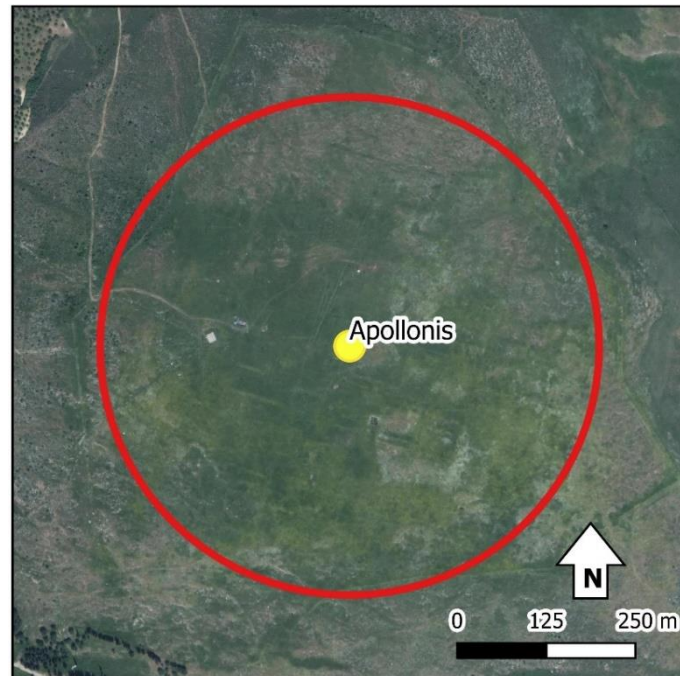
## 10. Apollonis

<b>Province</b> Manisa / Akhisar	<b>Period</b> 330 BC	<b>Coord.</b> UTME, N 558191 4307678
<b>GeoCont.</b> North of Mecidiye	AD 640	Lat, Long 38.91440 27.67073

Site plan or other supportive material (Conze and Schuchhardt 1899)



Google Earth View



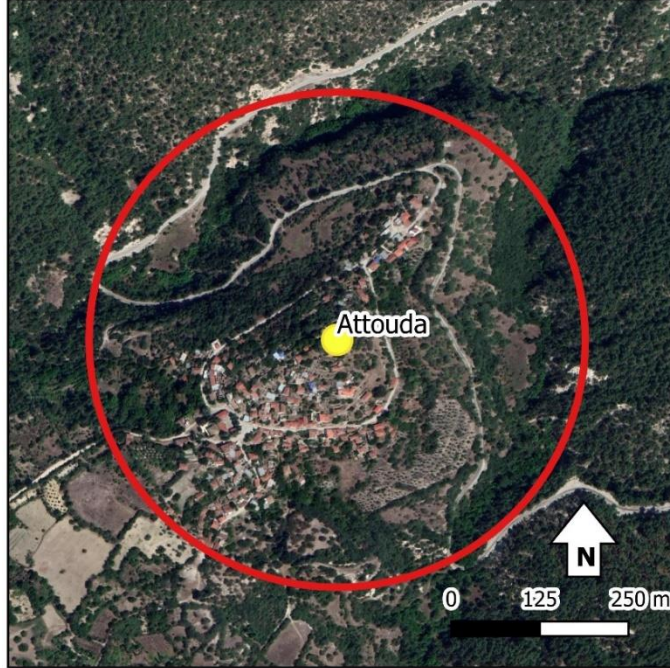
## 11. Attouda

<b>Province</b> Denizli / Sarayköy	<b>Period</b> 330 BC	<b>Coord.</b> UTME, N 659541 4189515
<b>GeoCont.</b> Hisar	AD 2100	Lat, Long 37.83746 28.81260

### Site plan or other supportive material

The ancient city of Attouda is located beneath the old Hisar village settlement (Söğüt 2016). The Hisar village has been moved to the edge of Sarayköy-Hisar road in the northeast of Arap Creek since new constructions are not allowed at the ancient city site.

### Google Earth View



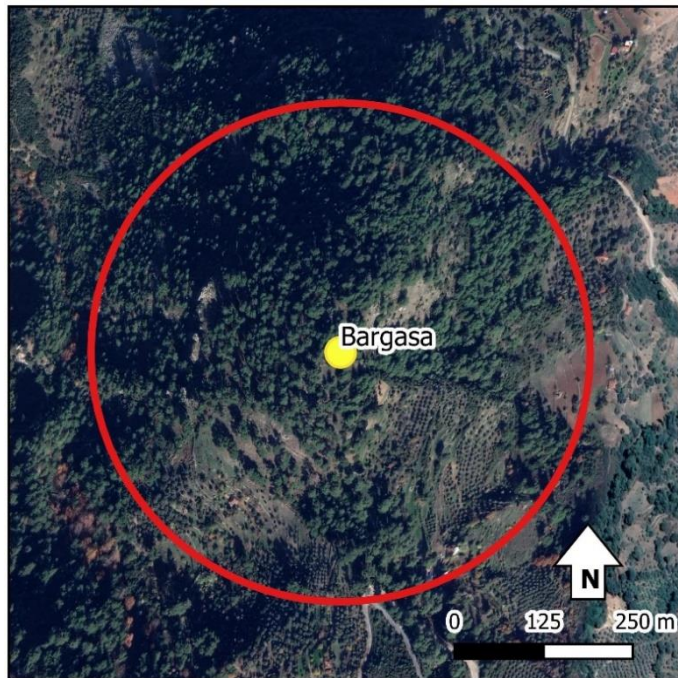
## 12. Bargasa

<b>Province</b> Aydın / Bozdoğan	<b>Period</b> 330 BC	<b>Coord.</b> UTME, N 625230 4162714
<b>GeoCont.</b> Haydere	AD 300	Lat, Long 37.60133 28.41820

**Site plan or other supportive material** (Debord and Varinlioğlu 2010)



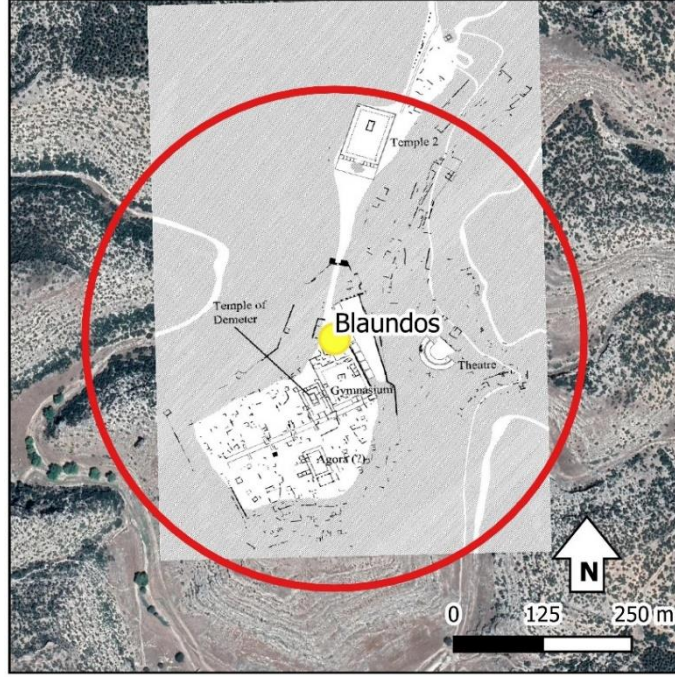
**Google Earth View**



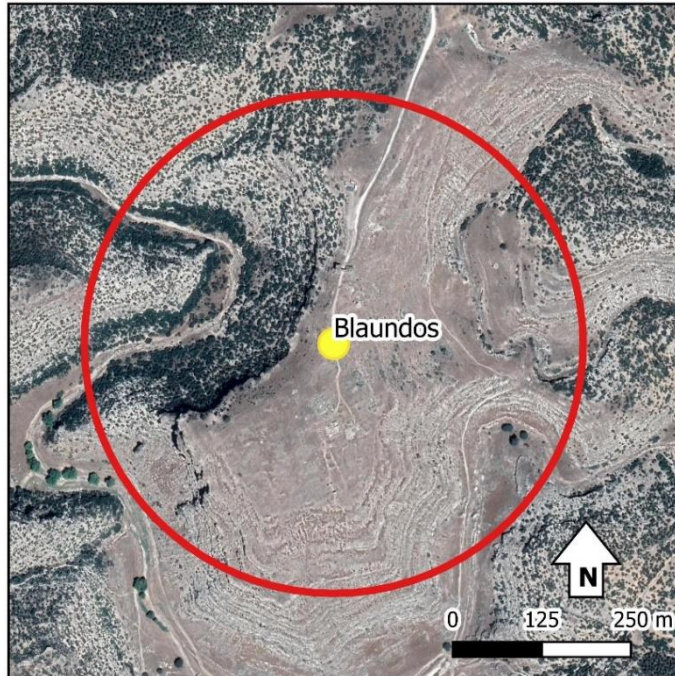
### 13. Blaundos

<b>Province</b> Uşak / Ulubey	<b>Period</b> 330 BC	<b>Coord.</b> UTME, N 693080 4248055
<b>GeoCont.</b> Sülümenli	AD 640	Lat, Long 38.35820 29.20934

Site plan or other supportive material (Filges 2006)



Google Earth View



## 14. Colossae

<b>Province</b> Denizli / Honaz	<b>Period</b> 550 BC	<b>Coord.</b> UTME, N 699058 4184717
<b>GeoCont.</b> Honaz	AD 640	Lat, Long 37.78649 29.26008

**Site plan or other supportive material** (Denizli İl Kültür ve Turizm Müdürlüğü 2020)



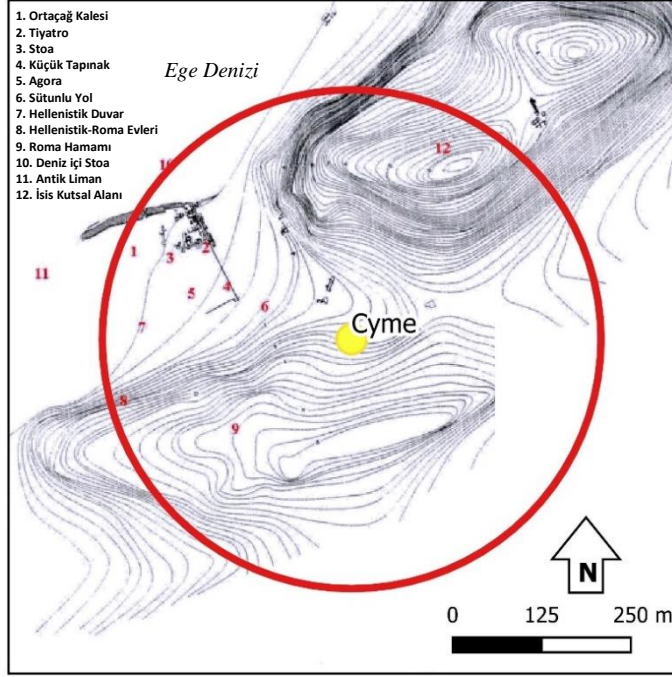
**Google Earth View**



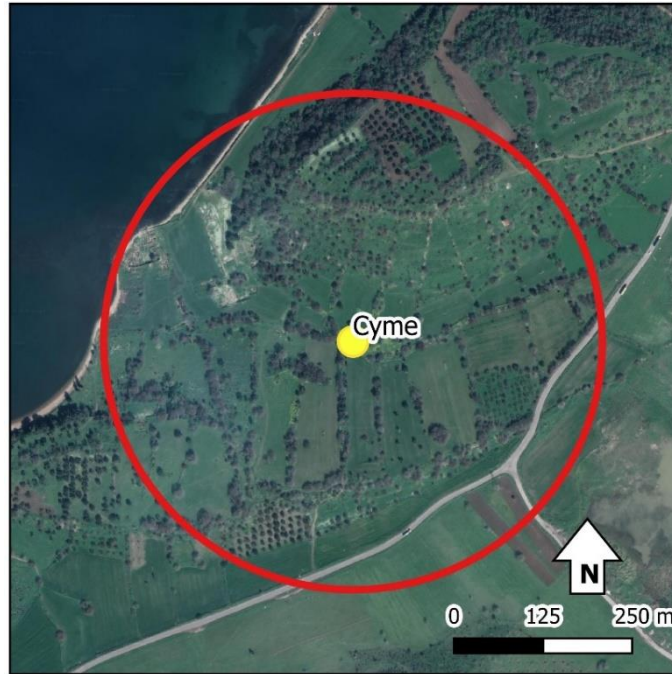
## 15. Cyme (Kyme)

<b>Province</b> İzmir / Aliğa	<b>Period</b> 750 BC	<b>Coord.</b> UTME, N 494748 4290135
<b>GeoCont.</b> Nemrut Limanı	AD 640	Lat, Long 38.75822 26.93908

Site plan or other supportive material (La Marca 2013)



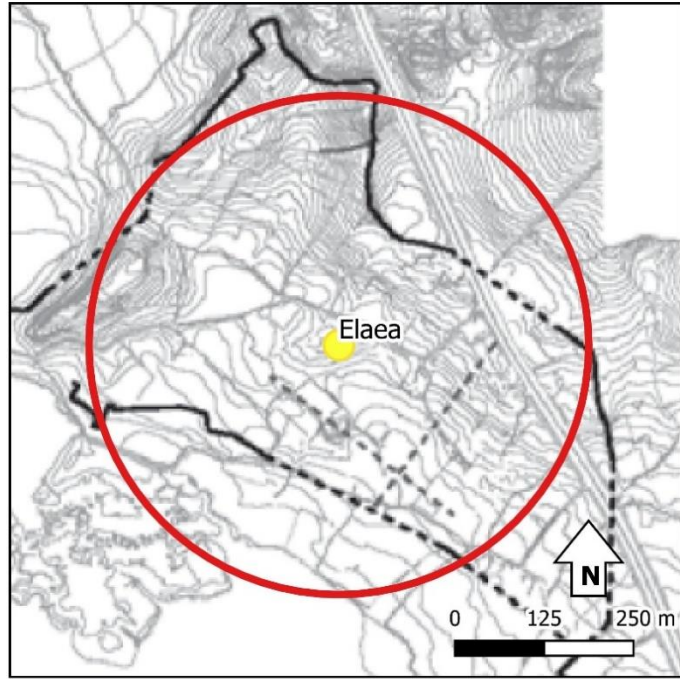
Google Earth View



## 16. Elaea (Elaiia)

<b>Province</b> İzmir / Bergama	<b>Period</b> 750 BC	<b>Coord.</b> UTME, N 503917 4310793
<b>GeoCont.</b> Kazıkbağları	AD 640	Lat, Long 38.94439 27.04472

Site plan or other supportive material (Pirson 2008)



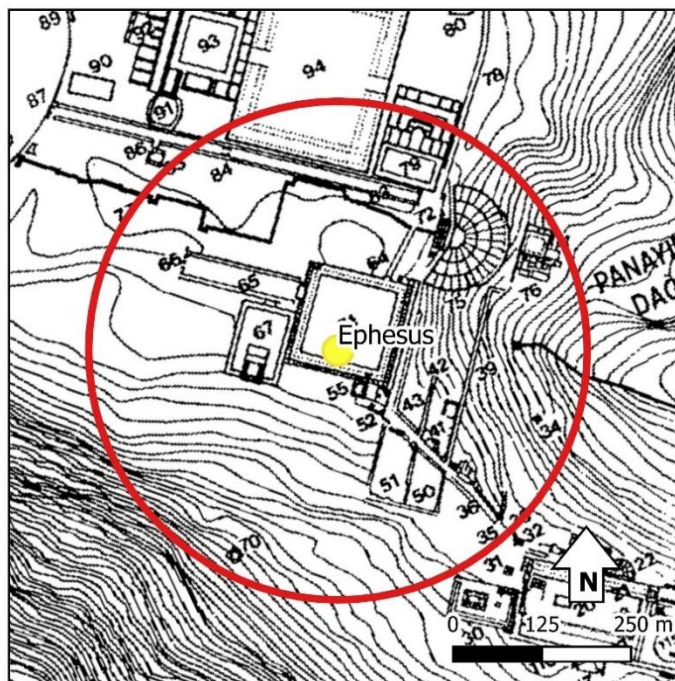
Google Earth View



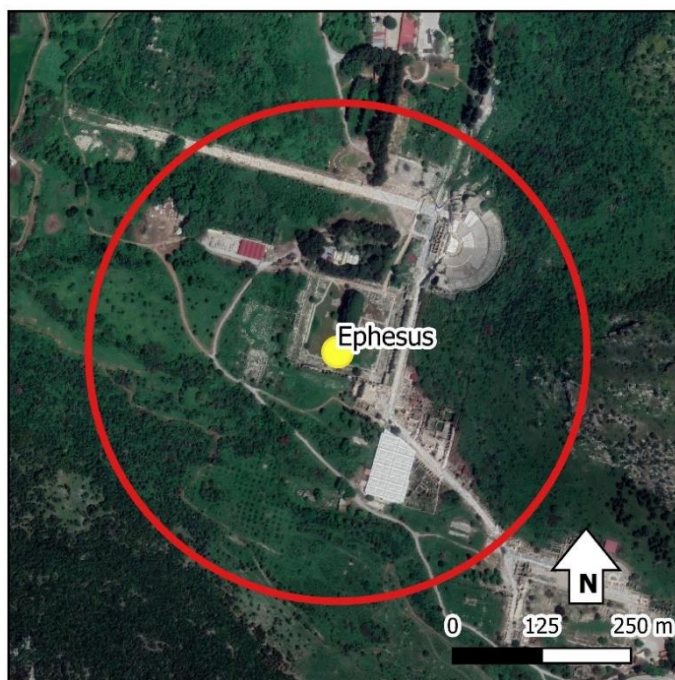
## 17. Ephesus/Arsinoe(ia) (Efes)

<b>Province</b> İzmir / Selçuk	<b>Period</b> 1200 BC	<b>Coord.</b> UTME, N 529966 4199358
<b>GeoCont.</b> Selçuk	AD 2000	Lat, Long 37.93963 27.34056

Site plan or other supportive material (Crouch 2003)



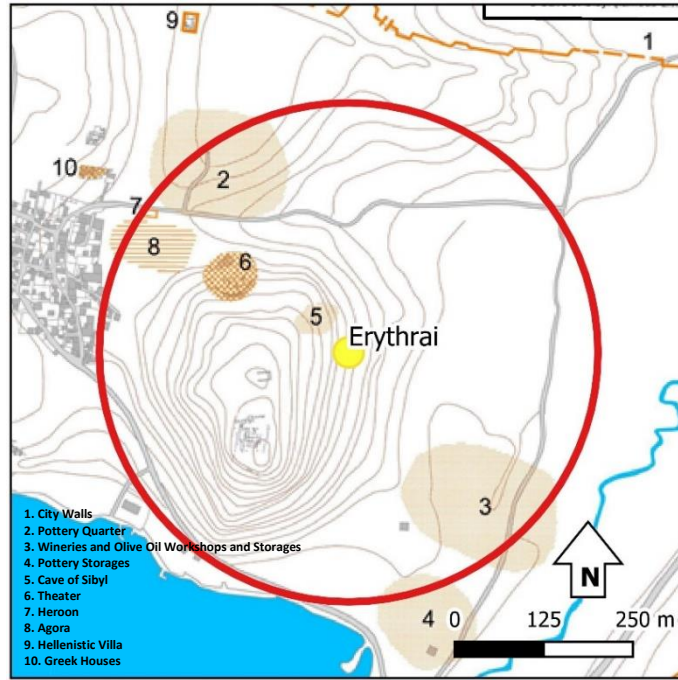
Google Earth View



## 18. Erythrai

<b>Province</b> İzmir / Çeşme	<b>Period</b> 550 BC	<b>Coord.</b> UTME, N 454859 4248478
<b>GeoCont.</b> Ildır	AD 640	Lat, Long 38.38168 26.48270

**Site plan or other supportive material** Hellenistic remains of Erythrai (Topaloğlu 2017)



**Google Earth View**



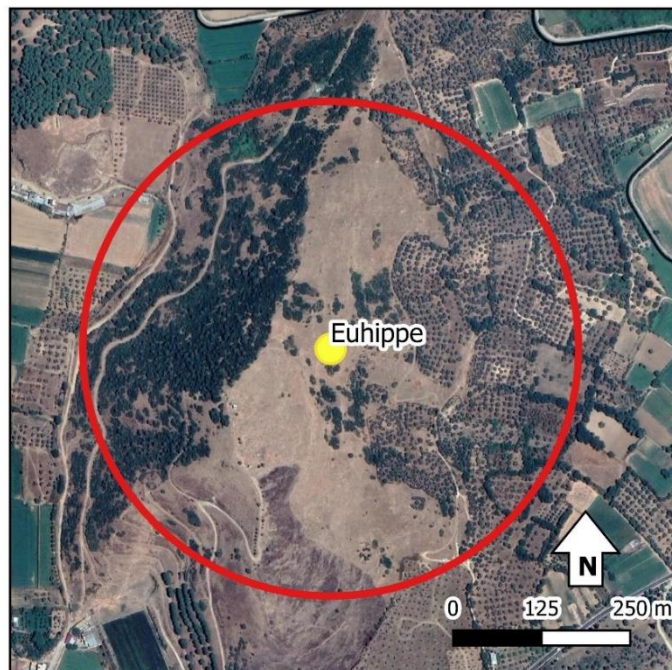
## 19. Euhippe

<b>Province</b> Aydın / Merkez	<b>Period</b> 330 BC	<b>Coord.</b> UTME, N 594991 4183840
<b>GeoCont.</b> Dalama	AD 300	Lat, Long 37.79533 28.07845

### Site plan or other supportive material

Settlement data provided by Willet (2020) for Euhippe includes mentions of coins minted in this city from the Hellenistic Period and remains of fortification and theater (confirmed on Google Earth).

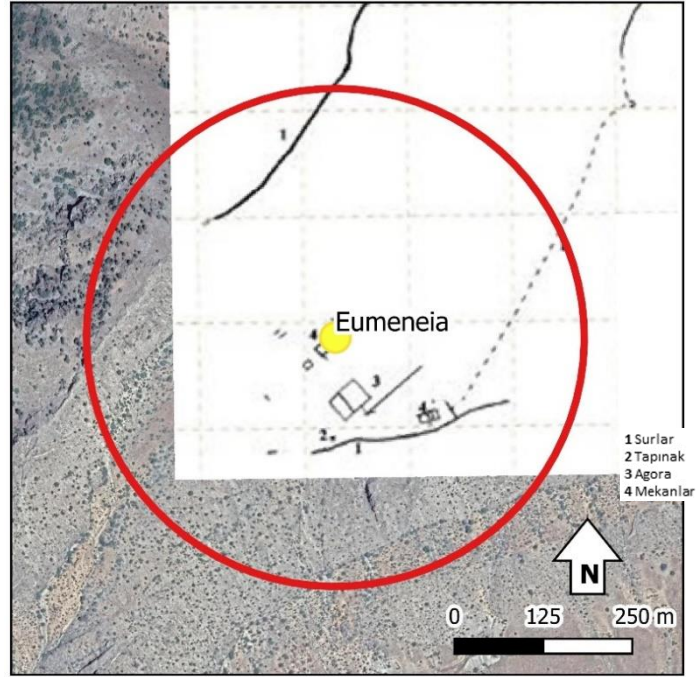
### Google Earth View



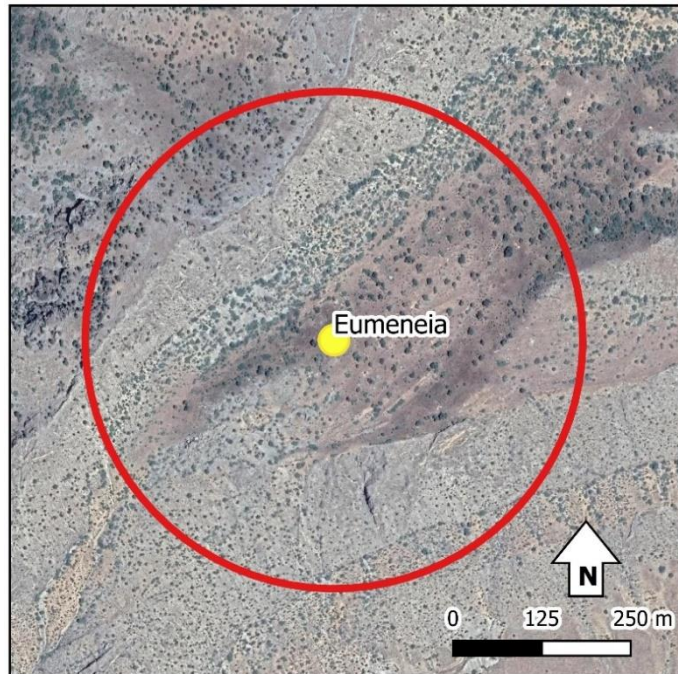
## 20. Eumeneia/Fulvia

<b>Province</b> Denizli / Çivril	<b>Period</b> 330 BC	<b>Coord.</b> UTME, N 749511 4246500
<b>GeoCont.</b> Işıklı	AD 640	Lat, Long 38.33026 29.85398

Site plan or other supportive material (Sezgin and Taşkıran 2011)



Google Earth View

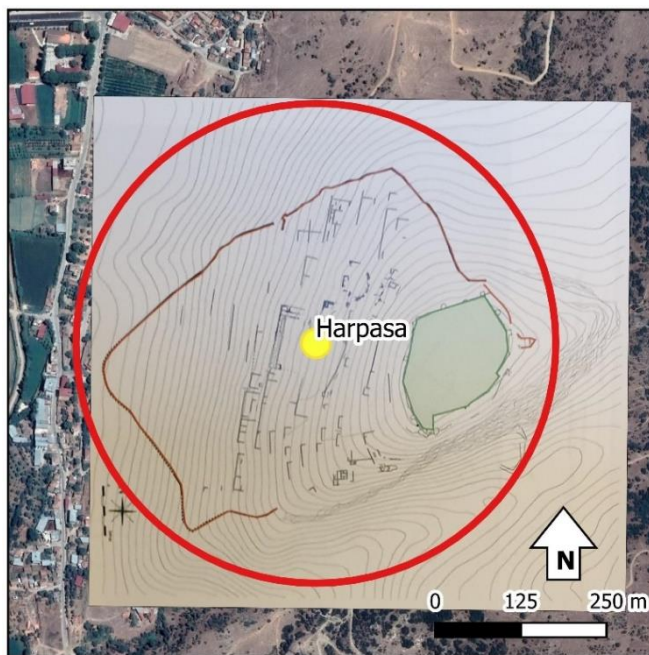


## 21. Harpasa

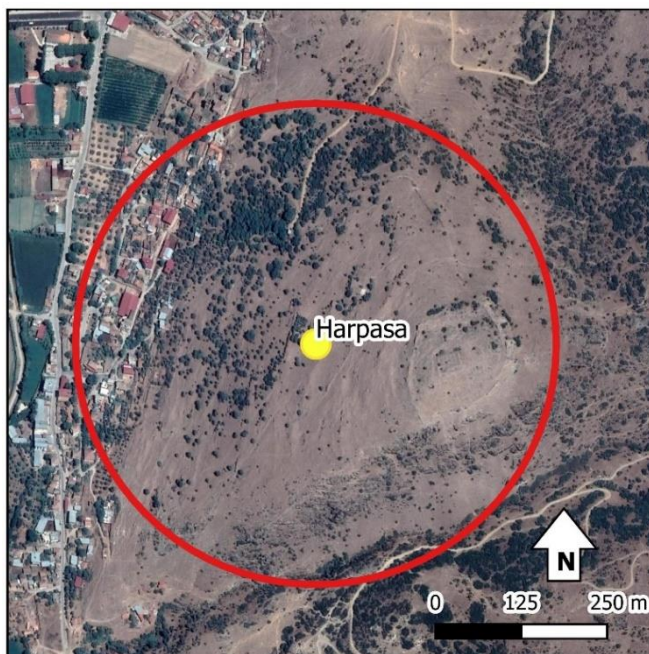
<b>Province</b> Aydın / Nazilli	<b>Period</b>	<b>Coord.</b> UTME, N 618930 4184972
<b>GeoCont.</b> Esenköy (prev. Arpaz)		Lat, Long 38.33026 29.85398

### Site plan or other supportive material

The site's period is attested to 30 BC- AD 640 in Pleiades Project database. However, there are architectural remains showing Hellenistic characteristics (Debord and Varinlioğlu 2010).



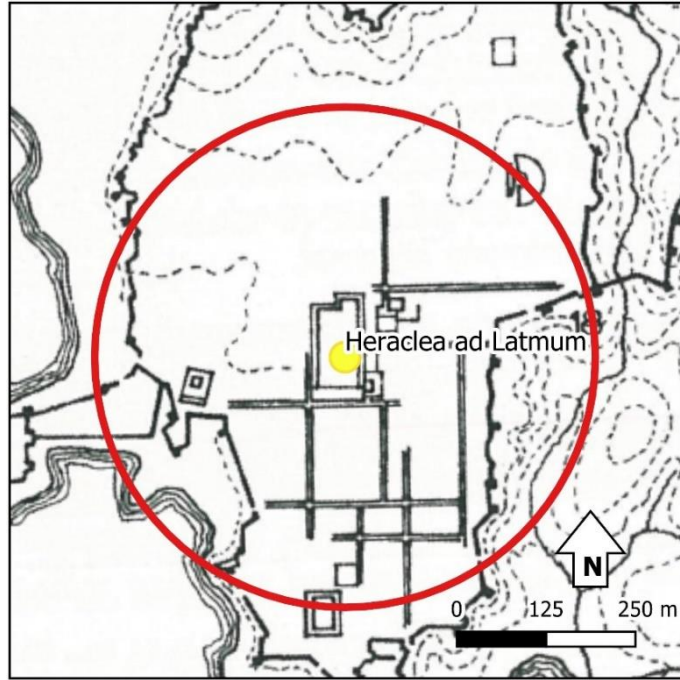
### Google Earth View



## 22. Heraclea ad Latmum/Pleistarcheia

<b>Province</b> Muğla / Milas	<b>Period</b> 550 BC	<b>Coord.</b> UTME, N 546559 4150850
<b>GeoCont.</b> Kapıkırı	AD 640	Lat, Long 37.50174 27.52628

Site plan or other supportive material (McNicoll and Milner 1997)



Google Earth View



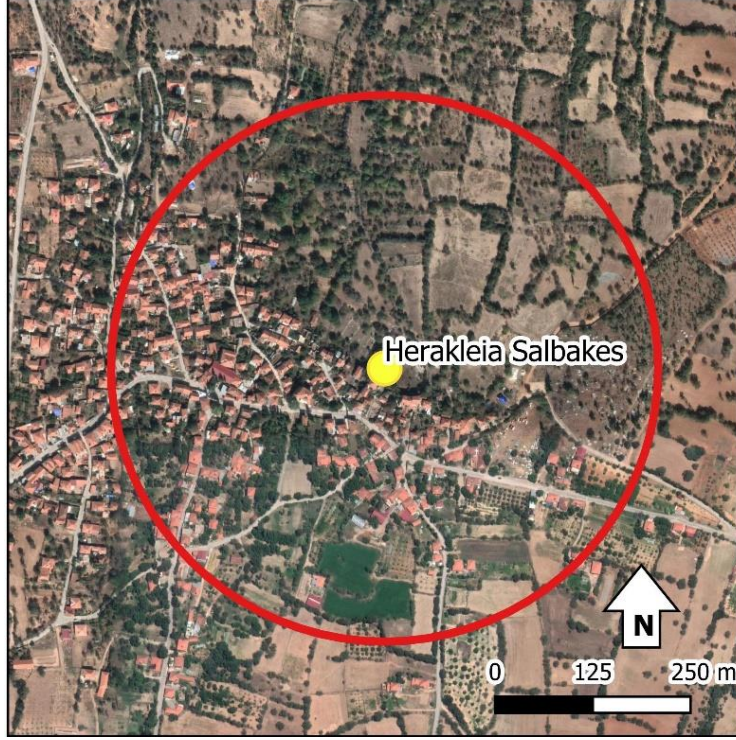
### 23. Herakleia Salbakes

<b>Province</b> Denizli / Tavas	<b>Period</b> 330 BC	<b>Coord.</b> UTME, N 675267 4165995
<b>GeoCont.</b> Vakıf	AD 640	Lat, Long 37.62271 28.98556

#### Site plan or other supportive material

The location of site is adjusted based on the descriptions given at the webpage of Denizli Provincial Directorate of Culture and Tourism and the remains of stadium seen in the Google Earth (Denizli İl Kültür ve Turizm Müdürlüğü 2020b).

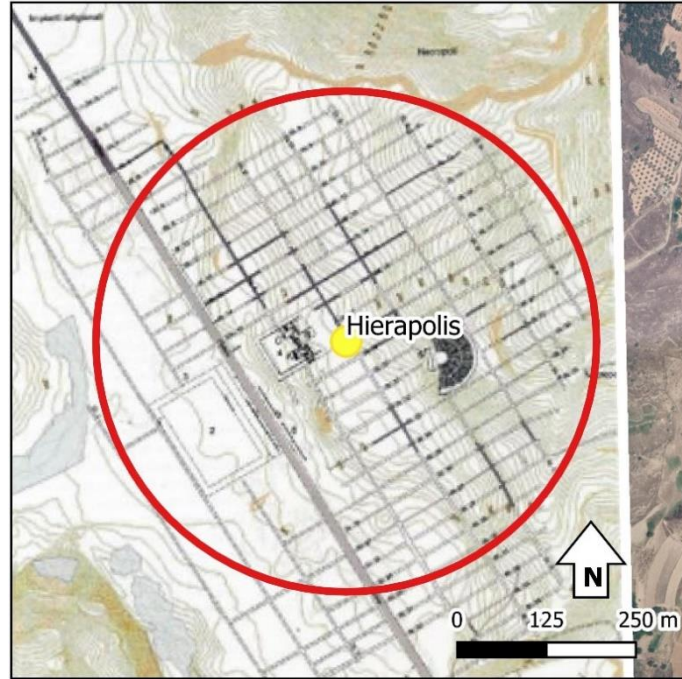
#### Google Earth View



## 24. Hierapolis

<b>Province</b> Denizli / Merkez	<b>Period</b> 550 BC	<b>Coord.</b> UTME, N 687032 4200032
<b>GeoCont.</b> Pamukkale	AD 640	Lat, Long 37.92696 29.12756

**Site plan or other supportive material** Plan of Hierapolis in the Hellenistic and early imperial periods (University of Salento 2013)



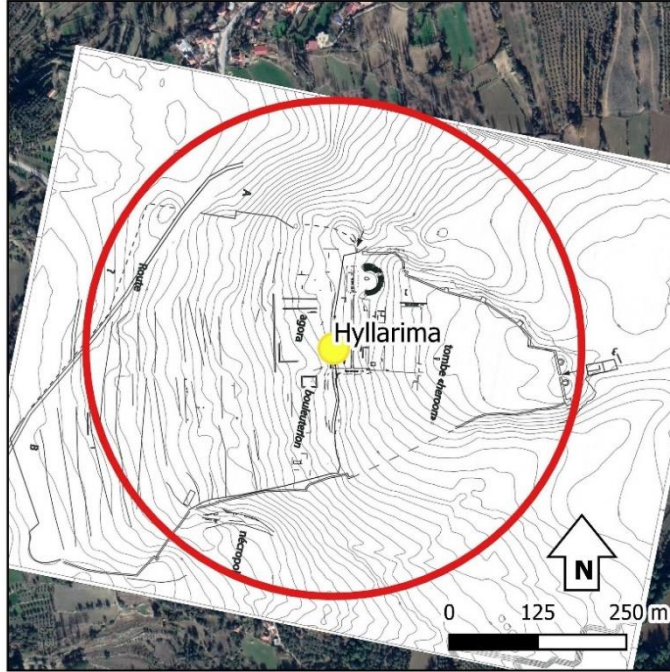
**Google Earth View**



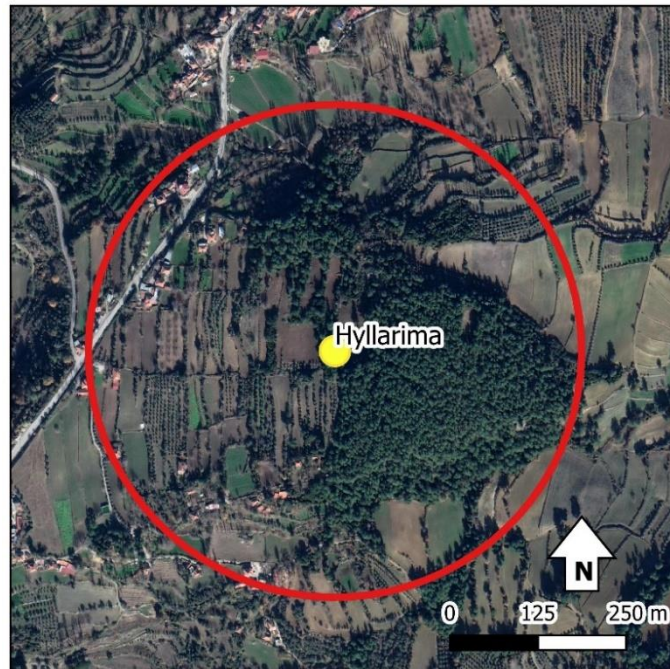
## 25. Hyllarima

<b>Province</b> Muğla / Kavaklıdere	<b>Period</b> 330 BC	<b>Coord.</b> UTME, N 619292 4151830
<b>GeoCont.</b> Derebağ	AD 640	Lat, Long 37.50404 28.34917

Site plan or other supportive material (Debord and Varinlioğlu 2018)



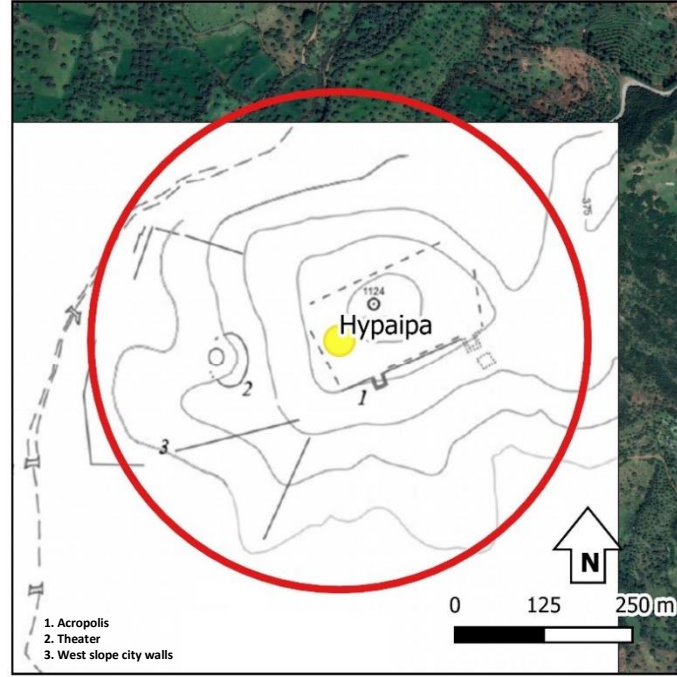
Google Earth View



## 26. Hypaipa

<b>Province</b> İzmir / Ödemiş	<b>Period</b> 330 BC	<b>Coord.</b> UTME, N 584010 4237041
<b>GeoCont.</b> Gönlüce (prev. Datbey)	AD 640	Lat, Long 38.27583 27.95998

**Site plan or other supportive material** (Kalkan and Koçak Yaldir 2013)



**Google Earth View**



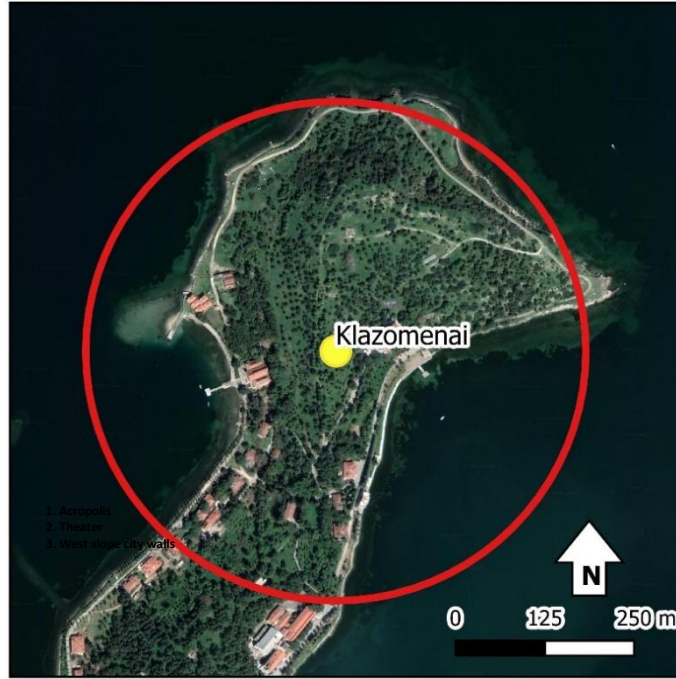
## 27. Klazomenai

<b>Province</b> İzmir / Urla	<b>Period</b> 550 BC	<b>Coord.</b> UTME, N 481485 4247569
<b>GeoCont.</b> Karantina Adası	AD 2000	Lat, Long 38.37444 26.78756

### Site plan or other supportive material

The location of site is adjusted based on the results of surveys and excavations carried out on the Karantina Island (Ersoy et al. 2015).

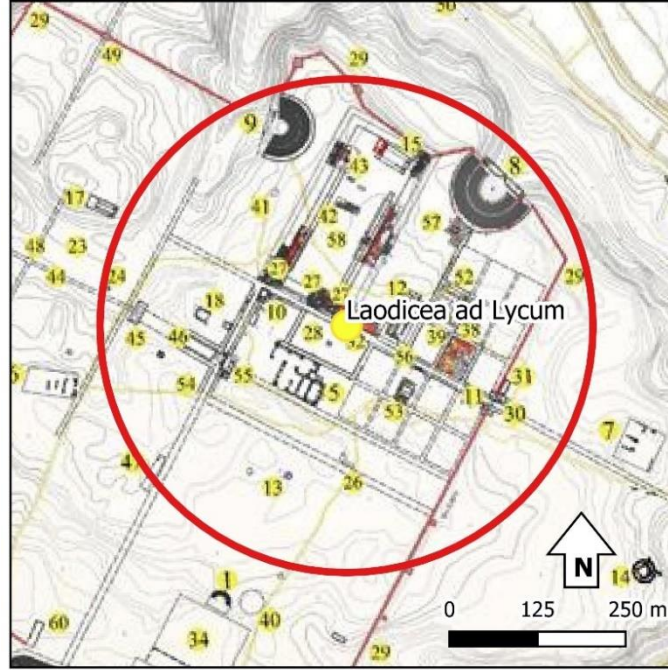
### Google Earth View



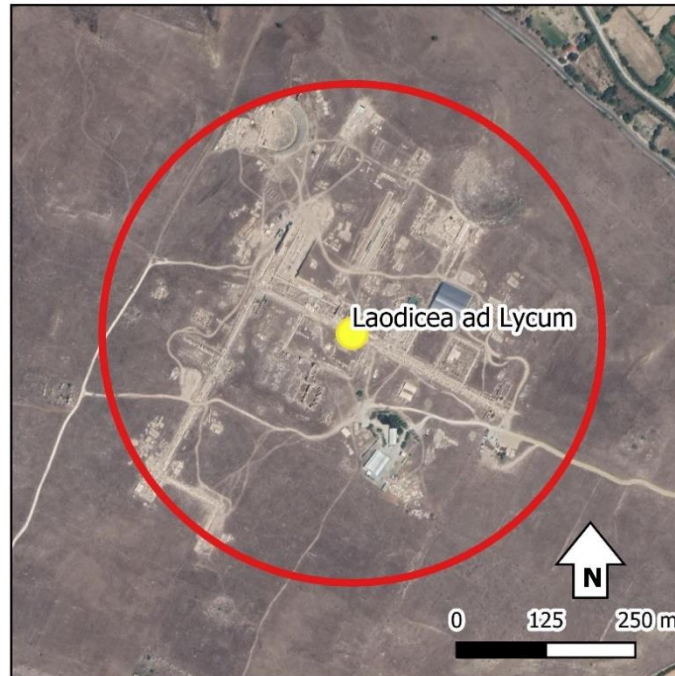
## 28. Laodicea ad Lycum/Diospolis/Roas

<b>Province</b> Denizli / Merkez	<b>Period</b> 550 BC	<b>Coord.</b> UTME, N 685621 4189909
<b>GeoCont.</b> Eski Hisar	AD 300	Lat, Long 37.83608 29.10891

Site plan or other supportive material (Denizli İl Kültür ve Turizm Müdürlüğü 2020c)



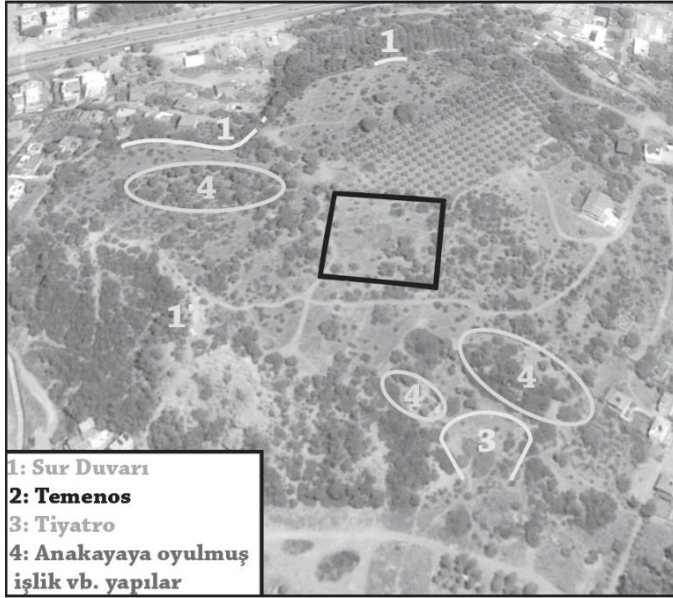
Google Earth View



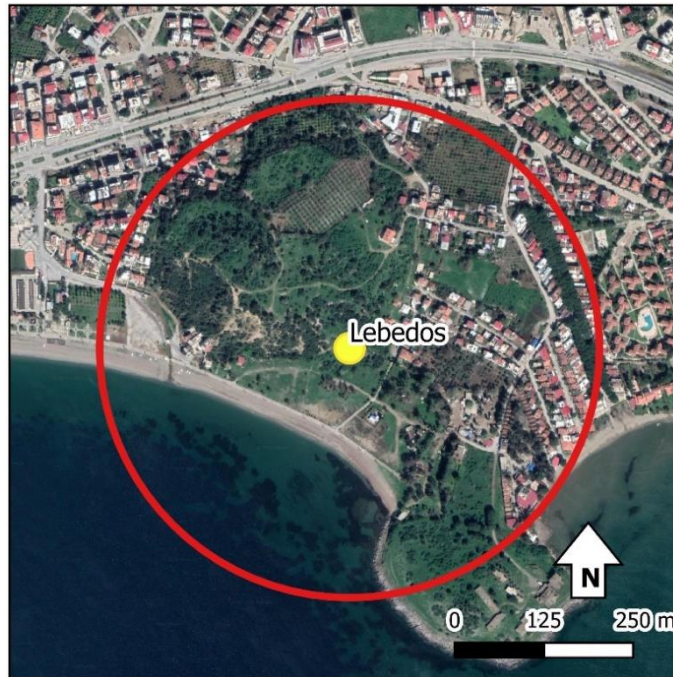
## 29. Lebedos/Ptolemais

<b>Province</b> İzmir / Seferihisar	<b>Period</b> 750 BC	<b>Coord.</b> UTME, N 497005 4214436
<b>GeoCont.</b> Kısık	AD 640	Lat, Long 38.07601 26.96538

**Site plan or other supportive material** Architectural remains on acropolis (Coşkun 2018)



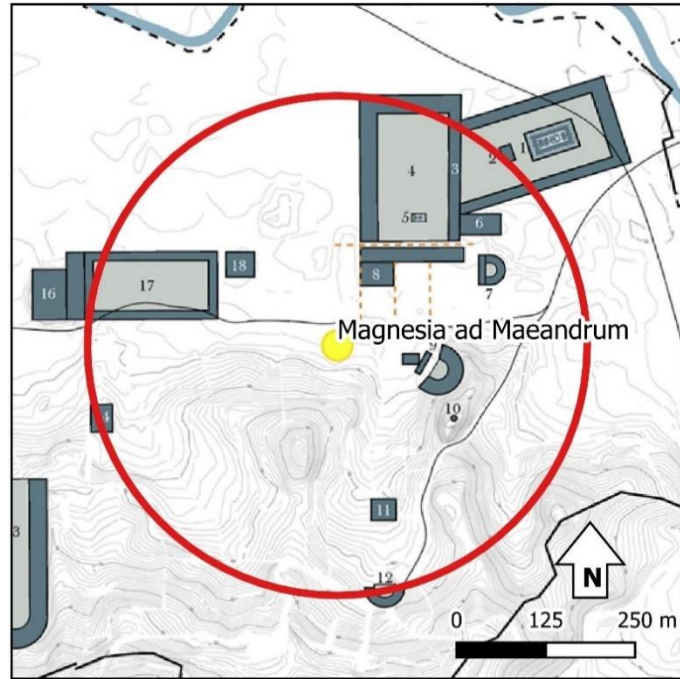
**Google Earth View**



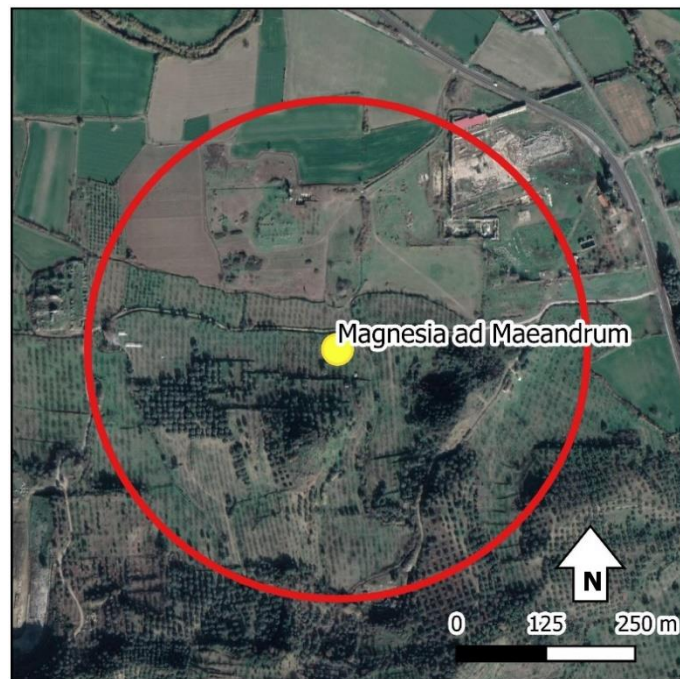
### 30. Magnesia ad Maeandrum/Leukophrys

<b>Province</b> Aydın / Germencik	<b>Period</b> 550 BC	<b>Coord.</b> UTME, N 546155 4189559
<b>GeoCont.</b> Tekin	AD 640	Lat, Long 37.85065 27.52417

Site plan or other supportive material (Saldaña 2018)



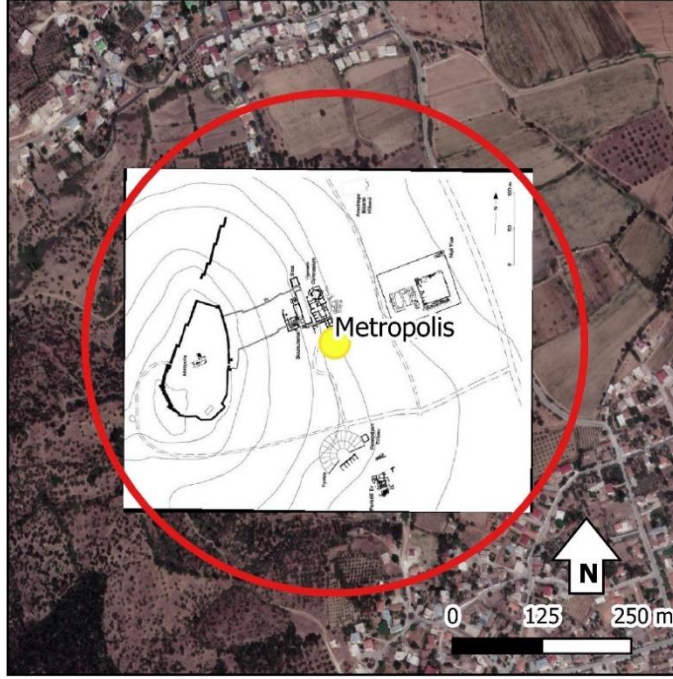
Google Earth View



### 31. Metropolis

<b>Province</b> İzmir / Torbalı	<b>Period</b> 330 BC	<b>Coord.</b> UTME, N 528493 4219948
<b>GeoCont.</b> Yeniköy	AD 640	Lat, Long 38.12526 27.32461

Site plan or other supportive material (Metropolis Kazı ve Araştırmaları 2017)



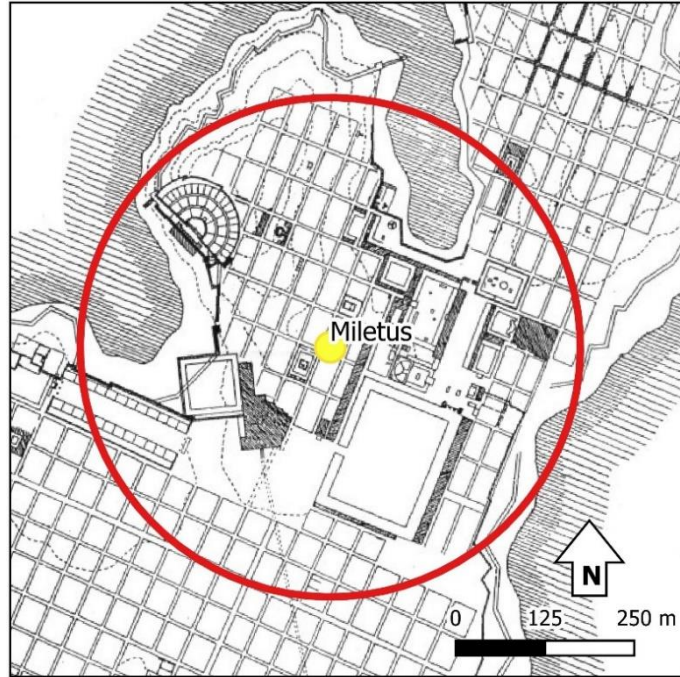
Google Earth View



### 32. Miletus (Milet)

<b>Province</b> Aydın / Didim	<b>Period</b> 1750 BC	<b>Coord.</b> UTME, N 524617 4153784
<b>GeoCont.</b> Balat	AD 2000	Lat, Long 37.52903 27.27814

Site plan or other supportive material (Weber 2002)



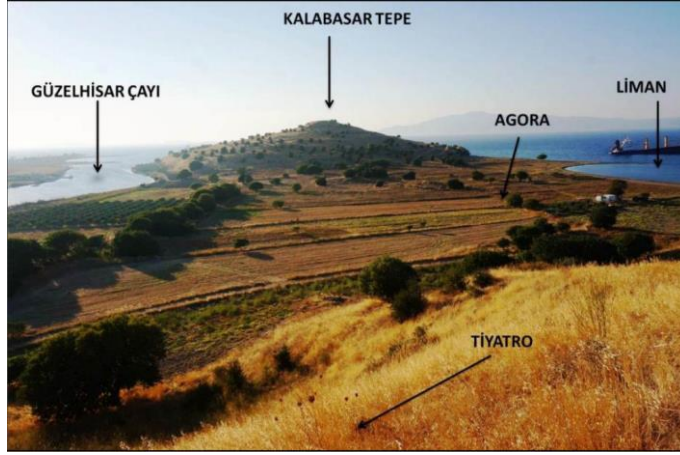
Google Earth View



### 33. Myrina/Sebastopolis

<b>Province</b> İzmir / Aliğa	<b>Period</b> 1750 BC	<b>Coord.</b> UTME, N 498531 4299879
<b>GeoCont.</b> Mouth of Güzelhisar R.	AD 2000	Lat, Long 38.84605 26.98260

Site plan or other supportive material (Çekilmez et al. 2016)



Google Earth View



### 34. Neonteichos

<b>Province</b> İzmir / Menemen	<b>Period</b> 750 BC	<b>Coord.</b> UTME, N 507964 4279099
<b>GeoCont.</b> Yanıkköy	AD 640	Lat, Long 38.65875 27.09106

#### Site plan or other supportive material

The location of site is adjusted observing the architectural remains, especially the city walls which were mentioned in (Erkanal Öktü et al. 2002)

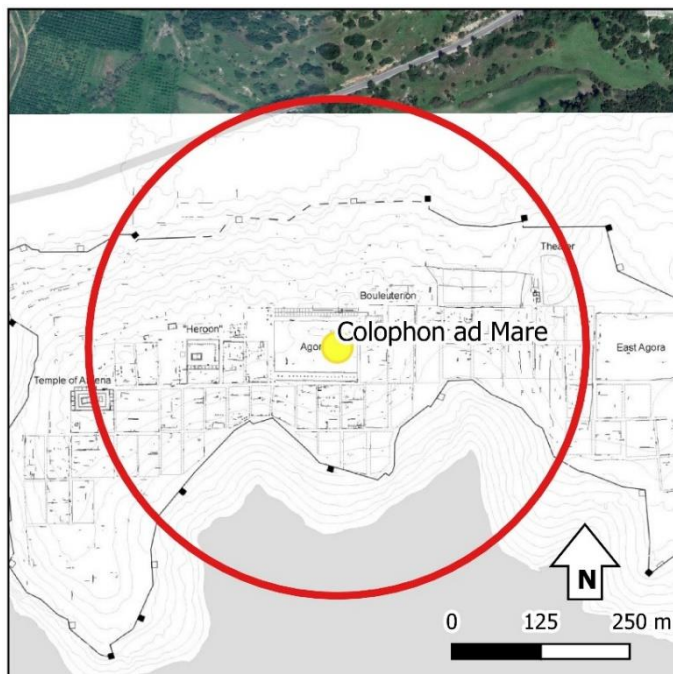
#### Google Earth View



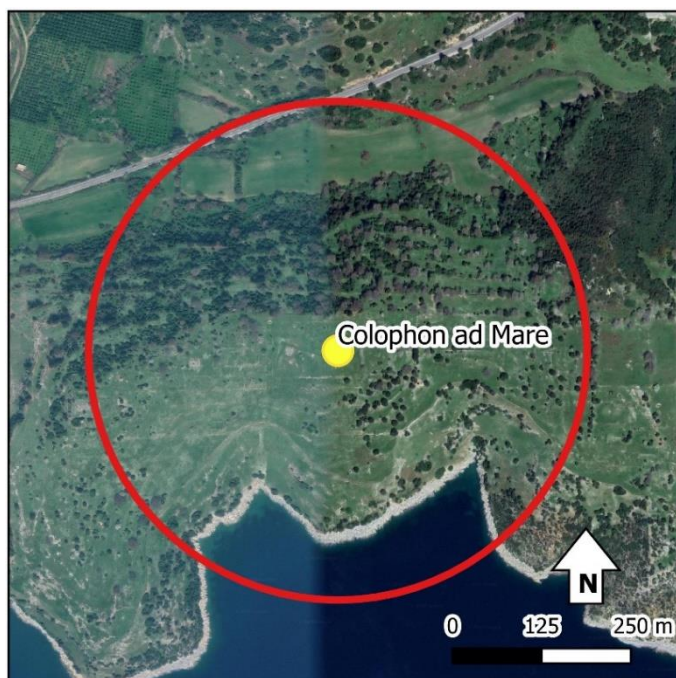
### 35. Notion/ Colophon ad Mare

<b>Province</b> İzmir / Menderes	<b>Period</b> 750 BC	<b>Coord.</b> UTME, N 517390 4205213
<b>GeoCont.</b> Ahmetbeyli	AD 640	Lat, Long 37.99273 27.19758

Site plan or other supportive material (Ratté et al. 2016)



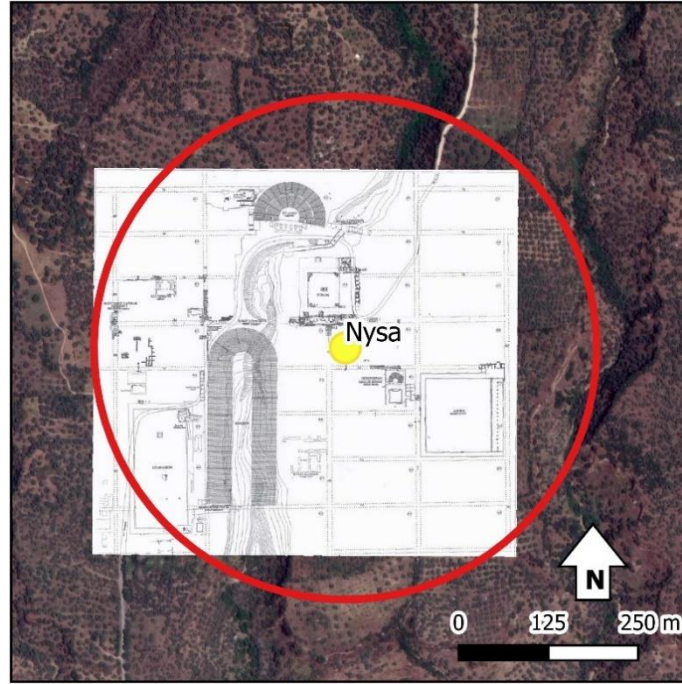
Google Earth View



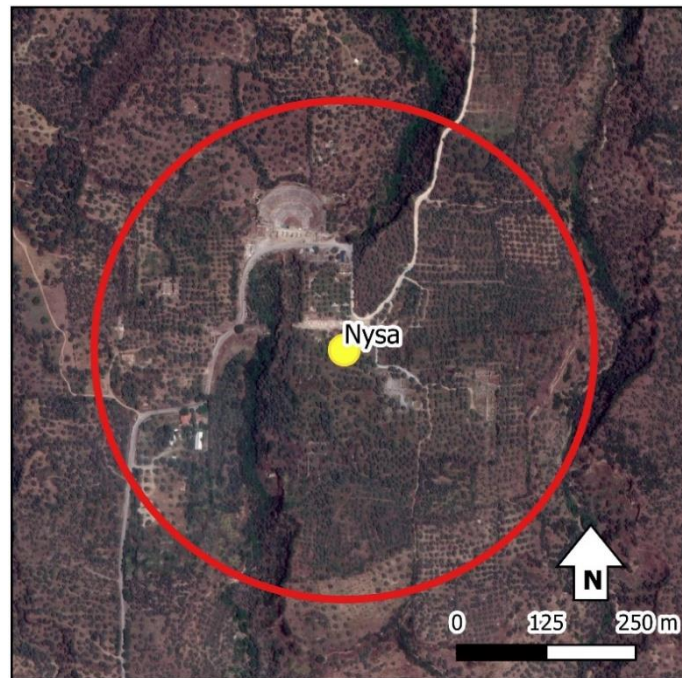
### 36. Nysa/Athymbra

<b>Province</b> İzmir / Sultanhisar	<b>Period</b> 550 BC	<b>Coord.</b> UTME, N 600821 4195731
<b>GeoCont.</b> Sultanhisar	AD 640	Lat, Long 37.90186 28.14631

Site plan or other supportive material (Öztaner 2018)



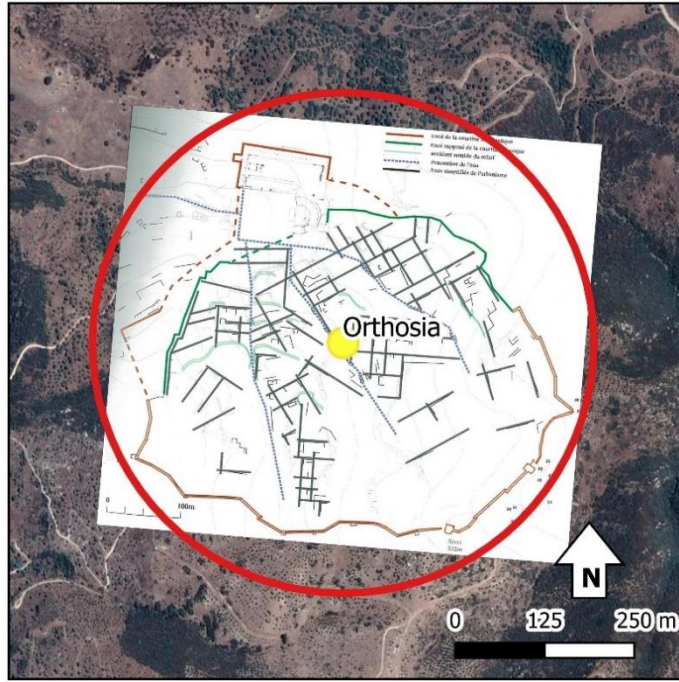
Google Earth View



### 37. Orthosia

<b>Province</b> Aydın / Yenipazar	<b>Period</b> 330 BC	<b>Coord.</b> UTME, N 608273 4186898
<b>GeoCont.</b> Ortas	AD 640	Lat, Long 37.82141 28.22974

Site plan or other supportive material (Debord and Varinlioğlu 2010)



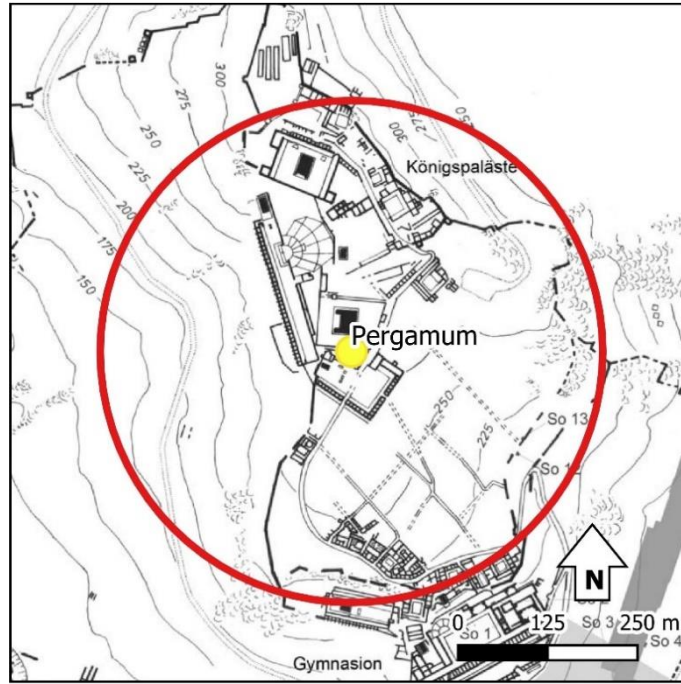
Google Earth View



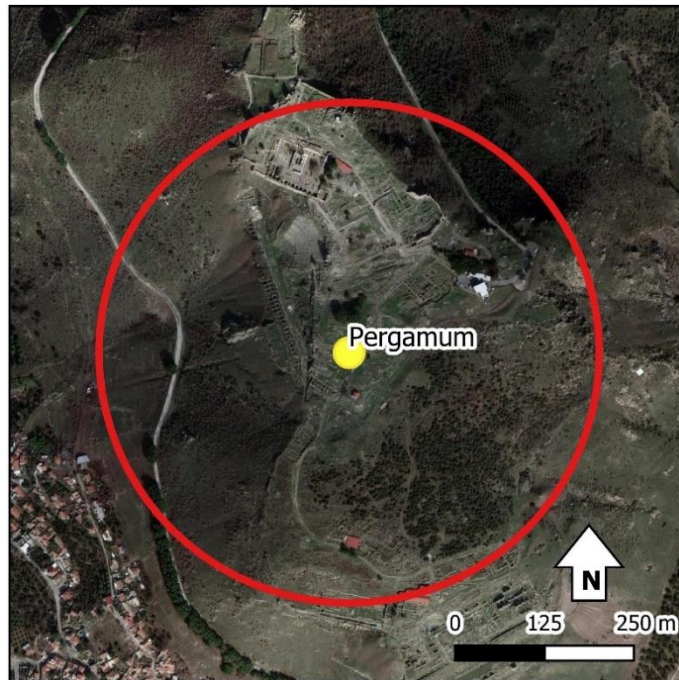
### 38. Pergamum

<b>Province</b> İzmir / Bergama	<b>Period</b> 1750 BC	<b>Coord.</b> UTME, N 515959 4331444
<b>GeoCont.</b> Bergama	AD 2000	Lat, Long 39.13035 27.18416

Site plan or other supportive material (Pirson 2007)



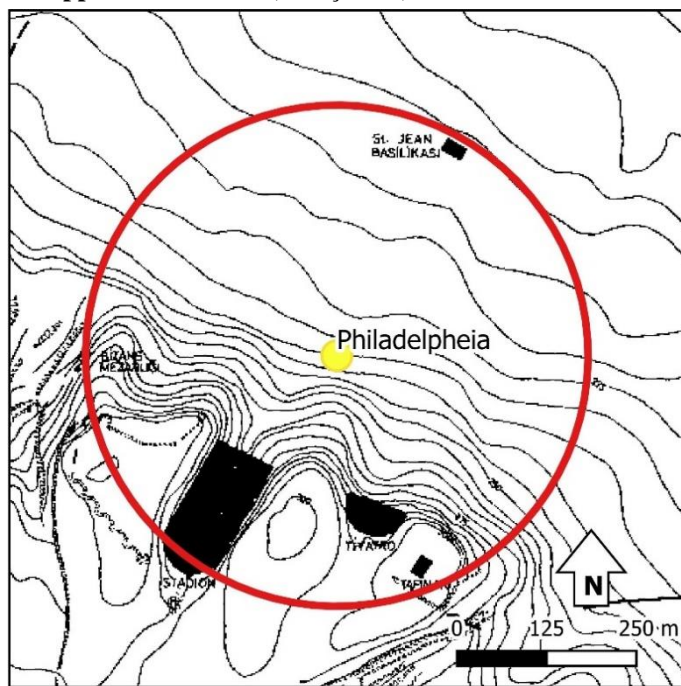
Google Earth View



### 39. Philadelphia

<b>Province</b> Manisa / Alaşehir	<b>Period</b> 330 BC AD 2100	<b>Coord.</b> UTM E, N 632296 4245633 Lat, Long 38.34742 28.51348
-----------------------------------	---------------------------------	--

Site plan or other supportive material (Meriç 1986)



Google Earth View



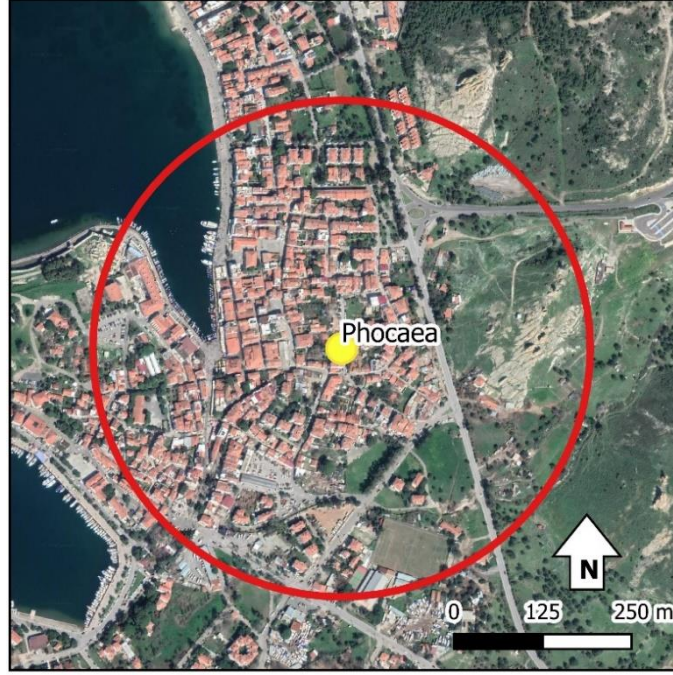
#### 40. Phocaea (Phokaia)

<b>Province</b> İzmir / Foça	<b>Period</b> 750 BC	<b>Coord.</b> UTME, N 478901 4280234
<b>GeoCont.</b> Foça	AD 2100	Lat, Long 38.66876 26.75699

##### Site plan or other supportive material(Çekilmez et al. 2016)

The location of site is adjusted considering the excavated theater dating to the years of 340-330 BC on the northwestern slope of Değirmenli hill (Özyiğit 2003).

##### Google Earth View



## 41. Pitane

<b>Province</b> İzmir / Dikili	<b>Period</b> 750 BC	<b>Coord.</b> UTME, N 494466 4309304
<b>GeoCont.</b> Çandarlı	AD 640	Lat, Long 38.93096 26.93568

### Site plan or other supportive material

The location of site is adjusted based on the few remains of theater situated at the half-way along the peninsula (Sear 2006).

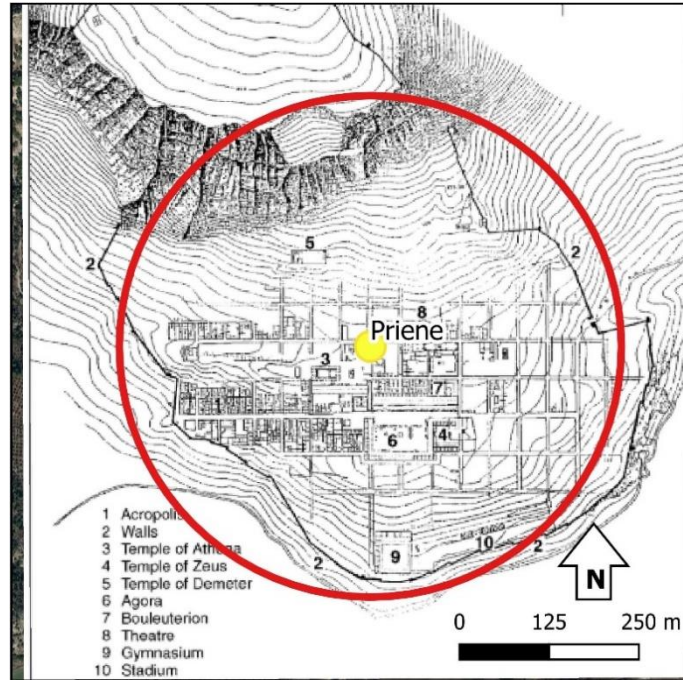
### Google Earth View



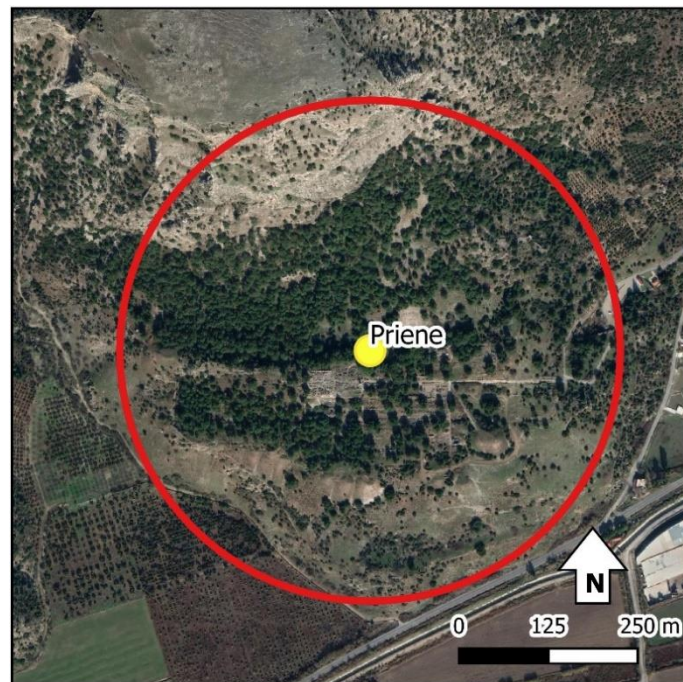
## 42. Priene

<b>Province</b> Aydın / Söke	<b>Period</b> 550 BC	<b>Coord.</b> UTME, N 526257 4168272
<b>GeoCont.</b> Güllübahçe	AD 640	Lat, Long 37.65957 27.29723

**Site plan or other supportive material** After Kummer G. and Wilberg, W. as cited in Erskine (2005)



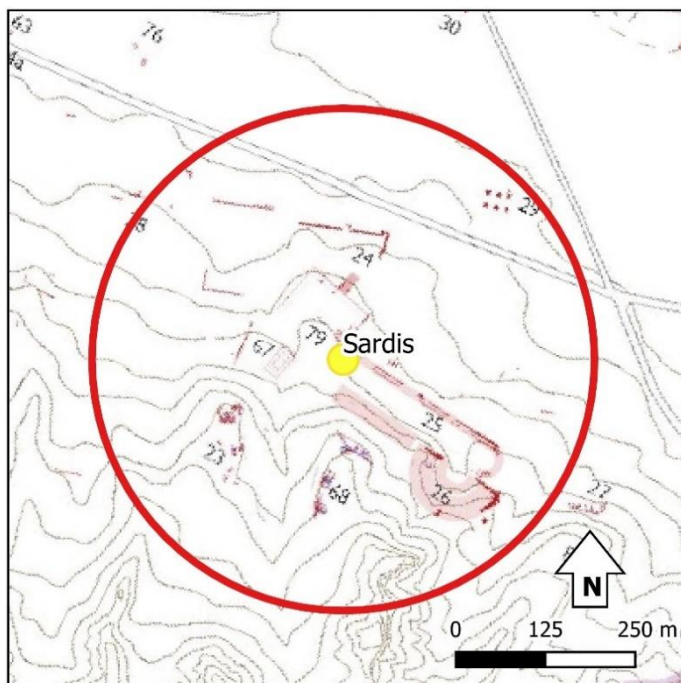
### Google Earth View



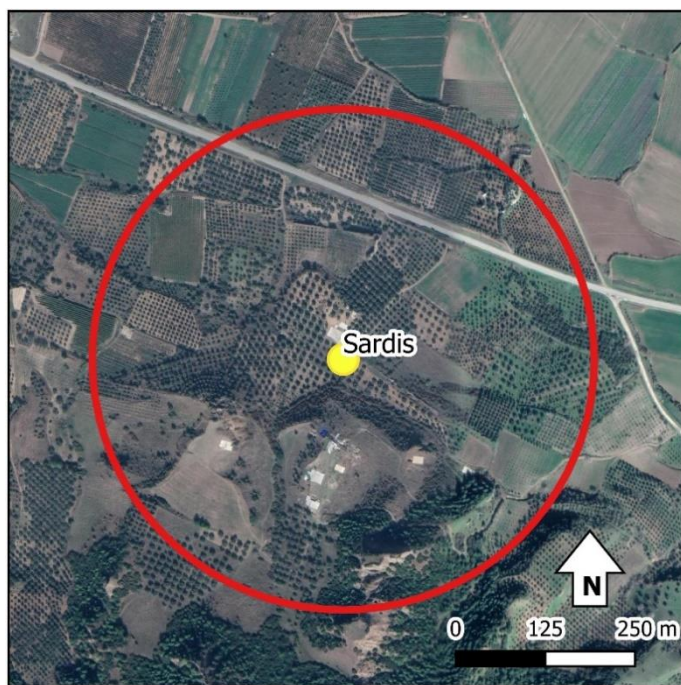
### 43. Sardis

<b>Province</b> Manisa / Salihli	<b>Period</b> 1750 BC	<b>Coord.</b> UTME, N 591306 4260149
<b>GeoCont.</b> Sart	AD 2000	Lat, Long 38.48333 28.04638

Site plan or other supportive material (Cahill 2018)



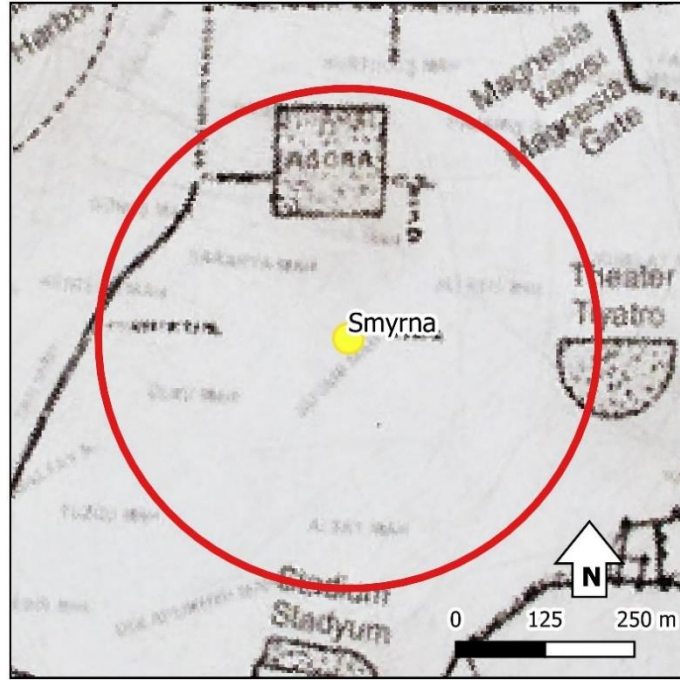
Google Earth View



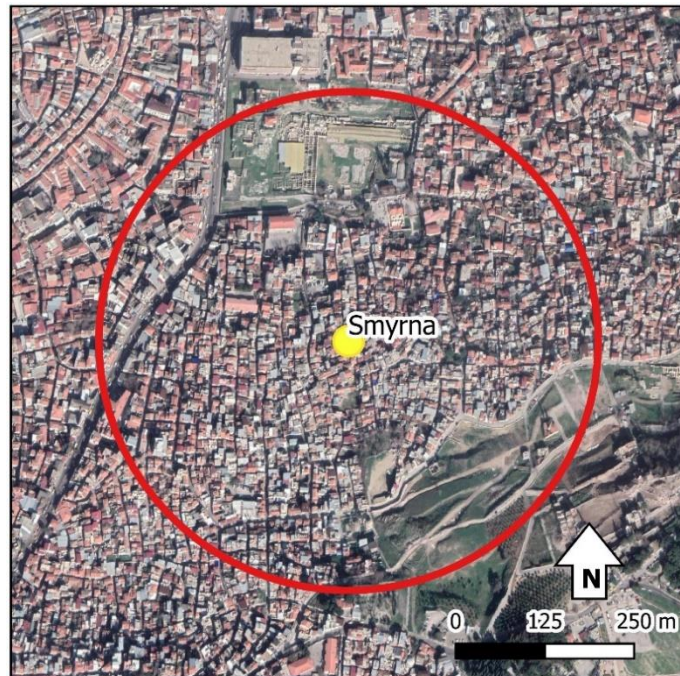
#### 44. Smyrna/Eurydikeia

<b>Province</b> İzmir / Konak	<b>Period</b> 550 BC	<b>Coord.</b> UTME, N 512178 4252222
<b>GeoCont.</b> İzmir	AD 2100	Lat, Long 38.41648 27.13902

Site plan or other supportive material (Naumann and Kantar 1950)



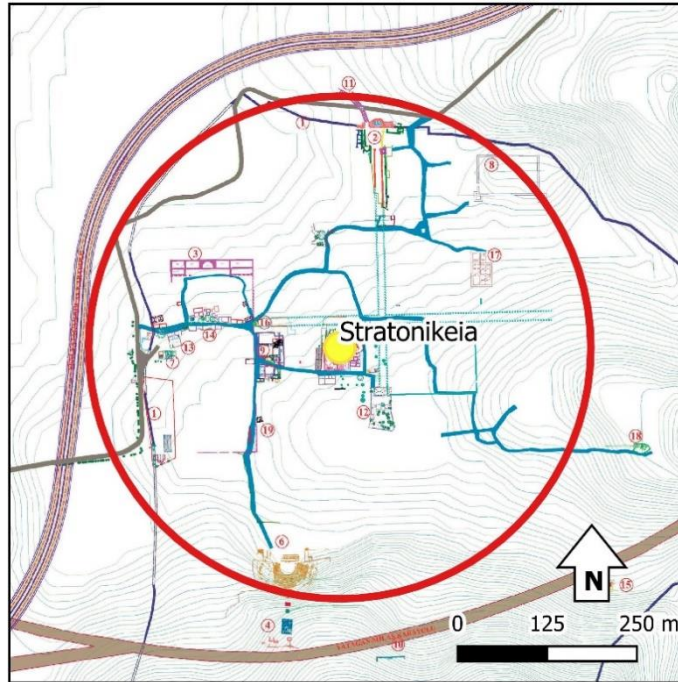
Google Earth View



## 45. Stratonikeia

<b>Province</b> Muğla / Yatağan	<b>Period</b> 330 BC	<b>Coord.</b> UTME, N 594493 4130335
<b>GeoCont.</b> Eskihisar	AD 640	Lat, Long 37.31319 28.06590

Site plan or other supportive material (Söğüt 2015)



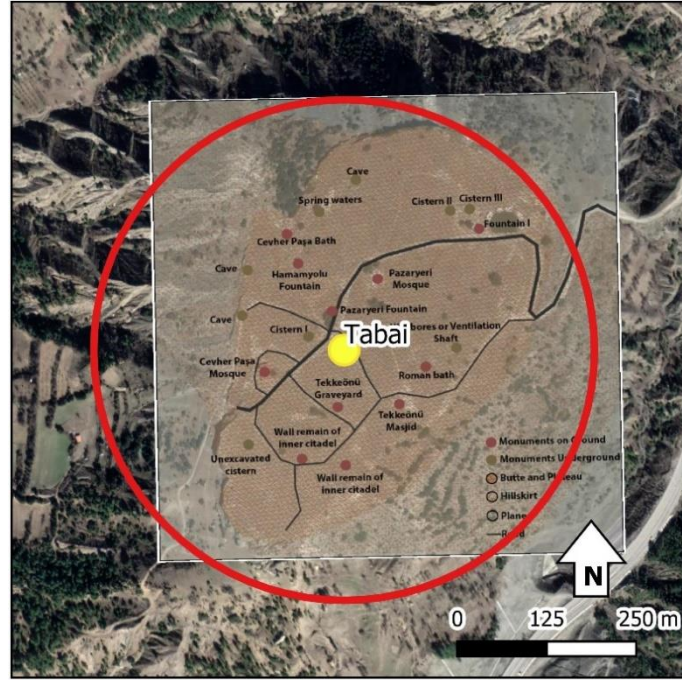
Google Earth View



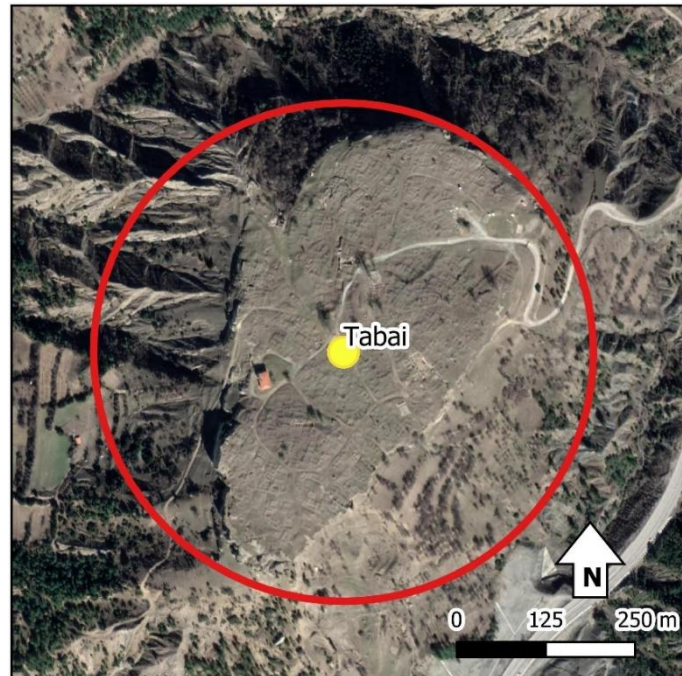
#### 46. Tabai (Tabae)

<b>Province</b> Denizli / Kale	<b>Period</b> 330 BC	<b>Coord.</b> UTME, N 663297 4144512
<b>GeoCont.</b> Kale	AD 640	Lat, Long 37.43138 28.84521

Site plan or other supportive material (Durmuşlar 2018)



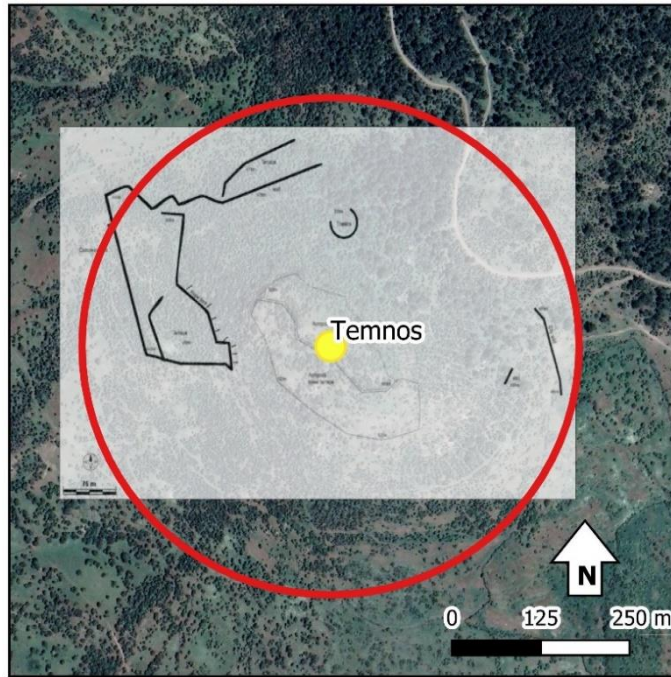
Google Earth View



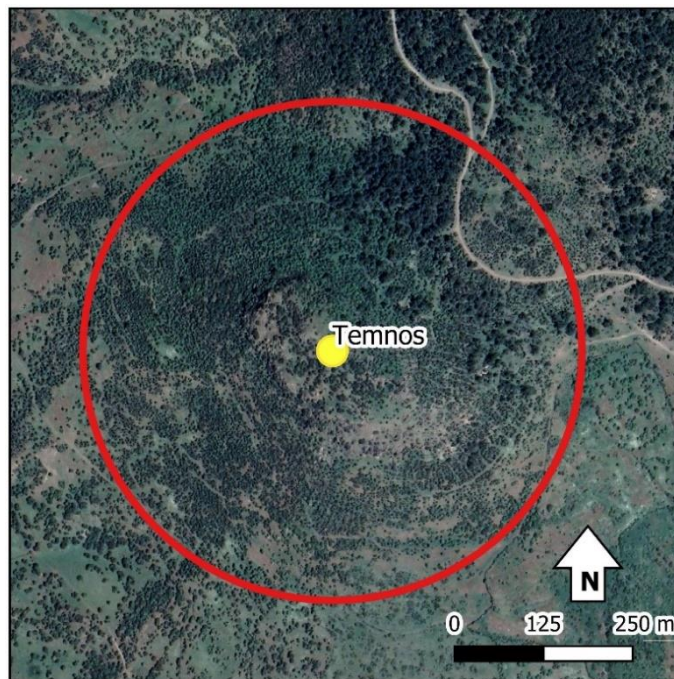
## 47. Temnos

<b>Province</b> İzmir / Menemen	<b>Period</b> 550 BC	<b>Coord.</b> UTME, N 515091 4281053
<b>GeoCont.</b> Görece Kalesi	AD 300	Lat, Long 38.67627 27.17302

Site plan or other supportive material (Ragone 2007)



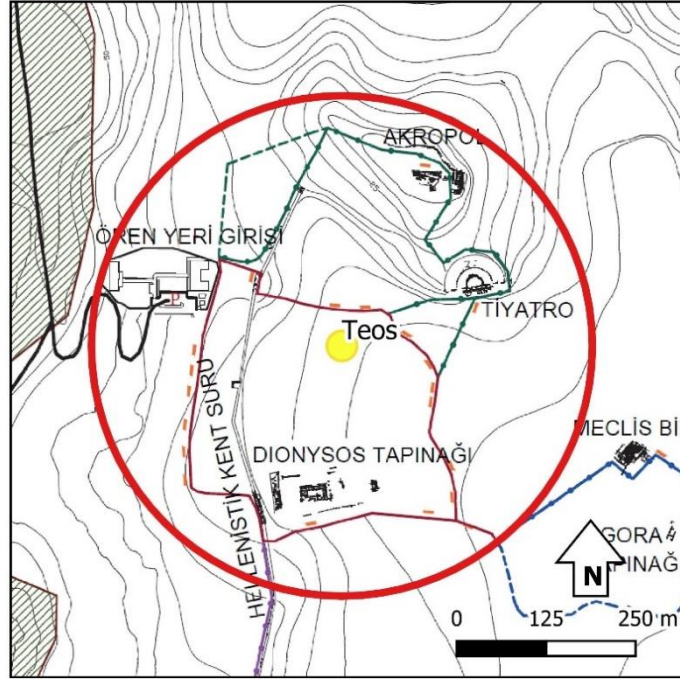
Google Earth View



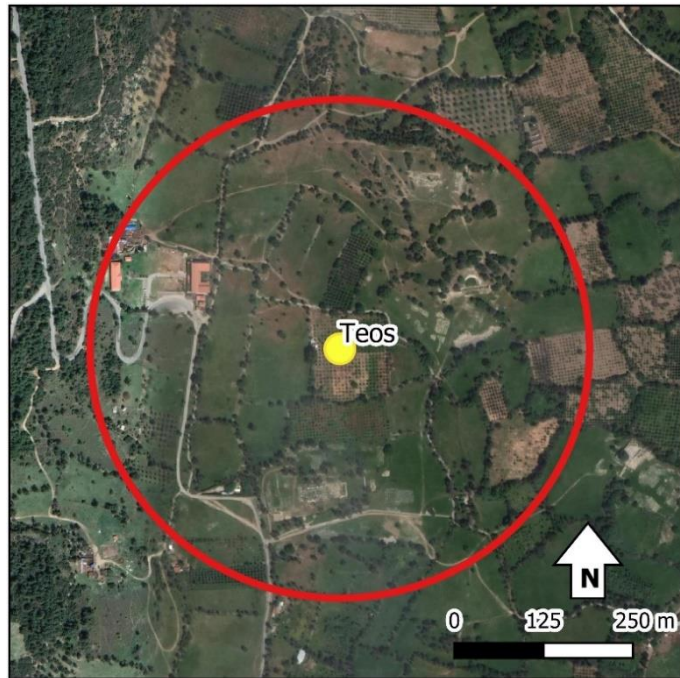
## 48. Teos

<b>Province</b> İzmir / Seferihisar	<b>Period</b> 750 BC	<b>Coord.</b> UTME, N 481253 4225883
<b>GeoCont.</b> Sığacık	AD 2100	Lat, Long 38.17900 26.78548

Site plan or other supportive material (Kadioğlu 2018)



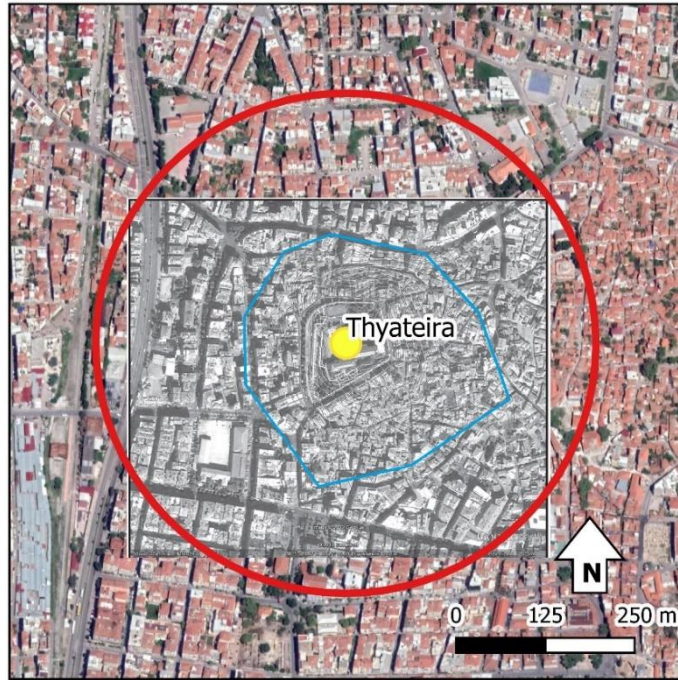
Google Earth View



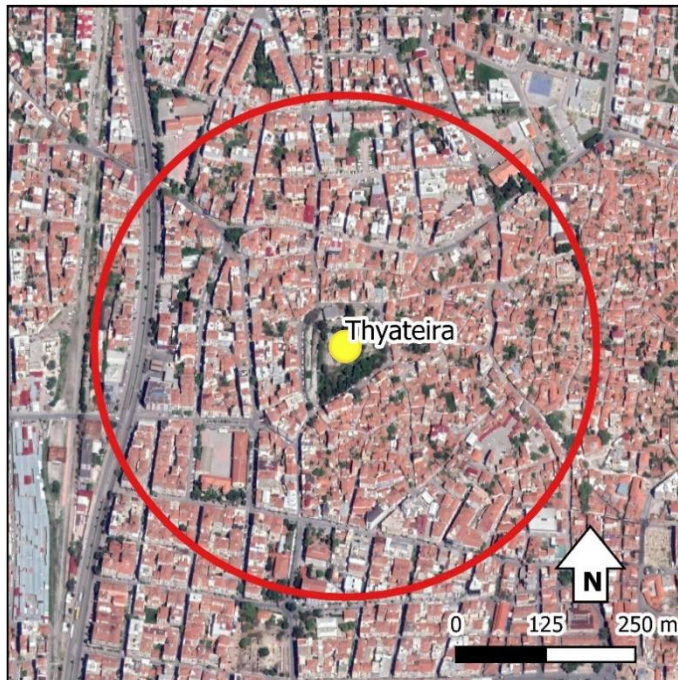
## 49. Thyateira

<b>Province</b> Manisa / Akhisar	<b>Period</b> 330 BC	<b>Coord.</b> UTME, N 572658 4308835
<b>GeoCont.</b> Akhisar	AD 640	Lat, Long 38.92375 27.83770

Site plan or other supportive material (Akdeniz et al. 2018)



Google Earth View

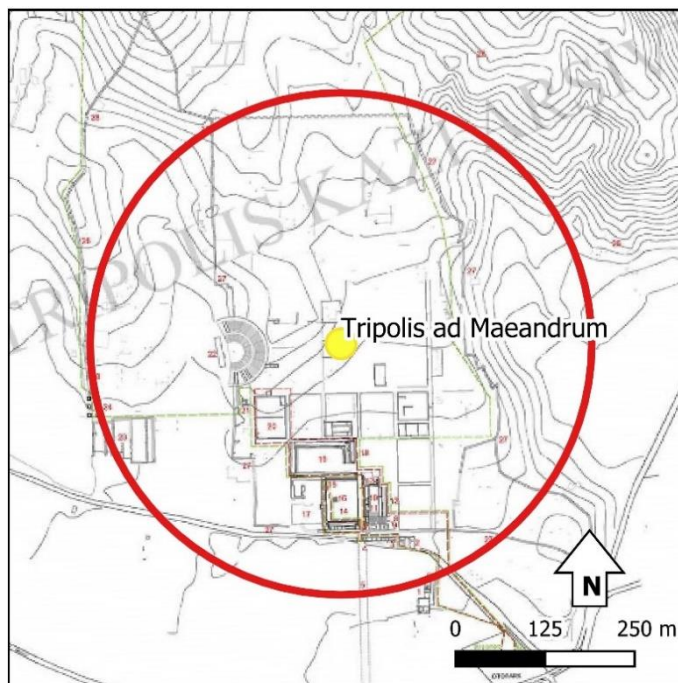




## 51. Tripolis ad Maeandrum/Apollonia ad Maeandrum/Antoniopolis

<b>Province</b> Denizli / Buldan	<b>Period</b> 330 BC	<b>Coord.</b> UTME, N 671260 4212230
<b>GeoCont.</b> Yenicekent	AD 850	Lat, Long 38.03995 28.95111

Site plan or other supportive material (Duman 2020)



Google Earth View



## B. CHARACTERISTICS OF ARCHAEOLOGICAL SITE LOCATIONS

At the first step of statistical analysis, characteristic data was derived using the known archaeological settlements' locations for each variable. The values derived for each variable for each settlement are given in the following tables (Table B1-B4).

Table B-1 Range of elevation values observed within the polygonal area and the median values with 95% confidence level for each archaeological site settled on in the study area in the Hellenistic Period.

ID	Name	Unimodality	Range		Median wt 95 % CI	
			Min	Max	Lower	Upper
1	Aegae	Unimodal	209	373	308.3	315.7
2	Akmonia	Multimodal	937	1011	958.0 996.9	961.2 998.7
3	Alabanda	Unimodal	66	140	79.4	82.0
4	Alinda	Unimodal	125	291	178.9	188.4
5	Amyzon	Multimodal	611	669	639.0 662.5	641.1 663.4
6	Anaia	Unimodal	0	14	7.3	7.7
7	Antiochia ad Maeandrum	Unimodal	93	151	119.1	121.8
8	Apamea	Unimodal	875	975	927.7	932.8
9	Aphrodisias	Unimodal	513	526	519.9	520.7
10	Apollonis	Unimodal	173	235	209.1	211.7
11	Attouda	Unimodal	636	754	691.2	696.9
12	Bargasa	Unimodal	417	630	553.4	560.9
13	Blaundos	Unimodal	595	683	632.4	639.2
14	Colossae	Multimodal	344	381	358.1 373.4	359.5 374.2
15	Cyme	Unimodal	0	39	13.6	14.7
16	Elaea	Unimodal	3	20	8.5	9.5
17	Ephesus	Unimodal	5	98	21.1	26.0
18	Erythrai	Multimodal	5	74	9.0 34.1	10.0 36.9
19	Euhippe	Unimodal	51	138	84.5	89.3
20	Eumeneia	Multimodal	1019	1269	1147.1 1246.8	1156.6 1251.5
21	Harpasa	Unimodal	69	277	160.5	173.8
22	Heraclea ad Latmum	Unimodal	0	77	30.1	34.0
23	Herakleia Salbakes	Unimodal	965	1000	981.8	983.0
24	Hierapolis	Unimodal	363	425	376.8	380.1
25	Hyllarima	Unimodal	738	824	783.9	788.3
26	Hypaipa	Unimodal	256	361	300.1	306.7

Table B-1 (cont'd)

ID	Name	Unimodality	Range		Median wt 95 % CI	
			Min	Max	Lower	Upper
27	Klazomenai	Multimodal	0	26	0.2 9.3	0.3 10.5
28	Laodicea ad Lycum	Unimodal	264	293	283.6	284.8
29	Lebedos	Unimodal	0	35	10.6	13.0
30	Magnesia ad Maeandrum	Unimodal	31	70	37.4	39.9
31	Metropolis	Unimodal	36	140	69.2	75.3
32	Miletus	Unimodal	3	21	5.5	5.7
33	Myrina	Unimodal	0	31	2.5	3.9
34	Neonteichos	Unimodal	102	216	153.1	160.4
35	Notion	Multimodal	0	66	22.3 56.2	25.0 57.8
36	Nysa	Unimodal	184	272	218.8	221.8
37	Orthosia	Unimodal	126	309	198.6	214.4
38	Pergamum	Unimodal	130	323	244.3	252.9
39	Philadelpheia	Multimodal	217	299	228.1 269.0	229.5 273.2
40	Phocaea	Unimodal	0	32	6.9	7.2
41	Pitane	Multimodal	0	19	5.0 14.7	5.7 15.7
42	Priene	Unimodal	11	338	83.7	89.4
43	Sardis	Unimodal	106	217	139.5	146.4
44	Smyrna	Unimodal	10	114	41.3	48.0
45	Stratonikeia	Unimodal	488	522	504.5	505.3
46	Tabai	Unimodal	1002	1110	1081.5	1086.6
47	Temnos	Unimodal	372	537	468.3	477.5
48	Teos	Multimodal	10	43	10.7 21.0	10.9 22.2
49	Thyateira	Unimodal	100	112	105.8	106.2
50	Tralles	Unimodal	156	193	169.7	171.3
51	Tripolis ad Maeandrum	Unimodal	168	233	200.0	202.3

Table B-2 Range of TRI values observed within the polygonal area and the median values with 95% confidence level for each archaeological site settled on in the study area in the Hellenistic Period.

ID	Name	Unimodality	Range		Median wt 95 % CI	
			Min	Max	Lower	Upper
1	Aegae	Unimodal	45.1	83.0	72.0	73.1
2	Akmonia	Unimodal	16.2	46.6	27.7	28.5
3	Alabanda	Multimodal	6.3	34.6	10.3 24.6	11.1 25.6
4	Alinda	Unimodal	32.3	83.6	50.3	51.2
5	Amyzon	Unimodal	13.1	40.9	20.9	21.8
6	Anaia	Unimodal	1.7	7.7	3.0	3.0
7	Antiochia ad Maeandrum	Unimodal	10.7	24.8	16.0	16.4

Table B-2 (cont'd)

ID	Name	Unimodality	Range		Median wt 95 % CI	
			Min	Max	Lower	Upper
8	Apamea	Unimodal	17.0	36.1	29.0	29.6
9	Aphrodisias	Unimodal	2.4	5.5	3.4	3.5
10	Apollonis	Unimodal	12.6	38.1	22.9	24.4
11	Attouda	Unimodal	22.9	64.5	37.4	39.6
12	Bargasa	Unimodal	40.2	94.6	67.7	71.7
13	Blaundos	Unimodal	18.7	60.5	28.9	30.1
14	Colossae	Unimodal	5.4	14.3	8.9	9.4
15	Cyme	Unimodal	5.6	24.4	9.5	10.1
16	Elaea	Unimodal	2.1	6.3	4.9	5.1
17	Ephesus	Unimodal	9.6	85.1	36.2	36.9
18	Erythrai	Unimodal	9.4	50.0	18.8	19.5
19	Euhippe	Unimodal	20.9	52.4	28.9	29.9
20	Eumeneia	Multimodal	51.6	97.5	62.5 86.1	63.9 87.5
21	Harpasa	Unimodal	32.1	78.4	55.5	57.5
22	Heraclea ad Latmum	Unimodal	9.8	33.8	17.6	18.5
23	Herakleia Salbakes	Unimodal	7.5	9.4	8.3	8.4
24	Hierapolis	Unimodal	10.8	27.4	16.8	17.9
25	Hyllarima	Unimodal	13.1	28.7	22.7	23.4
26	Hypaipa	Multimodal	19.4	60.7	24.2 39.6	24.7 41.2
27	Klazomenai	Unimodal	4.6	18.4	7.6	8.2
28	Laodicea ad Lycum	Unimodal	4.4	22.7	8.4	9.2
29	Lebedos	Unimodal	3.8	23.0	8.5	9.1
30	Magnesia ad Maeandrum	Unimodal	1.6	22.7	10.5	11.4
31	Metropolis	Unimodal	13.0	44.7	28.3	29.1
32	Miletus	Multimodal	1.1	15.0	1.5 4.0	1.6 4.4
33	Myrina	Unimodal	4.6	25.1	9.2	9.7
34	Neonteichos	Multimodal	17.3	48.9	25.6 36.9	26.6 37.9
35	Notion	Unimodal	15.3	43.7	25.0	25.8
36	Nysa	Unimodal	12.2	30.1	18.8	19.3
37	Orthosia	Unimodal	23.6	56.9	46.5	47.9
38	Pergamum	Unimodal	50.0	80.5	62.7	63.8
39	Philadelpheia	Unimodal	8.1	32.3	22.5	23.3
40	Phocaea	Unimodal	2.4	19.0	7.2	8.0
41	Pitane	Unimodal	2.2	12.0	5.3	5.5
42	Priene	Multimodal	30.8	136.5	41.3 88.5	43.3 92.6
43	Sardis	Unimodal	12.1	42.3	27.4	28.6
44	Smyrna	Unimodal	9.2	41.9	26.7	28.9
45	Stratonikeia	Unimodal	5.0	33.0	15.0	15.8
46	Tabai	Unimodal	25.0	63.0	42.9	44.3
47	Temnos	Unimodal	27.0	82.2	51.3	54.4
48	Teos	Multimodal	3.2	19.4	8.3 17.1	8.9 17.5
49	Thyateira	Multimodal	1.3	6.1	1.8 3.0	1.9 3.1

Table B-2 (cont'd)

ID	Name	Unimodality	Range		Median wt 95 % CI	
			Min	Max	Lower	Upper
50	Tralles	Unimodal	5.5	25.6	9.5	10.3
51	Tripolis ad Maeandrum	Unimodal	7.9	32.2	14.2	15.3

Table B-3 Range of slope values observed within the polygonal area and the median values with 95% confidence level for each archaeological site settled on in the study area in the Hellenistic Period.

ID	Name	Unimodality	Range		Median wt 95 % CI	
			Min	Max	Lower	Upper
1	Aegae	Unimodal	0.7	39.2	22.3	23.5
2	Akmonia	Multimodal	0.1	23.4	3.6	4.1
					13.7	14.5
3	Alabanda	Multimodal	0.9	17.2	7.6	8.2
					2.5	2.7
4	Alinda	Unimodal	2.3	33.4	16.7	17.9
5	Amyzon	Unimodal	0.2	13.7	5.9	6.6
6	Anaia	Multimodal	0.0	4.5	0.5	0.5
					1.7	1.8
7	Antiochia ad Maeandrum	Unimodal	0.4	12.6	6.0	6.4
8	Apamea	Unimodal	0.9	17.9	11.3	12.0
9	Aphrodisias	Unimodal	0.1	4.0	1.3	1.4
10	Apollonis	Unimodal	1.2	14.4	5.3	5.9
11	Attouda	Unimodal	0.7	28.1	15.9	17.3
12	Bargasa	Unimodal	1.1	40.6	24.3	25.5
13	Blaundos	Unimodal	0.5	30.3	13.1	14.6
14	Colossae	Unimodal	0.3	9.3	3.5	4.0
15	Cyme	Unimodal	0.1	11.1	3.2	3.8
16	Elaea	Unimodal	0.1	3.7	1.7	1.8
17	Ephesus	Unimodal	0.5	29.7	7.3	8.7
18	Erythrai	Unimodal	0.9	22.7	6.6	7.6
19	Euhippe	Unimodal	0.8	25.6	11.4	11.9
20	Eumeneia	Unimodal	0.3	36.1	22.2	24.4
21	Harpasa	Unimodal	2.8	34.5	21.3	22.3
22	Heraclea ad Latmum	Unimodal	1.4	18.4	6.5	7.0
23	Herakleia Salbakes	Unimodal	1.2	4.9	2.8	3.0
24	Hierapolis	Multimodal	0.6	11.0	1.5	1.7
					4.9	5.3
					9.2	9.5
25	Hyllarima	Unimodal	0.3	16.2	7.6	8.0
26	Hypaipa	Unimodal	2.0	25.9	12.2	13.4
27	Klazomenai	Unimodal	0.3	11.0	5.3	5.8
28	Laodicea ad Lycum	Unimodal	0.2	10.6	2.3	2.5
29	Lebedos	Multimodal	0.0	11.3	0.9	1.1
					4.9	5.4
30	Magnesia ad Maeandrum	Unimodal	0.0	10.1	2.6	3.1

Table B-3 (cont'd)

ID	Name	Unimodality	Range		Median wt 95 % CI	
			Min	Max	Lower	Upper
31	Metropolis	Multimodal	0.5	19.2	5.9 14.2	6.5 14.7
32	Miletus	Unimodal	0.0	7.1	1.0	1.2
33	Myrina	Multimodal	0.0	10.3	0.7 5.5	0.8 5.9
34	Neonteichos	Unimodal	1.0	18.1	10.4	11.0
35	Notion	Unimodal	0.4	23.2	10.8	12.2
36	Nysa	Unimodal	1.1	17.1	6.8	7.5
37	Orthosia	Unimodal	1.5	26.7	15.3	16.8
38	Pergamum	Unimodal	2.0	34.9	18.9	20.7
39	Philadelpheia	Unimodal	0.8	17.0	5.7	6.6
40	Phocaea	Unimodal	0.0	8.8	1.8	2.2
41	Pitane	Unimodal	0.0	10.4	2.3	2.5
42	Priene	Unimodal	5.5	53.0	18.8	20.1
43	Sardis	Multimodal	3.0	16.5	8.0 13.4	8.4 13.8
44	Smyrna	Unimodal	1.3	17.5	8.7	9.2
45	Stratonikeia	Unimodal	0.1	12.8	2.0	2.2
46	Tabai	Unimodal	0.5	30.7	15.3	16.5
47	Temnos	Unimodal	0.8	35.0	17.4	18.7
48	Teos	Multimodal	0.1	10.2	2.8 7.4	3.1 7.9
49	Thyateira	Unimodal	0.0	4.1	1.0	1.2
50	Tralles	Unimodal	1.3	11.5	2.6	2.6
51	Tripolis ad Maeandrum	Unimodal	0.2	13.2	4.4	4.8

Table B-4 Range of aspect values observed within the polygonal area and the median values with 95% confidence level for each archaeological site settled on in the study area in the Hellenistic Period.

ID	Name	Uniformity	Unimodality	Median with 95 % CI	
				Lower	Upper
1	Aegae	Non-uniform	Multimodal	114 245 337	121 253 344
2	Akmonia	Non-uniform	Multimodal	196 352	202 356
3	Alabanda	Non-uniform	Multimodal	28 356	36 360
4	Alinda	Non-uniform	Multimodal	0 52 140	2 66 144
5	Amyzon	Non-uniform	Unimodal	68	82
6	Anaia	Non-uniform	Unimodal	274	285
7	Antiochia ad Maeandrum	Non-uniform	Multimodal	1 150	6 166

Table B-4 (cont'd)

ID	Name	Uniformity	Unimodality	Median with 95 % CI	
				Lower	Upper
1	Aegae	Non-uniform	Multimodal	114 245 337	121 253 344
2	Akmonia	Non-uniform	Multimodal	196 352	202 356
3	Alabanda	Non-uniform	Multimodal	28 356	36 360
4	Alinda	Non-uniform	Multimodal	0 52 140	2 66 144
5	Amyzon	Non-uniform	Unimodal	68	82
6	Anaia	Non-uniform	Unimodal	274	285
7	Antiochia ad Maeandrum	Non-uniform	Multimodal	1 150	6 166
8	Apamea	Non-uniform	Multimodal	154 276	164 279
9	Aphrodisias	Non-uniform	Multimodal	132 240	143 250
10	Apollonis	Non-uniform	Unimodal	205	213
11	Attouda	Non-uniform	Multimodal	102 135 327	115 143 333
12	Bargasa	Non-uniform	Multimodal	78 281	83 288
13	Blaundos	Non-uniform	Multimodal	97 133 264	113 195 281
14	Colossae	Non-uniform	Multimodal	33 289	44 307
15	Cyme	Non-uniform	Multimodal	133 315	157 325
16	Elaea	Non-uniform	Unimodal	210	217
17	Ephesus	Non-uniform	Multimodal	19 287	22 293
18	Erythrai	Non-uniform	Multimodal	116 248	124 275
19	Euhippe	Non-uniform	Multimodal	95 300 307	97 308 337
20	Eumeneia	Non-uniform	Multimodal	143 290	147 311
21	Harpasa	Non-uniform	Multimodal	179 294	191 300
22	Heraclea ad Latmum	Non-uniform	Multimodal	155 222	165 227
23	Herakleia Salbakes	Non-uniform	Unimodal	190	195
24	Hierapolis	Non-uniform	Unimodal	242	246
25	Hyllarima	Non-uniform	Multimodal	212 263 298	218 267 306
26	Hypaipa	Non-uniform	Multimodal	178 291	184 301
27	Klazomenai	Non-uniform	Multimodal	94 284	117 307
28	Laodicea ad Lycum	Non-uniform	Unimodal	33	43

Table B-4 (cont'd)

ID	Name	Uniformity	Unimodality	Median with 95 % CI	
				Lower	Upper
29	Lebedos	Non-uniform	Multimodal	30 186	73 199
30	Magnesia ad Maeandrum	Non-uniform	Unimodal	7	13
31	Metropolis	Non-uniform	Unimodal	61	67
32	Miletus	Non-uniform	Multimodal	88 239	97 256
33	Myrina	Uniform		No mean	
34	Neonteichos	Non-uniform	Multimodal	200 235 297	205 244 307
35	Notion	Non-uniform	Multimodal	174 338	183 342
36	Nysa	Non-uniform	Multimodal	121 173 241	129 186 248
37	Orthosia	Non-uniform	Unimodal	329	333
38	Pergamum	Non-uniform	Multimodal	123 241	134 245
39	Philadelpheia	Non-uniform	Unimodal	22	27
40	Phocaea	Non-uniform	Multimodal	19 249	36 256
41	Pitane	Non-uniform	Multimodal	49 272	58 288
42	Priene	Non-uniform	Multimodal	155 208	166 211
43	Sardis	Non-uniform	Unimodal	19	21
44	Smyrna	Non-uniform	Unimodal	332	334
45	Stratonikeia	Non-uniform	Multimodal	4 86 151	9 113 159
46	Tabai	Non-uniform	Multimodal	128 295	136 302
47	Temnos	Non-uniform	Multimodal	205 308	226 325
48	Teos	Non-uniform	Unimodal	109	119
49	Thyateira	Non-uniform	Unimodal	265	278
50	Tralles	Non-uniform	Multimodal	202 242	207 251
51	Tripolis ad Maeandrum	Non-uniform	Multimodal	93 171	109 178



### C. RESPONSE OF ARCHAEOLOGICAL SETTLEMENTS TO THE POTENTIAL MAPS

Table C-1 Sorted archaeological settlements with decreasing potentiality for ruggedness variable. Gray colored rows are testing data and the others are training data.

Gr90/10-Set1	Gr90/10-Set2	Gr90/10-Set3	Gr80/20-Set1	Gr80/20-Set2	Gr80/20-Set3	Gr70/30-Set1	Gr70/30-Set2	Gr70/30-Set3	Gr60/40-Set1	Gr60/40-Set2	Gr60/40-Set3	Gr50/50-Set1	Gr50/50-Set2	Gr50/50-Set3
Hyllarima	Philadelpheia	Hyllarima	Hyllarima	Hyllarima	Hyllarima	Philadelpheia	Hyllarima	Euhippe	Hyllarima	Hyllarima	Euhippe	Colossae	Antiochia adM.	Hyllarima
Philadelpheia	Akmonia	Amyzon	Philadelpheia	Amyzon	Philadelpheia	Hyllarima	Amyzon	Apamea	Amyzon	Philadelpheia	Akmonia	Cyme	Hierapolis	Amyzon
Hypaipa	Euhippe	Notion	Notion	Nysa	Blaundos	Euhippe	Philadelpheia	Akmonia	Notion	Euhippe	Apamea	Tripolis adM.	Tripolis adM.	Notion
Blaundos	Hyllarima	Philadelpheia	Euhippe	Notion	Notion	Akmonia	Notion	Metropolis	Philadelpheia	Akmonia	Philadelpheia	Hierapolis	Stratonikeia	Philadelpheia
Notion	Notion	Nysa	Akmonia	Erythrai	Hypaipa	Notion	Nysa	Philadelpheia	Nysa	Notion	Metropolis	Myrina	Erythrai	Nysa
Akmonia	Blaundos	Erythrai	Hypaipa	Hierapolis	Amyzon	Blaundos	Hypaipa	Blaundos	Hierapolis	Blaundos	Notion	Antiochia adM.	Heraclea adLa.	Hierapolis
Euhippe	Hypaipa	Hierapolis	Blaundos	Philadelpheia	Akmonia	Hypaipa	Hierapolis	Notion	Erythrai	Hypaipa	Hyllarima	Magnesia adM.	Myrina	Erythrai
Amyzon	Metropolis	Apollonis	Amyzon	Apollonis	Euhippe	Metropolis	Blaundos	Sardis	Blaundos	Metropolis	Blaundos	Stratonikeia	Magnesia adM.	Hypaipa
Sardis	Apamea	Heraclea adLa.	Metropolis	Heraclea adLa.	Nysa	Apamea	Erythrai	Hyllarima	Hypaipa	Alabanda	Sardis	Tralles	Teos	Blaundos
Metropolis	Alabanda	Blaundos	Apamea	Antiochia adM.	Hierapolis	Alabanda	Apollonis	Neonteichos	Apollonis	Apamea	Hypaipa	Lebedos	Cyme	Apollonis
Apollonis	Sardis	Hypaipa	Sardis	Stratonikeia	Apollonis	Sardis	Akmonia	Alabanda	Akmonia	Sardis	Neonteichos	Phocaea	Colossae	Akmonia
Alabanda	Amyzon	Antiochia adM.	Alabanda	Smyrna	Erythrai	Amyzon	Heraclea adLa.	Hypaipa	Heraclea adLa.	Amyzon	Alabanda	Klazomenai	Phocaea	Heraclea adLa.
Apamea	Apollonis	Akmonia	Apollonis	Tripolis adM.	Sardis	Apollonis	Smyrna	Apollonis	Smyrna	Apollonis	Apollonis	Teos	Tralles	Smyrna
Heraclea adLa.	Heraclea adLa.	Stratonikeia	Heraclea adLa.	Sardis	Heraclea adLa.	Heraclea adLa.	Apamea	Smyrna	Euhippe	Heraclea adLa.	Smyrna	Erythrai	Nysa	Sardis
Hierapolis	Neonteichos	Smyrna	Smyrna	Alabanda	Metropolis	Neonteichos	Sardis	Amyzon	Sardis	Neonteichos	Amyzon	Laodicea adLy.	Lebedos	Apamea
Nysa	Smyrna	Sardis	Hierapolis	Magnesia adM.	Alabanda	Smyrna	Antiochia adM.	Heraclea adLa.	Apamea	Smyrna	Heraclea adLa.	Heraclea adLa.	Laodicea adLy.	Euhippe
Smyrna	Hierapolis	Apamea	Nysa	Teos	Apamea	Hierapolis	Euhippe	Attouda	Metropolis	Hierapolis	Attouda	Alabanda	Alabanda	Antiochia adM.
Erythrai	Tripolis adM.	Alabanda	Neonteichos	Metropolis	Smyrna	Nysa	Stratonikeia	Ephesus	Alabanda	Nysa	Ephesus	Herakleia Salb.	Klazomenai	Alabanda
Neonteichos	Erythrai	Tripolis adM.	Erythrai	Blaundos	Stratonikeia	Erythrai	Alabanda	Hierapolis	Antiochia adM.	Erythrai	Tripolis adM.	Nysa	Amyzon	Metropolis
Tripolis adM.	Nysa	Metropolis	Tripolis adM.	Hypaipa	Antiochia adM.	Attouda	Metropolis	Nysa	Stratonikeia	Tripolis adM.	Hierapolis	Amyzon	Apollonis	Stratonikeia
Stratonikeia	Stratonikeia	Euhippe	Stratonikeia	Tralles	Neonteichos	Tripolis adM.	Tripolis adM.	Erythrai	Tripolis adM.	Attouda	Nysa	Philadelpheia	Philadelpheia	Tripolis adM.
Antiochia adM.	Antiochia adM.	Magnesia adM.	Antiochia adM.	Akmonia	Tripolis adM.	Ephesus	Magnesia adM.	Tabai	Neonteichos	Stratonikeia	Cyme	Apollonis	Herakleia Salb.	Magnesia adM.
Magnesia adM.	Magnesia adM.	Teos	Magnesia adM.	Laodicea adLy.	Magnesia adM.	Stratonikeia	Teos	Tripolis adM.	Magnesia adM.	Ephesus	Colossae	Hyllarima	Hyllarima	Teos
Attouda	Tralles	Tralles	Teos	Myrina	Teos	Antiochia adM.	Neonteichos	Stratonikeia	Teos	Antiochia adM.	Myrina	Pitane	Smyrna	Tralles
Ephesus	Cyme	Laodicea adLy.	Tralles	Cyme	Tralles	Tabai	Tralles	Temnos	Tralles	Tabai	Tralles	Smyrna	Notion	Neonteichos
Teos	Myrina	Myrina	Laodicea adLy.	Apamea	Laodicea adLy.	Temnos	Laodicea adLy.	Antiochia adM.	Laodicea adLy.	Temnos	Erythrai	Notion	Sardis	Laodicea adLy.
Tralles	Teos	Cyme	Myrina	Euhippe	Myrina	Magnesia adM.	Myrina	Orthosia	Myrina	Magnesia adM.	Stratonikeia	Sardis	Pitane	Myrina
Laodicea adLy.	Laodicea adLy.	Neonteichos	Cyme	Lebedos	Cyme	Teos	Cyme	Alinda	Cyme	Orthosia	Herakleia Salb.	Metropolis	Metropolis	Cyme
Myrina	Lebedos	Lebedos	Ephesus	Phocaea	Lebedos	Orthosia	Lebedos	Magnesia adM.	Lebedos	Teos	Lebedos	Elaea	Blaundos	Lebedos
Cyme	Phocaea	Phocaea	Lebedos	Colossae	Phocaea	Tralles	Phocaea	Priene	Phocaea	Tralles	Magnesia adM.	Blaundos	Hypaipa	Phocaea
Lebedos	Colossae	Colossae	Phocaea	Neonteichos	Ephesus	Laodicea adLy.	Colossae	Harpasa	Colossae	Laodicea adLy.	Klazomenai	Hypaipa	Akmonia	Colossae
Phocaea	Ephesus	Klazomenai	Colossae	Klazomenai	Colossae	Myrina	Klazomenai	Teos	Ephesus	Alinda	Laodicea adLy.	Akmonia	Elaea	Klazomenai
Colossae	Klazomenai	Ephesus	Attouda	Ephesus	Klazomenai	Cyme	Ephesus	Tralles	Klazomenai	Myrina	Teos	Apamea	Apamea	Herakleia Salb.
Tabai	Attouda	Herakleia Salb.	Klazomenai	Tabai	Attouda	Lebedos	Herakleia Salb.	Pergamum	Herakleia Salb.	Priene	Tabai	Euhippe	Euhippe	Ephesus
Klazomenai	Herakleia Salb.	Attouda	Herakleia Salb.	Attouda	Herakleia Salb.	Phocaea	Attouda	Laodicea adLy.	Attouda	Cyme	Phocaea	Neonteichos	Neonteichos	Attouda

Table C-1 (cont'd)

Gr90/10-Set1	Gr90/10-Set2	Gr90/10-Set3	Gr80/20-Set1	Gr80/20-Set2	Gr80/20-Set3	Gr70/30-Set1	Gr70/30-Set2	Gr70/30-Set3	Gr60/40-Set1	Gr60/40-Set2	Gr60/40-Set3	Gr50/50-Set1	Gr50/50-Set2	Gr50/50-Set3
Temnos	Tabai	Tabai	Pitane	Orthosia	Pitane	Colossae	Tabai	Bargasa	Orthosia	Harpasa	Temnos	Orthosia	Miletus	Pitane
Orthosia	Temnos	Temnos	Tabai	Herakleia Salb.	Tabai	Klazomenai	Orthosia	Eumeneia	Alinda	Bargasa	Orthosia	Alinda	Ephesus	Elaea
Herakleia Salb.	Pitane	Orthosia	Temnos	Temnos	Temnos	Alinda	Temnos	Myrina	Temnos	Lebedos	Alinda	Ephesus	Pergamum	Tabai
Alinda	Orthosia	Pitane	Orthosia	Alinda	Elaea	Herakleia Salb.	Pitane	Cyme	Tabai	Phocaea	Priene	Miletus	Aphrodisias	Miletus
Priene	Alinda	Alinda	Elaea	Priene	Orthosia	Priene	Alinda	Aegae	Harpasa	Pergamum	Antiochia adM.	Tabai	Aegae	Temnos
Pitane	Elaea	Priene	Alinda	Pitane	Alinda	Pitane	Priene	Lebedos	Pitane	Colossae	Harpasa	Attouda	Anaia	Aphrodisias
Harpasa	Priene	Elaea	Priene	Harpasa	Miletus	Harpasa	Elaea	Phocaea	Priene	Eumeneia	Pitane	Aphrodisias	Thyateira	Anaia
Elaea	Harpasa	Harpasa	Harpasa	Elaea	Priene	Elaea	Harpasa	Colossae	Pergamum	Aegae	Elaea	Harpasa	Harpasa	Thyateira
Pergamum	Miletus	Miletus	Miletus	Miletus	Harpasa	Bargasa	Miletus	Klazomenai	Elaea	Klazomenai	Pergamum	Anaia	Attouda	Orthosia
Bargasa	Aphrodisias	Aphrodisias	Aphrodisias	Aphrodisias	Aphrodisias	Pergamum	Aphrodisias	Herakleia Salb.	Bargasa	Herakleia Salb.	Bargasa	Temnos	Bargasa	Alinda
Eumeneia	Anaia	Anaia	Anaia	Anaia	Pergamum	Aegae	Anaia	Pitane	Eumeneia	Pitane	Miletus	Thyateira	Temnos	Pergamum
Miletus	Thyateira	Thyateira	Thyateira	Thyateira	Bargasa	Miletus	Thyateira	Elaea	Aegae	Elaea	Eumeneia	Priene	Eumeneia	Harpasa
Aegae	Pergamum	Pergamum	Pergamum	Pergamum	Anaia	Eumeneia	Bargasa	Miletus	Miletus	Miletus	Aegae	Pergamum	Tabai	Priene
Aphrodisias	Bargasa	Bargasa	Bargasa	Bargasa	Thyateira	Aphrodisias	Pergamum	Aphrodisias	Aphrodisias	Aphrodisias	Aphrodisias	Bargasa	Priene	Eumeneia
Anaia	Eumeneia	Eumeneia	Eumeneia	Eumeneia	Aegae	Anaia	Aegae	Anaia	Anaia	Anaia	Anaia	Aegae	Alinda	Bargasa
Thyateira	Aegae	Aegae	Aegae	Aegae	Eumeneia	Thyateira	Eumeneia	Thyateira	Thyateira	Thyateira	Thyateira	Eumeneia	Orthosia	Aegae

Table C-2 Sorted archaeological settlements with decreasing potentiality for slope variable. Gray colored rows are testing data and the others are training data.

Gr90/10-Set1	Gr90/10-Set2	Gr90/10-Set3	Gr80/20-Set1	Gr80/20-Set2	Gr80/20-Set3	Gr70/30-Set1	Gr70/30-Set2	Gr70/30-Set3	Gr60/40-Set1	Gr60/40-Set2	Gr60/40-Set3	Gr50/50-Set1	Gr50/50-Set2	Gr50/50-Set3
Heraclea adLa.	Heraclea adLa.	Heraclea adLa.	Antiochia adM.	Antiochia adM.	Heraclea adLa.	Philadelpheia	Antiochia adM.	Tabai	Heraclea adLa.	Alinda	Alinda	Hyllarima	Antiochia adM.	Antiochia adM.
Antiochia adM.	Antiochia adM.	Antiochia adM.	Heraclea adLa.	Heraclea adLa.	Antiochia adM.	Hyllarima	Heraclea adLa.	Notion	Antiochia adM.	Notion	Apamea	Heraclea adLa.	Klazomenai	Hyllarima
Hyllarima	Hyllarima	Hyllarima	Hyllarima	Klazomenai	Klazomenai	Euhippe	Hyllarima	Metropolis	Hyllarima	Metropolis	Neonteichos	Antiochia adM.	Colossae	Heraclea adLa.
Klazomenai	Klazomenai	Klazomenai	Klazomenai	Apollonis	Hyllarima	Akmonia	Klazomenai	Heraclea adLa.	Klazomenai	Hypaipa	Metropolis	Klazomenai	Heraclea adLa.	Klazomenai
Apollonis	Apollonis	Apollonis	Apollonis	Hyllarima	Apollonis	Notion	Apollonis	Hypaipa	Myrina	Apamea	Notion	Amyzon	Apollonis	Apollonis
Myrina	Myrina	Lebedos	Myrina	Hierapolis	Lebedos	Blaundos	Myrina	Antiochia adM.	Apollonis	Akmonia	Hypaipa	Myrina	Tripolis adM.	Amyzon
Lebedos	Amyzon	Colossae	Lebedos	Lebedos	Colossae	Hypaipa	Colossae	Blaundos	Amyzon	Neonteichos	Akmonia	Apollonis	Lebedos	Myrina
Amyzon	Lebedos	Hierapolis	Amyzon	Colossae	Hierapolis	Metropolis	Hierapolis	Hyllarima	Lebedos	Temnos	Euhippe	Nysa	Hierapolis	Nysa
Colossae	Colossae	Amyzon	Colossae	Metropolis	Amyzon	Apamea	Lebedos	Klazomenai	Nysa	Tabai	Temnos	Lebedos	Metropolis	Lebedos
Hierapolis	Hierapolis	Myrina	Hierapolis	Amyzon	Myrina	Alabanda	Amyzon	Akmonia	Colossae	Blaundos	Orthosia	Sardis	Nysa	Sardis
Nysa	Nysa	Sardis	Nysa	Nysa	Sardis	Sardis	Sardis	Temnos	Hierapolis	Heraclea adLa.	Attouda	Hierapolis	Amyzon	Hierapolis
Sardis	Sardis	Tripolis adM.	Sardis	Sardis	Tripolis adM.	Amyzon	Nysa	Apollonis	Sardis	Attouda	Tabai	Colossae	Magnesia adM.	Colossae
Tripolis adM.	Tripolis adM.	Nysa	Tripolis adM.	Tripolis adM.	Nysa	Apollonis	Tripolis adM.	Priene	Tripolis adM.	Hyllarima	Smyrna	Tripolis adM.	Akmonia	Tripolis adM.
Magnesia adM.	Magnesia adM.	Magnesia adM.	Magnesia adM.	Myrina	Magnesia adM.	Heraclea adLa.	Magnesia adM.	Ephesus	Magnesia adM.	Euhippe	Blaundos	Smyrna	Teos	Magnesia adM.
Metropolis	Teos	Teos	Metropolis	Akmonia	Teos	Neonteichos	Teos	Erythrai	Smyrna	Orthosia	Sardis	Metropolis	Hypaipa	Smyrna
Smyrna	Cyme	Cyme	Teos	Notion	Cyme	Smyrna	Cyme	Orthosia	Metropolis	Priene	Philadelpheia	Alabanda	Erythrai	Metropolis
Erythrai	Metropolis	Erythrai	Cyme	Hypaipa	Metropolis	Hierapolis	Smyrna	Attouda	Cyme	Erythrai	Pergamum	Magnesia adM.	Tabai	Erythrai
Philadelpheia	Erythrai	Metropolis	Smyrna	Erythrai	Erythrai	Nysa	Metropolis	Nysa	Teos	Antiochia adM.	Erythrai	Erythrai	Notion	Teos
Akmonia	Philadelpheia	Philadelpheia	Erythrai	Tabai	Philadelpheia	Erythrai	Erythrai	Lebedos	Erythrai	Ephesus	Nysa	Teos	Philadelpheia	Cyme
Teos	Smyrna	Alabanda	Philadelpheia	Philadelpheia	Smyrna	Attouda	Philadelpheia	Colossae	Philadelpheia	Smyrna	Priene	Cyme	Myrina	Philadelpheia
Hypaipa	Alabanda	Smyrna	Alabanda	Magnesia adM.	Alabanda	Tripolis adM.	Alabanda	Hierapolis	Alabanda	Pergamum	Heraclea adLa.	Philadelpheia	Hyllarima	Alabanda
Notion	Pitane	Pitane	Ephesus	Smyrna	Phocaea	Ephesus	Phocaea	Sardis	Ephesus	Sardis	Apollonis	Ephesus	Sardis	Ephesus
Ephesus	Ephesus	Phocaea	Apamea	Ephesus	Pitane	Stratonikeia	Pitane	Amyzon	Phocaea	Harpasa	Tripolis adM.	Apamea	Pitane	Phocaea
Apamea	Phocaea	Akmonia	Akmonia	Blaundos	Ephesus	Antiochia adM.	Ephesus	Myrina	Pitane	Nysa	Ephesus	Neonteichos	Ephesus	Pitane
Tabai	Akmonia	Ephesus	Hypaipa	Apamea	Akmonia	Tabai	Akmonia	Tripolis adM.	Akmonia	Klazomenai	Antiochia adM.	Akmonia	Alabanda	Akmonia
Cyme	Apamea	Notion	Notion	Teos	Apamea	Temnos	Notion	Alinda	Apamea	Apollonis	Amyzon	Pitane	Cyme	Herakleia Salb.
Blaundos	Notion	Apamea	Blaundos	Cyme	Notion	Magnesia adM.	Tabai	Euhippe	Neonteichos	Aegae	Colossae	Phocaea	Blaundos	Stratonikeia
Alabanda	Hypaipa	Hypaipa	Neonteichos	Alabanda	Hypaipa	Teos	Hypaipa	Harpasa	Notion	Amyzon	Klazomenai	Stratonikeia	Phocaea	Apamea
Neonteichos	Blaundos	Tabai	Tabai	Neonteichos	Blaundos	Orthosia	Blaundos	Pergamum	Blaundos	Myrina	Lebedos	Notion	Herakleia Salb.	Laodicea adLy.
Euhippe	Neonteichos	Blaundos	Phocaea	Attouda	Neonteichos	Tralles	Apamea	Apamea	Herakleia Salb.	Philadelpheia	Hierapolis	Herakleia Salb.	Smyrna	Neonteichos
Temnos	Tabai	Herakleia Salb.	Pitane	Pitane	Tabai	Laodicea adLy.	Neonteichos	Aegae	Hypaipa	Eumeneia	Magnesia adM.	Hypaipa	Attouda	Notion
Attouda	Herakleia Salb.	Neonteichos	Euhippe	Temnos	Herakleia Salb.	Myrina	Herakleia Salb.	Smyrna	Stratonikeia	Bargasa	Teos	Blaundos	Temnos	Tralles
Orthosia	Stratonikeia	Laodicea adLy.	Temnos	Phocaea	Stratonikeia	Cyme	Attouda	Philadelpheia	Tabai	Lebedos	Alabanda	Laodicea adLy.	Orthosia	Blaundos
Alinda	Laodicea adLy.	Stratonikeia	Orthosia	Euhippe	Euhippe	Lebedos	Stratonikeia	Neonteichos	Laodicea adLy.	Hierapolis	Hyllarima	Tabai	Apamea	Hypaipa
Priene	Tralles	Euhippe	Attouda	Orthosia	Laodicea adLy.	Phocaea	Euhippe	Magnesia adM.	Tralles	Alabanda	Cyme	Euhippe	Tralles	Elaea
Phocaea	Euhippe	Tralles	Alinda	Alinda	Tralles	Colossae	Temnos	Teos	Attouda	Colossae	Myrina	Tralles	Laodicea adLy.	Euhippe
Pitane	Attouda	Temnos	Herakleia Salb.	Priene	Temnos	Klazomenai	Laodicea adLy.	Cyme	Euhippe	Tripolis adM.	Pitane	Orthosia	Priene	Anaia

Table C-2 (cont'd)

Gr90/10-Set1	Gr90/10-Set2	Gr90/10-Set3	Gr80/20-Set1	Gr80/20-Set2	Gr80/20-Set3	Gr70/30-Set1	Gr70/30-Set2	Gr70/30-Set3	Gr60/40-Set1	Gr60/40-Set2	Gr60/40-Set3	Gr50/50-Set1	Gr50/50-Set2	Gr50/50-Set3
Pergamum	Orthosia	Attouda	Priene	Herakleia Salb.	Orthosia	Alinda	Orthosia	Alabanda	Orthosia	Magnesia adM.	Phocaea	Attouda	Euhippe	Tabai
Herakleia Salb.	Temnos	Orthosia	Stratonikeia	Laodicea adLy.	Attouda	Herakleia Salb.	Tralles	Eumeneia	Temnos	Teos	Herakleia Salb.	Temnos	Neonteichos	Aphrodisias
Stratonikeia	Alinda	Alinda	Laodicea adLy.	Tralles	Alinda	Priene	Priene	Bargasa	Priene	Cyme	Stratonikeia	Priene	Stratonikeia	Miletus
Laodicea adLy.	Priene	Priene	Tralles	Stratonikeia	Priene	Pitane	Alinda	Phocaea	Pergamum	Pitane	Eumeneia	Elaea	Alinda	Attouda
Tralles	Elaea	Pergamum	Pergamum	Pergamum	Pergamum	Harpasa	Pergamum	Pitane	Harpasa	Phocaea	Laodicea adLy.	Pergamum	Pergamum	Orthosia
Eumeneia	Pergamum	Elaea	Eumeneia	Harpasa	Harpasa	Elaea	Harpasa	Herakleia Salb.	Elaea	Stratonikeia	Tralles	Alinda	Harpasa	Alinda
Harpasa	Anaia	Harpasa	Harpasa	Eumeneia	Eumeneia	Bargasa	Eumeneia	Stratonikeia	Alinda	Herakleia Salb.	Harpasa	Anaia	Aegae	Thyateira
Aegae	Aphrodisias	Anaia	Elaea	Elaea	Elaea	Pergamum	Elaea	Laodicea adLy.	Anaia	Laodicea adLy.	Aegae	Aphrodisias	Elaea	Temnos
Bargasa	Miletus	Eumeneia	Anaia	Aegae	Aegae	Aegae	Anaia	Tralles	Aegae	Tralles	Bargasa	Miletus	Eumeneia	Pergamum
Elaea	Eumeneia	Aphrodisias	Aphrodisias	Anaia	Bargasa	Miletus	Aegae	Elaea	Aphrodisias	Elaea	Elaea	Eumeneia	Anaia	Priene
Anaia	Harpasa	Miletus	Miletus	Aphrodisias	Anaia	Eumeneia	Aphrodisias	Anaia	Miletus	Anaia	Anaia	Harpasa	Bargasa	Harpasa
Aphrodisias	Thyateira	Aegae	Aegae	Miletus	Aphrodisias	Aphrodisias	Miletus	Aphrodisias	Eumeneia	Aphrodisias	Aphrodisias	Thyateira	Aphrodisias	Eumeneia
Miletus	Aegae	Thyateira	Thyateira	Thyateira	Miletus	Anaia	Thyateira	Miletus	Thyateira	Miletus	Miletus	Aegae	Miletus	Aegae
Thyateira	Bargasa	Bargasa	Bargasa	Bargasa	Thyateira	Thyateira	Bargasa	Thyateira	Bargasa	Thyateira	Thyateira	Bargasa	Thyateira	Bargasa

Table C-3 Sorted archaeological settlements with decreasing potentiality for aspect variable. Gray colored rows are testing data and the others are training data.

Gr90/10-Set1	Gr90/10-Set2	Gr90/10-Set3	Gr80/20-Set1	Gr80/20-Set2	Gr80/20-Set3	Gr70/30-Set1	Gr70/30-Set2	Gr70/30-Set3	Gr60/40-Set1	Gr60/40-Set2	Gr60/40-Set3	Gr50/50-Set1	Gr50/50-Set2	Gr50/50-Set3
Harpasa	Harpasa	Harpasa	Harpasa	Harpasa	Harpasa	Philadelpheia	Harpasa	Harpasa	Euhippe	Harpasa	Hyllarima	Harpasa	Eumeneia	Tripolis adM.
Tabai	Tabai	Tabai	Tabai	Tabai	Tabai	Hyllarima	Apamea	Tabai	Teos	Apamea	Harpasa	Tabai	Alinda	Hypaipa
Apamea	Apamea	Apamea	Anaia	Apamea	Eumeneia	Euhippe	Tabai	Hyllarima	Tabai	Tabai	Tabai	Apamea	Erythrai	Teos
Anaia	Anaia	Anaia	Hyllarima	Hypaipa	Apamea	Akmonia	Anaia	Anaia	Erythrai	Anaia	Anaia	Anaia	Attouda	Priene
Hyllarima	Hyllarima	Hyllarima	Apamea	Anaia	Alinda	Notion	Hyllarima	Apamea	Amyzon	Hyllarima	Euhippe	Hyllarima	Stratonikeia	Apollonis
Bargasa	Bargasa	Eumeneia	Bargasa	Eumeneia	Anaia	Blaundos	Bargasa	Hypaipa	Blaundos	Bargasa	Hypaipa	Bargasa	Priene	Herakleia Salb.
Hypaipa	Hypaipa	Bargasa	Eumeneia	Tripolis adM.	Attouda	Hypaipa	Ephesus	Eumeneia	Harpasa	Thyateira	Cyme	Hypaipa	Teos	Eumeneia
Eumeneia	Eumeneia	Alinda	Alinda	Apollonis	Erythrai	Metropolis	Thyateira	Alinda	Laodicea adLy.	Ephesus	Erythrai	Ephesus	Tripolis adM.	Stratonikeia
Thyateira	Thyateira	Aphrodisias	Hypaipa	Herakleia Salb.	Blaundos	Apamea	Hypaipa	Stratonikeia	Neonteichos	Eumeneia	Attouda	Thyateira	Blaundos	Euhippe
Alinda	Aphrodisias	Attouda	Attouda	Priene	Aphrodisias	Alabanda	Aphrodisias	Tripolis adM.	Tripolis adM.	Aphrodisias	Blaundos	Euhippe	Nysa	Apamea
Aphrodisias	Alinda	Hypaipa	Blaundos	Stratonikeia	Hypaipa	Sardis	Phocaea	Attouda	Klazomenai	Hypaipa	Apamea	Neonteichos	Pergamum	Blaundos
Blaundos	Blaundos	Blaundos	Klazomenai	Alinda	Stratonikeia	Amyzon	Blaundos	Herakleia Salb.	Metropolis	Alinda	Aegae	Phocaea	Apamea	Tabai
Attouda	Attouda	Erythrai	Aphrodisias	Notion	Hyllarima	Apollonis	Erythrai	Priene	Hypaipa	Blaundos	Eumeneia	Aphrodisias	Tabai	Erythrai
Stratonikeia	Erythrai	Thyateira	Erythrai	Nysa	Priene	Heraclea adLa.	Aegae	Apollonis	Myrina	Attouda	Klazomenai	Blaundos	Aegae	Nysa
Erythrai	Klazomenai	Stratonikeia	Euhippe	Aphrodisias	Klazomenai	Neonteichos	Euhippe	Erythrai	Lebedos	Erythrai	Teos	Eumeneia	Amyzon	Harpasa
Apollonis	Ephesus	Klazomenai	Cyme	Elaea	Cyme	Smyrna	Eumeneia	Aphrodisias	Priene	Apollonis	Bargasa	Attouda	Harpasa	Notion
Ephesus	Euhippe	Priene	Stratonikeia	Erythrai	Tripolis adM.	Hierapolis	Cyme	Blaundos	Hyllarima	Phocaea	Alinda	Cyme	Klazomenai	Anaia
Euhippe	Stratonikeia	Apollonis	Thyateira	Heraclea adLa.	Aegae	Nysa	Attouda	Nysa	Apollonis	Klazomenai	Amyzon	Erythrai	Euhippe	Hyllarima
Klazomenai	Cyme	Cyme	Priene	Blaundos	Teos	Erythrai	Pergamum	Notion	Miletus	Pergamum	Temnos	Temnos	Aphrodisias	Thyateira
Tripolis adM.	Temnos	Tripolis adM.	Temnos	Attouda	Apollonis	Attouda	Teos	Klazomenai	Anaia	Stratonikeia	Miletus	Klazomenai	Cyme	Bargasa
Priene	Apollonis	Temnos	Apollonis	Lebedos	Nysa	Tripolis adM.	Klazomenai	Cyme	Herakleia Salb.	Temnos	Stratonikeia	Aegae	Hypaipa	Aphrodisias
Cyme	Priene	Nysa	Tripolis adM.	Temnos	Bargasa	Ephesus	Temnos	Temnos	Tralles	Cyme	Aphrodisias	Pergamum	Apollonis	Lebedos
Temnos	Aegae	Aegae	Aegae	Cyme	Euhippe	Stratonikeia	Miletus	Bargasa	Colossae	Euhippe	Myrina	Alinda	Anaia	Elaea
Nysa	Tripolis adM.	Euhippe	Nysa	Neonteichos	Thyateira	Antiochia adM.	Alinda	Euhippe	Temnos	Nysa	Tripolis adM.	Myrina	Herakleia Salb.	Temnos
Herakleia Salb.	Nysa	Teos	Teos	Hyllarima	Temnos	Tabai	Hierapolis	Myrina	Elaea	Hierapolis	Priene	Miletus	Miletus	Myrina
Notion	Teos	Pergamum	Myrina	Teos	Pergamum	Temnos	Nysa	Elaea	Nysa	Priene	Metropolis	Teos	Bargasa	Ephesus
Pergamum	Pergamum	Herakleia Salb.	Notion	Pergamum	Amyzon	Magnesia adM.	Amyzon	Teos	Stratonikeia	Tripolis adM.	Thyateira	Nysa	Temnos	Amyzon
Myrina	Myrina	Myrina	Pergamum	Myrina	Miletus	Teos	Stratonikeia	Thyateira	Apamea	Neonteichos	Pergamum	Apollonis	Thyateira	Phocaea
Elaea	Notion	Ephesus	Herakleia Salb.	Klazomenai	Herakleia Salb.	Orthosia	Myrina	Pergamum	Bargasa	Myrina	Apollonis	Pitane	Hyllarima	Cyme
Aegae	Miletus	Amyzon	Miletus	Thyateira	Myrina	Tralles	Apollonis	Lebedos	Pitane	Aegae	Smyrna	Stratonikeia	Myrina	Klazomenai
Teos	Herakleia Salb.	Miletus	Amyzon	Tralles	Notion	Laodicea adLy.	Pitane	Aegae	Heraclea adLa.	Pitane	Notion	Priene	Notion	Miletus
Phocaea	Amyzon	Notion	Elaea	Amyzon	Ephesus	Myrina	Neonteichos	Heraclea adLa.	Cyme	Miletus	Colossae	Amyzon	Ephesus	Laodicea adLy.
Miletus	Phocaea	Elaea	Ephesus	Aegae	Elaea	Cyme	Priene	Amyzon	Aphrodisias	Elaea	Nysa	Hierapolis	Lebedos	Pitane
Lebedos	Elaea	Phocaea	Lebedos	Miletus	Lebedos	Lebedos	Tripolis adM.	Neonteichos	Akmonia	Teos	Laodicea adLy.	Orthosia	Phocaea	Colossae
Amyzon	Lebedos	Lebedos	Neonteichos	Euhippe	Phocaea	Phocaea	Metropolis	Miletus	Aegae	Notion	Lebedos	Tripolis adM.	Elaea	Aegae
Neonteichos	Neonteichos	Pitane	Phocaea	Bargasa	Neonteichos	Colossae	Elaea	Tralles	Pergamum	Herakleia Salb.	Herakleia Salb.	Notion	Pitane	Philadelpheia
Heraclea adLa.	Pitane	Neonteichos	Pitane	Phocaea	Pitane	Klazomenai	Colossae	Phocaea	Thyateira	Tralles	Pitane	Elaea	Neonteichos	Neonteichos

Table C-3 (cont'd)

Gr90/10-Set1	Gr90/10-Set2	Gr90/10-Set3	Gr80/20-Set1	Gr80/20-Set2	Gr80/20-Set3	Gr70/30-Set1	Gr70/30-Set2	Gr70/30-Set3	Gr60/40-Set1	Gr60/40-Set2	Gr60/40-Set3	Gr50/50-Set1	Gr50/50-Set2	Gr50/50-Set3
Pitane	Heraclea adLa.	Heraclea adLa.	Heraclea adLa.	Akmonia	Metropolis	Alinda	Tralles	Antiochia adM.	Attouda	Heraclea adLa.	Antiochia adM.	Smyrna	Hierapolis	Pergamum
Hierapolis	Hierapolis	Metropolis	Metropolis	Antiochia adM.	Heraclea adLa.	Herakleia Salb.	Notion	Akmonia	Phocaea	Orthosia	Elaea	Lebedos	Metropolis	Alinda
Tralles	Metropolis	Hierapolis	Colossae	Hierapolis	Colossae	Priene	Lebedos	Metropolis	Eumeneia	Amyzon	Neonteichos	Herakleia Salb.	Orthosia	Sardis
Orthosia	Tralles	Tralles	Laodicea adLy.	Metropolis	Hierapolis	Pitane	Herakleia Salb.	Ephesus	Notion	Lebedos	Heraclea adLa.	Metropolis	Heraclea adLa.	Tralles
Antiochia adM.	Colossae	Colossae	Tralles	Pitane	Tralles	Harpasa	Heraclea adLa.	Hierapolis	Alinda	Smyrna	Phocaea	Colossae	Colossae	Metropolis
Akmonia	Laodicea adLy.	Laodicea adLy.	Orthosia	Ephesus	Laodicea adLy.	Elaea	Orthosia	Pitane	Antiochia adM.	Antiochia adM.	Orthosia	Heraclea adLa.	Tralles	Alabanda
Metropolis	Orthosia	Antiochia adM.	Smyrna	Colossae	Orthosia	Bargasa	Laodicea adLy.	Colossae	Hierapolis	Colossae	Philadelphieia	Tralles	Smyrna	Heraclea adLa.
Colossae	Antiochia adM.	Orthosia	Antiochia adM.	Laodicea adLy.	Antiochia adM.	Pergamum	Smyrna	Laodicea adLy.	Philadelphieia	Laodicea adLy.	Akmonia	Laodicea adLy.	Laodicea adLy.	Attouda
Laodicea adLy.	Akmonia	Akmonia	Hierapolis	Orthosia	Smyrna	Aegae	Antiochia adM.	Orthosia	Ephesus	Metropolis	Magnesia adM.	Antiochia adM.	Antiochia adM.	Hierapolis
Smyrna	Smyrna	Smyrna	Akmonia	Philadelphieia	Akmonia	Miletus	Akmonia	Smyrna	Magnesia adM.	Akmonia	Ephesus	Akmonia	Akmonia	Antiochia adM.
Magnesia adM.	Magnesia adM.	Philadelphieia	Magnesia adM.	Magnesia adM.	Magnesia adM.	Eumeneia	Magnesia adM.	Philadelphieia	Sardis	Magnesia adM.	Tralles	Magnesia adM.	Magnesia adM.	Magnesia adM.
Philadelphieia	Philadelphieia	Magnesia adM.	Philadelphieia	Sardis	Philadelphieia	Aphrodisias	Philadelphieia	Magnesia adM.	Alabanda	Alabanda	Sardis	Philadelphieia	Alabanda	Akmonia
Alabanda	Alabanda	Sardis	Alabanda	Alabanda	Alabanda	Anaia	Alabanda	Sardis	Orthosia	Philadelphieia	Alabanda	Alabanda	Philadelphieia	Orthosia
Sardis	Sardis	Alabanda	Sardis	Smyrna	Sardis	Thyateira	Sardis	Alabanda	Smyrna	Sardis	Hierapolis	Sardis	Sardis	Smyrna

Table C-4 Sorted archaeological settlements with decreasing potentiality for arable land density variable. Gray colored rows are testing data and the others are training data.

Gr90/10-Set1	Gr90/10-Set2	Gr90/10-Set3	Gr80/20-Set1	Gr80/20-Set2	Gr80/20-Set3	Gr70/30-Set1	Gr70/30-Set2	Gr70/30-Set3	Gr60/40-Set1	Gr60/40-Set2	Gr60/40-Set3	Gr50/50-Set1	Gr50/50-Set2	Gr50/50-Set3	
Akmonia	Akmonia	Akmonia	Akmonia	Akmonia	Akmonia	Akmonia	Akmonia	Akmonia	Akmonia	Akmonia	Akmonia	Akmonia	Akmonia	Akmonia	
Alabanda	Alabanda	Alabanda	Alabanda	Alabanda	Alabanda	Alabanda	Alabanda	Alabanda	Alabanda	Alabanda	Alabanda	Alabanda	Alabanda	Alabanda	
Antiochia adM.	Antiochia adM.	Antiochia adM.	Antiochia adM.	Antiochia adM.	Antiochia adM.	Antiochia adM.	Antiochia adM.	Antiochia adM.	Antiochia adM.	Antiochia adM.	Antiochia adM.	Antiochia adM.	Antiochia adM.	Antiochia adM.	
Apamea	Apamea	Apamea	Apamea	Apamea	Apamea	Apamea	Apamea	Apamea	Apamea	Apamea	Apamea	Apamea	Apamea	Apamea	
Apollonis	Apollonis	Apollonis	Apollonis	Apollonis	Apollonis	Apollonis	Apollonis	Apollonis	Apollonis	Apollonis	Apollonis	Apollonis	Apollonis	Apollonis	
Colossae	Colossae	Colossae	Colossae	Colossae	Colossae	Colossae	Colossae	Colossae	Colossae	Colossae	Colossae	Colossae	Colossae	Colossae	
Elaea	Elaea	Elaea	Elaea	Elaea	Elaea	Elaea	Elaea	Elaea	Elaea	Elaea	Elaea	Elaea	Elaea	Elaea	
Euhippe	Euhippe	Euhippe	Euhippe	Euhippe	Euhippe	Euhippe	Euhippe	Euhippe	Euhippe	Euhippe	Euhippe	Euhippe	Euhippe	Euhippe	
Harpasa	Harpasa	Harpasa	Harpasa	Harpasa	Harpasa	Harpasa	Harpasa	Harpasa	Harpasa	Harpasa	Harpasa	Harpasa	Harpasa	Harpasa	
Herakleia Salb.	Herakleia Salb.	Herakleia Salb.	Herakleia Salb.	Herakleia Salb.	Herakleia Salb.	Herakleia Salb.	Herakleia Salb.	Herakleia Salb.	Herakleia Salb.	Herakleia Salb.	Herakleia Salb.	Herakleia Salb.	Herakleia Salb.	Herakleia Salb.	
Hierapolis	Hierapolis	Hierapolis	Hierapolis	Hierapolis	Hierapolis	Hierapolis	Hierapolis	Hierapolis	Hierapolis	Hierapolis	Hierapolis	Hierapolis	Hierapolis	Hypaipa	
Hypaipa	Hypaipa	Hypaipa	Hypaipa	Hypaipa	Hypaipa	Hypaipa	Hypaipa	Hypaipa	Hypaipa	Hypaipa	Hypaipa	Hypaipa	Hypaipa	Laodicea adLy.	
Laodicea adLy.	Laodicea adLy.	Laodicea adLy.	Laodicea adLy.	Klazomenai	Laodicea adLy.	Laodicea adLy.	Laodicea adLy.	Laodicea adLy.	Laodicea adLy.	Laodicea adLy.	Klazomenai	Laodicea adLy.	Laodicea adLy.	Klazomenai	Magnesia adM.
Magnesia adM.	Magnesia adM.	Magnesia adM.	Magnesia adM.	Laodicea adLy.	Magnesia adM.	Magnesia adM.	Magnesia adM.	Magnesia adM.	Magnesia adM.	Laodicea adLy.	Magnesia adM.	Magnesia adM.	Laodicea adLy.	Metropolis	
Metropolis	Metropolis	Metropolis	Metropolis	Magnesia adM.	Metropolis	Metropolis	Metropolis	Metropolis	Metropolis	Magnesia adM.	Metropolis	Metropolis	Magnesia adM.	Nysa	
Neonteichos	Neonteichos	Neonteichos	Nysa	Metropolis	Nysa	Nysa	Nysa	Nysa	Nysa	Metropolis	Neonteichos	Nysa	Metropolis	Orthosia	
Nysa	Nysa	Nysa	Orthosia	Neonteichos	Orthosia	Orthosia	Orthosia	Orthosia	Orthosia	Neonteichos	Nysa	Orthosia	Neonteichos	Philadelpheia	
Orthosia	Orthosia	Orthosia	Philadelpheia	Nysa	Philadelpheia	Philadelpheia	Philadelpheia	Philadelpheia	Philadelpheia	Nysa	Orthosia	Philadelpheia	Nysa	Sardis	
Pergamum	Philadelpheia	Philadelpheia	Sardis	Orthosia	Sardis	Sardis	Sardis	Sardis	Sardis	Orthosia	Pergamum	Sardis	Orthosia	Smyrna	
Philadelpheia	Sardis	Sardis	Smyrna	Pergamum	Smyrna	Smyrna	Smyrna	Smyrna	Smyrna	Pergamum	Philadelpheia	Smyrna	Pergamum	Thyateira	
Sardis	Smyrna	Smyrna	Thyateira	Philadelpheia	Thyateira	Thyateira	Thyateira	Thyateira	Thyateira	Philadelpheia	Sardis	Thyateira	Philadelpheia	Tralles	
Smyrna	Thyateira	Thyateira	Tralles	Sardis	Tralles	Tralles	Tralles	Tralles	Tralles	Sardis	Smyrna	Tralles	Sardis	Tripolis adM.	
Thyateira	Tralles	Tralles	Tripolis adM.	Smyrna	Tripolis adM.	Tripolis adM.	Tripolis adM.	Tripolis adM.	Tripolis adM.	Smyrna	Thyateira	Tripolis adM.	Smyrna	Hierapolis	
Tralles	Tripolis adM.	Tripolis adM.	Neonteichos	Thyateira	Neonteichos	Neonteichos	Neonteichos	Neonteichos	Neonteichos	Thyateira	Tralles	Neonteichos	Thyateira	Neonteichos	
Tripolis adM.	Pergamum	Pergamum	Pergamum	Tralles	Pergamum	Pergamum	Pergamum	Pergamum	Pergamum	Tralles	Tripolis adM.	Pergamum	Tralles	Pergamum	
Klazomenai	Klazomenai	Klazomenai	Klazomenai	Tripolis adM.	Klazomenai	Klazomenai	Klazomenai	Klazomenai	Klazomenai	Klazomenai	Tripolis adM.	Klazomenai	Klazomenai	Tripolis adM.	Klazomenai
Aphrodisias	Aphrodisias	Aphrodisias	Aphrodisias	Aphrodisias	Aphrodisias	Aphrodisias	Aphrodisias	Aphrodisias	Aphrodisias	Aphrodisias	Aphrodisias	Aphrodisias	Aphrodisias	Aphrodisias	Aphrodisias
Eumeneia	Eumeneia	Eumeneia	Eumeneia	Eumeneia	Eumeneia	Eumeneia	Eumeneia	Eumeneia	Eumeneia	Eumeneia	Eumeneia	Eumeneia	Eumeneia	Eumeneia	Eumeneia
Anaia	Alinda	Anaia	Alinda	Anaia	Alinda	Anaia	Anaia	Alinda	Blaundos	Anaia	Anaia	Anaia	Anaia	Anaia	Alinda
Alinda	Blaundos	Alinda	Blaundos	Alinda	Blaundos	Alinda	Alinda	Blaundos	Miletus	Alinda	Alinda	Alinda	Alinda	Alinda	Blaundos
Blaundos	Stratonikeia	Blaundos	Cyme	Blaundos	Stratonikeia	Blaundos	Blaundos	Anaia	Hyllarima	Blaundos	Blaundos	Blaundos	Blaundos	Blaundos	Anaia
Stratonikeia	Myrina	Stratonikeia	Stratonikeia	Stratonikeia	Anaia	Stratonikeia	Stratonikeia	Stratonikeia	Stratonikeia	Ephesus	Stratonikeia	Stratonikeia	Stratonikeia	Stratonikeia	Stratonikeia
Myrina	Cyme	Myrina	Myrina	Myrina	Cyme	Myrina	Myrina	Myrina	Myrina	Bargasa	Myrina	Myrina	Myrina	Myrina	Myrina
Cyme	Anaia	Cyme	Anaia	Cyme	Myrina	Cyme	Miletus	Cyme	Alinda	Hyllarima	Cyme	Cyme	Miletus	Cyme	Cyme
Miletus	Miletus	Hyllarima	Lebedos	Ephesus	Ephesus	Ephesus	Hyllarima	Ephesus	Aegae	Bargasa	Miletus	Hyllarima	Ephesus	Ephesus	Ephesus
Hyllarima	Ephesus	Bargasa	Ephesus	Miletus	Bargasa	Bargasa	Bargasa	Miletus	Priene	Miletus	Ephesus	Bargasa	Hyllarima	Tabai	Tabai
Bargasa	Bargasa	Miletus	Tabai	Pitane	Pitane	Pitane	Ephesus	Bargasa	Myrina	Priene	Aegae	Miletus	Bargasa	Bargasa	Bargasa

Table C-4 (cont'd)

Gr90/10-Set1	Gr90/10-Set2	Gr90/10-Set3	Gr80/20-Set1	Gr80/20-Set2	Gr80/20-Set3	Gr70/30-Set1	Gr70/30-Set2	Gr70/30-Set3	Gr60/40-Set1	Gr60/40-Set2	Gr60/40-Set3	Gr50/50-Set1	Gr50/50-Set2	Gr50/50-Set3
Ephesus	Hyllarima	Priene	Pitane	Tabai	Tabai	Miletus	Priene	Pitane	Stratonikeia	Ephesus	Bargasa	Priene	Aegae	Pitane
Pitane	Pitane	Ephesus	Bargasa	Bargasa	Miletus	Tabai	Aegae	Tabai	Anaia	Aegae	Hyllarima	Ephesus	Priene	Hyllarima
Tabai	Aegae	Pitane	Priene	Aegae	Hyllarima	Hyllarima	Cyme	Hyllarima	Teos	Cyme	Pitane	Aegae	Cyme	Priene
Priene	Tabai	Tabai	Hyllarima	Hyllarima	Priene	Aegae	Pitane	Aegae	Pitane	Pitane	Tabai	Pitane	Pitane	Miletus
Aegae	Priene	Aegae	Miletus	Priene	Aegae	Priene	Teos	Priene	Cyme	Teos	Priene	Tabai	Teos	Lebedos
Teos	Teos	Teos	Teos	Lebedos	Lebedos	Lebedos	Tabai	Lebedos	Tabai	Tabai	Teos	Teos	Tabai	Teos
Lebedos	Lebedos	Temnos	Aegae	Teos	Teos	Teos	Temnos	Teos	Lebedos	Temnos	Lebedos	Temnos	Temnos	Aegae
Temnos	Temnos	Erythrai	Temnos	Temnos	Temnos	Temnos	Lebedos	Temnos	Temnos	Erythrai	Temnos	Erythrai	Lebedos	Temnos
Erythrai	Erythrai	Lebedos	Erythrai	Erythrai	Erythrai	Erythrai	Erythrai	Erythrai	Erythrai	Lebedos	Erythrai	Lebedos	Erythrai	Erythrai
Notion	Notion	Notion	Notion	Notion	Notion	Notion	Notion	Notion	Notion	Notion	Notion	Notion	Notion	Notion
Phocaea	Phocaea	Phocaea	Phocaea	Phocaea	Phocaea	Phocaea	Phocaea	Phocaea	Phocaea	Phocaea	Phocaea	Phocaea	Phocaea	Phocaea
Heraclea adLa.	Heraclea adLa.	Heraclea adLa.	Heraclea adLa.	Heraclea adLa.	Heraclea adLa.	Heraclea adLa.	Heraclea adLa.	Heraclea adLa.	Heraclea adLa.	Heraclea adLa.	Heraclea adLa.	Heraclea adLa.	Heraclea adLa.	Heraclea adLa.
Amyzon	Amyzon	Amyzon	Amyzon	Amyzon	Amyzon	Amyzon	Amyzon	Amyzon	Amyzon	Amyzon	Amyzon	Amyzon	Amyzon	Amyzon
Attouda	Attouda	Attouda	Attouda	Attouda	Attouda	Attouda	Attouda	Attouda	Attouda	Attouda	Attouda	Attouda	Attouda	Attouda

## CURRICULUM VITAE

### PERSONAL INFORMATION

Surname, Name: Er, Melek

### EDUCATION

Degree	Institution	Year of Graduation
MS	Vrije Universiteit Amsterdam, Geoarchaeology	2009
BS	METU, Mining Engineering	2005

### WORK EXPERIENCE

Year	Place	Enrollment
2020-Present	İka Madencilik A.Ş.	Mine Manager
2013 - 2020	Küçükasya Madencilik A.Ş.	Project Coordinator
2012 - 2013	Küçükasya Madencilik A.Ş.	Lands and IT Department Manager
2010 - 2012	Küçükasya Madencilik A.Ş.	Land Officer

### LANGUAGES

Turkish (Native), English (Advanced)

### COMPUTER SKILLS

Advanced understanding and user experience in 3D modelling, spatial analysis and statistical evaluation. Some of the programs I use: Micromine 8/10, Datamine 8/10, Leapfrog 7/10, MapInfo 9/10, ArcGIS 9/10, Discover & 3D 8/10, Microsoft Office Programs 9/10 (including Access), R Software 7/10

## **PUBLICATIONS**

1. Tendürüs, M., van Wijngaarden, G. J., Kars, H. "Long-term effect of seismic activities on archaeological remains, a test study from Zakynthos, Greece", (M. Sintubin, I. S. Stewart, T. Niemi, & E. Altunel, ed.), *The Geological Society of America Special Paper - Ancient Earthquakes*, 471:145-156, 2010.
2. Van Wijngaarden, G. J., Sotiriou, A., Pieters, N., Abed, K., Tendürüs, M. "The Zakynthos Archaeology Project. Preliminary report of the 2007 season", *Pharos. Journal of the Netherlands Institute in Athens XV (2007)*, 2009.
3. Pieters, N., Stoker, A., Tendürüs, M., van Wijngaarden, G. J. "Archeologie in een extreem dynamisch landschap: het Zakynthos Archeologie Project", *Tijdschrift voor Mediterrane Archeologie (TMA)*, 19 (1), 26-32, 2007.
4. Tendürüs, M., van Wijngaarden, G. J., Kars, H. "A study on quantifying the influence of seismic activities on the archaeological remains of Zakynthos, Greece", *Preserving archaeological remains in situ (PARIS)*, Proceedings of the 3rd conference, 7 - 9 December 2006. *Geoarchaeological and Bioarchaeological Studies* 10, pp. 273-279, 2008.

## **PRESENTATIONS**

1. Er, M., "Arkeolojik Yerleşim Yerlerinin CBS ile Öngörü Modellemesi: Batı Anadolu Helenistik Dönem Yerleşimleri", Presentation, 40. Uluslararası Kazı, Araştırma ve Arkeometri Sempozyumu, Çanakkale, May 2018.
2. Er, M. "A GIS-based Archaeological Predictive Model from Turkey: Preliminary Results for the Hellenistic Period Settlements of Asia Minor", Presentation, *Historic Landscapes: Character, Assessment and Visualization*, Izmir Institute of Technology Faculty of Architecture, Urla, June 2017
3. Tendürüs, M., van Wijngaarden, G. J., Kluiving, S., Soetens, S. "Landscape evolution of the southern coastal plain of Zakynthos, Greece, since the Mid-Holocene", Poster, *Landscape Archaeology Conference (LAC2010)*. Vrije Universiteit Amsterdam, Amsterdam, The Netherlands, Jan. 2010.
4. Tendürüs, M. "Quantifying the influence of seismic activities on the archaeological remains of Zakynthos, Greece", Presentation, *Workshop on Mediterranean Survey Methodology: Sampling Problems and Recent Fieldwork*. Universiteit Gent, Ghent, Belgium, Nov. 2007.
5. Tendürüs, M., van Wijngaarden, G. J., Kars, H. "A study on quantifying the influence of seismic activities on the archaeological remains of Zakynthos, Greece", Poster, *Conference: Preserving Archaeological Remains in situ 3 (PARIS3)*. Vrije Universiteit Amsterdam, Amsterdam, The Netherlands, Dec. 2006.